

IDENTIFICATION AND CHARACTERIZATION OF MOLECULAR MODULATORS OF
METHYLMERCURY-INDUCED TOXICITY AND DOPAMINE NEURON
DEGENERATION IN *CAENORHABDITIS ELEGANS*

Natalia M. VanDuyn

Submitted to the faculty of the University Graduate School
in partial fulfillment of the requirements
for the degree
Doctor of Philosophy
in the Department of Pharmacology & Toxicology,
Indiana University

March 2014

Accepted by the Faculty of Indiana University, in partial fulfillment of the requirements for the degree of Doctor of Philosophy.

Richard M. Nass, Ph.D., Chair

William D. Atchison, Ph.D.

Doctoral Committee

Nickolay Brustovetsky, Ph.D.

Theodore R. Cummins, Ph.D.

July 31, 2013

William J. Sullivan, Jr., Ph.D.

Ronald C. Wek, Ph.D.

DEDICATION

This thesis is dedicated to my grandparents, Harmon and Betty Jorritsma, who provided me with constant love and support. They both suffered from Parkinson's disease, and sadly passed before the completion of my work, however I know they are smiling down on me, overwhelmed with pride for my accomplishments.

ACKNOWLEDGEMENTS

I am beyond grateful for all my family and friends who have shown me never-ending support throughout my years in graduate school and during the completion of this thesis.

I would like to thank my mentor, Dr. Nass, for all the opportunities that he has provided me during my time in his lab, including the chance to attend numerous meetings and to be involved in a variety of projects and publications. I am honored to have received several fellowships and awards, and none of them would have been possible without his encouragement. Also, I appreciate his advice throughout my career as well as during the preparation of this thesis.

I would like to thank all the other faculty members who have shared with me their time and expertise, especially my thesis committee, including Dr. Bill Sullivan, Dr. Theodore Cummins, Dr. Nick Brustovetsky, Dr. Ron Wek and Dr. Bill Atchison. Dr. Atchison (Michigan State University) also gave me guidance in the field of toxicology and allowed me to spend time in his lab learning calcium-imaging techniques. Dr. Michael Wagner (IUSM) provided assistance with ICP-MS and was always available for troubleshooting. Dr. Lihsia Chen and the members of her lab were essential for my studies of *C. elegans* embryonic development. Dr. Jennifer Kowalski (Butler University) provided advice and the use of her microscope. Dr. Wayne Forrester (Indiana University) assisted me with analysis of cell migration and other *C. elegans* techniques. Dr. Garry Wong has shared his insight and experience with bioinformatics and gene expression analysis in *C. elegans*. I am grateful for the time that Dr. Malgorzata Kamocka (Center for Biological Microscopy, IUSM) has spent helping me with confocal microscopy and also for the assistance of Jim Powers (Light Microscopy Imaging Center, Indiana University). Rosalice Buehrer (IUPUI) shared her expertise in Hg analysis during the early stages of my project.

I am very appreciative to the funding agencies who provided the financial support for my research. I was fortunate to receive both the PhRMA Foundation Pre Doctoral Fellowship in Pharmacology/Toxicology and a Science to Achieve Results (STAR) Graduate Fellowship from the U.S. Environmental Protection Agency (EPA). There are many previous members of the Nass lab who have been teachers, colleagues and friends. I learned many techniques from Dr. Raja Settivari and I am grateful for his contributions to my project. I appreciate all the conversations and interactions I have had with Dr. Shaoyu Zhou, Jenny LeVora and Gary Sinclair and also their assistance

with experiments. Pam Torkelson shared many of her technical and lab management skills with me. Brittany Flores played an important role in the ICP-MS experiments for my project. I want to thank all of the work-study students who have done so much to keep the lab running smoothly through the years, especially Sarmed Toma and Rosene Salmo. Also, thanks goes to all of the summer, rotation and MS-MS students who I have had the pleasure of mentoring, especially Vera Obinwanne, Dieria Moore, Rosalinda Campos and Lauren Roach, who all contributed to my dissertation project. Finally, I am very thankful for all the support and encouragement from Sakha Jamadar during the past year.

I also would like to acknowledge the members of the Pharm/Tox department who have contributed to creating the great environment that I am thankful to have been a part of. I owe a huge thank you to all the past and present students and post docs who have shared advice and reagents and have also become friends. The administrative staff of this department have also been incredible resources and always helped me in any way they could. I greatly appreciate the interactions with and feedback from the Pharm/Tox faculty, which have been an essential contributor to my growth as a scientist.

ABSTRACT

Natalia M. VanDuyn

IDENTIFICATION AND CHARACTERIZATION OF MOLECULAR MODULATORS OF METHYLMERCURY-INDUCED TOXICITY AND DOPAMINE NEURON DEGENERATION IN *CAENORHABDITIS ELEGANS*

Methylmercury (MeHg) exposure from occupational, environmental and food sources is a significant threat to public health. MeHg poisonings in adults may result in severe psychological and neurological deficits, and *in utero* exposures can confer significant damage to the developing brain and impair neurobehavioral and intellectual development. Recent epidemiological and vertebrate studies suggest that MeHg exposure may contribute to dopamine (DA) neuron vulnerability and the propensity to develop Parkinson's disease (PD). I have developed a novel *Caenorhabditis elegans* (*C. elegans*) model of MeHg toxicity and have shown that low, chronic exposure confers embryonic defects, developmental delays, reduction in brood size, decreased animal viability and DA neuron degeneration. Toxicant exposure results in an increase in reactive oxygen species (ROS) and the robust induction of several glutathione-S-transferases (GSTs) that are largely dependent on the PD-associated phase II antioxidant transcription factor SKN-1/Nrf2. I have also shown that SKN-1 is expressed in the DA neurons, and a reduction in SKN-1 gene expression increases MeHg-induced animal vulnerability and DA neuron degeneration. Furthermore, I incorporated a novel genome wide reverse genetic screen that identified 92 genes involved in inhibiting MeHg-induced animal death. The putative multidrug resistance protein MRP-7 was identified in the screen. I have shown that this transporter is likely expressed in DA neurons, and reduced gene expression increases cellular Hg accumulation and MeHg-

associated DA neurodegeneration. My studies indicate that *C. elegans* is a useful genetic model to explore the molecular basis of MeHg-associated DA neurodegeneration, and may identify novel therapeutic targets to address this highly relevant health issue.

Richard M. Nass, Ph.D., Chair

TABLE OF CONTENTS

LIST OF TABLES.....	xii
LIST OF FIGURES	xiii
LIST OF ABBREVIATIONS	xv
I. Introduction	1
A. Methylmercury	1
1. MeHg in the environment and routes of exposure	1
2. Human health effects of MeHg exposure	6
3. Cellular and molecular effects of MeHg exposure.....	7
a. Glutathione and reactive oxygen species	7
b. Mitochondria	8
c. Calcium signaling.....	9
d. Neurotransmission and the dopaminergic system.....	10
e. Protein synthesis and interactions.....	12
f. MeHg-associated developmental effects.....	13
g. MeHg-induced cell death.....	13
4. Genetic studies associated with MeHg toxicity	14
5. Selenium inhibits MeHg toxicity.....	16
B. Parkinson's disease	17
1. Background	17
2. MeHg and Parkinson's disease.....	18
C. Nrf2.....	20
1. MeHg and Nrf2	20
2. Role of Nrf2 in PD	21
3. Expression and regulation of Nrf2.....	22
4. Role of Nrf2 and GSH in cellular toxicity	23
5. Nrf2 and Glutathione S-transferases.....	24
6. Nrf2 and heat shock proteins	24
7. Nrf2 and multidrug resistance proteins.....	25
D. Multidrug resistance proteins.....	25

1. Expression, function and regulation of MRPs	26
2. MRPs and MeHg toxicity	28
3. Role of MRPs in PD	29
E. <i>C. elegans</i>	30
1. Characteristics of the model system	30
2. Use of <i>C. elegans</i> in toxicology	31
3. <i>C. elegans</i> DA system and PD model	32
4. SKN-1.....	34
5. GSTs	36
6. HSPs	36
7. MRPs.....	37
8. RNAi and RNAi screens	37
9. Limitations of <i>C. elegans</i> as a model system	39
F. Hypothesis and key questions	40
II. Methods	42
A. <i>C. elegans</i> strains and maintenance	42
B. Synchronization	43
C. Genetic crosses.....	43
D. RNAi	43
E. Toxicant exposures.....	44
F. Viability assay	45
G. Pharyngeal pumping assay	46
H. Brood size assay	46
I. Larval development rate assay	46
J. Embryonic development assay	47
K. ROS analysis	47
L. RNA extraction	47
M. cDNA synthesis.....	48
N. RT-PCR.....	48
O. Protein preparation.....	50
P. Western blot analysis.....	50
Q. DA neuron degeneration	51
R. Immunohistochemistry.....	51
S. ICP-MS	52

1. Collecting samples for ICP-MS	52
2. Digesting samples for ICP-MS	53
3. ICP-MS analysis	54
T. Transgenic animals	55
1. Constructs	55
2. Microinjections	55
U. RNAi screen	56
V. RNAi clone sequencing	57
W. Determination of SKN-1 binding sites	58
X. DAVID analysis	58
Y. BLAST search and sequence alignment	58
Z. Statistical analysis	59
III. Characterization of MeHg toxicity in <i>C. elegans</i>	60
A. Viability	60
1. Chronic exposure to MeHg confers animal death	60
2. Selenium inhibits MeHg toxicity	61
3. MeHg reduces pharyngeal pumping rate	63
B. Reproduction and development	64
1. MeHg reduces brood size	64
2. MeHg causes embryonic defects	65
3. MeHg decreases growth rate	67
4. MeHg delays larval development	67
C. Biochemistry	68
1. MeHg induces <i>C. elegans</i> stress response	68
2. MeHg increases total ROS	69
3. Microarray analysis	70
4. RT-PCR	72
IV. SKN-1 inhibits MeHg-induced toxicity	75
A. SKN-1 inhibits MeHg-induced animal death	75
B. SKN-1 regulates MeHg-induced gene expression	77
C. SKN-1 regulates GST-38 expression	78
D. SKN-1 is expressed in DA neurons	79
E. SKN-1 inhibits MeHg-induced DA neuron degeneration	81
F. SKN-1 inhibits AI-induced DA neuron degeneration	85

V. RNAi screen for mediators of MeHg toxicity.....	87
A. Development and implementation of a MeHg-sensitive RNAi screen	87
B. Results.....	93
VI. The transporter MRP-7 inhibits MeHg toxicity	97
A. MRP-7 is homologous to human MRP1	97
B. MRP-7 inhibits MeHg-induced animal death	99
C. MRP-7 inhibits accumulation of Hg	100
D. MRP-7 expression reduces the MeHg-associated stress response	102
E. <i>mrp-7</i> mRNA levels are increased following MeHg exposure	103
F. MRP-7 inhibits DA neuron degeneration	104
G. MRP-7 is expressed in DA neurons	105
H. Other types of neurons do not degenerate after MeHg exposure	107
VII. Discussion	109
A. Viability	109
B. SKN-1	111
C. RNAi screen	113
D. MRP-7	116
E. Implications in PD	119
VIII. Future directions.....	126
A. Cell-type specific RNAi	126
B. Epigenetics, acetylation and ubiquitination.....	126
C. Further studies on RNAi screen hits.....	127
IX. References	130
CURRICULUM VITAE	

LIST OF TABLES

Table 1. Summary of <i>C. elegans</i> strains	42
Table 2. RT-PCR primer sequences	49
Table 3. DAVID analysis of genes upregulated > 2-fold in microarray	72
Table 4. Composition of <i>C. elegans</i> growth media	90
Table 5. Classification of genes identified in an RNAi screen for MeHg sensitivity	94

LIST OF FIGURES

Figure 1. Illustration of the Hg cycle in the environment and routes of human exposure	3
Figure 2. Diagram of an MRP transporter	26
Figure 3. MeHg confers concentration-dependent animal death	60
Figure 4. MeHg exposure inhibits egg-laying.....	61
Figure 5. Selenium inhibits MeHg-induced lethality	62
Figure 6. Hg levels are reduced by co-exposure with Se	63
Figure 7. MeHg exposure reduces the pharyngeal pumping rate.....	64
Figure 8. Exposure to MeHg causes a reduction in brood size	65
Figure 9. Exposure to MeHg causes embryonic defects	66
Figure 10. Growth on MeHg decreases nematode size.....	67
Figure 11. MeHg delays animal development.....	68
Figure 12. MeHg induces DAF-16 nuclear localization.....	69
Figure 13. MeHg increases ROS	70
Figure 14. MeHg induces the expression of GST mRNAs.....	73
Figure 15. MeHg induces the expression of HSP mRNAs.....	74
Figure 16. <i>skn-1</i> mRNA knockdown increases whole animal vulnerability to MeHg	76
Figure 17. Overexpression or increased activity of SKN-1 increases resistance to MeHg	77
Figure 18. SKN-1 regulates the expression of GSTs.....	78
Figure 19. MeHg-induced expression of GST-38 protein is dependent on <i>skn-1</i>	79
Figure 20. SKN-1 is expressed in DA neurons	80
Figure 21. A specific complementary peptide blocks the reactivity of the SKN-1 antibody	81
Figure 22. SKN-1 inhibits MeHg-induced DA neuron degeneration	83
Figure 23. Viability of <i>skn-1</i> RNAi nematodes exposed to low concentrations of MeHg is not decreased for up to 5 days.....	84
Figure 24. <i>cat-4</i> RNAi increases sensitivity to MeHg-induced DA neuron degeneration	85
Figure 25. SMF-3 contributes to Al ³⁺ -induced DA neuron degeneration.....	86
Figure 26. Work-flow diagram for the genome wide RNAi screen	89
Figure 27. The reduction of Ca ²⁺ or Mg ²⁺ levels does not significantly affect nematode growth.....	92
Figure 28. A graphic summary of the screen results	95

Figure 29. Sequence alignment of human MRP1 with <i>C. elegans</i> MRP-7	98
Figure 30. MRP-7 inhibits MeHg-induced whole animal death	99
Figure 31. Other MRPs do not affect MeHg-induced lethality.....	100
Figure 32. MRP-7 inhibits the accumulation of MeHg.....	101
Figure 33. GST and HSP mRNA expression are increased following MeHg exposure	103
Figure 34. <i>mrp-7</i> mRNA levels are increased following chronic MeHg exposure	104
Figure 35. MRP-7 inhibits MeHg-associated DA neuron degeneration	105
Figure 36. Expression pattern of P _{<i>mrp-7</i>} ::CFP in whole animals.....	106
Figure 37. MRP-7 is expressed in <i>C. elegans</i> DA neurons	107
Figure 38. MeHg exposure does not cause GABA neuron degeneration.....	108
Figure 39. A model for MRP-7 mediated transport of MeHg.....	117
Figure 40. A model for MeHg-induced DA neuron degeneration.....	123

LIST OF ABBREVIATIONS

6-OHDA	6-hydroxydopamine
AAADC	aromatic amino acid decarboxylase
ABC	ATP-binding cassette
ACh	acetylcholine
AD	Alzheimer's disease
AMPK	adenosine monophosphate-activated protein kinase
ARE	antioxidant response element
ATP	adenosine triphosphate
BBB	blood brain barrier
BLAST	basic local alignment search tool
bp	base pairs
CBS	cystathionine B-synthase
cDNA	complementary DNA
CEP	cephalic process
CFP	cyan fluorescent protein
CGC	<i>Caenorhabditis elegans</i> Genetic Center
ChIP-seq	chromatin immunoprecipitation sequencing
CNS	central nervous system
CYP	cytochrome P450
DA	dopamine
DAT	dopamine transporter
DAVID	database for annotation, visualization and integrated discovery
DCFDA	2',7'-dichlorofluorescein-diacetate
DIC	differential interference contrast
DMPS	dimercaptopropane-1-sulfonate
DMSA	dimercaptosuccinic acid
DMSO	dimethyl sulfoxide
DNA	deoxyribonucleic acid
dsRNA	double-stranded RNA
EGTA	ethylene glycol tetraacetic acid
<i>egl</i>	egg-laying defective

EPA	Environmental Protection Agency
ER	endoplasmic reticulum
ETC	electron transport chain
FDA	Food and Drug Administration
FIF	formaldehyde-induced fluorescence
GABA	gamma-Aminobutyric acid
GAPDH	glyceraldehyde 3-phosphate dehydrogenase
GFP	green fluorescent protein
GPx	glutathione peroxidase
GSH	glutathione
GST	glutathione S-transferase
GTPCH	GTP cyclohydrolase I
HAT	histone acetyltransferase
HDAC	histone deacetylase
Hg	mercury
HO-1	heme-oxygenase 1
HPLC	high-performance liquid chromatography
HSP	heat shock protein
ICP-MS	inductively coupled plasma mass spectrometry
IPTG	Isopropyl β -D-thiogalactoside
kb	kilobase
kD	kiloDalton
Keap1	kelch-like ECH-associated protein 1
LB	Luria broth
LC50	lethal concentration 50
MDR	multiple drug resistance
MEF	mouse embryonic fibroblast
MeHg	methylmercury
MPTP	1-methyl-4-phenyl-1,2,3,6-tetrahydropyridine
MPTP	mitochondrial permeability transition pore
MRP	multidrug resistance protein
NAC	N-acetylcysteine
NBD	nucleotide-binding domain
NCBI	National Center for Biotechnology Information

NGM	nematode growth media
NLS	nuclear localization sequence
Nrf2	nuclear factor (erythroid-derived 2)-like 2
NT	neurotransmitter
OD ₆₀₀	optical density 600 nm
PAGE	polyacrylamide gel electrophoresis
PCR	polymerase chain reaction
PD	Parkinson's disease
Ppb	parts per billion
ppm	parts per million
PTPS	6-pyruvoyl tetrahydrobiopterin synthase
RNAi	RNA interference
ROS	reactive oxygen species
RT-PCR	real time polymerase chain reaction
SAGE	serial analysis of gene expression
Se	selenium
SEM	standard error of the mean
SFN	sulforaphane
SH	thiol
SH-SY5Y	a human cell line with dopaminergic properties
shRNA	short hairpin RNA
siRNA	small interfering RNA
SN	substantia nigra
SNP	single nucleotide polymorphism
TBST	tris-buffered saline Tween-20
TH	tyrosine hydroxylase
UPS	ubiquitin proteasome system
VMAT	vesicular monoamine transporter
WT	wild type
YFP	yellow fluorescent protein

I. INTRODUCTION

Methylmercury (MeHg) is an environmental contaminant that is known to damage the nervous system, however the genes and molecular pathways involved in the pathology are largely unknown. The following **Introduction** will provide important background information to understand the results of my studies and the relevance of this dissertation to the field of MeHg toxicity. I first introduce MeHg, discussing its prevalence in the environment and effects on human health and reviewing the current understanding of the cellular effects of MeHg. I then provide a brief review of Parkinson's disease (PD) and how MeHg may be contributing to the development of this very common neurodegenerative disease. My studies support a role for the transcription factor Nrf2 and multidrug resistance proteins (MRPs) in inhibiting MeHg toxicity. I summarize the function, expression and regulation of these proteins and describe their relevance to MeHg. Finally, I introduce *C. elegans* as a model system and present information on its use in toxicology and the genes relevant to my thesis project.

A. Methylmercury

1. Methylmercury in the environment and routes of exposure

Methylmercury (MeHg) is ubiquitously present in the environment, as it originates from both natural and industrial sources. Inorganic mercury (Hg(0)) vapor is released into the atmosphere from volcanoes as well as coal-burning power plants and other types of factories (Clarkson & Magos 2006). The Hg circulates and becomes deposited in the sediment at the bottom of bodies of water where microorganisms and bacteria methylate it, through a process recently shown to require the genes *hgcA* and *hgcB*, to result in the formation of MeHg (Wood 1974, Parks *et al.* 2013). MeHg then enters the aquatic food chain as the bacteria are consumed by small fish, which are eaten by larger fish and so on, up to the highest predator fish. The MeHg accumulates through this food chain and can be found at high levels in the muscles of the fish and marine mammals at the top (ex. shark, tuna, swordfish and pike). In healthy aquatic ecosystems, sharks may contain up to 4 ppm MeHg and in polluted areas, levels as high as 20 parts per million (ppm) have been reported (Clarkson & Magos 2006). Therefore, the main source for human MeHg exposure is through the consumption of contaminated fish, marine mammals and shellfish, putting populations worldwide at risk for the toxic effects of exposure (**Fig. 1**).

Two widespread outbreaks of MeHg poisonings in humans provided much of the basis for determining the toxic effects of MeHg and revealed the severe neurotoxic potential of the contaminant. Outcomes of both acute and chronic exposure to MeHg have been well documented since the 1950s in Minamata, Japan where people ate fish containing high levels of mercury for an extended period of time and developed a condition later termed “Minamata disease”. The most common symptoms in adults included alterations of sight, hearing, taste and smell, impaired movement, tremors, numbness and psychiatric changes (Takeuchi 1982, Ekino *et al.* 2007). In cases of the highest exposure, brain MeHg levels as high as 25 ppm were observed and often resulted in lethality. Autopsies revealed damage to the cortex of the cerebrum and cerebellum, and lesions in brain regions consistent with the symptoms observed (Eto *et al.* 2010). The detrimental effects of fetal exposure were also revealed during the Minamata outbreak. Numerous miscarriages were attributed to the MeHg poisoning, and children born following exposure suffered from cerebral palsy and other defects in brain development resulting in neurobehavioral changes and delayed intellectual development in addition to the symptoms experienced by adults (Harada 1995). The effects on the brain due to infant or prenatal exposure were long lasting, with symptoms persisting throughout life and the brain damage obvious upon autopsy more than 20 years after exposure (Eto *et al.* 2010). In 1992, the number of confirmed cases of Minamata disease totaled 2,252 and nearly half of the cases ended in fatality (Harada 1995).

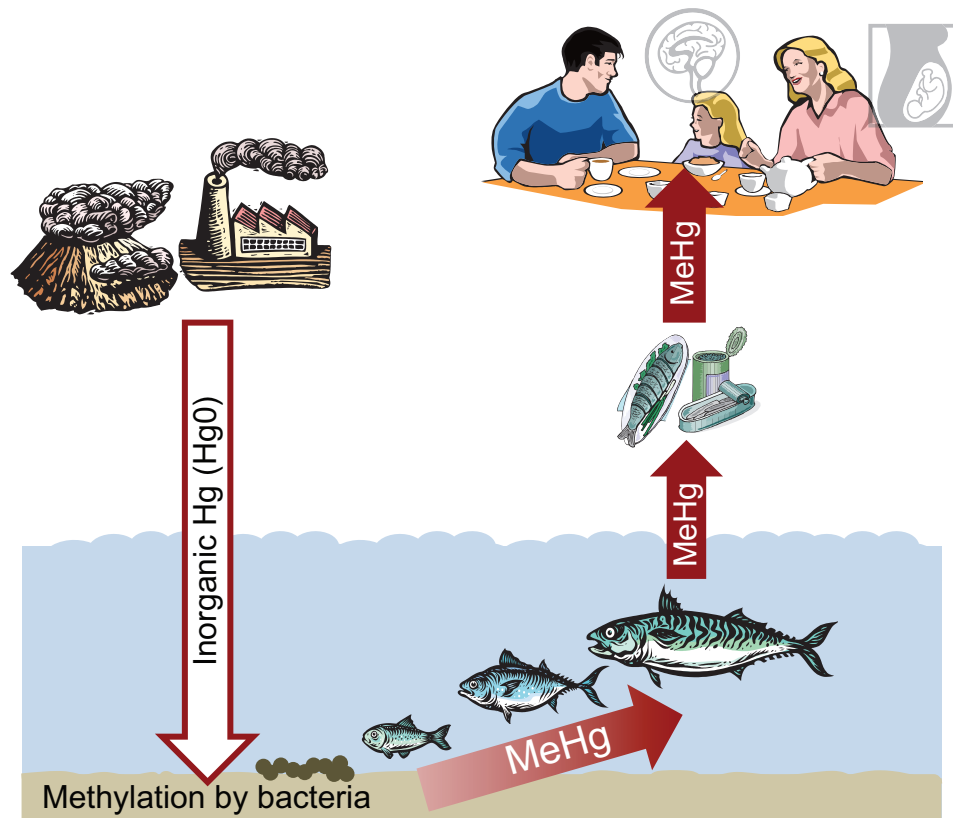


Figure 1. Illustration of the Hg cycle in the environment and routes of human exposure to MeHg. Created with images from Microsoft Clip Art.

A larger occurrence of poisonings happened in 1971 in the rural population of Iraq as a result of the consumption of wheat that had been intended for planting and was coated with a MeHg-containing fungicide (Clarkson & Magos 2006). In total, 6,530 people were admitted to the hospital as a result of exposure and 459 of those people died. MeHg in hair was recorded as high as almost 600 ppm and blood levels reached 3.7 ppm (Bakir *et al.* 1973). The observations of brain damage in both adults and infants ranged from mild to severe and symptoms correlated with total body burden of MeHg: paresthesia, ataxia, dysarthria, deafness, and death, from low to high. The effects on infants were well characterized. Infants exposed *in utero* had blood concentrations at least as high as in the mother, however those who were born before the outbreak and therefore only exposed through milk had concentrations equal to or lower than the mother (Bakir *et al.* 1973). Autopsies of prenatally exposed infants revealed defects in brain development including “abnormal neuronal migration and deranged cerebral

cortical organization” (Choi *et al.* 1978). These studies and others have led to the conclusion that MeHg poses a significant risk to the unborn fetus.

These initial observations revealed the severe neurotoxic potential of MeHg, and numerous studies have been conducted to investigate the dose response profile of the toxicant and the environmental levels that lead to a risk of toxicity. Limits for MeHg exposure have been based on correlations between Hg levels and the risk for toxicity. Studies of populations in New Zealand, the Seychelles islands and the Faroe Islands have been carried out because of the high levels of seafood in the diets of these people. Maternal hair Hg concentrations were recorded for hundreds of women, and their children were monitored for several years following birth. The scores on various neurological tests in relation to the maternal hair Hg were used to estimate the BMDL, which indicates the lower statistical bounds on the benchmark dose (BMD). It was determined that maternal hair levels higher than 20 ppm may contribute to an increased risk for neurological deficits in their children (van Wijngaarden *et al.* 2006).

The data from epidemiological studies were taken into account and the Environmental Protection Agency (EPA) reference dose of 0.1 ug/kg bw/day was ultimately based largely on developmental endpoints from the Faroe Islands study (USEPA 2001). In 2001, the Food and Drug Administration (FDA) released a consumer advisory warning pregnant women and young children against eating high-level predator fish including shark, swordfish, king mackerel and tilefish and suggesting they consume less than 12 oz. of other fish per week (USFDA 2001). The EPA extended these guidelines in 2004 and suggested that no more than 6 oz. of tuna should be eaten per week (Rheinberger & Hammitt 2012). These warnings are warranted based on an analysis of the National Health and Nutrition Examination Survey (NHANES) 1999-2000 study that indicated nearly 10% of women of child-bearing age in the U.S. had blood mercury levels above the advisable limit and this number increases to over 25% in Korea (Schober *et al.* 2003, Kim & Lee 2010). It was estimated by the National Academy of Sciences that over 60,000 children are born every year in the U.S. at risk for neurological impairments caused by prenatal exposure to MeHg and analysis by another group estimated this number to be as high as 600,000 (Trasande *et al.* 2005, Zuckerman *et al.* 2007). As the fetus can accumulate higher levels of MeHg than the mother, exceeding these suggested limits can lead to significant effects on the child. In the population as a whole, it has been estimated that by 2020, the decreased IQ and other

impacts on human health due to MeHg exposure could cost society billions of dollars annually (Sundseth *et al.* 2010).

As a result of the continuing efforts of the EPA and the FDA to establish safe limits of exposure, as of December 2008, all 50 states in the U.S. had issued Hg advisories for fish consumption (USEPA 2010). This was based on the water quality criterion of 0.3 mg/kg (MeHg/fish tissue wet weight). In 2009, the National Lake Fish Tissue Study found that half of the lakes sampled (all in the US) contained fish that exceeded the limit of 0.3 mg MeHg/kg (USEPA 2009). These observations indicate that MeHg remains high in the environment and Hg emissions continue to be a problem worldwide. While countries are improving methods to reduce Hg burden, Asia still contributes in high amounts due to the burning of fossil fuels (Pacyna *et al.* 2010). Because of the long half-life of Hg(0) in the atmosphere, the toxicant does not just affect Asia, but can travel long distances and contribute to the problem of MeHg in other areas of the world (Driscoll *et al.* 2013). In an effort to reduce the effects of Hg on the environment, a treaty called the Minamata Convention on Mercury is being signed by over 140 countries in the fall of 2013 and will require governments to monitor and regulate Hg pollution (Poulain & Barkay 2013). Current research is also addressing the methylation and demethylation of Hg, as the true impact of toxicant is determined by the amount of Hg that is converted to MeHg (Driscoll *et al.* 2013, Poulain & Barkay 2013).

Despite monitoring and regulations by the EPA and FDA, the consumption of contaminated fish is still a worldwide problem. Several populations and groups of people rely on the fish they catch themselves as a primary food source (Driscoll *et al.* 2013). It is not feasible, financially or logistically, to monitor the Hg consumption in situations like this, placing these groups at risk for MeHg-associated toxicities.

Limiting intake is the best way to prevent MeHg poisoning, however if high exposures do occur, drugs used for the treatment of inorganic Hg poisoning can be helpful in MeHg poisoning. Penicillamine, N-acetyl-DL-penicillamine and sodium 2,3-dimercaptopropane-1-sulfonate (DMPS) and dimercaptosuccinic acid (DMSA) increase the excretion rate of Hg in humans exposed to MeHg (Clarkson *et al.* 1981, Rusyniak *et al.* 2010). These drugs have free thiol groups that can bind MeHg, and a resin synthesized to contain sulfhydryl groups also increased excretion. These chelation therapies rely on the normal physiological excretion routes, but chelation combined with a hemodialysis device can further enhance the removal of Hg from the body (Al-Abbasi *et al.* 1978, Lund *et al.* 1984). These compounds have limited solubility and low efficacy

but N-acetylcysteine (NAC) is clinically available and had a greater effect on MeHg clearance (Ballatori *et al.* 1998). These drugs can increase the excretion rate of MeHg, but unfortunately often have little effect on overall clinical improvement (Rusyniak *et al.* 2010). Often there is a long latency period between exposure and the development of symptoms, limiting the efficacy of any treatment.

2. Human health effects of MeHg exposure

The majority of the effects of MeHg have been described above in relation to the poisonings in Iraq and Minamata disease. The symptoms such as numbness, tremors and sensory disturbances can occur soon after exposure, but may also manifest much later (Yorifuji *et al.* 2008). Psychiatric and behavioral symptoms can be detected long after the exposure occurred or following low chronic exposure (Yorifuji *et al.* 2011). Other possible long-term neurological outcomes of MeHg exposure include delayed development, lower IQ scores, and deficits in language, memory and attention (Clarkson & Magos 2006). These effects have been documented following the acute MeHg poisonings described above, as well as in longitudinal studies that monitor the development of children exposed *in utero* as a result of maternal fish consumption. In the Faroe Islands, where people regularly consume pilot whale meat that contains up to 2 ppm Hg, significant effects on several neurological endpoints were observed even when maternal hair Hg levels were lower than the advisable limit at that time (Grandjean *et al.* 1997, Bourdineaud *et al.* 2011). Another smaller study of prenatal exposure in New Zealand also found significant effects of MeHg exposure on developmental tests. However the maternal hair levels associated with impairment in the child were slightly higher, around 15 ppm (Rice *et al.* 2003). In contrast, the Seychelles Child Development Study has found no correlation between fish consumption and a negative impact on the neurological development on children (Myers *et al.* 2009, Davidson *et al.* 2011). This lack of correlation may be explained by lower overall Hg consumption, or by the protective effects afforded by long chain poly-unsaturated fatty acids (LCPUFAs) also present in fish.

Early life exposure to neurotoxicants can cause changes in the brain that may not manifest symptoms for several years. Minamata disease can remain latent until the nervous system is again compromised, by another stress or through the normal process of aging (Weiss 2010). Even if the effects of MeHg exposure do not result in classic Minamata disease, the damage can sensitize the nervous system making it more

susceptible to memory loss, cognitive defects and age-related neurodegenerative diseases such as Alzheimer's disease (AD) and Parkinson's disease (PD) (Trasande *et al.* 2005, Weiss 2010). These subtle changes induced by MeHg are a significant problem because there are no signs of toxicity until later in life when age-related processes are exacerbated by the pre-existing damage.

Although the nervous system is the most prominent target of MeHg, effects on other parts of the body are also observed. The effects of MeHg on the cardiovascular system were first recognized in a population of men in Finland who consumed high amounts of fish and had an increased risk of acute myocardial infarction and death from coronary heart disease and cardiovascular disease (Salonen *et al.* 1995, Salonen *et al.* 2000). Further epidemiological and animal studies also reported this association (Virtanen *et al.* 2007).

3. Cellular and molecular effects of MeHg exposure

Given the detrimental effects of MeHg on human health, the mechanisms underlying the toxicity have been an area of extensive research. Reviewed below are studies in animal models, cell culture and *in vitro* systems that have provided insight into the consequences of MeHg exposure at the cellular and molecular level.

a. Glutathione and reactive oxygen species

Oxidative damage is one of the key mechanisms by which MeHg exerts its toxic effects. Reactive oxygen species (ROS) are reactive molecules that contain oxygen such as hydrogen peroxide (H₂O₂), hydroxyl radicals and superoxide radicals (Forman *et al.* 2009). ROS are important in intracellular signaling pathways, but excess ROS can attack and damage other molecules including DNA, lipids and proteins. There are multiple cellular mechanisms that regulate the balance between oxidized and reduced conditions, but disruption of this balance in the favor of oxidation is termed oxidative stress (Roberts *et al.* 2009). The glutathione system is a significant regulator of the oxidative balance (Forman *et al.* 2009).

Glutathione (GSH) is a tripeptide comprised of glutamate, glycine and cysteine and is important for detoxification of xenobiotics and maintaining the oxidative balance of cells. GSH is the reduced form of the molecule as the thiol (-SH) group can participate in conjugation reactions (Forman *et al.* 2009). MeHg has a high affinity for -SH groups and can bind GSH, which may inhibit MeHg from reacting with other cellular targets and

also increase the excretion of MeHg from the cell (Ballatori & Villalobos 2002). Glutathione peroxidase (GPx) catalyzes the reaction between GSH and H₂O₂ to form H₂O and GSSG, the oxidized form of the molecule. Under normal conditions, glutathione reductase converts GSSG back to GSH and the redox balance is maintained. However, excessive amounts of ROS can deplete GSH and increase level of GSSG leading to oxidative stress and cellular damage.

There are numerous reports of the role of oxidative stress in MeHg toxicity. MeHg exposure significantly increases lipid peroxidation in cell culture and in mouse liver, kidney and brain (Sarafian & Verity 1991, Andersen & Andersen 1993). Oxidative DNA damage and the formation of 8-hydroxydeoxyguanosine (8-OHdG) are another consequence of MeHg exposure, contributing to its genotoxic effects (Ogura *et al.* 1996, Belletti *et al.* 2002). Total ROS, as detected by the fluorescent dye 2,7-dichlorodihydrofluorescein-diacetate (DCFDA), are increased by MeHg (Kaur *et al.* 2006, Mori *et al.* 2011). Superoxide and H₂O₂ were increased in mouse brains following MeHg exposure (Yee & Choi 1994). Mitochondria from mice administered MeHg show a significant increase in ROS, and this effect is specific to the cerebellum (LeBel *et al.* 1990). ROS are increased in primary astrocytic cultures by MeHg exposure, and the increase can be prevented by antioxidants (Shanker *et al.* 2002). Consistent with increased ROS, GSH levels are often decreased following MeHg exposure (Yee & Choi 1996, Kaur *et al.* 2006, Mori *et al.* 2007). However, the decrease is usually transient and followed by an increase in GSH synthesis and total levels in order to compensate and reduce the oxidative stress (Sarafian *et al.* 1996). Drugs that increase GSH, such as 15-deoxy-delta-12,14-prostaglandin J2 (15d-PGJ2), can help mitigate the oxidative stress induced by MeHg (Chang & Tsai 2008). Overall, these studies indicate that MeHg exposure can contribute to oxidative stress by increasing ROS and decreasing GSH.

b. Mitochondria

Mitochondria are a major source of ROS in the cell and appear to be a key cellular target of MeHg. Mitochondrial respiration is impaired by MeHg in synaptosomes and in brain slices (Fox *et al.* 1975, Verity *et al.* 1975). MeHg impairs mitochondrial function and leads to an increased production of ROS (Atchison & Hare 1994). In zebrafish muscle, MeHg inhibits mitochondrial energy metabolism (Cambier *et al.* 2009). Protein expression levels of subunits of the electron transport chain (ETC) are increased in the hippocampus and kidneys of mice fed a diet containing MeHg levels similar to that of

human consumption (Bourdineaud *et al.* 2011). MeHg decreased the activity of complex II in the cerebellum of exposed rats (Mori *et al.* 2011). MeHg may disrupt complex II or III to lead to the increased ROS observed following exposure (Yee & Choi 1996). The disruption of the ETC can lead to cellular toxicity both by decreasing ATP levels available to maintain normal cellular function as well as by increasing the levels of damage-inducing ROS. It has also been demonstrated that the mitochondrial permeability transition pore (MPTP) opens and the mitochondrial membrane potential is decreased in the presence of MeHg (Shenker *et al.* 1999, Limke & Atchison 2002). Opening of the MPTP can increase ROS levels and impair ATP production, and also lead to a release of Ca^{2+} into the cytosol, which can in turn have a significant impact on cellular function.

c. Calcium signaling

Calcium plays a role in important cellular processes and dysregulation of Ca^{2+} can be toxic. MeHg exposure results in an increase in intracellular Ca^{2+} , both from intracellular stores (endoplasmic reticulum (ER) and mitochondria) and from the influx of extracellular Ca^{2+} (Hare *et al.* 1993). This increased Ca^{2+} is likely a contributor to the cell death induced by MeHg. Ca^{2+} can activate pro-apoptotic calpains and caspases and cause the opening of the MPTP, facilitating the release of pro-apoptotic cytochrome c. Ca^{2+} is also required for the functioning of proteins with various roles in apoptotic signaling including calcineurin, nitric oxide synthase, endonucleases, phospholipases, transglutaminases and proteases (Orrenius *et al.* 2003). The Ca^{2+} chelators ethylene glycol tetraacetic acid (EGTA) and 1,2-bis(2-aminophenoxy)ethane-N,N,N',N'-tetraacetic acid tetrakis(acetoxymethyl)ester (BAPTA) can partially reduce the cytotoxicity of MeHg suggesting that the high intracellular Ca^{2+} levels are a key factor in the toxicity (Sarafian & Verity 1991, Marty & Atchison 1998).

MeHg may also interact with or pass through calcium channels, disrupting their function and further altering intracellular Ca^{2+} levels (Bailey *et al.* 2013). Voltage-sensitive Ca^{2+} currents can be inhibited by MeHg in PC12 cells (derived from a rat pheochromocytoma in the adrenal medulla) and Ca^{2+} channel blockers can prevent MeHg-induced neurotoxicity in cells and rats (Sakamoto *et al.* 1996, Marty & Atchison 1998, Shafer *et al.* 2002). Recent studies show that the Ca^{2+} channel blocker nimodipine can attenuate MeHg-induced neurobehavioral changes in mice (Atchison & Narahashi 1982). Ca^{2+} channels facilitate neurotransmission in many excitable cells of the nervous

systems and blockage of these channels, along with others, can lead to severe defects in nervous system function.

d. Neurotransmission and the dopaminergic system

MeHg disrupts neurotransmission and has multiple effects on ion channels (Sirois & Atchison 1996). The toxicant can both increase and decrease excitatory synaptic transmission, blocking evoked neurotransmitter (NT) release while stimulating the spontaneous release of dopamine (DA), gamma-Aminobutyric acid (GABA), acetylcholine (ACh) and serotonin (Tuomisto & Komulainen 1983, Minnema *et al.* 1989, Juárez *et al.* 2002, Surmeier *et al.* 2010). MeHg can also bind and inhibit NT receptors and the transporters involved in re-uptake (Atchison 2005).

Early observations in synaptosomes showed spontaneous release of several neurotransmitters (including DA) following MeHg exposure, and at the time, this was attributed to a general increase in membrane permeability (Minnema *et al.* 1989). Later studies sought to explain the source of DA release. Varying K^+ and Ca^{2+} during MeHg-evoked DA release from mouse striatal slices showed that, in addition to spontaneous release, K^+ stimulated release is significantly enhanced (Kalisch & Racz 1996). This suggests that membrane permeability cannot be the only source of increased DA release. Much research has been performed to investigate these mechanisms *in vivo*. In live rats, MeHg can be perfused into the brain and direct collection and measurement of DA is carried out by high-performance liquid chromatography (HPLC). In this system, an immediate response to MeHg exposure is DA release and increased extracellular DA (Faro *et al.* 1997). The release was shown to be independent of Ca^{2+} and to originate from a source other than vesicles (Faro *et al.* 2002a). There are some inconsistencies among systems and exposure conditions, as this experiment showed that KCl-stimulated release was inhibited by MeHg, rather than enhanced. Further, vesicular stores play a significant role in DA release in MeHg-exposed PC12 cells (Tiernan *et al.* 2013). N-methyl-D-aspartate (NMDA) receptors and nitric oxide synthase (NOS) may play a role in the MeHg-induced DA release, likely through an indirect mechanism involving Ca^{2+} (Faro *et al.* 2002b).

There is also evidence for an interaction of MeHg with the dopamine transporter (DAT). MeHg can inhibit DAT function but MeHg-evoked DA release was shown to be dependent on DAT (Faro *et al.* 2002a, Dreiem *et al.* 2009). Increased extracellular DA can come from increased release or decreased reuptake. MeHg may bind to the -SH

groups on DAT to block the transporter and inhibit the reuptake of DA. GSH and cysteine prevent the MeHg-induced DA release, likely by binding MeHg and preventing its interaction with DAT (Bonnet *et al.* 1994, Faro *et al.* 2002a, Faro *et al.* 2005). MeHg could also have a similar effect as amphetamine, causing DA efflux through DAT (Faro *et al.* 2002a, Leviel 2011).

In addition to affecting DA release, MeHg can cause overall changes in DA signaling. Decreased tyrosine levels and a reduction in the DA synthesis rate were observed in the brains of MeHg exposed rats (Sharma *et al.* 1982). However, studies in PC12 cells showed that MeHg increased tyrosine hydroxylase (TH) activity and DA synthesis in short term exposures (Tiernan *et al.* 2013). In mice, a diet containing MeHg led to decreased DA levels and impairment of DA-associated behaviors (Bourdineaud *et al.* 2011, Bourdineaud *et al.* 2012).

Early life exposure to MeHg can cause lasting changes in the DA system. Gestational exposure to a single dose of MeHg in rats altered DA-related behavioral responses up to 22 days of age (Cuomo *et al.* 1984). Female rats exposed to low levels of MeHg during pregnancy and lactation produced offspring with altered motor activity in the first month of life, decreased spatial learning ability at 2 months and impaired mobility at 6 months of age (Rossi *et al.* 1997, Giménez-Llort *et al.* 2001, Daré *et al.* 2003). Function of the DA system can be analyzed by its response to chemical challenges. Amphetamine is a DA agonist and increases activity of the DA system. Exposure to MeHg during early postnatal development caused an increased sensitivity to amphetamine-induced behaviors later in life (Wagner *et al.* 2007). Cocaine also targets the DA system, and rats exposed to MeHg *in utero* showed enhanced response to this drug, but not other drugs that target other NT systems (Reed & Newland 2009).

Aside from DA signaling and NT release, the viability of dopaminergic cells can also be affected by MeHg. The morphology of the DA neurons in primary mesencephalic neuronal cultures was affected by MeHg such that the number of neurites per cell was significantly decreased (Götz *et al.* 2002). Furthermore, apoptotic indicators including decreased cell size and increased chromatin condensation were observed following MeHg exposure (Götz *et al.* 2002). Embryonic stem cells can be differentiated in mixed neuronal cultures *in vitro*. The addition of MeHg during this period of differentiation resulted in gene expression changes that decreased the number of cells that matured into dopaminergic neurons (Zimmer *et al.* 2011). Together, these

studies indicate that DA neurons are sensitive to MeHg, both during early development and adulthood.

e. Protein synthesis and interactions

MeHg impairs protein synthesis and can also bind proteins containing -SH groups (Syversen 1977, Clarkson 1987, Kasama *et al.* 1989, Atchison & Hare 1994). Binding by MeHg can alter the function of enzymes or cause modifications to other proteins impairing their function (LoPachin & Barber 2006). The accumulation of misfolded and damaged proteins contributes to the pathology of several neurodegenerative diseases and may also play a role in MeHg-induced cytotoxicity (Stefani & Dobson 2003). The ubiquitin-proteasome system (UPS) is a cellular mechanism for targeting and degrading damaged proteins and several studies demonstrate a role of the UPS in protecting against MeHg toxicity (Hershko & Ciechanover 1998). Enhancement of the UPS system promotes cell survival in the presence of MeHg as yeast overexpressing a ubiquitin-conjugating enzyme (Cdc34), a ubiquitin binding protein (Rad23) or an F-box protein (Ymr258c) show enhanced resistance to the toxicant (Hwang *et al.* 2002, Hwang *et al.* 2007, Hwang *et al.* 2009). Furthermore, UPS genes are upregulated by MeHg exposure in mouse embryonic fibroblast (MEF) cells, supporting their role in inhibiting the toxicity (Yu *et al.* 2010).

One specific protein target of MeHg is tubulin. Microtubules are a component of the cytoskeleton that help to maintain cellular structure, participate in the intracellular transport of vesicles and organelles and play an integral role in cytokinesis. MeHg binds the sulfhydryl groups in tubulin monomers and results in depolymerization (Abe *et al.* 1975). This disruption of microtubules can inhibit mitosis, creating micronucleated or multinucleated cells (Sager & Syversen 1984). Axonal transport of proteins is impaired by MeHg, likely due to the effects on microtubules (Abe *et al.* 1975). Microtubules also participate in cell migration. One of the key pathological findings of fetal Minamata disease was abnormal organization of the cerebellar granule cells, which suggested impaired migration. Experimental evidence shows that MeHg impairs cell migration *in vitro* and in cerebellar organotypic slice cultures, inhibiting the migration of the cells from the external layer towards the internal layer (Kunimoto & Suzuki 1997, Sass *et al.* 2001, Mancini *et al.* 2009). Further *in vivo* studies demonstrate that MeHg disrupts neuronal migration and patterning of the nervous system in developing *Drosophila* (Rand *et al.*

2009). Tubulin is one well-characterized protein target of MeHg binding, but numerous other targets exist with a variety of cellular consequences.

f. MeHg-associated developmental effects

In addition to the damage on the nervous system, *in utero* MeHg exposure can affect other cellular processes and structures. MeHg exposure in mice during pregnancy resulted in the death of embryos, defects in those that survived and chromosomal aberrations (Curle *et al.* 1987). Tail development in zebrafish is altered by MeHg exposure (Yang *et al.* 2010). Fish embryos exposed to MeHg during development exhibit abnormalities in multiple systems from the skeleton to the nervous system (Weis 2009). One way that MeHg could be altering development is through a direct regulation of the transcription of genes involved in developmental pathways such as Enhancer-of-split and Bearded complex genes in *Drosophila* (Rand *et al.* 2008).

g. MeHg-induced cell death

The increases in ROS and intracellular Ca^{2+} following MeHg exposure likely contribute to the cell death associated with MeHg toxicity (Ceccatelli *et al.* 2010). Both apoptosis and necrosis have been observed following MeHg exposure, and ROS and Ca^{2+} can play a role in both types of cell death (Castoldi *et al.* 2000, Orrenius *et al.* 2003, Zong & Thompson 2006). Apoptosis may occur at lower MeHg concentrations, and necrosis often predominates at higher concentrations or prolonged exposure times (Kunimoto & Suzuki 1997, Castoldi *et al.* 2000). The apoptotic cell death following MeHg exposure has been described in numerous systems, ranging from cell culture to rats and these studies have been extensively reviewed (Ceccatelli *et al.* 2010). The pathways leading to apoptosis vary in the different models. The classic pathway of cytochrome c release followed by activation of caspases has been observed (Tamm *et al.* 2006). Also, lysosomal proteases may play a role, as do calpains activated by the increased intracellular Ca^{2+} (Ceccatelli *et al.* 2010, Tofighi *et al.* 2011). MeHg induces apoptosis and increases Bax, Bad, cytochrome c and caspases 12, 9, 8 and 3 (Usuki *et al.* 2008, Cuello *et al.* 2010, Sokolowski *et al.* 2011). The mechanism of MeHg-induced cell death may vary depending upon cell type, however multiple mechanisms can also be activated simultaneously in a single cell (Ceccatelli *et al.* 2010).

4. Genetic studies associated with MeHg toxicity

Although a genome-wide reverse genetic screen for modulators of MeHg toxicity in an animal has not been previously reported, in yeast, screens of genomic libraries have identified several genes that when overexpressed facilitate resistance to MeHg. Overexpression of CDC34/UBC3 (a ubiquitin conjugating enzyme) or Ymr258c (an F-box protein) may increase resistance to MeHg by enhancing the function of the UPS and removal of damaged proteins or proteins that contribute to MeHg toxicity (Hwang *et al.* 2009, Furuchi *et al.* 2002). In another screen, MeHg-resistant clones were identified to have increased expression of GFAT (L-glutamine:D-fructose-6-phosphate). The GFAT enzyme is essential for amino acid biosynthesis and may be inhibited by MeHg, so increased expression of the protein could attempt to compensate for the impaired function (Miura *et al.* 1999). Bop3 and proteins that interact with it were also found to increase resistance to MeHg, but the function of Bop3 and the mechanism of resistance is unknown (Miura *et al.* 1999, Furuchi *et al.* 2002, Hwang *et al.* 2005, Hwang *et al.* 2009). In human cell culture (HEK293 cells), a small interfering RNA (siRNA) screen of 8,500 genes revealed a single gene, PIGB, for which knockdown made the cells resistant to MeHg (Hwang *et al.* 2007). PIGB encodes the phosphatidylinositol glycan class B, which is involved in the synthesis of membrane-associated glycosylphosphatidylinositol (GPI) anchors. The mechanism by which PIGB may contribute to MeHg toxicity had not yet been identified. More recently, an siRNA screen targeting nearly 50,000 human mRNA transcripts in HEK293 cells revealed that PRKAA1 (a subunit of adenosine monophosphate-activated protein kinase (AMPK)) is also involved in MeHg toxicity (Hwang *et al.* 2010). The AMPK activator (AICAR) suppressed MeHg-induced cell death, suggesting that AMPK and its role in regulating cellular energy metabolism may promote survival in the presence of MeHg. These unbiased, screen-based studies have implicated signaling pathways in MeHg toxicity that may not have been identified through targeted studies.

More mechanistic studies have also identified genes associated with MeHg toxicity. As the mitochondria and ROS have been implicated in MeHg toxicity, the role of genes associated with the ETC were analyzed in response to MeHg in yeast. Loss of Rip1, part of complex III, increased resistance to MeHg, however this effect was not observed for any other components of complex III, suggesting that Rip1 may contribute to MeHg-induced ROS production through a novel function independent of the ETC (Lee *et al.* 2009). To determine if attenuation of ROS may inhibit MeHg toxicity, several

antioxidant enzymes were overexpressed in HeLa cells, and it was shown that increased expression of manganese superoxide dismutase (Mn-SOD) increased the resistance to MeHg (Naganuma *et al.* 1998). Pharmacological inhibition of another antioxidant enzyme, GPx1, in mitochondria isolated from mouse brain and human SH-SY5Y cells significantly increased MeHg toxicity (Franco *et al.* 2009). Overexpression of GPx1 in cerebellar granule cells increased the resistance to MeHg (Farina *et al.* 2009). Considering that hydrogen sulfide (H₂S) can provide the -SH group for detoxification of MeHg and that the enzyme cystathionine B-synthase (CBS) catalyzes the production of H₂S, the role of CBS in MeHg toxicity was investigated. In SH-SY5Y cells, siRNA knockdown of the CBS gene was found to enhance MeHg-induced cell death and overexpression reduced toxicity in the presence of MeHg, suggesting that this gene contributes to cellular protection against MeHg (Yoshida *et al.* 2011).

Gene expression studies in several different systems have provided insight into the cellular response to MeHg. Microarray analysis of mouse embryonic fibroblast (MEF) cells exposed to MeHg or the proteasome inhibitor MG132 showed increases in genes associated with the UPS/ubiquitin system, phase II enzymes, cell cycle regulation, and genes associated with PD (Yu *et al.* 2010). Microarray analyses have also been used to characterize the gene expression profile in the brains of mice exposed to MeHg *in utero* (Glover *et al.* 2009). Serial analysis of gene expression (SAGE) revealed genes associated with MeHg in zebrafish muscle including ribosomal genes, protein synthesis, ETC, mitochondria, ER, detoxification and stress response (Cambier *et al.* 2010). A further study investigated the gene expression changes in zebrafish brain following a chronic exposure to MeHg at environmentally relevant doses (Cambier *et al.* 2012). Analysis of protein expression in the brain of the Atlantic cod showed alterations in proteins associated with the mitochondria, tubulin, oxidative stress and calcium (Berg *et al.* 2010). One of the most significant changes was in the protein pyridoxine kinase, which plays a role in the synthesis of several neurotransmitters, including DA (Berg *et al.* 2010). Insight into the mechanisms of how MeHg affects development was gained by microarray analysis of gene expression during the specific time period of neural tube closure (Robinson *et al.* 2010). Comparison of the various microarray data sets shows genes associated with mitochondria, ER, the UPS and stress response are commonly upregulated by MeHg exposure. The microarray studies are consistent with other reports of the mechanisms of MeHg toxicity, suggesting that microarray analysis may be a useful method for identifying novel MeHg-associated genes.

5. Selenium inhibits MeHg toxicity

Identifying approaches to inhibit the toxicity of a chemical may contribute to understanding the mechanisms of toxicity. Studies show that supplementing selenium (Se) is one method of protecting against MeHg toxicity. Se is a trace element that is required for normal cellular function and is a cofactor of several enzymes. Se supplementation can reduce MeHg toxicity in whole animals and it has been shown that co-exposure prevents toxicant-associated morphological changes to the kidney and animal death (Parížek & Ostádalová 1967). Se reduced or delayed the onset of behavioral deficits induced by chronic exposure to MeHg, indicating Se can also inhibit the neurotoxicity of MeHg (Heath *et al.* 2010).

The affinity of Hg for Se is approximately a million times higher than its affinity for sulfur (i.e. -SH groups), therefore in biological systems Hg and Se are often tightly bound (Ralston & Raymond 2010). It was first believed that a biological function of Se was to sequester the Hg, however recent studies suggest that Hg sequesters the Se. The excess Se is beneficial by overcoming the deficit to keep selenoenzymes functioning properly (Ralston & Raymond 2010). Selenoproteins are often antioxidants or participate in redox balance, including glutathione peroxidases and thioredoxin reductases (Gromer *et al.* 2005). The interaction of Hg and Se suggest several other mechanisms by which Se could be decreasing the toxicity of MeHg (Khan & Wang 2009).

The Hg-Se complex can also form another species with glutathione, $(GS)_5(HgSe)_{core}$ (Gailer *et al.* 2002). The similar $[(GS)_2AsSe]^-$ complex promotes the excretion of arsenic (As) through the liver, and the same could be true for the Hg complex (Carew & Leslie 2010). Furthermore, the export of the As complex is mediated by the multidrug resistance protein MRP2, which also transports the MeHg-GSH complex. As the reaction between Hg and Se can occur in the absence of a biological system, it is possible that the Hg-Se complex is formed in the environment thus limiting the uptake of MeHg. In rice plants, high Se levels in the soil and plants correlates with low MeHg content (Zhang *et al.* 2012). Although the protective effect of Se against MeHg toxicity is well documented, the mechanism(s) contributing to this effect are still debated and a better understanding of the interaction may provide opportunities to reduce the effects of MeHg on the environment or human health.

B. Parkinson's disease

1. Background

PD is an age-related neurodegenerative disorder that affects about 1-2% of the population over 65 and the prevalence is higher in those over 85 (Nuytemans *et al.* 2010). PD presents clinically with a set of symptoms including tremor, rigidity, bradykinesia, postural instability, flexed posture and the freezing phenomenon (Fahn 2008, Jankovic 2008). Other symptoms include depression, sleep disorders and impairment of cognitive and sensory function (Jankovic 2008). Pathologically, PD is defined by the loss of DA neurons in the substantia nigra pars compacta (Damier *et al.* 1999, Petrucelli & Dickson 2008). Lewy bodies and Lewy neurites, which contain α -synuclein, are also found in the brain of people with PD, and the lesions resulting from these inclusions spread through the brain as the disease progresses (Braak *et al.* 2003). Currently, there is no cure for PD. Treatment involves either drug therapy to increase DA synthesis, such as L-DOPA, or deep brain stimulation. Both options only relieve the symptoms and do not inhibit the progression of the disease, and the efficacy of treatment can decrease over time (Fahn 2008).

The precise etiology of PD remains unknown, but it is likely that both genetic and environmental factors contribute to the development of most cases of PD. Mutations in several genes have been associated with the development of PD, however less than 10% of cases are classified as the "familial" (inherited) form of the disease (Corti *et al.* 2011). The most well-known and well-studied genes are α -synuclein, parkin, PINK1, DJ-1, and LRRK2 (Nuytemans *et al.* 2010, Vistbakka *et al.* 2012). The majority of PD cases (over 90%) are considered sporadic or idiopathic. Similar molecular mechanisms may be associated with DA neuron cell death, whether the cause is genetic or environment-related, and include mitochondrial dysfunction, oxidative stress and proteasomal dysfunction (Thomas & Beal 2011).

There are numerous environmental factors that may contribute to the development of PD. Pesticides, herbicides and insecticides have all been positively correlated with the disease, and the exposures can be occupational by those who use them or due to living on a farm and drinking well water (Freire & Koifman 2012). Specifically, the use of paraquat and rotenone is positively correlated with PD (Tanner *et al.* 2011). Other environmental and industrial contaminants can also contribute to PD: polychlorinated biphenyls (PCBs), the solvent trichloroethylene (TCE), and metals including lead, copper and MeHg (Petersen *et al.* 2008, Caudle *et al.* 2012).

2. MeHg and Parkinson's disease

Epidemiological evidence suggests a correlation between exposure to MeHg and the development of PD. The prevalence of PD in people from the Faroe Islands is approximately two times higher than the prevalence expected in other populations and it is thought that the diet of these native people may explain the increased risk (Petersen *et al.* 2008). The traditional Faroe diet consists of large amounts of pilot whale meat and blubber, which contain high levels of MeHg and PCBs. Although prenatal MeHg exposure was not correlated with the risk of PD, a study comparing the dietary history of PD patients with normal controls showed that there was a significant association between the adulthood consumption of whale meat and blubber and the development of PD (Petersen *et al.* 2008). These results, as well as several cohort studies of children born in the Faroes, have led to the recommendation that pilot whale should no longer be consumed in any amounts (Weihe & Joensen 2012). Occupational PCB exposure has been associated with an increased incidence of PD, so the presence of PCBs along with MeHg in the Faroe diet may contribute to the higher prevalence of PD observed in this study (Steenland *et al.* 2006). However, several other reports support the role of MeHg in PD independent of PCBs (Ohlson & Hogstedt 1981, Ngim & Devathanan 1989, Finkelstein *et al.* 1996, Seidler *et al.* 1996).

A study based on the direct measurement of Hg content, rather than interviews or self-reporting of past exposure, showed a significant and dose dependent correlation between blood and urinary Hg levels and PD (Ngim & Devathanan 1989). A single case study of a female dentist with parkinsonism suggested a link between Hg and parkinsonism. Chelation therapy with d-penicillamine resulted in an increase in urinary Hg excretion and sustained improvement of the parkinsonism (Finkelstein *et al.* 1996). In 1981 a small case-control study was carried out on PD patients and a control population. Questionnaire reporting revealed that 6 of the PD patients, but only 2 controls, had been exposed to mercury (organic and inorganic were both included) (Ohlson & Hogstedt 1981). Due to the small sample size the results were not statistically significant, but these findings are supportive of a possible connection between the metal and the disease. A much larger case-control study in Germany surveyed several possible risk factors for PD, including exposure to chemicals and heavy metals. This study detected an increase in the odds ratio for occupational mercury exposure (not significant) and a positive association between dental amalgams and PD (Seidler *et al.* 1996).

Identifying correlations between toxicant exposure and the development of neurodegenerative diseases is challenging due to varied exposure conditions and the lack of accurate reporting methods (Cannon & Greenamyre 2013). Furthermore, early life exposures to environmental toxicants can contribute to neurodegenerative disorders later in life, but a long latency period greatly impairs the ability to establish a causal relationship (Weiss *et al.* 2002, Trasande *et al.* 2005). Although the epidemiological evidence is inconclusive, the similarities between the cellular effects of MeHg toxicity and the dysfunctions that contribute to PD are supportive of an association between the toxicant and the disease. Oxidative stress is involved in DA neuron cytotoxicity, and results from sources including dysfunctional mitochondria, reduced ability to buffer ROS and altered DA metabolism (Dawson & Dawson 2003, Drechsel & Patel 2008, Zeevalk *et al.* 2008). Oxidative stress is one of the well-documented effects of MeHg exposure. In PD, mitochondrial dysfunction is associated with both genetic and environmental causes of the disease and the mitochondria may be the organelle most highly damaged by MeHg (Thomas & Beal 2011). MeHg disrupts Ca^{2+} signaling and the sustained elevation of intracellular Ca^{2+} in DA neurons due to autonomous pacemaking may contribute to the selective sensitivity of these cells (Surmeier *et al.* 2010). There is also evidence of ER stress in both PD and MeHg toxicity (Hoozemans *et al.* 2007, Zhang *et al.* 2013). There is an emerging role of the immune response in the progression of PD and MeHg can alter the function of glia and astrocytes (Bassett *et al.* 2012). Although Hg was not included in the study, several other metals were shown to contribute to the formation of the α -synuclein fibrils that form Lewy bodies and are toxic to DA neurons (Uversky *et al.* 2001). Finally, PD is an age-related disorder with the incidence increasing dramatically in older individuals. MeHg accumulates in the brain and other tissues, which could allow for a compounding effect that slowly increases over time before resulting in observable damage.

The UPS is another molecular target of both MeHg and PD (Yu *et al.* 2010). Two of the genes that cause familial PD are components of the UPS; parkin is a ubiquitin ligase and UCHL1 is a ubiquitin hydrolase. Function and activity of the UPS is inhibited in several PD models (Lim & Tan 2007). This could lead to accumulation of damaged or misfolded proteins (ex. α -synuclein) that contribute to the cytotoxicity. In the brains of human PD patients, a gene called SKP1A, which is associated with ubiquitin-mediated protein degradation was significantly decreased in comparison to healthy controls. This led to the development of a new model for sporadic PD in which small hairpin RNA

(shRNA) knockdown of SKP1A confers cell death in a substantia nigra (SN)-derived cell line (Mandel *et al.* 2009). SKP1A is an F-box binding protein and a member of the SCF ubiquitin ligase complex, similar to the yeast gene Ymr258c that confers resistance to MeHg (Hwang *et al.* 2009). Microarray analysis in MEF cells exposed to MeHg identified 20 genes involved in PD-related pathways, including the ubiquitin hydrolase Uchl1 (Yu *et al.* 2010). These studies suggest that the UPS plays a role in MeHg toxicity and PD, and the pathologies may involve common molecular pathways.

C. Nrf2

Cellular stress results in increased expression of genes and proteins that function to minimize the insult and promote survival. In the case of oxidative stress, genes containing an antioxidant response element (ARE) are induced by the transcription factor nuclear factor (erythroid-derived 2)-like 2 (NFE2L2 or Nrf2) (Kensler *et al.* 2007). Nrf2 binds to the ARE in the promoter of the target gene and increases the transcription of the gene. Genes encoding phase II detoxification enzymes (ex. glutathione s-transferases (GSTs)), antioxidant enzymes (ex. heme oxygenase 1 (HO-1)) and phase III enzymes (ex. MRPs) are under the control of Nrf2 (Jaiswal 2004). Nrf2 is activated during oxidative and ER stresses and by a wide range of insults including xenobiotics, heavy metals, natural compounds, pharmacological agents and radiation (Kensler *et al.* 2007). This diversity in inducers implicates Nrf2 in a variety of conditions and disease, from cancer to neurodegenerative diseases to heavy metal toxicity, and the transcription factor plays a significant role in the cellular response to MeHg.

1. MeHg and Nrf2

MeHg exposure can activate Nrf2 and expression of Nrf2 inhibits MeHg toxicity in several cell types. In SH-SY5Y cells, overexpression of Nrf2 increases resistance to MeHg and siRNA mediated knockdown of Nrf2 results in sensitivity to MeHg (Toyama *et al.* 2007). Nuclear Nrf2 levels are higher following MeHg exposure, and levels of Nrf2 target proteins in whole-cell extracts also increased (Toyama *et al.* 2007). In a whole animal model, Nrf2 *-/-* hepatocytes were more sensitive to MeHg-induced cytotoxicity (Toyama *et al.* 2007). Nrf2 is also induced following MeHg exposure in astrocytes. MeHg exposure increased nuclear localization of Nrf2, ARE-driven luciferase activity and the expression of three Nrf2 target genes (Wang *et al.* 2009a). Reduced Nrf2 activity, via inhibition of PI3 kinase (an upstream regulator of Nrf2), decreased cell viability in the

presence of MeHg (Wang *et al.* 2009a). MeHg exposure in microglia increased nuclear Nrf2 and expression of its target genes as well (Ni *et al.* 2010). shRNA-mediated knockdown of Nrf2 sensitizes the microglia to MeHg-induced cell death (Ni *et al.* 2010). Although Nrf2 is involved in the MeHg response in both microglia and astrocytes, the nuclear translocation and upregulation of target genes occurs more quickly and at lower MeHg concentrations in microglia and the sensitizing effect of Nrf2 knockdown is also more dramatic in these cells (Ni *et al.* 2011). Nrf2 is conserved across species and in *Drosophila* overexpressing Nrf2, the hatching rate in the presence of MeHg is greatly increased relative to wild type (WT) flies (Rand *et al.* 2009).

In addition to genetic manipulation of Nrf2, pharmacological and chemical activators of the transcription factor can also inhibit MeHg toxicity. Carbon monoxide (CO) (a product of the enzymatic reaction mediated by HO-1) activates Nrf2, and through this pathway, is able to reduce the toxicity of MeHg in SH-SY5Y cells (Toyama *et al.* 2010). Two different Nrf2 activators, 6-methylsulfinylhexyl isothiocyanate (6-HITC) and sulforaphane (SFN), can inhibit MeHg toxicity in primary mouse hepatocytes, and SFN decreases the neurotoxicity and mortality induced by MeHg in mice (Toyama *et al.* 2011a).

Gene expression studies suggest that Nrf2 is induced and regulates transcription following MeHg exposure. Microarray analysis of SH-SY5Y cells exposed to MeHg indicated that 4 out of the 15 genes upregulated over 10-fold have been shown to be regulated by Nrf2 (Toyama *et al.* 2011b). Nrf2-regulated genes are also among the transcripts increased in Atlantic cod following MeHg exposure (Yadete *et al.* 2013).

2. Role of Nrf2 in PD

Nrf2 is activated in response to oxidative stress. Oxidative stress may contribute to the DA neuron cell death that occurs in PD, suggesting that Nrf2 may be an attractive therapeutic target for the disease (Johnson *et al.* 2007). Studies have shown that Nrf2 is activated and inhibits 1-methyl-4-phenyl-1,2,3,6-tetrahydropyridine (MPTP)-induced cytotoxicity in a mouse model of PD (Burton *et al.* 2006). Overexpression of Nrf2 in astrocytes reduces MPTP toxicity (Chen *et al.* 2009). Nrf2 knockout mice also had a greater loss of DA neurons following MPTP and 6-hydroxydopamine (6-OHDA) exposure than WT (Burton *et al.* 2006, Jakel *et al.* 2007, Innamorato *et al.* 2010). SFN can reduce the striatal DA neuron loss caused by MPTP and 6-OHDA in WT mice (Siebert *et al.* 2009, Jazwa *et al.* 2011). Another Nrf2 activator, tert-Butylhydroquinone (tBHQ),

decreases 6-OHDA-induced cytotoxicity in mouse neuronal cells (Jakel *et al.* 2007). Nrf2 overexpression also inhibits the toxicity induced by α -synuclein in a *Drosophila* PD model (Barone *et al.* 2011). In addition to the animal and cell culture evidence, epidemiological data shows that a variation in the promoter of *NFE2L2* (the gene coding for Nrf2) is associated with delayed onset and reduced risk of PD (von Otter *et al.* 2010). As this genetic variant of the Nrf2 gene is suggested to suppress the disease, this change in the promoter sequence is likely to result in increased expression or activity of Nrf2.

The oxidative stress associated with DA neuron degeneration is likely due in part to DA auto-oxidation producing H_2O_2 and DA quinones, both of which can contribute to the induction of Nrf2 transcriptional activity (Shih *et al.* 2007). Nrf2 activity has also been shown to decline with age, and as PD is an age-related disease, this decline may contribute to the sensitivity of the neurons (Suh *et al.* 2004, Sykiotis & Bohmann 2010). Nrf2 activating compounds have been shown to inhibit DA neuron toxicity in cell culture models, suggesting the possible utility of Nrf2 as a therapeutic target for PD (Cuadrado *et al.* 2009). DA agonists with catechol rings may disrupt the association between Nrf2/Keap1 and promote Nrf2 activity, in addition to their role in supplementing endogenous DA. GSK-3B inhibitors may also stimulate Nrf2 mediated transcription and increase oxidative stress resistance (Cuadrado *et al.* 2009). Deprenyl is a candidate PD therapeutic that offers neuroprotection via multiple mechanisms, including the activation of Nrf2 and its antioxidant target genes (Nakaso *et al.* 2006).

3. Expression and regulation of Nrf2

The activity of Nrf2 is tightly regulated to allow rapid increases in gene expression in response to stress. This regulation is achieved mainly at the level of Nrf2 localization and protein turnover, with Nrf2 sequestered in the cytoplasm under non-stressed conditions by the protein kelch-like ECH-associated protein 1 (Keap1) (Itoh *et al.* 1999). Besides the physical association of Nrf2 with Keap1, which is further enhanced by Keap1 binding to actin, Keap1 also acts as an adaptor protein to facilitate the ubiquitination and eventual proteasomal degradation of Nrf2 (Zhang *et al.* 2004a, Kensler *et al.* 2007). Upon stress, the interaction between Keap1 and Nrf2 is disrupted, allowing accumulation of higher amounts of Nrf2, which can translocate to the nucleus (Nguyen *et al.* 2009). The interaction between Keap1 and Nrf2 can be disrupted by electrophiles, including MeHg. Keap1 is rich in cysteines and the binding of

electrophiles to the reactive SH groups causes the dissociation from Nrf2 (Dinkova-Kostova *et al.* 2002, Nguyen *et al.* 2009). Nrf2 is then free to translocate to the nucleus, via a process involving its nuclear localization sequence (NLS) and importin α and importin β (Theodore *et al.* 2008).

Keap1 is a key player in controlling Nrf2, yet other mechanisms may also participate in the regulation of the localization or transcriptional activity of Nrf2. Mammalian studies have implicated the histone deacetylase (HDAC) SIRT1 in the regulation of Nrf2, such that overexpression or inhibition of SIRT1 affected the binding of Nrf2 to the ARE, Nrf2 regulated transcription and nuclear localization (Kawai *et al.* 2011). SIRT1 inhibitors increase Nrf2 activity, suggesting that increased acetylation is a positive regulator of the transcription factor. Consistent with these studies, the histone acetyltransferase (HAT) p300/CBP acts as a transcription co-activator, and can directly acetylate Nrf2 to enhance the binding to target genes (Sun *et al.* 2009, Kawai *et al.* 2011). Specific protein kinases are also involved in both inhibition and enhancement of Nrf2 activity. GSK-3B phosphorylates Fyn and Fyn phosphorylates Nrf2 resulting in nuclear export of Nrf2 and an inhibition of the response to oxidative stress (Jain & Jaiswal 2007, Rojo *et al.* 2008b). In contrast, phosphorylation of Nrf2 via MAPK pathways, including those involving ERK and p38, lead to increased activity of Nrf2 (Yu *et al.* 2000, Zipper & Mulcahy 2000).

4. The role of Nrf2 and GSH in cellular toxicity

The expression of several of the genes involved in the GSH system is increased by exposure to xenobiotics under the regulation of Nrf2 (Kensler *et al.* 2007). The first evidence that Nrf2 was a regulator of this process was in Nrf2 knockout mice, which showed a reduced GST response in the presence of butylated hydroxyanisole (BHA) compared to WT mice (Itoh *et al.* 1997). A more comprehensive identification of genes regulated by Nrf2 involved microarray analysis of WT and Nrf2 *-/-* mice with or without SFN treatment (Thimmulappa *et al.* 2002). Several GSTs were identified, along with other antioxidant genes that had been previously linked to Nrf2 and also new genes. Chromatin immunoprecipitation sequencing (ChIP-Seq) provided direct evidence that Nrf2 can bind the ARE in several GST genes (Malhotra *et al.* 2010).

Although GSH plays a role in the detoxification of numerous xenobiotics, it is particularly important for MeHg due to the high affinity of Hg compounds for the -SH group (Sarafian *et al.* 1996, Clarkson & Magos 2006). The -SH group on GSH can bind

MeHg, preventing MeHg from attacking other molecules and proteins. Further, the GS-MeHg complex is a substrate for ATP binding cassette (ABC) transporters, expediting the excretion of MeHg from the cell (Sarafian *et al.* 1996). Conjugation with GSH is an important route of MeHg excretion from astrocytes (Fujiyama *et al.* 1994). Cell lines with increased GSH levels are more resistant to MeHg toxicity (Miura & Clarkson 1993).

5. Nrf2 and Glutathione S-transferases

Conjugation of GSH to xenobiotics can occur in a reaction catalyzed by GSTs (Forman *et al.* 2009). GSTs belong to the phase II class of cellular detoxification enzymes. This conjugation of electrophiles to the reduced GSH molecule typically inactivates and prepares the electrophile for excretion (Wilce & Parker 1994, Armstrong 1997). As organisms are confronted with a multitude of stressors and toxicants, they have also developed a large number of detoxification mechanisms (Hayes *et al.* 2005). Organisms usually express several GSTs so they can react to a variety of substrates in different locations. GSTs have been grouped into seven species-independent classes based on sequence similarity (Hayes *et al.* 2005). GST expression is dependent upon sex, age and tissue type and this is controlled primarily through transcriptional regulation by Nrf2 among other factors (Eaton & Bammler 1999). There are numerous substrates for GSTs, including environmental toxicants, pesticides, drugs and endogenous molecules (Eaton & Bammler 1999).

6. Nrf2 and heat shock proteins

Heat shock proteins (HSPs) are proteins induced in response to cellular stress and function to minimize damage to the cell. They typically act as molecular chaperones either assisting in the localization or transport of another protein or binding to damaged proteins and targeting them for degradation in the proteasome or to another organelle for repair (Samali & Orrenius 1998a). HSPs are induced following exposure to thermal stress, oxidative stress and heavy metals, including Hg (Sanders 1993, Stacchiotti *et al.* 2004, Yu *et al.* 2006). These proteins mitigate cellular insults and have a diverse range of functions, including promoting protein folding, regulating protein trafficking, stabilizing proteins and regulating protein degradation (Sarafian *et al.* 1996). The induction of HSPs is under the control of heat shock factors (HSFs) that translocate to the nucleus, bind to heat shock elements (HSEs) in the genome and upregulate transcription of HSPs (Samali & Orrenius 1998a).

7. Nrf2 and multidrug resistance proteins

Nrf2 can also regulate the expression of phase III detoxification enzymes including MRPs. In primary rat hepatocytes, MRP1 and MRP2 levels were decreased in Nrf2^{-/-} cells and increased in cells with decreased Keap1 expression (Toyama *et al.* 2007). One of the main routes of MeHg excretion is through MRPs and, following exposure, Hg content was correlated with the level of MRP expression (Toyama *et al.* 2007). Nrf2 activators can inhibit MeHg toxicity, both by increasing expression of genes to combat ROS and by increasing the transporters necessary for MeHg export. Isothiocyanates, which activate Nrf2, increased cell viability in the presence of MeHg and decreased the total Hg content *in vitro*. The effect was also observed *in vivo*, as Hg was decreased in the brain and liver of mice (Toyama *et al.* 2011a). MRP1 expression is decreased by Nrf2 siRNA, and some tumor tissues that had high levels of Nrf2 were found to have high levels of MRP1 (Ji *et al.* 2013).

D. MRPs

ABC transporters are proteins that utilize energy from ATP to transport substances across cellular membranes, often against a concentration gradient. They are characterized by the presence of (at least) two membrane-spanning domains and two nucleotide-binding domains (NBDs), but differ by substrate specificity and localization or tissue expression (Sharom 2008). NBDs are located in the cytoplasmic loops of the protein and contain conserved sequences referred to as the Walker A and Walker B motifs and a third sequence between them called Walker C or the ABC signature sequence (**Fig. 2**). The hydrophobic transmembrane domains form the opening that allows the substrate to pass through the membrane. The Walker A, B and C motifs are involved in ATP binding and ATPase activity to provide the energy for substrate transport (Dean *et al.* 2001, Jones & George 2002). The ABC transporters are grouped into classes based on the overall structure and phylogenetic analysis. Proteins in the ABCC class are termed MRPs. Some in this class have an additional N-terminal transmembrane domain (for a total of 3) and the typical two NBDs (**Fig. 2**).

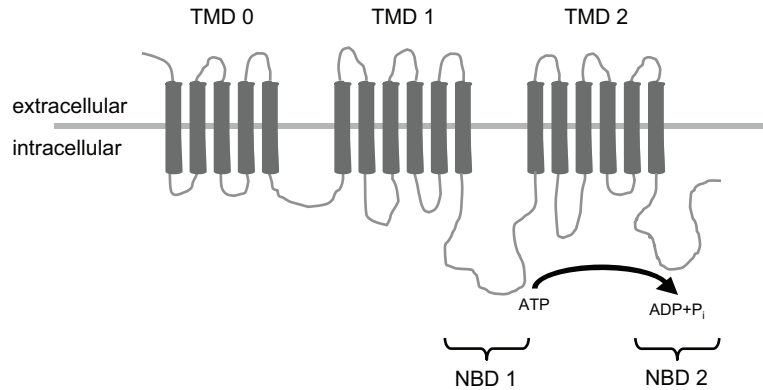


Figure 2. Diagram of an MRP transporter. The protein contains at least 2 transmembrane domains (TMD) and two nucleotide-binding domains (NBD). The NBDs participate in ATP hydrolysis and contain three conserved sequences, termed Walker A, Walker B and Walker C. Shown is a member of the ABCC/MRP class of transporters that contains an extra transmembrane domain (TMD 0).

The classes of ABC transporters also differ by substrate. The ABCC/MRP family transports several different drugs (anticancer agents, antibiotics, etc.), endogenous molecules, metalloids, pesticides and toxins, but the preferred substrates appear to be GSH conjugates of endogenous and exogenous compounds (Dallas *et al.* 2006, Sharom 2008). Functionally, ABC transporters are often thought of in the context of multidrug resistance and cancer chemotherapeutics. However their ability to transport toxins, pesticides, metals and GSH-conjugated metabolites gives them an important role in detoxification and removal of these compounds from the cell (Sharom 2008). GSH is required for the transport of certain substrates. MRP1 was shown to transport $As(GS)_3$ but not unconjugated arsenite and GST π was closely associated with this process, likely facilitating the conjugation of GSH to As and therefore increasing export (Leslie *et al.* 2004).

1. Expression, function and regulation of MRPs

MRPs are widely expressed in the body and their function has been characterized in several organs including liver, kidney, gut, pancreas, bladder, muscle, skin and brain (Borst *et al.* 2000). MRPs can be expressed on both sides of polarized epithelial cells, and the different isoforms may facilitate either the uptake or the excretion of their substrates (Dallas *et al.* 2006). For example, MRP1 is localized to the basolateral membrane in the liver and likely participates in uptake, but MRP2 is found primarily at

the apical membrane and transports its substrates into the bile for excretion (Borst *et al.* 2000, Dallas *et al.* 2006). In the blood brain barrier (BBB), MRP1, 4 and 5 are expressed on the apical membrane and may serve to prevent compounds from crossing into the central nervous system (CNS) (Zhang *et al.* 2004b). MRPs can be expressed in tumor tissues, but overexpression of another family of ABC transporters, the multiple drug resistance proteins (MDRs), is more highly implicated in chemoresistance to cancer therapeutics (Sharom 2008).

MRPs play a crucial role in uptake and excretion, especially in the organs that facilitate these processes (ex. liver, kidney, gut), however their role in the CNS is largely undefined (Dallas *et al.* 2006). Although much information has been gathered about the expression of MRPs in the CNS, there seems to be considerable variability between species and between studies. Dallas *et al.* 2006 has provided a comprehensive summary of expression studies and concludes that either mRNA or protein of all MRPs (1-9) are expressed in some part of the CNS in at least one species (Dallas *et al.* 2006). Hartz and Bauer also provide an in depth review of MRP expression in the CNS and at least some evidence is presented for expression of MRP1 – 8 in either brain capillary endothelial cells, glia or neurons (Hartz & Bauer 2011). Functional characterization of MRPs in the BBB suggests a role for inhibiting the accumulation of substances in the CNS, however information regarding the function of MRPs in glia and astrocytes is more limited, and almost nonexistent in neurons (Dallas *et al.* 2006). The exception is MRP1, which has been documented in brain cancer to be expressed and involved in chemoresistance (Dallas *et al.* 2006). The first study in non-diseased tissue to identify MRP1 expression (mRNA and protein) was performed in rat neurons (Falcão *et al.* 2007). They also show that the MRP1 is functional as inhibition by MK571 increases the toxicity of unconjugated bilirubin (Falcão *et al.* 2007).

As the expression of MRPs is quite varied between cell types, there are multiple mechanisms that contribute to their regulation. Nrf2 regulates the expression of phase II and phase III enzymes, including GSTs and MRPs. Several antioxidants and Nrf2 activators can increase the expression of MRPs (Kauffmann *et al.* 2002, Shinkai *et al.* 2006, Vollrath *et al.* 2006). The involvement of Nrf2 in MRP activation has also been shown genetically. In Nrf2 *-/-* mouse fibroblasts, the basal expression level of MRP1 is significantly decreased compared to WT, and the induction of MRP1 by diethyl maleate is also abolished (Hayashi *et al.* 2003). Like GSTs, ARE sequences can be found in the promoter region of MRP2 and other MRPs (Vollrath *et al.* 2006). A recent study has

identified two ARE sequences in the promoter of MRP1, and both play a role in Nrf2-mediated induction of the gene (Ji *et al.* 2013).

Other signaling pathways can also contribute to the regulation of MRP expression. JNK, c-Jun, MAPK, STAT3, NF-KB, TNF-R1 and AP-1 have been implicated in the regulation of ABC transporter function or expression (Miao & Ding 2003, Dreuw *et al.* 2005, Zhou *et al.* 2006, Ronaldson *et al.* 2008, Hartz & Bauer 2010). Drugs or endogenous compounds that serve as ligands for nuclear receptors can alter the expression of ABC transporter genes (van de Water *et al.* 2005, Ronaldson *et al.* 2008). In the absence of exogenous stimuli, inflammation and other pathological conditions can modulate MRP expression (van de Water *et al.* 2005).

2. MRPs and MeHg toxicity

MeHg has been shown to bind tightly with thiol groups, including those on the cysteine of GSH, and ABCC transporters have been previously associated with the export and detoxification of MeHg. The main focus has been on the family member ABCC2/MRP2 and its expression in the liver and kidneys. MRP2 was shown to participate in the transport of a NAC-MeHg complex to increase urinary excretion in rats (Madejczyk *et al.* 2007). Other chelating agents, DMPS and DMSA, also increase the excretion of MeHg through the kidneys and it was demonstrated that this effect is greatly reduced in MRP2 knockout rats (Zalups & Bridges 2009). DMPS/DMSA can also reduce the fetal burden of MeHg following maternal exposure, and the elimination of Hg from fetal tissue is dependent on MRP2 (Bridges *et al.* 2009, Bridges *et al.* 2012). More detailed mechanistic studies of membrane vesicles confirmed that MeHg-cysteine (Cys) conjugates are substrates of MRP2 (Bridges *et al.* 2011). This role of the transporter may be expected as the liver and kidneys are an important route of excretion for MeHg in the body (Clarkson & Magos 2006). However, there are few data concerning the role of ABCC transporters and MeHg in neurons.

In one study, SH-SY5Y cells were treated with MeHg and microarray analysis showed that ABCC3 was upregulated following the exposure (Toyama *et al.* 2011b), but it was not reported which other MRPs may be expressed in these cells. In mixed cortical neuron cultures (containing neurons and glia) GSH supplementation decreased MeHg cytotoxicity, but this effect required the activity of a transporter inhibited by MK571 (MRP1, MRP2, MRP4 or MRP5) (Reid *et al.* 2003, Łania-Pietrzak *et al.* 2005, Pratt *et al.*

2005, Yamazaki *et al.* 2005, Rush *et al.* 2012). This is consistent with the reported role of MRP1 in GSH export from astrocytes (Minich *et al.* 2006).

3. Role of MRPs in PD

While there are presently no reports of ABCC family transporters directly contributing to DA neuron degeneration or the development of PD in vertebrates, MRPs are found in the BBB, which functions to limit the accumulation of toxicants in the brain (Dallas *et al.* 2006). Neuroimaging studies have revealed that Pgp (an MDR) function in the BBB decreases with age (Bartels *et al.* 2009). The function of MRPs in the BBB may also decline with age. PD is an age-related disorder and decreased protection by the BBB may contribute to increasing neuronal sensitivity. Furthermore, GSH plays an important role in the regulation and reduction of elevated ROS levels in PD (Hirrlinger & Dringen 2005). In astroglial cells, extracellular DA can react with GSH in a superoxide-dependent manner to form DA adducts and deplete GSH, inhibiting the antioxidant potential (Hirrlinger *et al.* 2002). Also, DA auto-oxidation can produce H₂O₂, which causes the export of GSSG out of cells through MRP1 (Hirrlinger *et al.* 2002). The key role of ABCC family transporters in the export of GSH conjugates could have multiple implications for the cellular effects involved in PD.

Polymorphisms in the ABC transporter gene Pgp/MDR1/ABCB1 have been associated with the development of PD. In a study of Chinese PD patients, three single nucleotide polymorphisms (SNPs) in MDR1 were significantly associated with the risk for PD in males over age 60 (Lee *et al.* 2004). Pesticide exposure can also have an effect on the contribution of MDR1 to PD. PD patients exposed to pesticides with at least one mutated copy of MDR1 (C3435T) had a 5 fold increased risk of the disease compared to the non-exposed patients (Drożdżik *et al.* 2003). The correlation between MDR1 polymorphism, pesticide exposure and PD was also significant in a study of French patients, however it was the G2677(A,T) variant rather than C3435T (Dutheil *et al.* 2010). Although these results are for MDR1, not MRP1, there are several reported polymorphisms in ABCC family genes. Mutations lead to disease including Dubin-Johnson syndrome (ABCC2), Pseudoxanthoma elasticum (ABCC6), cystic fibrosis (ABCC7/CFTR) and persistent hyperinsulinemic hypoglycemia of infancy (ABCC8/SUR1) (Conseil *et al.* 2005). It is quite plausible that polymorphisms in these or other MRP genes could contribute to the sensitivity to MeHg and the toxicity resulting from its accumulation. Single mutations can have a dramatic effect on transporter

function or specificity and it may be possible for individuals to differ in their ability to detoxify MeHg. Identifying these populations could lead to better precautionary or preventative methods for reducing MeHg-induced toxicities.

E. *C. elegans*

1. Characteristics of the model system

The nematode *C. elegans* is a useful model for toxicological studies (Nass & Hamza 2007). *C. elegans* are small, inexpensive to maintain in the laboratory and have a short generation time and large number of clonal progeny. Each adult nematode is about 1 mm in length and thousands of animals can be grown in a petri dish filled with agar and seeded with a lawn of *E. coli* (Riddle 1988). *C. elegans* are primarily hermaphrodites and each animal can produce over 300 progeny via self-fertilization. Males occur at a low frequency but can be used for genetic crosses to generate strains with multiple mutations. The nematodes can grow from egg to egg-laying adult, transitioning through four larval stages (termed L1 – L4) in about 3.5 days at 20°C (Brenner 1974). The nematodes contain 959 somatic cells and have highly developed and organized reproductive, digestive, muscular and neuronal systems. Both the developmental lineage and the synaptic connectivity for each neuron of the 302 cell nervous system have been mapped (Hope 1999).

C. elegans are a genetically tractable model organism and possess several characteristics that allow for facile genetic manipulation (Nass & Settivari 2008). The genome has been fully sequenced and annotated. A large collection of mutant strains is available to the *C. elegans* community, and mutations can be identified and mapped in as little as a week. RNAi can be utilized to knock down gene expression if a mutant is unavailable and the RNAi techniques are convenient for large-scale genetic screens (Kamath & Ahringer 2003). The nematodes are transparent allowing for the visualization of fluorescent reporters in living animals, and animals expressing transcriptional or translational fusion reporters can be generated within a few days (Boulin *et al.* 2006).

The genome of *C. elegans* contains nearly the same number of genes as the human genome and numerous proteins, cellular processes and molecular pathways are conserved between the nematode and humans (Peterson *et al.* 2008). Of particular importance to this project is the conservation of stress response pathways and the nervous system. *C. elegans* and humans share nearly all molecular components involved in neurotransmission including neurotransmitter biosynthetic enzymes, release

mechanisms, ionotropic and G-protein coupled receptors, ion channels (except voltage gated Na⁺ channels) and second messenger systems (Bargmann 1998). *C. elegans* have both phase I and phase II detoxification enzymes including cytochrome P450s, short-chain dehydrogenases, UDP-glucuronosyl or glycosyl transferases, and GSTs (Lindblom & Dodd 2006). Induced expression of these and other stress response genes and proteins have been demonstrated in *C. elegans* in several studies, including those of cadmium (Cd) (Cui *et al.* 2007), di(2-ethylhexyl)phthalate (Roh *et al.* 2007) and oxidative stress (Leiers *et al.* 2003). Further facilitating research is the wide array of resources available to the *C. elegans* community. Wormbase.org is an integrated database that provides gene information including sequence, expression profiles, function and a collection of gene specific literature. The *Caenorhabditis* Genetics Center (CGC) coordinates the sharing of nematode strains among laboratories. There are also databases for RNAi screen results, microarray gene expression data, protein networks and nematode anatomy, among others (Antoshechkin & Sternberg 2007).

2. Use of *C. elegans* in toxicology

As the development, morphology, behaviors and lifespan of *C. elegans* are consistent and well characterized, changes in any of these traits may be used to indicate and monitor toxicity, as well as the response to exogenous compounds or stressors (Peterson *et al.* 2008). Common endpoints of toxicological studies are lethality, reproductive capacity, growth rate and motility (Leung *et al.* 2008). Animal viability has been used to monitor the toxicity of ethanol and several metals, including Hg and Cd (Tatara *et al.* 1997, Traunspurger *et al.* 1997, Dhawan *et al.* 1999). Decreased brood size and slow growth have been observed with exposure to ethanol, Cd, sodium arsenite and sodium fluoride (Traunspurger *et al.* 1997, Dhawan *et al.* 1999, Wang *et al.* 2007, Li *et al.* 2012). These parameters have also been utilized for high-throughput screening of chemicals such as pesticides and metals, exposing at L1 stage to monitor growth and L4 stage to measure reproductive capacity, with automated detection by the COPAS Biosort (Boyd *et al.* 2010). Morphological changes during development can also be characterized, and ethanol, a human teratogen, caused physical defects in *C. elegans* larvae following embryonic exposure (Davis *et al.* 2008). Behaviors can be used to indicate toxicity and possible neurological damage. Movements such as head thrashing and body bends were decreased by sodium fluoride exposure (Li *et al.* 2012). Computer monitored locomotion assays have been used to characterize toxicity and lethal

concentration 50s (LC50s) for metals and organophosphate pesticides (Dhawan *et al.* 2000, Cole *et al.* 2004). Neurotoxicity and neurodegeneration can also be observed by the morphology of green fluorescent protein (GFP)-expressing neurons. Alterations in DA or GABA neurons have been reported following exposure to metals including Mn, Al, Hg, Pb, Cu, and Cd (Du & Wang 2009, Settivari *et al.* 2009, VanDuyn *et al.* 2013).

Gene expression changes can also be observed in the transparent nematode using reporter genes expressed behind stress-inducible promoters (Link *et al.* 1999). For example, the promoter from an HSP gene fused to GFP results in increased fluorescence in the presence of heat, superoxide-generating quinones and the human B-amyloid protein (Link *et al.* 1999). These reporter strains allow for convenient visualization of gene expression in intact living animals and have even been proposed for use as biosensors (Hasegawa *et al.* 2008). Gene expression profiles measured by microarray or real time polymerase chain reaction (RT-PCR) may also be used to indicate toxicity as well as characterize the physiological effects of a toxicant (Swain *et al.* 2010). Biochemical assays including GSH level, ROS level, mitochondrial membrane potential and oxygen consumption have also been successfully applied in *C. elegans* studies of Mn, Al, sodium arsenite and sodium fluoride (Settivari *et al.* 2009, Li *et al.* 2012, VanDuyn *et al.* 2013).

3. *C. elegans* DA system and PD model

Although the *C. elegans* nervous system is fairly simple in terms of the relatively low number of cells and synapses (302 and ~5000, respectively in the hermaphrodite), the nematode contains nearly all the neurotransmitters and synaptic components present in humans and mammals (White *et al.* 1986, Bargmann 1998). DA is detectable by HPLC, and formaldehyde-induced fluorescence (FIF) indicates the presence of the neurotransmitter in 8 cells in hermaphrodites, and an additional 6 cells in the tail of the male (Sulston *et al.* 1975, Nass & Blakely 2003). To identify genes involved in DA synthesis and regulation, mutants with reduced FIF staining were identified and named *cat-1* to *cat-5* (Sulston *et al.* 1975). *cat-1* was later identified as the *C. elegans* homolog of the vesicular monoamine transporter (VMAT) (Duerr *et al.* 1999). *cat-1* mutants do not exhibit the basal slowing response on bacteria, as seen in animals that have had their DA neurons laser ablated (Duerr *et al.* 1999, Sawin *et al.* 2000). *cat-2* encodes TH, and is expressed in the cells identified as dopaminergic by FIF (Lints & Emmons 1999). These mutants are also defective in the basal slowing response (Sawin *et al.* 2000).

Other enzymes necessary for the synthesis of DA also have homologues in the nematode; *cat-4* encodes a GTP cyclohydrolase and *bas-1* encodes an aromatic amino acid decarboxylase. Therefore, *C. elegans* likely contain all the proteins necessary for the synthesis and packaging of DA.

The mechanism of DA re-uptake is also conserved between the nematode and humans. The *C. elegans* DAT *dat-1* was identified by homology of the predicted sequence, and the protein transports DA and is inhibited by DAT antagonists *in vitro* and *in vivo* (Jayanthi *et al.* 1998, Nass *et al.* 2002). The similarity between the DA neurons in nematodes and humans has allowed for the establishment of an *in vivo* model for DA neuron degeneration in which the DA neurons can be observed in a living animal. To visualize the DA neurons in a living animal, GFP was expressed behind the *dat-1* promoter, which resulted in a strong fluorescent signal specifically in these cells (Nass *et al.* 2001, Nass *et al.* 2002). Importantly, exposure to toxicants that cause DA neuron cell death in mammals also causes DA neurodegeneration in *C. elegans*. 6-OHDA is a neurotoxicant that primarily enters cells through DAT, causing selective degeneration of the DA neurons (Sachs & Jonsson 1975). This effect is also observed in *C. elegans*, as exposure to 6-OHDA results in a loss of GFP in the DA neurons (Nass *et al.* 2002). Other PD-associated toxicants are also effective in killing the DA neurons in the nematode, including MPP+ and rotenone (Braungart *et al.* 2004, Saha *et al.* 2009). Furthermore, *C. elegans* can be used to model the mechanisms of familial PD as overexpression of human α -synuclein or LRRK2 causes DA neuron degeneration (Lakso *et al.* 2003, Yao *et al.* 2010).

Exposure to heavy metals is believed to be a contributing factor to the development of PD (Caudle *et al.* 2012). A *C. elegans* model of manganese has been developed that supports this claim, as well as allows characterization of the molecular mechanisms of neurotoxicity induced by metals (Settivari *et al.* 2009). In *C. elegans*, Mn exposure increases ROS and GSH, and causes alterations in mitochondrial function. The divalent metal transporter SMF-1 (human DMT-1) contributes to the neurotoxicity induced by Mn, and SKN-1 and GST-1 inhibit DA neuron cytotoxicity (Settivari *et al.* 2009, Settivari *et al.* 2013). Al^{3+} is another metal associated with the development of PD (Zayed 1990). In *C. elegans*, Al^{3+} induces DA neuron degeneration and this effect is dependent on SMF-3, a homologue of the human divalent metal transporter (VanDuyn *et al.* 2013).

4. SKN-1

SKN-1 is the *C. elegans* homolog of the transcription factor Nrf2 and has several functions in *C. elegans*. The *skn-1* gene was originally identified to code for a maternally-expressed gene product that is necessary for normal cell fate determination in the early embryo, such that offspring of *skn-1* mutants fail to develop a pharynx or intestine (Bowerman *et al.* 1992). These structures originate from the EMS cell of the blastomere, and the fate of the EMS cell is specified by GATA factors, which are direct targets of SKN-1 (Bowerman *et al.* 1992, Maduro *et al.* 2001). Later studies revealed that SKN-1 binds DNA as a monomer to act as a transcription factor and likely functions in the same way as human Nrf2 (Walker *et al.* 2000).

In larval and adult stages, SKN-1 is expressed in the intestine and the two ASI (chemosensory) neurons (An & Blackwell 2003). Similar to Nrf2, a functional SKN-1::GFP fusion protein localizes to intestinal nuclei after external stress. Furthermore, the SKN-1 dependent activation of antioxidant genes has also been shown in *C. elegans*. Acrylamide treatment causes an upregulation of *gst-4* that is not present after RNAi knockdown of SKN-1 (Hasegawa *et al.* 2008). Heat and paraquat induce expression of the *C. elegans* glutamylcysteine synthetase (*gcs-1*) except in a *skn-1(zu67)* background, where SKN-1 was not functional, and deletion of the SKN-1 binding site in the promoter of *gcs-1* also reduces this expression (An & Blackwell 2003). Lack of induction of these genes plays a significant role in the animals as SKN-1 mutants are both sensitive to oxidative stress (paraquat) and exhibit a decreased lifespan (An & Blackwell 2003).

As a transcription factor, SKN-1 likely functions primarily in the nucleus. A GFP reporter strain was used to demonstrate that upon stress, the SKN-1 protein translocates from the cytoplasm to the nucleus, where it binds to DNA at AREs (An & Blackwell 2003). The consensus sequence for the ARE in *C. elegans* has been identified as WWTRTCAT, where R = G or A and W = T or A. This sequence (termed canonical) should be randomly found about every 2000 base pairs (bp), but sequence analysis has shown that several phase II detoxification enzymes have two or more SKN-1 binding sites in their promoter region (5' of the ATG start codon) (An & Blackwell 2003). Further bioinformatic analysis revealed a slightly more restrictive sequence than the canonical one (Oliveira *et al.* 2009). Microarray was used to identify lists of genes upregulated and downregulated by SKN-1, both in the presence and absence of stress. Weeder Web analysis for overrepresented motifs in the regions 2 kb upstream of genes regulated by

SKN-1 revealed a consensus sequence slightly different than the canonical one, as well as a novel motif present in SKN-1 downregulated genes (Oliveira *et al.* 2009).

SKN-1 is located in the cytoplasm under normal conditions in intestinal cells (An & Blackwell 2003). Cytoplasmic localization of SKN-1 is maintained by WDR-23, a functional homolog of Keap1. In mammals, Keap1 is a ubiquitin ligase that ubiquitinates Nrf2, targeting it for degradation in the proteasome. Loss of *wdr-23* (*xrep-1*) results in constitutive expression of GST-4, suggesting constitutive activation of SKN-1 (Hasegawa & Miwa 2010). There is evidence that MAPK pathways may also participate in the activation of Nrf2 (Owuor & Kong 2002). Phosphorylation of Nrf2 by PKC releases it from being targeted for proteasomal degradation and increases nuclear localization and target gene expression (Bloom & Jaiswal 2003). In *C. elegans*, SKN-1 must also be phosphorylated for nuclear translocation, by *pmk-1*, *nekl-2*, *pdhk-2*, *mkk-4* and *ikke-1* (Inoue *et al.* 2005, Kell *et al.* 2007). The SEK-1/PMK-1 pathway is activated by oxidative stress, as indicated by phosphorylation of PMK-1 following treatment with As, paraquat and tert-butyl hydroperoxide (t-BOOH) (Inoue *et al.* 2005). Phosphorylation can also be a negative regulator of Nrf2/SKN-1. GSK-3 (glycogen synthase kinase-3) has widespread cellular targets and effects, from growth to apoptosis, and is implicated in disorders from diabetes to AD (Jope & Johnson 2004). Inactivation of GSK-3B leads to the nuclear localization of Nrf2 (Rojo *et al.* 2008a, Rojo *et al.* 2008b).

A functional UPS is also required for proper SKN-1 regulation in *C. elegans* as RNAi knockdown of proteasome subunits caused nuclear localization of SKN-1 (Kahn *et al.* 2008). The authors suggest that this is a result of the activation of the SKN-1 stress response, for example damaged proteins may accumulate and activate SKN-1, or the dysfunctional proteasome itself could induce a signaling pathway leading to SKN-1 activation. However, given the mechanism of Nrf2 regulation by Keap1 in mammals, it seems likely that a decrease in proteasome or ubiquitination function could inhibit the cytoplasmic degradation of SKN-1 and lead to its accumulation in the nucleus. The effects on SKN-1 nuclear localization were different for different subunits or proteasome genes and there was often a disconnect between *skn-1* activation and *gst-4* expression, suggesting that there are other regulatory mechanisms at play (Kahn *et al.* 2008). Translation initiation factors (TIFs) also appear to play a role in SKN-1 regulation as SKN-1 activity is increased following RNAi of the TIFs (Wang *et al.* 2010).

5. GSTs

A comprehensive analysis of the *C. elegans* databases, including literature and genomic BLAST searches, revealed 48 genes encoding GSTs including members of the Alpha, Pi and Sigma classes (Leiers *et al.* 2003, Lindblom & Dodd 2006). Several of the *C. elegans* GSTs are of the sigma class, which are mainly found in invertebrates, but the sigma class also includes the hematopoietic prostaglandin D synthase in mammals (Kanaoka *et al.* 1997). The role of GSTs in conjugation is the most widely recognized, but they can also participate in cellular signaling, metabolism, catabolism and even apoptosis, explaining the presence of multiple genes (van Rossum *et al.* 2001). The proteins may differ in function, and they also have different expression patterns (Hasegawa *et al.* 2008). As in vertebrates, *C. elegans* GSTs participate in stress response. RNAi knockdown of multiple GSTs sensitizes and overexpression of *gst-10* provides resistance to the oxidative stress inducer 4-hydroxynonenal (4-HNE) (Ayyadevara *et al.* 2005, Ayyadevara *et al.* 2007). Overexpression of *gst-4* increases resistance to paraquat and juglone (Leiers *et al.* 2003). GST mRNA expression is induced by stress caused by exposure to acrylamide and allyl isothiocyanate, among other compounds, and this can be regulated by SKN-1 (Hasegawa *et al.* 2008, Hasegawa & Miwa 2010).

6. HSPs

C. elegans contain several HSPs that are highly conserved with vertebrates. The *C. elegans* HSP genes include the small HSPs (*hsp-16.1*, *16.2*, *16.41*, *16.48*) and up to 9 members of the HSP70 gene family (Candido *et al.* 1989, Heschl & Baillie 1990). The small HSPs are homologous to the mammalian protein alphaB-crystallin, which is expressed in multiple tissues (Parcellier *et al.* 2005, Mineva *et al.* 2008). The *C. elegans* HSPs have been shown to regulate protein synthesis and degradation and participate in stress response (Prahlad & Morimoto 2009). GFP expression driven by the *hsp-16.2* reporter can be induced by heat, the oxidative stressor juglone and expression of the human β -amyloid peptide and observed in the living nematode (Link *et al.* 1999). Metals, including Cd, Al, Mn, Cu and Hg, can also increase the expression of HSPs (Guyen & de Pomerai 1995, Guven *et al.* 1995, Dennis *et al.* 1997).

7. MRPs

The first MRPs described in *C. elegans* were MRP-1 to 4 and these were identified based on sequence homology to the human protein MRP1 (Broeks *et al.* 1996). Further sequence analysis has revealed that *C. elegans* contains 9 MRPs (*mrp-1* to *8* and *cft-1*) and the proteins were classified based mostly on the position of their nucleotide binding domains (Sheps *et al.* 2004). An *mrp-1* mutant strain was generated and found to be sensitive to Cd and arsenite, compared to WT (Broeks *et al.* 1996). Both Cd and arsenite form GSH complexes and are substrates for human MRP1. *C. elegans* MRPs can transport more than metals. Ivermectin, an anthelmintic drug, is likely a MRP-1 substrate. An ivermectin resistant strain of nematodes was generated and found to have increased expression of several ABC transporters (Yan *et al.* 2012). Several parameters of viability were assessed following knockdown of individual transporters, and decreased MRP-1 seemed to cause the greatest sensitivity to ivermectin (Yan *et al.* 2012). Some endogenous molecules may also be substrates for MRP-1. The insulin-signaling pathway regulates nematode growth and entry into the dauer phase, and this regulation is disrupted in *mrp-1* mutants. Therefore, MRP-1 likely transports a substance or molecule critical for the insulin-signaling pathway (Yabe *et al.* 2005). The similarity between human and *C. elegans* MRPs extends beyond sequence and the types of substrates. Human MRP1 can rescue the dauer regulatory defect in *mrp-1* mutants, suggesting an equivalent function of the two proteins (Yabe *et al.* 2005). Other ABC transporters can also contribute to heavy metal transport in *C. elegans* including *pgp-1* and *hmt-1* (Broeks *et al.* 1996, Vatamaniuk *et al.* 2005).

8. RNAi and RNAi Screens

RNA interference (RNAi) is a method of reducing the levels of endogenous mRNA by introducing exogenous double stranded RNA (dsRNA) (siRNA – small/short interfering or silencing RNAs) with a corresponding sequence. dsRNA can be introduced into the nematode by three methods: injection, soaking or feeding. In *C. elegans*, the RNAi effect likely involves more than anti-sense binding and degradation of the endogenous RNA as the interference effect can spread from cell to cell throughout most of the body of the nematode and also pass from one generation to the next, such that progeny of an injected mother can show the phenotype associated with gene knockdown (Fire *et al.* 1998). Early observations indicated that although RNAi was effective in most cells, neurons were quite resistant to the effects (Kamath *et al.* 2001, Timmons *et al.* 2001).

To overcome this resistance, researchers have employed the use of a nematode strain that has a mutation in the *rrf-3* gene (Simmer *et al.* 2003). RRF-3 is a RNA-directed RNA polymerase that is involved in the processing of siRNAs and it has been shown that *rrf-3* mutants are more sensitive to RNAi than WT nematodes, especially in the neurons (Simmer *et al.* 2002). Further characterization using strains that express GFP in specific neuronal types showed that RNAi is enhanced in the DA and GABA neurons in the *rrf-3* mutants (Asikainen *et al.* 2005). Another mutant, *eri-1*, is sensitive to RNAi as the gene encodes an siRNA-degrading RNase (Kennedy *et al.* 2004).

For RNAi by feeding, consumption of bacteria expressing dsRNA results in a decrease in the complementary mRNA in the nematode (Timmons *et al.* 2001). The bacterial feeding strain has been optimized for maximum efficiency of this procedure. The dsRNA sequence is flanked by T7 promoters in a vector referred to as L4440 (Fire *et al.* 1998). The *E. coli* genome encodes the T7 polymerase downstream of a lac operon, which normally represses the expression of the polymerase. When isopropyl β -D-1-thiogalactopyranoside (IPTG) is added, the repression of the lac operon is released and T7 is expressed, allowing transcription of the dsRNA sequence. A lambda prophage DE3 was introduced that allows for IPTG-inducible production of T7 polymerase (Fire *et al.* 1998, Timmons *et al.* 2001). Thus, dsRNA is not produced in the bacteria until IPTG is present. Bacteria express an enzyme that degrades dsRNA (RNaseIII), which was found to limit the effectiveness of feeding RNAi, therefore the *E. coli* strain HT115 was utilized as it has a mutation in the *rnc* gene and does not express RNaseIII (Timmons *et al.* 2001). Antibiotic selection can be used to maintain the HT115 *rnc*- strain (tetracycline) and cells with the dsRNA plasmid (ampicillin) (Timmons *et al.* 2001).

Libraries of feeding RNAi bacterial clones have been generated to facilitate RNAi screens (Kamath & Ahringer 2003, Rual *et al.* 2004). The first RNAi library to be constructed (the Ahringer library) was based on the GenePairs primers, which are designed to amplify polymerase chain reaction (PCR) products from all 19,000 genes predicted by the initial sequencing of the *C. elegans* genome. The PCR products were cloned into the L4440 vector and transformed into HT115(DE3) *E. coli* as described above (Kamath & Ahringer 2003). The final library was prepared as glycerol stocks of each bacterial strain (16,757 total) contained in 52 384-well plates (Kamath & Ahringer 2003). A screen was performed using the library and phenotypes such as sterility, lethality and slow growth were observed for approximately 10% of the strains (1,722 clones) (Kamath *et al.* 2003).

A second RNAi feeding library, the ORFeome-RNAi v1.1 Library (Open Biosystems, OBS), was generated that offers several advantages over the Ahringer library (Rual *et al.* 2004). First, the library sequences are obtained from the *C. elegans* ORFeome, which is a collection of the open reading frames (ORFs), or cDNAs, from the genome. The fragments include the entire ORF, which can improve specificity over the randomly placed primer pairs of the Ahringer library. Also, the lack of introns increases the sequence that can be included in the siRNAs, further facilitating binding. These traits may enhance the effectiveness of the RNAi, but the real advantage is in the vector construction and the versatility of the library. The *C. elegans* ORFeome was constructed from all predicted ORFs in the genome, 11,942 in Version 1.1. Researchers utilized the Gateway cloning system, which allows for recombinational cloning and easy transfer of the ORF between different types of vectors for various applications. The final RNAi library contains 10,953 clones, 1,736 of which were not present in the Ahringer library (Rual *et al.* 2004). An initial screen with this library revealed 1,066 bacterial strains that produced a phenotype different than WT, which is approximately 10% and similar to the results observed in the screen using the Ahringer library (Rual *et al.* 2004).

RNAi screens are designed to identify genes for which decreased expression results in a particular phenotype. Genome wide screens have been utilized to identify genes involved in development, lifespan, fat content and osmoregulation (Ashrafi *et al.* 2003, Hamilton *et al.* 2005, Lamitina *et al.* 2006). In addition to the study of normal physiological processes, the use of RNAi screens for toxicological studies in *C. elegans* has proven to be successful (Cui *et al.* 2007, Kim & Sun 2007). After identifying 94 genes involved in Cd toxicity by microarray, a low throughput RNAi screen of those genes resulted in 50 genes that when knocked down increased the nematodes' sensitivity to Cd (Cui *et al.* 2007). In a more unbiased study, RNAi knock-down of the available genes on chromosomes III and IV (about 6000) revealed 608 paraquat-resistant clones (Kim & Sun 2007). These studies suggest that a genome wide RNAi screen for clones showing differential sensitivity to MeHg may identify novel genes and pathways involved in MeHg-associated toxicity.

9. Limitations of *C. elegans* as a genetic model system

All model systems have limitations that should be acknowledged when applying experimental results to the study of human disease. As *C. elegans* are in contact with numerous compounds and chemicals in their natural soil habitat, they have an

exoskeleton called the cuticle that guards them from the environment. This covering is comprised of collagen and is largely impermeant (Dengg & van Meel 2004). Therefore, some drugs, toxicants or other compounds may need to be used at higher concentrations to facilitate entry into the animal (Nass & Settivari 2008). Despite high exposure conditions, once inside the cells of the nematode, many compounds have similar binding affinities and kinetics as would be observed in other organisms (Nass & Settivari 2008). If solubility of the chemical at high concentrations is an issue, nematodes can tolerate up to 2% dimethyl sulfoxide (DMSO) and several mutants exist that have increased cuticle permeability (Dengg & van Meel 2004, Page & Johnstone 2007).

Although *C. elegans* contain most of the neuronal types found in mammals, the number of neurons and cell-cell interactions is greatly reduced (Bargmann 1998). The proximity of certain cells to each other and the connections that neurons make can have a significant impact on neuronal function and pathology that may not be fully represented in *C. elegans* (Nass & Settivari 2008). Genetically, there is high homology between human and *C. elegans* genes, however the abundance of proteins that affect toxicity or pathology may be different (Nass & Settivari 2008). For example, the stress response proteins (GSTs, CYPs, HSPs) in *C. elegans* may be expressed at higher levels than in mammals due to their exposure to such a variety of compounds in their natural environment (Lant & Storey 2010).

F. Hypothesis and key questions

Despite years of study, the molecular basis of MeHg toxicity remains largely unknown. The environmental contaminant continues to pose a significant risk to human health. Of particular concern is the contribution of MeHg exposure to PD. The increasing lifespan of the population increases the number of individuals at risk for developing PD and other age-related neurodegenerative disorders. The role of MeHg in the pathology of these disorders has not been elucidated. A significant hindrance to studies of MeHg toxicity in vertebrates is the complexity of the nervous system and the lack of convenient genetic techniques. Cell culture has provided some insight, however it does not always recapitulate in vivo conditions. I propose the use of *C. elegans* to investigate the genes and pathways involved in MeHg-induced toxicity and DA neuron pathology.

1. What endpoints of MeHg-associated toxicity can be measured in *C. elegans*?

To facilitate the use of *C. elegans* as a model to study the genetics of MeHg-associated toxicity, it is important to characterize the effects of MeHg exposure in the nematode and identify assays that may be utilized to indicate toxic endpoints. I will study animal viability, reproduction and development, as well as ROS and stress-response gene expression following MeHg exposure.

2. What are the genes and molecular pathways involved in MeHg toxicity?

I will utilize microarray analysis of gene expression and RT-PCR to determine how mRNA levels are altered following MeHg toxicity. Furthermore, I will incorporate a reverse genetic screen to identify genes and pathways involved in MeHg toxicity. The expression of over 90% of the genes in the *C. elegans* genome will be reduced individually and then I will determine how the reduction of each gene affects viability in the presence of MeHg.

3. Does MeHg decrease DA neuron viability in *C. elegans*?

I will utilize a GFP reporter strain to examine the morphology of the DA neurons following MeHg exposure in live animals. The contribution of genes identified to be involved in MeHg toxicity to DA neuron vulnerability will also be examined.

II. Methods

A. *C. elegans* strains and maintenance.

Nematode growth media (NGM) plates with a lawn of OP50 bacteria were used for standard maintenance (Brenner 1974, Hope 1999). 8P plates (an enriched media) with a lawn of NA22 bacteria were used to grow large amounts of nematodes for synchronization and also for the early MeHg experiments. Nematodes were cultured in a 20°C incubator during growth and experiments, unless noted otherwise. The strains used in all experiments are summarized in **Table 1**.

Strain	Genotype	Source	Description
N2	wild type	CGC	wild type
BY250	$P_{dat-1}::GFP$	Injection into N2	GFP in DA neurons
NL2099	<i>rrf-3(pk1426)</i>	CGC	RNAi sensitive
OD70	<i>unc-119(ed3)III</i> ; <i>ltIs44</i> [<i>pie-1p-mCherry::PH</i> (PLC1delta)+ <i>unc119</i> (+)]	CGC	mCherry on plasma membrane of embryonic cells
TJ356	zIs356 IV	CGC	DAF-16::GFP reporter
RJ934	$P_{dat-1}::GFP$; <i>smf-3(ok1035)</i>	Cross BY250 x RB1074	GFP in DA neurons, <i>smf-3</i> mutant
RJ928	$P_{dat-1}::GFP$; <i>rrf-3(pk1426)</i>	Cross BY250 x NL2099	GFP in DA neurons, RNAi sensitive
RJ1040	$P_{unc-47}::GFP$; <i>rrf-3(pk1426)</i>	Cross EG1285 x NL2099	GFP in GABA neurons, RNAi sensitive
RJ1046		Cross DR2022 x NL2099	GFP in ASI neurons, RNAi sensitive
RJ1072	$P_{eat-4}::GFP$; <i>rrf-3(pk1426)</i>	Cross DA1240 x NL2099	GFP in glutamatergic neurons, RNAi sensitive
RJ1074	$P_{unc-17}::GFP$; <i>rrf-3(pk1426)</i>	Cross LX929 x NL2099	GFP in cholinergic neurons, RNAi sensitive
RJ1082	$P_{tph-1}::GFP$; <i>rol-6(su1006)</i> ; <i>rrf-3(pk1426)</i>	Cross GR1366 x NL2099	GFP in serotonergic neurons, RNAi sensitive
RJ1089	$P_{mrp-7}::CFP$; $P_{dat-1}::YFP$	Injection into N2	YFP in DA neurons, CFP behind MRP-7 promoter

Table 1. Summary of *C. elegans* strains with genotype and phenotypic description. Source column shows from where the strain was acquired or how it was generated.

B. Synchronization

To obtain an age-synchronized population of nematodes, gravid adults (full of embryos) were collected in a 15 ml tube and washed. 5 ml of a sodium hypochlorite solution (1.25 ml 10 M NaOH, 5 ml Clorox bleach, 18.75 ml H₂O) was added to the pellet. Animals were mixed gently and monitored for approximately 4 – 7 minutes until the majority of the adults had broken open and released their eggs. M9 buffer (22 mM KH₂PO₄, 22 mM Na₂HPO₄, 85 mM NaCl, 1 mM MgSO₄) was added to fill the tube and the eggs were pelleted by centrifugation at 2000 RPM for 2 minutes. The synchronization solution was discarded and the eggs were washed three additional times with M9. The tube was filled with M9 and allowed to incubate for 18 hours while mixing on a Nutator at room temperature (Nass *et al.* 2002, Nass & Hamza 2007). During this time, the eggs hatch and arrest at the L1 stage due to the lack of food.

C. Genetic crosses

Genetic crosses were performed to generate strains containing multiple mutations or transgenes. Transgenic strains expressing GFP in each neuronal type were obtained from the CGC. Each strain was crossed with the RNAi sensitive strain NL2099 [*rrf-3(pk1426)*] so the morphology of each type of neuron could be analyzed following RNAi and MeHg exposure. Males from the GFP strain were mated with NL2099 hermaphrodites and progeny (F1) resulting from mating rather than self-fertilization were selected by the expression of GFP. F1 nematodes were allowed to self-fertilize, and F2 progeny were isolated onto individual plates. Animals from plates with 100% GFP-expressing F3 progeny were picked for single worm PCR to determine if the *rrf-3* mutation was present. Lines with 100% GFP and 100% homozygous *rrf-3* mutants were isolated and used in further experiments.

D. RNAi

RNAi by feeding was carried out on NGM plates containing 1 mM IPTG and 100 µg/ml ampicillin largely as described (Ahringer 2006). The bacterial strain used for feeding RNAi is HT115 (DE3), an RNase III-deficient *E. coli* strain carrying the L4440 vector (Fire Lab Vector Kit). For control (no gene knockdown) experiments, the empty L4440 vector was used. To achieve knockdown of a specific gene, the L4440 vector contained a sequence complementary to the target gene. These gene-specific clones are available in the ORFeome-RNAi v1.1 Library (Open Biosystems/Thermo Fisher

Scientific, Waltham, MA) and the RNAi feeding library (Source BioScience Life Sciences, Nottingham, UK). Cultures of RNAi bacteria were streaked from the frozen glycerol stocks onto (Luria broth) LB plates with 100 µg/ml ampicillin and grown overnight at 37°C. For liquid cultures, LB broth with 50 µg/ml ampicillin was inoculated with an individual colony from the LB plate and grown for 14 – 16 hours at 37°C. Plates were spotted with the overnight culture and allowed to dry for at least 24 hours before use.

The RNAi sensitive strains NL2099 or RJ928 were used for all RNAi experiments. Second-generation RNAi nematodes were used for experiments when possible: animals (P0) were fed RNAi bacteria from L1 to adult stage, then their progeny (F1) were also fed RNAi bacteria until the desired stage was reached and the experiment was carried out. For *skn-1*, knockdown of the gene produces an embryonic lethal phenotype, such that the embryos are produced but fail to hatch (Bowerman *et al.* 1992). Therefore, first generation nematodes were used for all *skn-1* RNAi experiments, and the presence of unhatched eggs was an indication of gene knockdown.

E. Toxicant exposures

Methylmercury chloride (CH₃HgCl, 442534-5G-A, Sigma-Aldrich, St. Louis, MO) was prepared as a 1 mM solution in H₂O. The powder was carefully weighed into a 50 ml conical tube, the appropriate amount of H₂O was added and the tube was mixed on a Nutator 1 – 2 hours in the hood to dissolve. The tubes containing MeHg were sealed with parafilm, covered in foil and stored at 4°C for up to 10 days. For all assays except DA neuron degeneration, MeHg was added to the agar before it was poured into the plates. Plates containing 10 µM MeHg required 10 ml 1 mM MeHg in 1 L of agar, so MeHg makes up 1% of the total volume. Up to this concentration, no H₂O was removed from the agar preparation to account for the additional volume. However, at concentrations above 10 µM (1%), the volume of H₂O used in the preparation of the agar was adjusted to account for the addition of the MeHg solution. For DA neuron degeneration exposures, MeHg was added to the top of plates that were already spread with bacteria and completely dry. The final concentration of MeHg was determined using the volume of agar added to the plate as the final volume. For example, to prepare large plates with 1 µM MeHg, 25 µl of 1 mM MeHg (1 mM x volume = 1 µM x 25 ml) and 725 µl H₂O were combined as 750 µl is the amount that covers a large plate evenly. The MeHg-H₂O mixture was pipetted onto the plate, the plate was tilted to spread out the liquid and allowed to dry. Small (35 mm) petri dishes (containing 3 ml

agar) were used for viability assays. DA neuron degeneration exposures were carried out on medium (60 mm) or large (90 mm) petri dishes (no difference was observed based on plate size). For experiments requiring a large amount of nematodes (RT-PCR, Western blots, ROS, etc.) large petri dishes containing MeHg were used.

Selenium was used in the form of sodium selenite, Na_2SeO_3 (214485, Sigma-Aldrich, St. Louis, MO). A 30 mM solution was prepared in H_2O , filter sterilized with a 2 μm filter and stored at 4°C. Selenium was added on top of the agar in plates that had been previously poured, before seeding with bacteria. Live bacterial cultures spotted onto plates containing selenium turned a red-orange color, with higher [Se] leading to a deeper color. This effect only occurred when the bacteria was alive. Dead bacterial cultures were prepared by first growing cultures, then either autoclaving or microwaving the culture. When the heat-killed culture was spotted onto plates with selenium, there was no color change and the inhibitory effects on MeHg-induced lethality were at least partially, and sometimes fully, impaired.

The bacteria spotted onto MeHg plates does not grow or thicken as it does on control plates. To overcome this, concentrated cultures were prepared to have a larger number of bacterial cells in a smaller volume of liquid. Overnight cultures were centrifuged at 4000 RPM for 10 minutes (in either 15 or 50 ml conical tubes) to pellet the cells. The LB broth was removed, leaving 10% of the original volume for the NA22 culture for 8P plates. For example, 50 ml was used to resuspend the pellets resulting from 500 ml of culture. For later RNAi experiments, and the third round of the screen, 5 ml original culture was concentrated to 1.25 ml final volume.

F. Viability assay

For measurements of whole animal viability, a synchronized population of nematodes was used. Animals were grown to the desired stage on plates without MeHg. Then, animals were transferred to plates containing MeHg either by picking or washing the animals into a tube and pipetting the desired amount onto the new plate. Nematodes were then incubated for the desired amount of time, usually 24 or 48 hours, at 20°C. Viability was determined by manual counting of the number of live animals and the total number of animals on the plate. Nematodes were considered alive if they moved in response to light touch on the nose with a metal pick (Strange 2006). To ensure that the nematodes considered dead were not just paralyzed, “dead” animals were carefully picked onto a fresh plate (without MeHg). After 24 hours, the animals had not moved

from the initial location, confirming that this was an effective method for determining if animals are dead or alive. At least 20 nematodes were counted per [MeHg] and the experiment was repeated at least three times. Results are reported as mean \pm standard error of the mean (SEM).

G. Pharyngeal pumping assay

Synchronized L4 stage nematodes were exposed for 24 hours on 8P plates containing MeHg at 20°C. Animals were imaged on the exposure plates, using StreamPix (NorPix Inc., Montreal, Quebec, Canada) to obtain video clips with the camera zoomed in on the pharynx. Videos were taken for at least 30 seconds, or longer if the animal moved out of the field of view. The number of pumps in 30 seconds was counted and multiplied by 2 to obtain the number of pumps per minute and the data was presented as % of control. At least 10 nematodes were recorded for 0 and 5 μ M MeHg, and 6 nematodes on 20 μ M were observed. Data is presented as mean \pm SEM.

H. Brood-size assay

N2 nematodes were synchronized and grown to L4 stage on 8P plates. L4s were then placed individually onto 8P plates containing various concentrations of MeHg (0-15 μ M). After 24 hours, each nematode was moved to a fresh plate every 12 hours to limit the number of progeny on each plate and to ensure the adult could be distinguished from its progeny. Animals were transferred to new plates until egg laying stopped. The number of live progeny on each plate was counted after 48 – 72 hours of growth and the plates for each nematode were totaled. At least 15 animals were assayed for each [MeHg].

I. Larvae development rate assay

Synchronized L1 stage N2 nematodes were placed on 8P plates with 0 or 10 μ M MeHg and incubated at 20°C. The nematodes were examined every 12 hours and the time was recorded when the animals reached L4 and adult stage, as indicated by the presence of the “white patch” at the vulva (L4) or embryos (adult). All animals on a single plate developed at essentially the same rate. The experiment was repeated at least 4 times.

J. Embryonic development assay.

Synchronized L1 stage OD70 nematodes were incubated on 8P plates containing 0 or 10 μM MeHg for 72 hours. OD70 nematodes contain a fusion of the pleckstrin homology domain derived from mammalian PLC1d1, which binds to a phosphoinositide lipid on the plasma membrane, to the red fluorescent protein mCherry (Audhya *et al.* 2005). The *pie-1* promoter drives expression specifically in germ cells. When the nematodes reached adult stage and contained embryos, they were immobilized on 2% agarose pads with 2% sodium azide for examination and imaging with a fluorescent inverted microscope (Axioplan 2 and Axiovision Release 4.5, Carl Zeiss, Jena, Germany). At least 50 animals were observed for each condition and representative images are shown.

K. ROS analysis

Total ROS formation was evaluated in the whole nematode using the dye DCFDA. DCFDA is a non-fluorescent molecule that can easily enter cells (Kampkötter *et al.* 2007). The dye is cleaved in the presence of ROS to yield the fluorescent DCF, which can be monitored and quantitated. ROS levels were determined using previously reported protocols (Kampkötter *et al.* 2007, Schulz *et al.* 2007). Synchronized L4 stage nematodes were exposed to 25 μM MeHg for 8 hours. Following exposure, nematodes were washed off the plates with M9 buffer and washed three additional times. Nematodes in M9 (50 μl) were combined with 50 μl of 100 μM DCFDA (for a final concentration of 50 μM) in a 96 well plate with black sides and a clear bottom, 4 wells per condition. Controls included nematodes without DCFDA and DCFDA without nematodes. The fluorescence was measured at excitation and emission wavelengths of 485 and 520 nm in a Spectrafluor Plus plate reader (Tecan, Durham, NC). An initial read was obtained, the plates were incubated at room temperature for 1 hour with shaking and the final fluorescence was measured. The fluorescence intensity of the control wells was subtracted from all other wells and the change in fluorescence was determined by subtracting the initial value from the final value. The experiment was repeated in triplicate and average values were calculated.

L. RNA extraction

After the desired exposure or growth condition, nematodes were collected from the plates by washing with water and washed at least 3 times to remove bacteria. TRIzol

reagent (Life Technologies, Grand Island, NY) was added to the pellet of nematodes, approximately 1 ml TRIzol per 100 μ l of pellet. Samples were frozen at -80°C and later thawed for processing, or RNA was isolated immediately as previously described (Novillo *et al.* 2005). Samples were vortexed and incubated in TRIzol for 10 minutes at room temperature, then centrifuged for 10 minutes at 14K RPM at 4°C . The debris was pelleted to the bottom and the top layer was removed to a new tube. 200 μ l chloroform was added to separate the protein and other impurities, samples were vortexed and allowed to sit at room temperature for 3 minutes. Samples were centrifuged for 10 minutes at 12K RPM at 4°C and the top clear layer was removed to a new tube. 500 μ l isopropanol was added to precipitate the RNA, the tube was inverted to mix and incubated at room temperature for 10 minutes. The RNA was pelleted by centrifugation for 10 minutes at 12K RPM at 4°C and then the pellet was washed with 75% ethanol. After air drying, the pellet was dissolved in nuclease free H_2O and the concentration was measured using a ND-1000 spectrophotometer (Nanodrop Technology, Wilmington, DE). RNA samples were stored at -80°C .

M. cDNA synthesis

cDNA synthesis was carried out using the iScript cDNA Synthesis Kit (Bio-Rad, Hercules, CA) or the Maxima First Strand cDNA Synthesis Kit for RT-qPCR (Thermo Fisher Scientific, Waltham, MA) following manufacturer's instructions. Both kits use a mixture of oligo dT and random hexamer primers and 1 μ g of total RNA was used as the template. cDNA was quantified using a ND-1000 spectrophotometer and stored at -20°C .

N. RT-PCR measurements

Primers were designed using Primer3 software to be gene specific and exon spanning to avoid amplification of contaminating genomic DNA. Glyceraldehyde-3-dehydrogenase (GAPDH) was selected as the gene for normalization in the RT-PCR because its expression does not change as a result of MeHg treatment (data not shown, Wilson *et al.* 2005, Yin *et al.* 2007). Primer sequences are listed in **Table 2**. Real-time PCR was performed using 2X SYBR Green PCR master mix (Life Technologies, Grand Island, NY) or Maxima SYBR Green/ROX qPCR Master Mix (Thermo Fisher Scientific, Waltham, MA) and the StepOnePlus Real-Time PCR System (Life Technologies, Grand Island, NY). 25 μ g of cDNA was used as the template, reactions were performed in

triplicate and each experiment was repeated with three independent cDNA samples. Primer specificity and the formation of a single product were verified by a melting curve. Relative fold change in expression of each gene was calculated using the $\Delta\Delta C_t$ method, normalized to GAPDH.

Gene	Primer Sequence (5' – 3')
<i>gapdh</i>	F: CAATGCTTCCTGCACCACTA R: CTCCAGAGCTTTCTGATGG
<i>gst-1</i>	F: CAAGGACGTTCTTCCAGGAG R: CTGGAACACCATCAAGAGCA
<i>gst-4</i>	F: TGCTCAATGTGCCTTACGAG R: AGTTTTTCCAGCGAGTCCAA
<i>gst-5</i>	F: CCGGACAACAATACGAGGAT R: GAGCCAAGAAACGAGCAATC
<i>gst-10</i>	F: ATTCGAAGACATTCGGTTCG R: TTGCTCCAGTCTGCACAATC
<i>gst-12</i>	F: GGAGTTCCGTTTGAGGATGA R: CGACGTTTAGGACAGGCATT
<i>gst-21</i>	F: AATGCTGACGCATGAAGATG R: GCCTTGACGCAATGTATCCT
<i>gst-38</i>	F: TCCAATGCTCGAGGTAGATGGCAA R: ACGAGCCTCCGCGTAATAGTCTTT
<i>hsp-4</i>	F: TTGAAGCCGGTTCAGAAAGT R: GCTCCTTGCCGTTGAAGTAG
<i>hsp-6</i>	F: AACGCCGTTGTTACAGTTCC R: GCTCGTTGATGACACGAAGA
<i>hsp-16.1</i>	F: CAATGTCTCGCAGTTCAAGCCAGA R: GCACCAACATCAACATCTTCGGGT
<i>hsp-16.2</i>	F: CTCAACGTTCCGTTTTTGGT R: CGTTGAGATTGATGGCAAAC
<i>hsp-16.41</i>	F: GAAACAAAATCGGAACATGGA R: TCTTTGGAGCCTCAATTTGG
<i>hsp-16.48</i>	F: CATGCTCCGTCCTCCATTTT R: TTGTGATCAGCATTTCTCCAA
<i>hsp-70</i>	F: TTAAGTGAATCCCACCAGCTCCA R: ATCTCGTTGTGCTGCGTCTTCTCT
<i>mrp-7</i>	F: CGAGAAGACGTTGCAGGAC R: ATTTGGGCCGATTACCTTCT

Table 2. RT-PCR primer sequences.

O. Protein preparation

Protein extracts from whole nematodes were prepared for Western blot analysis following previously established methods with slight modifications (Weimer *et al.* 2003, Li *et al.* 2009). Following exposure, animals were washed from plates with H₂O and washed an additional three times. 150 µl of mito buffer (20 mM HEPES, pH 7.5, 250 mM sucrose, 1 mM EDTA, 1 mM EGTA, 10 mM KCl, 1.5 mM MgCl₂, 1 mM DTT, 0.1 mM PMSF, 2 µg/ml leupeptin, 2 µg/ml pepstatin, 2 µg/ml aprotinin) was added to 300-400 µl of pelleted nematodes and the tubes were frozen at -20°C until protein purification or processed immediately. Animals were homogenized on ice with 50 – 60 strokes in a 2 ml glass tissue grinder. The lysate was centrifuged for 4 minutes at 400xg at 4°C and the supernatant was collected without disturbing the insoluble debris. The protein concentration was determined using the Quick Start Bradford assay (Bio-Rad, Hercules, CA) with bovine gamma globulin as the standard.

P. Western blot analysis

NuPAGE LDS buffer (Invitrogen, Carlsbad, CA) and β-mercaptoethanol were added to 50 µg of protein and samples were heated at 95°C for 20 minutes. Total cell lysates were separated by SDS-polyacrylamide gel electrophoresis (PAGE) using pre-cast NuPAGE 10% Bis-Tris gels and NuPAGE MOPS running buffer (Invitrogen, Carlsbad, CA). Proteins were transferred to polyvinylidene difluoride (PVDF) membranes in a Tris-glycine transfer buffer (Bio-Rad, Hercules, CA). Membranes were blocked with 5% non-fat dry milk dissolved in TBST (tris-buffered saline, 0.1% Tween-20) for 2 hours at room temperature and then incubated in primary antibody overnight at 4°C. The GST-38 antibody was generated against amino acids 6-92 of the putative *C. elegans* GST-38 sequence (WP:CE15958) using Genomic Antibody Technology at Strategic Diagnostics Inc. (SDI, Newark, DE). This rabbit polyclonal antibody was affinity purified by SDI and used at a 1:20,000 dilution. A mouse monoclonal antibody to GAPDH (ab36840, Abcam, Cambridge, MA) was used to ensure equal loading of the wells (1:5,000 dilution). Membranes were washed three times in TBST for 15 minutes and incubated with horseradish peroxidase-conjugated secondary anti-rabbit IgG (611-1302 Rockland, Gilbertsville, PA) for 1 hour at room temperature. Proteins were detected using Amersham enhanced chemiluminescence (ECL) reagent (GE Healthcare, Piscataway, NJ) and the image was captured with the ChemiDoc XRS system (Bio-Rad, Hercules,

CA). The intensity of each band was quantified using the Quantity One software (Bio-Rad, Hercules, CA).

Q. Dopamine neuron degeneration

For DA neuron degeneration assays, RJ928 gravid adults were used for the synchronization procedure and L1 stage nematodes were washed with H₂O and placed on RNAi plates containing the appropriate bacteria and MeHg. Nematodes were incubated for 4 days at 20°C. For scoring of DA neuron degeneration, 50 – 60 animals were picked into 10 µl of H₂O on a 2% agarose pad on a glass slide (Nass & Hamza 2007). For immobilization, 2% sodium azide (10 µl) was added and the nematodes were covered with a glass coverslip. A fluorescent microscope (Leica MZ 16FA, Switzerland) was used to examine the GFP-expressing DA neurons. Nematodes were scored as either “normal” or “degeneration” based on our previously reported method (Nass *et al.* 2002). To be considered normal, the GFP must be intact from the nerve ring to the tip of the nose in all 4 CEP processes (cephalic dendrites).

R. Immunohistochemistry.

For localization and expression studies, primary *C. elegans* cultures were created (Bianchi & Driscoll 2006, Settivari *et al.* 2009). Nematodes were grown to the gravid adult stage, collected and lysed with sodium hypochlorite solution. The eggs were pelleted and washed with egg buffer (118 mM NaCl, 48 mM KCl, 2 mM CaCl₂, 2 mM MgCl₂, 25 mM HEPES). A 60% sucrose solution was used to separate the eggs from the debris and the eggs were washed again with egg buffer. The eggs were incubated in chitinase (C6137, Sigma, St. Louis, MO) at 4 mg/ml, or later 1 unit/ml, for 50 minutes to dissolve the egg shells (Frokjaer-Jensen 2003, Bianchi 2006, Strange *et al.* 2007). The embryonic cells were dissociated by passing the solution through a 21 gauge needle, then collected and grown on polylysine-coated coverslips in L-15 media containing 10% fetal bovine serum (FBS) and 1% pen/strep. Cells were cultured for 3 days at 20°C.

For immunocytochemistry, cells were fixed in 4% paraformaldehyde and permeabilized with 0.5% triton X-100 (Settivari *et al.* 2009). Cells were incubated in a blocking buffer of 1% normal donkey serum followed by the SKN-1 primary antibody (sc-9244, Santa Cruz Biotechnology, Santa Cruz, CA) at a 1:1,000 dilution overnight at 4°C. A Cy5-conjugated donkey anti-goat secondary antibody (AP180S, EMD Millipore

Corporation, Billerica, MA) was used at a 1:1,000 dilution and incubated for 1 hour at room temperature. Coverslips were mounted onto slides with VECTASHIELD HardSet Mounting Medium (Vector Laboratories, Burlingame, CA, USA). As a control for the specificity of the SKN-1 antibody, cells were incubated in a mixture of primary antibody and the complementary antigenic peptide (sc-9244p; Santa Cruz Biotechnology, Santa Cruz, CA) at a ratio of 1:5, followed by secondary antibody as described above.

For expression analysis in transgenic strains, the nematode cultures were enriched for transgenic animals by picking rollers and then processed as above. After a 72 hour incubation, cells were fixed with 4% paraformaldehyde and then directly mounted onto slides with the VECTASHIELD HardSet Mounting Medium.

Confocal microscopy was used to obtain images of the cells. The Zeiss LSM 510 microscope (Carl Zeiss, Jena, Germany) was used for the SKN-1 experiments and the Nikon Eclipse Ti with NIS Elements AR software (Nikon Instruments Inc., Melville, NY) was used for CFP/YFP expression in the MRP-7 experiments (440 nm and 514 nm lasers, respectively). Z-stacks were assembled in ImageJ (Rasband 1997-2012).

S. Inductively coupled plasma mass spectrometry (ICP-MS)

1. Collecting samples for ICP-MS analysis

a. MeHg

Gravid adult NL2099 nematodes were bleached and synchronized L1s were placed onto RNAi plates seeded with RNAi bacteria. Nematodes (P0) were grown to the adult stage and synchronized again. L1s (F1) were grown on RNAi for 3 days to the adult stage and then transferred to RNAi plates containing 1 μ M MeHg and seeded with the appropriate RNAi bacteria. Nematodes were grown on the RNAi + MeHg plates for the indicated amount of time at 20°C. After exposure, animals were washed off of the plates with ice cold H₂O into pre-weighed metal-free 1.5 ml tubes and the tubes were kept on ice throughout the washing process. Nematode pellets were washed 3 times with ice cold H₂O. L1s were present on the plate, therefore the adults were allowed to settle by gravity on ice and the L1s were removed during the washes to ensure that the Hg measurement reflected only the content in adults. After the final wash, the H₂O was removed and samples were frozen at -20°C until further processing.

b. Aluminum

Synchronized L1 stage WT (BY250) and *smf-3* mutant (RJ934) nematodes were placed on NGM plates and grown for 48 hours at 20°C. L4 stage nematodes were washed off the plates with W5 H₂O (Thermo Fisher Scientific, Waltham, MA, submicron filtered HPLC grade H₂O to minimize contamination of aluminum from diH₂O) and washed three times to remove bacteria. Nematodes were added to 15 ml tubes and exposed to W5 H₂O or 100 µM AlCl₃ for 30 minutes at room temperature. Ice-cold W5 H₂O was added to each tube to stop the exposure, nematodes were moved to pre-weighed tubes, and additionally washed 4 more times with ice-cold W5 H₂O. All H₂O was removed from the pellet and the tubes were frozen at -80°C.

2. Digesting samples for ICP-MS analysis

a. MeHg

Frozen nematode samples were thawed, centrifuged to collect any liquid to the bottom of the tube and H₂O was removed down to the top of the pellet. The total weight of the tube and pellet was recorded. Digestion was carried out using the MARSXpress microwave digestion system with 20 ml capacity vessels (CEM, Matthews, NC). Concentrated HNO₃ (1 ml) (Optima grade, Thermo Fisher Scientific, Waltham, MA) was used to transfer the sample to the digestion vessel. Millipore filtered H₂O (1 ml) was added to achieve a final concentration of 50% acid. The vessels were evenly distributed and secured into the carousel and placed into the digestion chamber. The following parameters were used: Max – 1600W, % – 100, Ramp – 20 min, °C – 200, Hold – 15 min. The Max was determined based on the total volume of all vessels in the chamber: 10 to 20 ml – 400W, 20 to 60 ml – 800W, > 60ml – 1600W. After heating and cool-down, the contents of each vessel were transferred to a 50 ml metal-free tube by filling the vessel with Millipore filtered H₂O, pouring the acid + H₂O into the 50 ml tube and adding H₂O to bring the volume to 50 ml. This resulted in a final acid concentration of 2%. Samples were stored at 4°C before analysis by ICP-MS.

b. Aluminum

Samples were thawed and the open tubes were placed in an oven overnight (12 – 14 hours) at 60°C to dry the pellets. The dry weight of each sample was determined and then the dried pellet was transferred to the digestion vessel. Samples were digested in 45% HNO₃, 5% HCl using the parameters as above. Digested samples were diluted

with W5 H₂O to achieve a solution containing 2% acid and stored at room temperature before analysis.

3. ICP-MS analysis

a. MeHg

A standard curve for Hg was prepared from 0.1 – 5.0 parts per billion (ppb) Hg in 2% HNO₃ (Wilbur & Soffey 2003). All samples contained the internal standard mix #71 at 1 ppb (⁸⁹Y and ²⁰⁹Bi were monitored) and 200 ppb Au. Au was added to prevent the loss of Hg due to binding to the container and to limit Hg build up in the instrument, as Au maintains Hg²⁺ rather than Hg in solution (Thermo Scientific Application Note 40612 2008). Digested samples were diluted in 2% HNO₃ to achieve a final concentration of 0.1 mg nematode tissue/ml. Although the nematode matrix did not appear to cause interference with the Hg measurement, the total dissolved solids were kept constant to ensure consistency. Also, maintaining this concentration resulted in nearly all sample measurements falling within the range of the standard curve. The pellet obtained following exposure needed to be > 5 mg so that the concentration of sample would be > 0.1 mg/ml (5 mg / 50 ml = 0.1 mg/ml). Samples containing less than this amount were either repeated, or the sample was not diluted and the actual tissue weight was used in the final calculation. Samples were introduced into the X Series ICP-MS (Thermo Fisher Scientific, Waltham, MA) and the isotopes ²⁰¹Hg and ²⁰²Hg were monitored. ²⁰²Hg was used for data analysis as it is the most abundant Hg isotope (Reyes *et al.* 2008). The [Hg] in ng/ml (ppb) was divided by the concentration of tissue in the sample (usually 0.1 mg/ml) and the data was expressed as ng Hg/mg nematodes (wet weight) or ppm Hg.

b. Aluminum

A standard curve for Al was prepared in 2% HNO₃ ranging from 0 to 100 ppb Al. Beryllium and gallium were used as internal standards (⁹Be and ⁷¹Ga were monitored). Samples were introduced into the ICP-MS and ²⁷Al was monitored. Al content was normalized to dry weight of the nematode pellet and expressed as µg Al/g nematodes or ppm Al.

T. Transgenic animals

1. Constructs

Cyan fluorescent protein (CFP) and yellow fluorescent protein (YFP) were used as the reporters for co-expression studies (Miller *et al.* 1999). The GFP in pRN200 (Nass *et al.* 2002) was replaced with YFP from the vector L4817 (Fire Lab Vector Kit, Addgene, Cambridge, MA). The plasmids were digested with AgeI and ApaI, which flank the GFP or YFP regions of the plasmids. ExpressLink T4 DNA Ligase (Invitrogen, Carlsbad, CA) was used to ligate the YFP fragment into the pRN200 vector. The method was also used to generate a promoterless CFP expression vector by replacing the GFP in pPD95.73 with the CFP fragment from L4816. To generate a transcriptional fusion of *mrp-7* with CFP, the *mrp-7* promoter was amplified from genomic DNA based on primers designed by The Genome BC *C. elegans* Gene Expression Consortium, which amplify 3466 bp 5' of the start codon (Hunt-Newbury *et al.* 2007). The PCR product was generated using Elongase Enzyme Mix (10480-010, Invitrogen, Carlsbad, CA) as this mixture of polymerases has proofreading ability and allows for amplification of targets over 5 kb, and the following primers: F – GTCGACTAGAGGATCCTTTAAAATCTCGTCGACATCACT, R – CCAATCCCGGGGATCCCTAATTTTTGGAGTTTGTGTT. The *mrp-7* promoter was inserted into the promoterless CFP vector at the BamHI site using the In-Fusion HD cloning system (Clontech, Mountain View, CA). Ligation reactions were transformed into Max Efficiency DH5 α supercompetent cells (Invitrogen, Carlsbad, CA). Single colonies were grown for miniprep (QIAprep Spin Miniprep Kit, Qiagen, Germantown, MD) and the ligation was confirmed by restriction digest or PCR.

2. Microinjections

C. elegans microinjections were performed largely as described (Evans 2006). A drop of halocarbon oil (H8898, Sigma-Aldrich, St. Louis, MO) was placed onto an injection pad (2% agarose with small bits of glass baked at 60°C overnight in a vacuum oven) and young adult nematodes were picked into the oil. The animals were carefully pressed onto the agarose and allowed to stick to immobilize them. Injection needles were pulled and loaded with 1.2 μ l of injection mixture (1x Injection Buffer with DNA constructs totaling 100-200 ng/ μ l). The injection mix for the *mrp-7* transcriptional fusion contained P_{*mrp-7*}::CFP at 75 ng/ μ l, P_{*dat-1*}::YFP at 50 ng/ μ l, pRF4 (*rol-6*) at 50 ng/ μ l and pUC19 at 25 ng/ μ l. The needle was inserted into the gonad of the nematode and DNA was injected

into the animal. M9 buffer was used to re-hydrate the animals and they were picked onto an NGM plate to recover.

U. RNAi Screen

An RNAi screen by feeding in liquid culture was performed in a 96 well format as previously described by (Kamath & Ahringer 2003, Ahringer 2006). First, the bacterial cultures for feeding were prepared from the RNAi libraries. Cultures from the RNAi library glycerol stocks were spotted onto rectangular LB plates (Nunc OmniTray, 12-565-450, Thermo Fisher Scientific, Waltham, MA) containing 50 µg/ml ampicillin and 10 µg/ml tetracycline using sterile disposable inoculators (Nunc Disp Inoculator, 14-245-101, Thermo Fisher Scientific, Waltham, MA). The spots were allowed to dry and plates were incubated overnight at 37°C. To grow liquid cultures, 500 µl of LB broth with 50 µg/ml ampicillin was dispensed into each well of a 96-well deep well plate (Scienceware 96 Deep-Well Plate, F378600001, Bel-Art Products, Wayne, NJ) using a multi-drop dispenser (Multidrop DW, 5840177, Thermo Fisher Scientific, Waltham, MA) immediately prior to use. The LB broth was inoculated from the colonies on the flat LB plate and the plates were covered with lids (96 Deep-Well Plate Covers, 378600004, Bel-Art Products, Wayne, NJ), secured with a rubber band and grown overnight at 37°C with shaking at 300 RPM. IPTG was added to each well to a final concentration of 1 mM and the plates were shaken 1 hour to induce the dsRNA expression. To concentrate the cultures, the bacteria was pelleted by centrifugation and the LB broth was removed. The pellets were resuspended in 160 µl S basal with 100 µg/ml ampicillin and 1 mM IPTG. 50 µl was transferred to each well of a standard 96 well plate (Nunc MicroWell 96-Well Microplate, 260860, Thermo Fisher Scientific, Waltham, MA).

Synchronized L1 stage NL2099s were resuspended in S basal + 100 µg/ml ampicillin + 1 mM IPTG + 0.01% Tween and ~40 nematodes were added to each well. Tween was used to prevent the animals from sticking to the tips and ensure that an equal number was added to each well (Lagido *et al.* 2008). The initial OD₆₀₀ of each well was determined by measuring the OD₆₀₀ in a plate reader (Synergy HT, BioTek, Winooski, VT) following a 30 second shake. Plates containing nematodes were grown in a refrigerated shaking incubator set at 20°C and 160 RPM. After 48 h of incubation, MeHg was added to each well to a final concentration of 5 µM and the OD₆₀₀ (t=2 days) was recorded again. The shaking step in the plate reader helped to mix the MeHg into the solution and resuspended any bacteria that had settled to the bottom of the well.

The plates were again incubated for 2 days. At the end of the exposure, the final OD₆₀₀ (t=4 days) was recorded. A ratio of growth was determined by dividing the OD₆₀₀ t=4 / OD₆₀₀ t=2. If the nematodes were healthy and consumed all the bacteria, the t=4 would be close to 0, resulting in a ratio close to 0. If the nematode viability was impaired and little bacteria was consumed, the t=4 would be near t=2 and the ratio would be close to 1. To select genes that may affect viability, clones with a ratio greater than 0.5 (or wells which were obviously different from other wells based on visual observation) were identified and subjected to a second round of testing.

For the second round of the screen, each gene was tested again in liquid +/- MeHg. HT115 (empty vector) and *skn-1* bacteria were included in every plate as a control (VanDuyn *et al.* 2010). 50 µl of bacteria was pipetted into two wells of a 96 well plate, nematodes were added and the plates were incubated as above. After 48 hours, MeHg was added to one well per clone, and H₂O was added to the other well for control. The OD₆₀₀ was measured at day 0, 2 and 4 and the t=4/t=2 ratio was calculated. Clones for which the MeHg ratio was greater than 2 times the control ratio (as observed for *skn-1* RNAi), or for which there was a clear difference between control and MeHg based on visual observation, were selected to undergo a third round of screening.

For the third round, a live/dead assay on agar plates was carried out for each clone. Synchronized NL2099 L1 stage nematodes were grown on plates seeded with each individual RNAi clone for 48 hours. L4 stage nematodes were transferred onto RNAi plates containing 10 µM MeHg and seeded with the RNAi bacteria. After 48 hours, the number of live animals was determined as described in the viability assay above. Each clone was tested in triplicate (> 20 animals per replicate) and clones for which the average percent live nematodes was significantly different from WT (HT115) were identified as “screen hits”.

V. RNAi clone sequencing

The RNAi feeding clone in well III-6J08 of the Source BioScience library was grown overnight in LB broth + 50 µg/ml ampicillin and a miniprep kit was used to isolate plasmid DNA (QIAprep Spin Miniprep Kit, Qiagen, Hilden, Germany). Sequencing services were carried out by ACGT, Inc. (Wheeling, IL, USA) using their provided M13F(-20) primer. The resulting nucleotide sequence was mapped to the *C. elegans* genome using the BLASTN feature at WormBase.org.

W. Determination of SKN-1 binding sites

To determine if genes have SKN-1 binding sites, the region 2 kb (or until the start of another gene) upstream (5') of the ATG start codon was identified using the genome browser on Wormbase.org. This sequence is always given for the + strand but the consensus sequence can be found on either the + or – strand, so the search includes both the forward sequence and its reverse complement, with all combinations of the variable bases.

A method of experimentally determining SKN-1 binding sites is through the use of ChIP-seq analysis (Niu *et al.* 2011). A SKN-1::GFP translational fusion (which produces functional SKN-1 protein) was utilized to generate transgenic animals. Synchronized nematodes were collected at the L1 stage and formaldehyde was used to cross-link DNA to proteins before a GFP antibody was used to pull down SKN-1::GFP. Any DNA fragments that were bound by SKN-1 were isolated and sequenced. A program called PeakSeq and other statistical analysis was used to identify regions of DNA that were bound by SKN-1. The genes that were bound by SKN-1 are presented as a table in the publication, but also annotated as a “Track” in the genome browser on Wormbase.org. Therefore, regions bound by SKN-1 are indicated by peaks in the promoter region when viewing the genome browser. The presence of SKN-1 binding sites is not conclusive evidence that the gene is regulated by SKN-1 but it supports the hypothesis.

X. DAVID analysis of screen hits and microarray data

DAVID (the database for annotation, visualization and integrated discovery) is a program for the analysis of large gene lists, such as those generated by microarray experiments (Huang *et al.* 2009). DAVID compares a list of genes input by the user to a reference gene list, first assigning a biological annotation to each gene and then determining the classes of genes or related gene groups that are over-represented based on their frequency in the input list versus the reference list. The list of genes upregulated > 2-fold by MeHg exposure in the microarray was submitted and the Affymetrix *C. elegans* Array was used as the reference list.

Y. BLAST searches and sequence alignment

To determine putative homologues, the NCBI BLAST program was utilized (Altschul *et al.* 1990). Protein sequences were compared using the blastp feature. *C. elegans*

protein sequences were obtained from WormBase.org and subjected to search against the human genome, or human protein sequences were obtained from the NCBI protein database and used as the query sequence for a search of the most recent build of the *C. elegans* genome.

Sequence alignment was carried out using the ClustalW program with the default parameters (Larkin *et al.* 2007). In the output, an asterisk represents a fully conserved residue, a colon (:) indicates strongly conserved residues (> 0.5 in the Gonnet PAM 250 matrix) and a period (.) indicates a weakly conserved residue (≤ 0.5 in the Gonnet PAM 250 matrix).

Z. Statistical analysis

Statistical analysis was performed using GraphPad Prism software (GraphPad Software, San Diego, CA). For comparison of two groups, a student's t-test was used. For multiple groups, one-way ANOVA analysis was performed. When two variables were compared, two-way ANOVA was done. All ANOVA tests were followed by Bonferroni post-tests (which are preferred over the Tukey test for small samples). Error bars represent the standard error of the mean (SEM).

III. Characterization of MeHg toxicity in *C. elegans*

MeHg exposure in vertebrates confers animal death and impairs development and reproduction (Verschuuren *et al.* 1976, Curle *et al.* 1987). MeHg also increases ROS and induces stress response gene expression (Kaur *et al.* 2006, Yu *et al.* 2010). These endpoints were evaluated to determine if *C. elegans* recapitulates key features of mammalian MeHg toxicity.

A. Viability

1. Chronic exposure to MeHg confers animal death

Chronic exposure of *C. elegans* to MeHg results in animal death that is increased with increasing concentrations of MeHg. Initial experiments were performed on 8P plates containing MeHg at concentrations between 0 and 125 μM . Wild type (N2) nematodes were synchronized and grown to the fourth larval stage (L4) on standard media before being transferred to the plates containing MeHg. After 48 hours, the number of live animals was determined. Based on the results of this experiment, the LC50 was approximately 95 μM after a 48 hour exposure on 8P plates (**Fig. 3**).

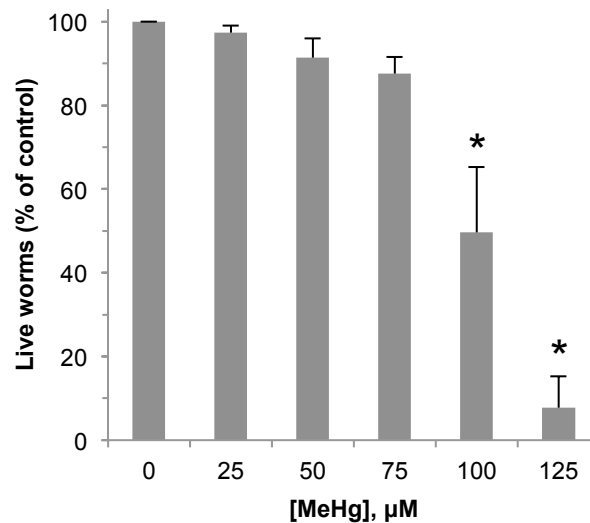


Figure 3. MeHg confers concentration-dependent animal death. WT (N2) L4 stage nematodes were exposed to various concentrations of MeHg on 8P plates for 48 hours. The number of live animals was determined and expressed as % of control. Data was analyzed using one-way ANOVA followed by a Dunnett's multiple comparison test. * indicates a significant difference from 0 μM MeHg with $p < 0.01$.

MeHg-induced lethality appears dependent on the age of the nematodes when the exposure begins. Adult nematodes appear to be the most sensitive, as they develop a severe “egg-laying defective” (*egl*) phenotype that may contribute to the overall toxicity resulting in death. L4 stage nematodes placed on 5 μ M MeHg exhibit a significant reduction in egg-laying and accumulation of embryos that hatch inside the adult (**Fig. 4A and B**) and 20 μ M results in the *egl* phenotype combined with non-viable embryos (**Fig. 4C and D**). MeHg exposure beginning at early larval stages (L2 – L3, 24 hours post synchronization) inhibits the formation of embryos, suggesting that the lethality observed may be due to direct effects on that animal.

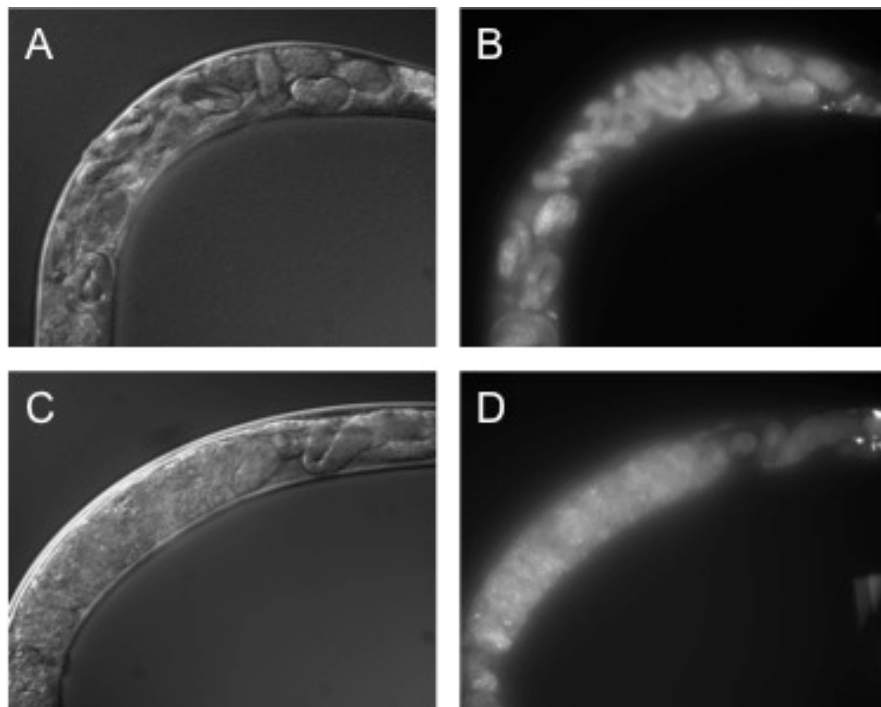


Figure 4. MeHg exposure inhibits egg-laying and results in an accumulation of embryos inside the hermaphrodite. Under normal/control conditions, 10 – 15 embryos are present in the uterus at this age and eggs are laid before the 44-cell stage of development (see Fig. 8A). Growth on 5 μ M MeHg causes the *egl* phenotype, in which egg-laying is inhibited and larvae hatch inside the hermaphrodite (A and B). At higher MeHg concentrations (20 μ M), the embryos accumulate but are not viable (C and D).

2. Selenium inhibits MeHg toxicity

Nematodes are able to survive exposure to high concentrations of MeHg when selenium (1 mM) is also present on the plates (**Fig. 5**). The bacteria turns red in the presence of Se, and this may be due to a metabolic process as the bacteria must be alive for the red

color to develop. Also, when Se is added to dead bacteria, the compound is unable to inhibit MeHg toxicity.

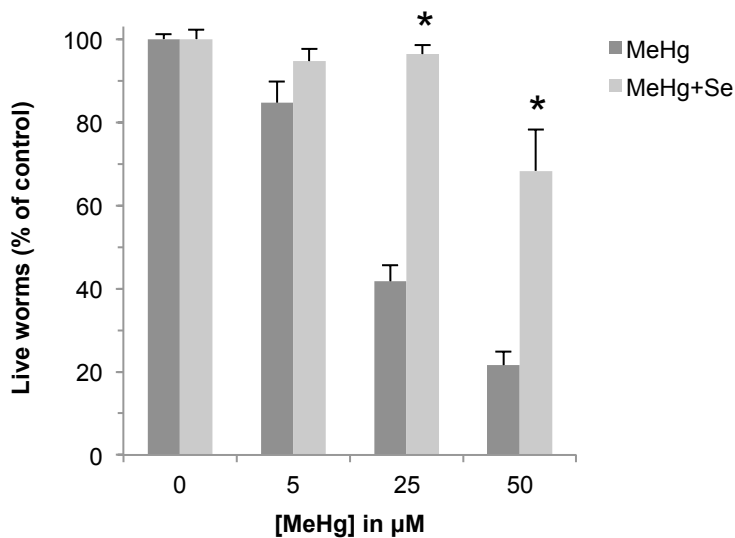


Figure 5. Selenium inhibits MeHg-induced lethality. L4 stage N2 nematodes were exposed to MeHg or MeHg + Se (1 mM Na₂SeO₃) on 8P plates for 48 hours. The number of live animals was determined and expressed as % of control. The combination exposure is significantly different than MeHg alone; * indicates p < 0.001 by two-way ANOVA followed by Bonferroni post test.

Although the ability of Se to inhibit MeHg toxicity has been documented in multiple systems, the mechanisms involved are still debated (Khan & Wang 2009). One hypothesis is that supplemental Se increases the Se available for selenoproteins and therefore the antioxidant capacity of the cell, enhancing the ability to buffer the oxidative stress induced by MeHg (Ralston & Raymond 2010). However, Se can bind MeHg with a high affinity (Ralston & Raymond 2010). Intracellular binding could sequester MeHg and prevent it from reacting with other molecules and may also enhance excretion (Ralston *et al.* 2007). A third possibility is that Se may bind MeHg outside the cell and inhibit uptake. Analysis of Hg levels shows that the Hg in the nematodes is dramatically reduced when co-exposed with Se (**Fig. 6**), suggesting either impaired uptake or increased excretion of MeHg when Se is present.

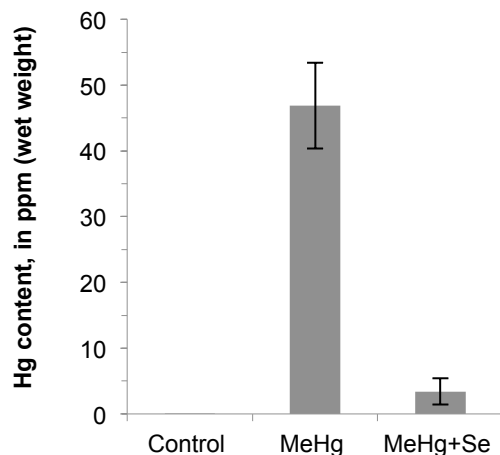


Figure 6. Hg levels are reduced by co-exposure with Se. L4 stage N2 nematodes were exposed to 25 μM MeHg or 25 μM MeHg + 1 mM Na_2SeO_3 for 8 hours and then collected for Hg analysis. The LECO Advanced Mercury Analyzer 254 was used to measure total Hg in the nematode samples, and the data was normalized to wet weight. Analysis was completed by Rosalice Buehrer in the Department of Earth Sciences at IUPUI.

3. MeHg exposure reduces pharyngeal pumping rate

Pharyngeal pumping is a *C. elegans* behavior that may be impaired when the nervous system is not functioning properly (Avery & You 2012). Several neurotransmitters, including DA, are involved in the regulation of pumping rate (Marr *et al.* 2003). Pharyngeal pumping rate can also be an indicator of overall animal health. L4 stage nematodes were exposed to MeHg for 24 hours and the number of pumps per minute was determined. There was a significant decrease in the pumping rate at 5 μM and 20 μM MeHg (**Fig. 7**).

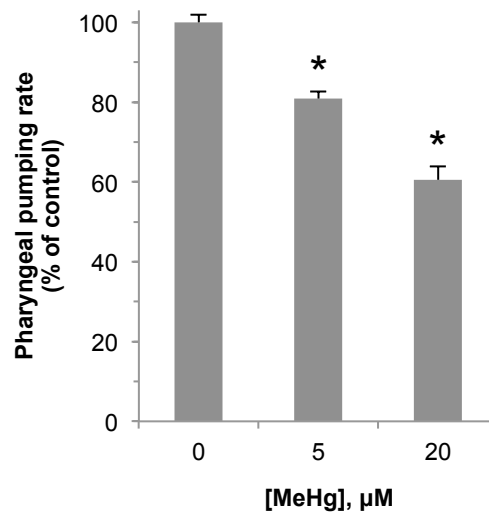


Figure 7. MeHg exposure reduces the pharyngeal pumping rate. L4 stage N2 nematodes were placed on 8P plates containing the indicated MeHg concentration for 24 hours. Individual animals were recorded on the plates for 30 seconds, the number of pumps was counted and multiplied by 2 to obtain pumps per minute. Data is expressed as percent of control and is the average of at least 6 animals. The pharyngeal pumping rate is significantly decreased by MeHg compared to control as determined by one-way ANOVA, * indicates $p < 0.001$.

B. Reproduction and development

1. MeHg reduces brood size

To determine the reproductive capacity of nematodes exposed to MeHg, a brood size assay was incorporated to quantify the total number of progeny produced by a single animal. Synchronized N2 animals were placed on 8P plates and grown to the L4 stage. Animals were transferred individually to plates containing MeHg from 2.5 – 15 μM . The adult nematodes were moved to a new plate (with the same [MeHg]) every 24 hours until egg-laying stopped. The number of progeny (larval stage) on each plate was counted and the counts from each plate were combined to determine the total number of progeny from a single animal. The progeny were counted once they had hatched into larvae rather than un-hatched embryos, however no eggs were observed that failed to hatch on any plates. At concentrations of MeHg as low as 2.5 μM , the brood size is significantly lower than for unexposed nematodes and 10 μM MeHg reduces the brood size by over 90% (Fig. 8).

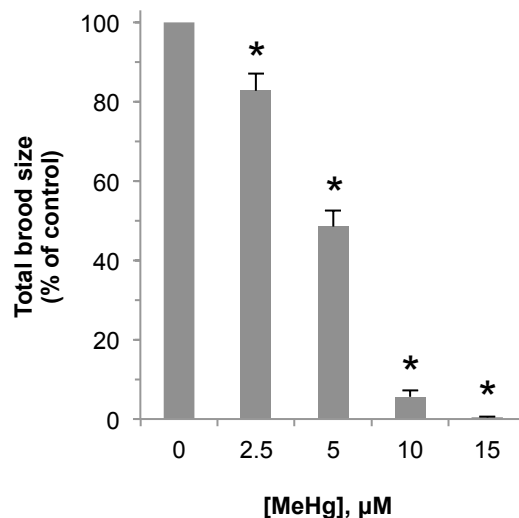


Figure 8. Exposure to MeHg causes a reduction in brood size. L4 stage nematodes were transferred to plates containing MeHg, one animal per plate, and the parent was moved to a new plate every 24 hours. The total number of progeny produced by each animal was calculated over its entire period of egg-laying. One-way ANOVA was used to determine that the brood size is significantly different from 0 μM on all concentrations of MeHg; * indicates $p < 0.01$.

As mentioned above, MeHg exposure inhibits egg-laying, so the reduction in brood size may be a combinatorial effect of decreased embryo production and decreased egg-laying. Sodium arsenite is another toxicant that reduces the brood size of *C. elegans* and following exposure, DAPI staining was used to identify and count mitotic cells and apoptotic cells in the gonad (Wang *et al.* 2007). A correlation was found between the reduced brood size, decreased mitotic cells and increased apoptotic cells (Wang *et al.* 2007). Increased apoptosis and decreased mitosis could likely be occurring during MeHg exposure as well, contributing to the reduction in brood size.

2. MeHg causes embryonic defects

Studies in several systems show that MeHg can cause embryonic defects and teratogenic effects (Curle *et al.* 1987, Carvalho *et al.* 2008, Weis 2009). Fluorescent reporters and the transparency of the nematode allow us to study embryonic development *in vivo* and over time in living animals. The strain OD70 was used to visually monitor cell division in the embryos (Audhya *et al.* 2005). This strain expresses mCherry behind the *pie-1* promoter to drive expression only in germ cells, and fused to a plekstrin homology domain to target the protein to the cell membrane. Normal

development occurs through a series of tightly regulated cell divisions, resulting in embryos as shown in **Fig. 9A**. However, growth of L1 animals on 10 μ M MeHg until adulthood produces significant changes in the appearance of the embryos. Shown are representative images, but nearly all animals displayed some degree of embryonic defects. The cell division becomes abnormal, resulting in embryos that appear to be a random jumble of cells (**Fig. 9B**). Defects in mitosis are suspected as multinucleated cells were also observed (**Fig. 9C and D**). Abnormal fertilization or formation of the oocyte during embryogenesis could also contribute to multinucleated embryos. MeHg has been shown to cause multinucleated cells in PtK2 cells by interfering with microtubules and mitotic division (Sager & Syversen 1984).

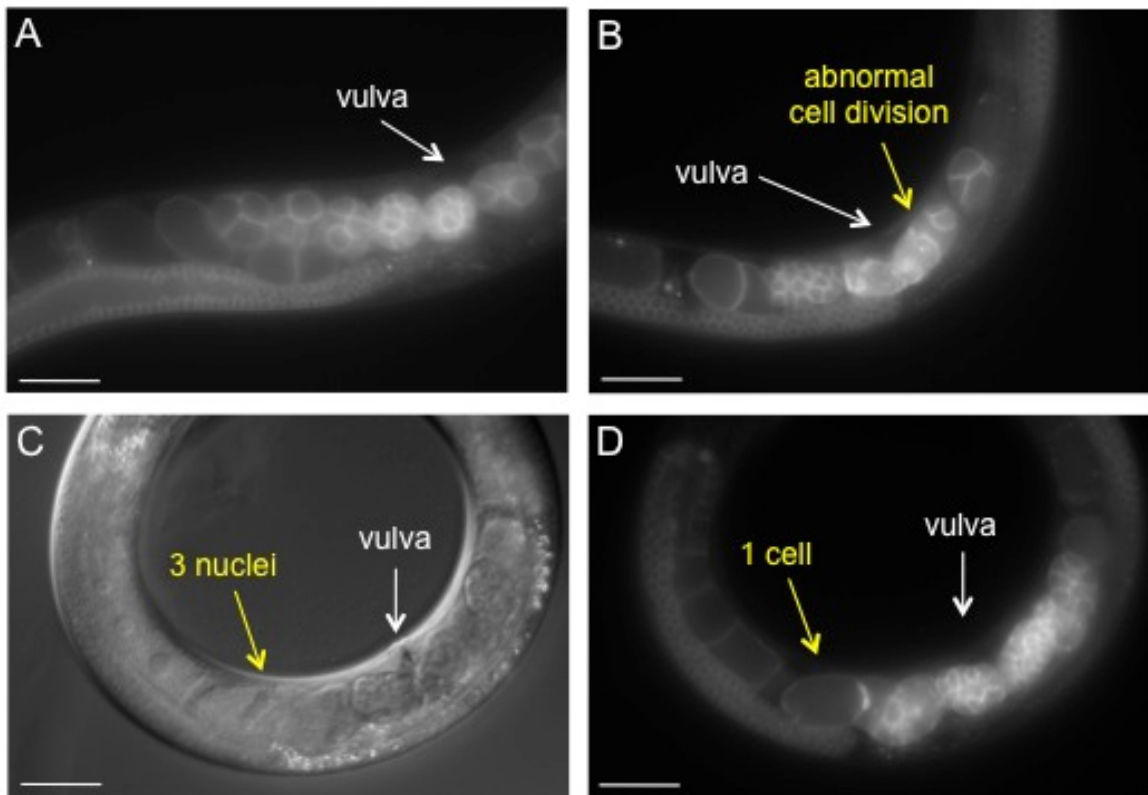


Figure 9. Exposure to MeHg causes embryonic defects. L1 nematodes expressing the mCherry fluorophore behind the *pie-1* promoter were grown to adulthood on 8P plates in the presence of water (A) or 10 μ M MeHg (B-D), and fluorescence (A,B and D) or DIC (C) images were obtained. Relative to control (A), MeHg causes irregular cell division (B), and some cells are multinucleated (C and D). The scale bar is 50 μ m.

3. MeHg decreases growth rate

Measuring animal size is a method of monitoring growth rate. L1 stage nematodes were put on plates containing MeHg up to 50 μM and images of the animals were captured after 72 hours. ImageJ was used to measure the length of each nematode and values were presented at percent of control. Nematodes on 50 μM MeHg appear to remain near the L1 stage and reach a size less than 20% of control animals (**Fig. 10**).

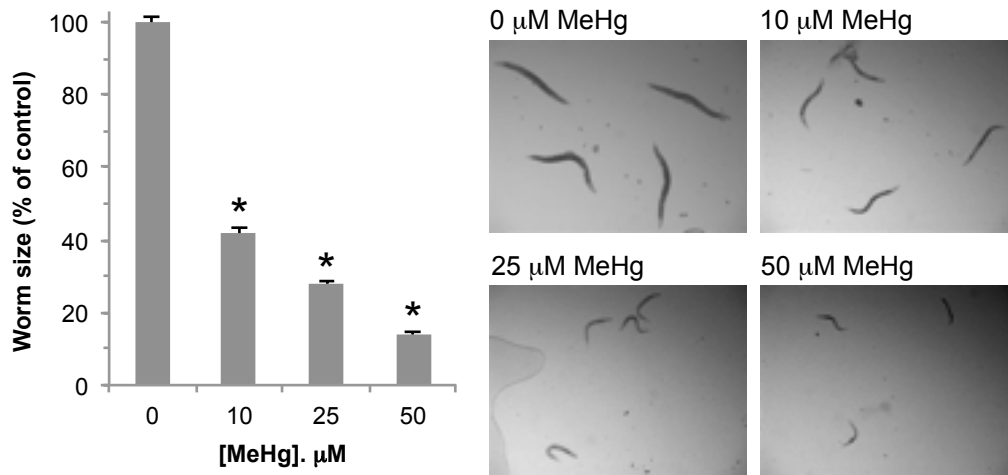


Figure 10. Growth on MeHg decreases nematode size. L1 stage N2 nematodes were placed on 8P plates with the indicated concentration of MeHg and grown for 72 hours. Images were obtained and the size of at least 10 animals was measured using the ImageJ software. Control (0 μM) nematodes reached adult size by this time, but all MeHg conditions significantly decreased size (one-way ANOVA, * $p < 0.001$).

4. MeHg delays larval development

As *C. elegans* have a consistent and well-defined life cycle, the time to reach developmental milestones can be monitored in addition to measuring the body size. Synchronized L1 stage N2 animals were placed on 8P plates containing 10 μM MeHg and were monitored during exposure until the adult stage was reached, as determined by the presence of embryos inside the nematode. For nematodes exposed to MeHg, the time to reach adulthood was about 1.4 times longer than for unexposed controls (56 hours vs. 78 hours) (**Fig. 11**). At concentrations higher than 10 μM , animals rarely produced embryos or fully developed to the adult stage.

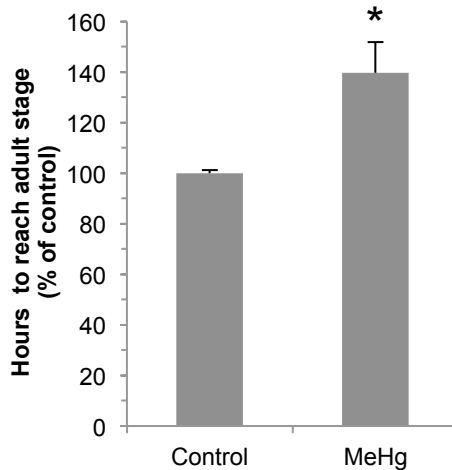


Figure 11. MeHg delays animal development. L1 stage N2 nematodes were placed on 8P plates containing 10 μ M MeHg. The time to reach adulthood (as determined by the presence of eggs in the gonad) was recorded and expressed as percent of control. The time to reach adulthood was significantly increased in the presence of MeHg (student's t-test, * indicates $p < 0.01$).

C. Biochemistry

1. MeHg induces *C. elegans* stress response

C. elegans have been proposed for use as biosensors because of the availability of stress-inducible reporter strains (David *et al.* 2003). DAF-16 is a transcription factor involved in the insulin-like signaling pathway that regulates life span and stress resistance (Henderson & Johnson 2001). In unfavorable conditions, DAF-16 is localized to the nucleus to enhance the expression of genes that promote survival and longevity. A DAF-16::GFP reporter strain (TJ356) shows nuclear localization of GFP following exposure to stress such as starvation, heat and oxidative stress (ex. juglone) (Henderson & Johnson 2001). I exposed TJ356 L4 stage nematodes to MeHg and observed a distinct nuclear localization of DAF-16::GFP within 4 hours (**Fig. 12**). The activation and nuclear localization of DAF-16 suggests that MeHg induces a nematode stress response pathway and DAF-16 and insulin-like signaling may be involved in the cellular response to MeHg.

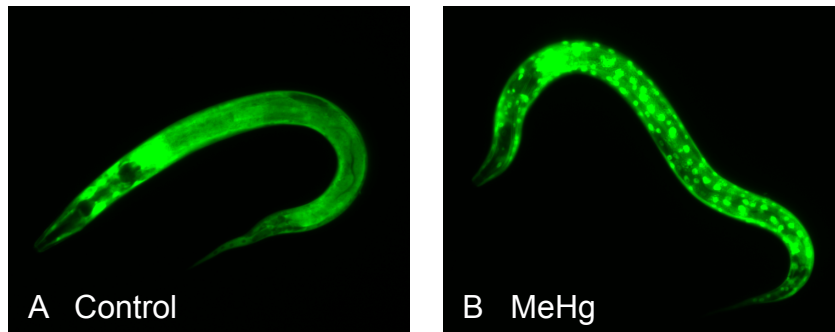


Figure 12. MeHg induces DAF-16 nuclear localization. L4 stage TJ356 nematodes have a diffuse expression of GFP under non-stressed conditions, indicating cytoplasmic localization of DAF-16 (A). After 4 hours of exposure to 25 μ M MeHg 30% of nematodes exhibited nuclear localization of DAF-16::GFP (B). After 24 hours of exposure, DAF-16::GFP was localized to the nucleus in 70% of animals.

2. MeHg increases total ROS

DAF-16 can be activated in response to oxidative stress and one of the effects of MeHg exposure is an increase in cellular ROS (InSug *et al.* 1997, Limke *et al.* 2004). Therefore, I determined total ROS following MeHg exposure utilizing the dye DCFDA (Kampkötter *et al.* 2007). DCFDA is a non-fluorescent molecule that can easily enter cells. The dye is cleaved in the presence of ROS to yield the fluorescent DCF, which can be monitored and quantitated. To determine if MeHg increases ROS in *C. elegans*, N2 animals were grown to the L4 stage, then incubated on plates containing 25 μ M MeHg for 8 hours. Following incubation, DCFDA was added to the nematodes and the fluorescence was measured at $t=0$ and after 1 hour and normalized to the protein content of each well. After MeHg exposure, the level of ROS increases more than two-fold compared to untreated nematodes (**Fig. 13**).

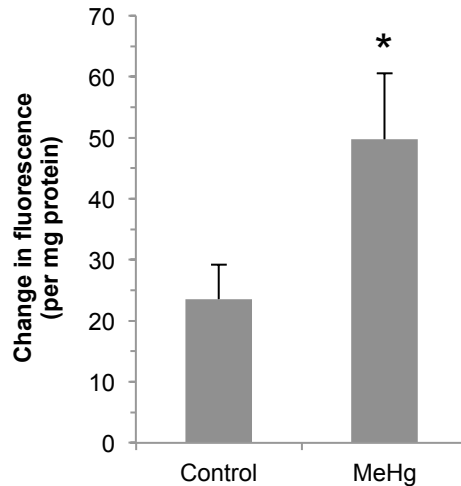


Figure 13. Exposure of *C. elegans* to MeHg increases ROS. Synchronized L4 stage N2 nematodes were exposed to 25 μ M MeHg on 8P plates for 8 hours and then incubated with DCFDA for 60 minutes. Change in fluorescence was normalized to protein concentration. Shown are mean \pm SEM of four replicates. A student's t-test indicates that MeHg significantly increases ROS compared to control, * indicates $p = 0.02$.

The assay using DCFDA measures ROS non-specifically (Karlsson *et al.* 2010). Using other methods to quantify the various species of ROS (ex. H_2O_2 , superoxide radical) may give further insight into the cellular targets of MeHg, as the disruption of different processes can produce different species of ROS.

3. Microarray analysis

The *C. elegans* Affymetrix chip, which contains probes for 22,500 transcripts, was used to compare global gene expression between control and MeHg treated animals (Affymetrix). L4 stage N2 nematodes were exposed to 25 μ M MeHg and control conditions for 8 hours then collected and the RNA was prepared for microarray analysis. A single replicate of the microarray was performed and a cut-off value of 2-fold change was used to determine which genes were significantly different between MeHg and control. With a single replicate, more advanced statistical methods could not be applied, however some evidence suggests that the fold change may be more restrictive and provide a more biologically relevant interpretation of the data compared with other statistical methods (Dalman *et al.* 2012). Based on the cut-off of 2-fold, 508 genes were upregulated and 165 genes were downregulated following MeHg exposure. Phase II

detoxification enzymes were some of the highest upregulated genes, including HSPs and GSTs. DAVID analysis was performed on the list of upregulated genes and the gene groups with enrichment scores greater than 1 were identified (**Table 3**). Phase I and II detoxification enzymes (GSTs, UGTs, CYPs) were some of the highest upregulated genes. HSPs are another class stress response proteins (Samali & Orrenius 1998b). The F-box and SKp1 genes are related to the UPS system, which plays a role in the cellular stress response (Hershko & Ciechanover 1998). These microarray results are similar to those obtained in other systems, especially MeHg-treated MEF cells (Yu *et al.* 2010). There were also 5 *dod* genes (“downstream of *daf-16*”) upregulated by MeHg, suggesting that the transcription factor DAF-16 is activated by the toxicant. The DAF-16 regulated genes are likely involved in stress resistance or survival and the induction of these *dod* genes is consistent with the nuclear localization of DAF-16 observed following MeHg exposure (**Fig. 12**).

Of the 165 down-regulated genes, DAVID analysis did not indicate any enriched gene groups. However three of the 20 most decreased genes were heme responsive genes, *hrg-1*, *hrg-3* and *hrg-4*. In humans and other mammals, Hg and MeHg are known to alter heme biosynthesis and the profile of the amounts of heme intermediates (porphyrins) in the urine can be used as a biomarker for Hg and MeHg exposure (Woods 1996). Although HO-1 is often believed to function as an antioxidant and provide cytoprotection, when heme is broken down it releases free iron (Fe) and carbon monoxide (CO), which are both pro-oxidants (Ponka 1999). Heme serves many other functions in the cell, but one hypothesis is that the nematode may downregulate the genes necessary for heme uptake in response to MeHg in an attempt to limit additional cellular stress caused by Fe or CO.

Gene class	Enrichment score
Glutathione S-transferase	9.64
F-box A protein	5.08
UDP-glucuronosyl transferase	3.75
Heat shock protein	3.36
CYtochrome P450 family	2.96
Neuropeptide-like protein	2.28
SKp1 related (ubiquitin ligase complex component)	1.44

Table 3. DAVID analysis of genes upregulated > 2-fold in microarray revealed 7 gene classes with enrichment scores greater than 1.

4. RT-PCR

The redox balance in cells is maintained by increasing the expression of antioxidant proteins, including GSTs, in response to increased amounts of ROS (Prester *et al.* 1993). In the microarray results, the expression of 18 GSTs was increased and 8 of these were in the top 100 genes. The induction of GSTs was indicated by the microarray results, so RT-PCR was used to verify these results and measure the expression of two other GSTs associated with stress response but not found in the microarray results. L4 stage animals were exposed to 25 μ M MeHg for 2 hours or 8 hours and then mRNA was isolated from each sample. *gst-4*, 12, and 21 were increased at 2 hours, and *gst-4*, 5, 12, 21 and 38 were significantly increased after 8 hours of exposure (**Fig. 14**), consistent with the results obtained from the microarray analysis. These GSTs are of the Sigma class and homologous to hematopoietic prostaglandin D synthase (H-PGDS), the only vertebrate member of the Sigma class of GSTs (Kanaoka & Urade 2003). Among the GSTs tested, *gst-38*, which is expressed in the intestines and nervous system, showed the largest change, with a 50-fold increase in mRNA levels. *gst-38* expression levels have previously been shown to increase 5-fold or less following exposure to Cd, acrylamide, arsenite, or hyperoxia, suggesting that *gst-38* expression is likely a sensitive indicator of tissue-associated oxidative stress (Liao & Freedman 1998, Hasegawa *et al.* 2008, Oliveira *et al.* 2009, Park *et al.* 2009).

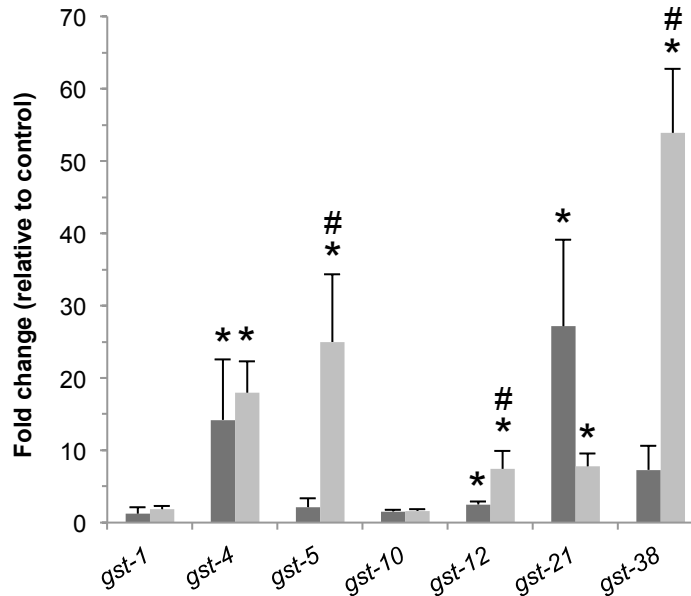


Figure 14. MeHg induces the expression of GST mRNAs. L4 stage N2s were exposed to 25 μ M MeHg for 2 hours (black bars) or 8 hours (gray bars). RT-PCR was used to quantify gene expression. The ddCt method was used to calculate the fold change, and data was normalized to GAPDH. The log fold-change values of control and MeHg exposure were compared by a t-test. * indicates a significant difference from unexposed nematodes ($p < 0.05$). A t-test was used to determine if the induction following an 8 hour exposure was different from a 2 hour exposure, # indicates $p < 0.05$.

HSPs have been shown to be upregulated following stress (Yu *et al.* 2006). The small HSPs and *hsp-70* were induced greater than 2-fold by MeHg as indicated in the microarray results. *hsp-6* was not included in the list of upregulated genes. RT-PCR showed that the small HSPs were upregulated greater than 2-fold, but none of the genes were significantly different between control and MeHg-exposed at either time point (**Fig. 15**). In contrast to the microarray, RT-PCR did not show an increase in *hsp-70*. *hsp-6* expression was essentially unchanged as indicated by RT-PCR and was also not found to be upregulated by microarray. This suggests that the increase in HSPs is specific and not general to the whole gene class.

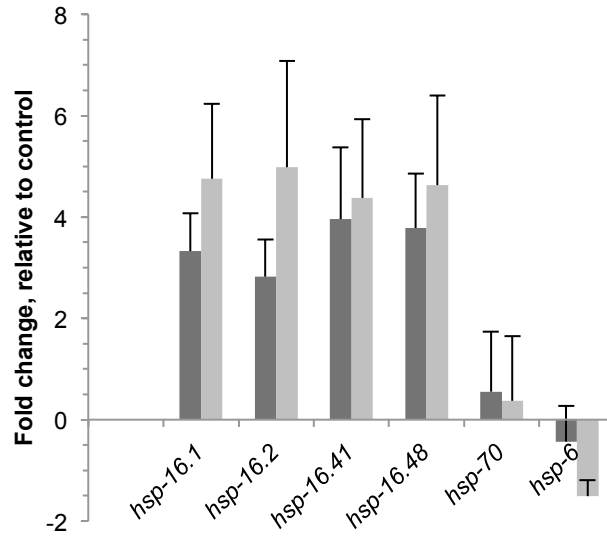


Figure 15. MeHg induces expression of HSP mRNAs. L4 stage N2s were exposed to 25 μ M MeHg for 2 hours (black bars) or 8 hours (gray bars). RT-PCR was used to quantify gene expression. The ddCt method was used to calculate the fold change, and data was normalized to GAPDH. The log fold-change values of control and MeHg exposure were compared by a t-test. No significant difference was found.

IV. SKN-1 inhibits MeHg-induced toxicity

Mammalian studies have demonstrated a role for Nrf2 in inhibiting MeHg toxicity. Nrf2 regulates the expression of stress response genes following MeHg exposure and decreased Nrf2 levels often increase sensitivity to MeHg (Toyama *et al.* 2007). I found that MeHg exposure in *C. elegans* increases the expression of GSTs, and many GSTs are regulated by SKN-1, so I evaluated the role of SKN-1 in my newly developed *C. elegans* model of MeHg toxicity.

A. SKN-1 inhibits MeHg-induced animal death

The transcription factor Nrf2 regulates the expression of phase II detoxification enzymes and has been shown to play a significant role in inhibiting MeHg toxicity in vertebrate systems (Toyama *et al.* 2007). As the expression of several GSTs was induced following MeHg exposure, I asked whether SKN-1 may inhibit MeHg-induced lethality in *C. elegans*. RNAi-sensitive NL2099 animals were fed bacteria containing either an empty vector (control) or a vector expressing *skn-1* dsRNA to reduce *skn-1* mRNA expression. The decrease in *skn-1* mRNA levels was confirmed by RT-PCR, and the protein levels are also likely decreased as the nematodes exhibit the *skn-1* deletion phenotype of non-viable embryos (Simmer *et al.* 2003, data not shown). Although SKN-1 is required for reproduction, loss of *skn-1* does not affect viability at larval and adult stages under non-stressed conditions (An & Blackwell 2003) (**Fig. 23**). However, when exposed to MeHg, the *skn-1* RNAi animals are up to 5 times more sensitive to the toxicant than WT controls (**Fig. 16**). The nematodes have decreased viability when exposed to much lower concentrations than WT. These results indicate that SKN-1 increases *C. elegans* survival in the presence of MeHg and identifies a common molecular pathway of MeHg toxicity conserved from nematodes to higher mammalian systems.

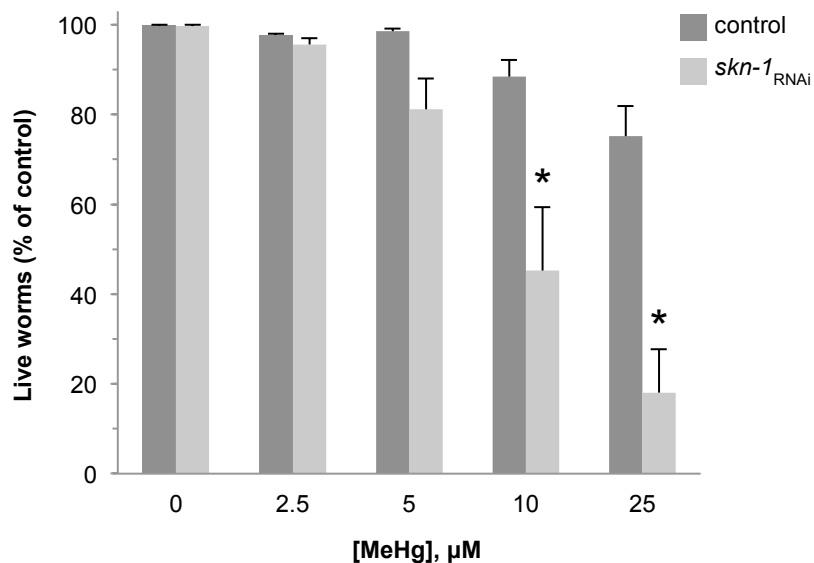


Figure 16. *skn-1* mRNA knockdown increases whole animal vulnerability to MeHg. RNAi sensitive NL2099 animals were grown on RNAi plates to knockdown *skn-1* for 48 hours, then transferred to plates containing MeHg for 24 hours. The number of live animals was determined and expressed as percent of control. Two-way ANOVA analysis indicates that *skn-1* RNAi is significantly different than control, * indicates $p < 0.001$.

Lower concentrations of MeHg are necessary in this experiment due to the increased sensitivity of *skn-1* RNAi nematodes. However, the sensitivity of WT animals is also slightly increased when the exposures are done on NGM (or RNAi) plates rather than 8P plates. Approximately 20% of WT animals are dead at 25 μM on RNAi plates, however this level of lethality is reached at 75 – 100 μM on 8P plates (compare **Fig. 3** to **Fig. 16**). It is important to consider this difference when comparing the results of various experiments and the concentrations of MeHg.

A reduction in expression of *skn-1* increases sensitivity to MeHg, therefore I asked if overexpression of SKN-1 could increase resistance. A transgenic strain (LD1) containing the full-length SKN-1 protein fused to GFP expresses this construct and the SKN-1 protein is functional (An & Blackwell 2003). LD1 strain nematodes exhibit increased viability in the presence of MeHg compared to WT (**Fig. 17A**). WDR-23 is a negative regulator of SKN-1 function, therefore decreased expression of *wdr-23* allows greater SKN-1 activity (Choe *et al.* 2009). RNAi mediated knockdown of *wdr-23* results in decreased animal death following MeHg exposure (**Fig. 17B**). These results indicate that increased expression and/or activity of SKN-1 can reduce MeHg toxicity.

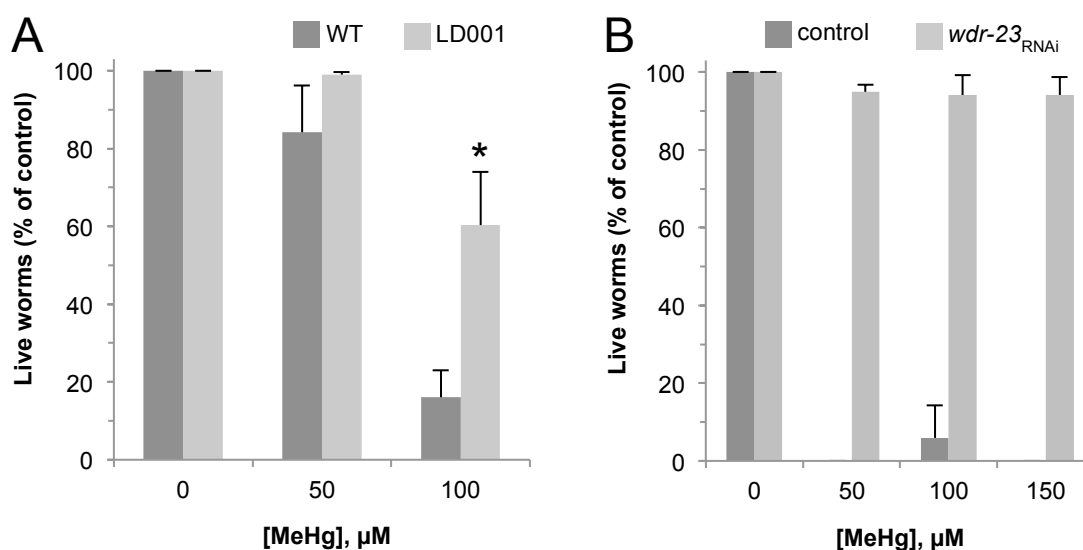


Figure 17. Overexpression or increased activity of SKN-1 increases resistance to MeHg. LD1 (SKN-1::GFP) animals are more resistant to MeHg than WT (A). RNAi knockdown of *wdr-23*, a negative regulator of SKN-1, also inhibits MeHg-induced animal death (B). Note that exposure in A was on 8P plates and B was on RNAi plates, explaining the discrepancy between the % live WT animals at 50 μM .

B. SKN-1 regulates MeHg-induced gene expression

It has been reported that SKN-1 regulates the expression of several GSTs in *C. elegans* (An *et al.* 2005). At least 3 SKN-1 binding sites are found in the promoter region (1 kb upstream of the start codon) of *gst-4*, *gst-5*, *gst-12* and *gst-38*, however *gst-21* has no SKN-1 binding sites. Given the microarray and RT-PCR results, and the involvement of SKN-1 in whole-animal viability, I determined if the expression of the upregulated GSTs was dependent on SKN-1. Nematodes were grown on control or *skn-1* RNAi bacteria for 48 hours, then exposed to 25 μM MeHg for 4 hours and RNA was isolated from the animals. RT-PCR was used to measure gene expression, and results are presented as fold change in MeHg-treated samples relative to unexposed. The induction of *gst-4* and *gst-38* is significantly decreased after *skn-1* RNAi relative to WT, approximately 15 and 55 fold less (**Fig. 18**). This is consistent with the inhibition of induction of *gst-4* and *gst-38* by *skn-1* RNAi following hyperbaric oxygen exposure (Park *et al.* 2009). *skn-1* is also necessary for the induction of *gst-12* by hyperbaric oxygen, however this gene is not significantly different in my results, indicating that the *skn-1* response may vary with different toxicants (hyperbaric oxygen versus MeHg). There may be a reduction in *gst-5*

and *gst-12* following *skn-1* RNAi, although not significant in this experiment. *gst-21* expression does not decrease after *skn-1* RNAi consistent with the lack of SKN-1 binding sites in its promoter. These results indicate that MeHg-associated induction of *gst-4* and *gst-38* is largely dependent on the expression of *skn-1*, and suggests that the corresponding proteins levels may also be *skn-1*-dependent.

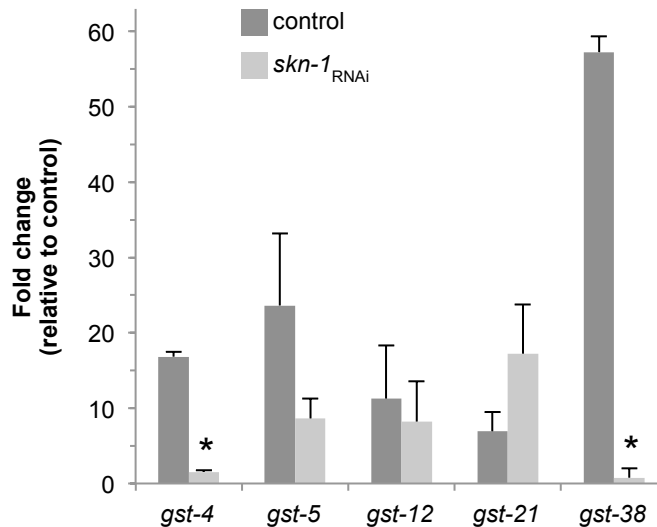


Figure 18. SKN-1 regulates the expression of GSTs. RNAi sensitive NL2099s were grown on *skn-1* RNAi or control bacteria for 48 hours, then exposed to 25 μ M MeHg for 4 hours. RT-PCR was used to quantify mRNA expression by the ddCt method. Fold change in mRNA levels after MeHg exposure relative to control is presented for WT and *skn-1* RNAi animals. The expression of *gst-4* and *gst-38* is significantly lower in *skn-1* RNAi animals compared to WT. Paired t-tests were performed on log-transformed fold-change values, * indicates $p < 0.01$.

C. SKN-1 regulates GST-38 expression

To determine if GST-38 protein expression is also dependent on *skn-1*, antibodies to GST-38 were generated, and protein levels were determined following exposure to 25 μ M MeHg for 4 hrs. Consistent with the induction of *gst-38* mRNA expression, exposure to the toxicant results in an approximate 12-fold increase in GST-38 protein levels (**Fig. 19**). Furthermore, MeHg-associated induction of the GST-38 protein appears to be highly dependent on *skn-1* as genetic knockdown of the transcription factor inhibits the increase in GST-38 following exposure to MeHg.

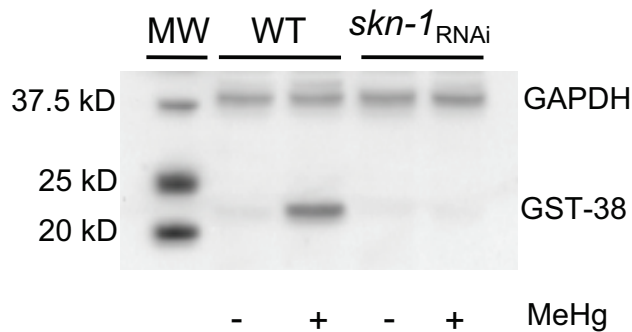


Figure 19. MeHg-induced expression of GST-38 protein is dependent on *skn-1*. Animals were exposed as for RT-PCR and protein lysates were prepared. Western blot analysis with primary antibodies to GAPDH and GST-38 showed an increase in GST-38 expression following MeHg exposure in WT nematodes, but not after *skn-1* RNAi. Western blots were performed in triplicate and one representative image is shown.

D. SKN-1 is expressed in DA neurons

Nrf2 is expressed in DA neurons in mammals, and a decrease in Nrf2 gene expression *in vitro* and *in vivo* renders cells vulnerable to DA neurotoxins (Jakel *et al.* 2007, Siebert *et al.* 2009). Previous studies of SKN-1 expression and localization have included analysis of transgenic animals overexpressing SKN-1 fused to GFP (SKN-1::GFP) and suggested protein expression in the intestines and the chemosensory ASI neurons (Bishop & Guarente 2007, Tullet *et al.* 2008). However, translational reporter fusions may not give a complete representation of endogenous protein expression levels and cellular localization (Boulin *et al.* 2006). To determine whether the *C. elegans* DA neurons express SKN-1, *C. elegans* primary cultures were generated from RJ928 animals that have robust expression of GFP in DA neurons both *in vivo* and *in vitro* (Nass *et al.* 2002, Carvelli *et al.* 2004). The cells in primary cultures have been shown to express proteins and fluorescent reporters that are observed in the corresponding cells in the whole animal (Christensen *et al.* 2002). Therefore, cell type specific genes and proteins likely exhibit similar expression patterns in cell culture and whole nematodes. Differences may be seen if the protein is stage-specific; proteins only expressed in adults may not be present in the embryonic cell culture.

A primary antibody to SKN-1 was used to evaluate cellular SKN-1 expression levels. SKN-1 immunoreactivity is observed in DA neurons (**Fig. 20A-D**). Although intracellular organelle markers were not utilized, most cells had SKN-1 specific staining that

appeared to be largely localized to the nucleus, although some DA neurons were observed in which SKN-1 was present in the cytoplasm (**Fig. 20A-D**; data not shown). No specific staining was observed in any cells from animals in which *skn-1* mRNA levels were reduced using RNAi (**Fig. 20E-H**; data not shown). These results indicate that SKN-1 is expressed in DA neurons, and that a reduction in the transcription factor mRNA levels by RNAi results in a significant loss of SKN-1 immunoreactive protein expression in the DAergic cells.

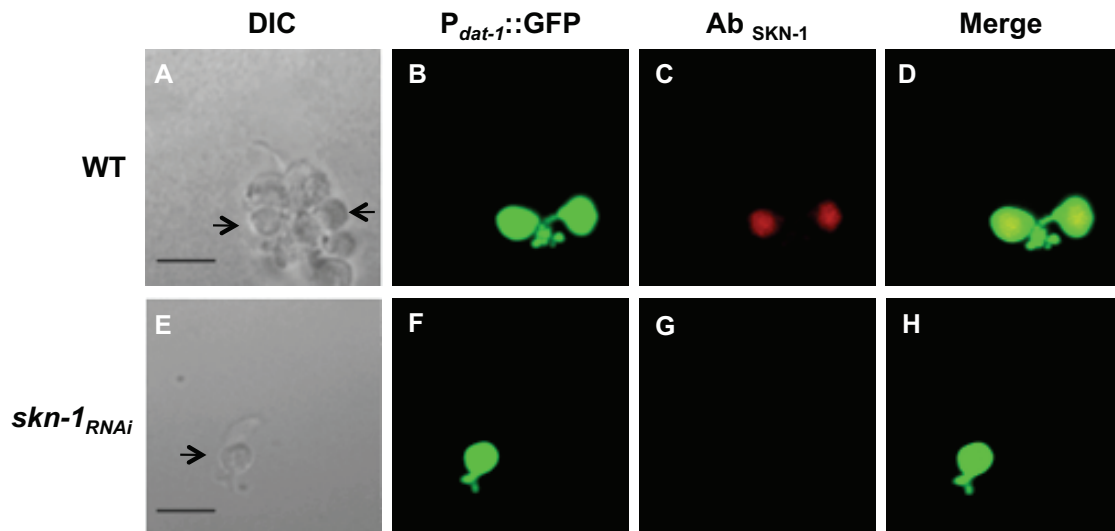


Figure 20. SKN-1 is expressed in DA neurons. Primary *C. elegans* cultures expressing GFP in the DA neurons were generated with WT (A-D) or *skn-1* RNAi animals (E-H). Cells were incubated with a SKN-1 primary antibody followed by incubation with Texas Red conjugated donkey anti-goat secondary antibodies. DIC images of WT (A) and *skn-1* RNAi (E) cultures. DA neurons from WT (B) and *skn-1* RNAi (F) animals expressing GFP driven by the *dat-1* promoter. SKN-1 is expressed in DA neurons in WT animals (C) but not in *skn-1* RNAi animals (G). (D) overlay of B-C and (H) overlay of F-G. Images were obtained with a confocal microscope, scale bar represents 5 μ m.

To further show that the antibody is specific for SKN-1, a blocking peptide complementary to the antibody was utilized. The peptide is able to bind to the antibody and prevent its reactivity with endogenous SKN-1. No reactivity is seen in WT cells when exposed to the antibody-peptide mixture, suggesting that the primary antibody is specific for SKN-1 (**Fig. 21**).

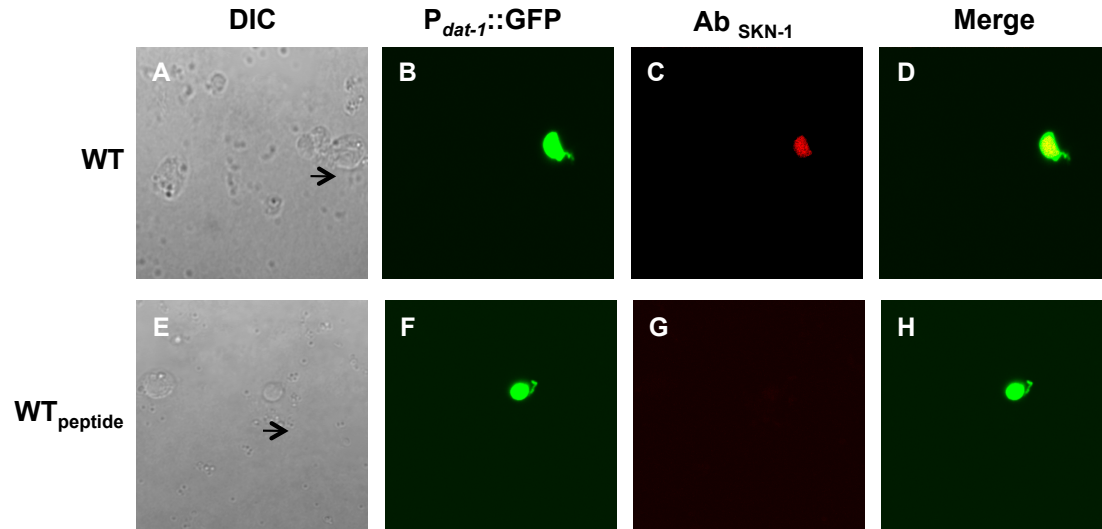


Figure 21. A specific complementary peptide blocks the reactivity of the SKN-1 antibody. Primary *C. elegans* cultures expressing GFP in the DA neurons were generated with WT animals. (E-H). Cells were incubated with a SKN-1 primary antibody (A-D) or a mixture of the SKN-1 antibody and its blocking peptide (1:5 ratio) (E-H), followed by incubation with Texas Red conjugated donkey anti-goat secondary antibodies. DA neurons are identified by GFP (B and F). SKN-1 immunoreactivity is seen in DA neurons in cells from WT animals, but not when the antibody is mixed with the blocking peptide (G). DIC (A and E) and overlay (D and H) images.

Transcriptional and translational fusion reporter strains often provide an accurate representation of a gene's expression pattern, however there are some factors that may inhibit the transgene from being observed in cells that actually express the endogenous gene. The construct may not include all the endogenous regulatory elements, such as introns and UTRs, necessary for expression in a particular cell type (Boulin *et al.* 2006). The reduced stability of GFP when fused to another protein can also decrease the fluorescence intensity and inhibit detection. Subcellular localization of a translational fusion may also impair visualization of the reporter (Boulin *et al.* 2006). Studies have shown that *C. elegans* embryonic cells in culture exhibit gene expression patterns similar to that of early larval stage nematodes (Strange *et al.* 2007). Our results demonstrate for the first time that SKN-1 is expressed in the DA neurons of *C. elegans*.

E. SKN-1 inhibits MeHg-induced DA neuron degeneration

Neuronal degeneration has been observed following MeHg exposure. In rat cortical neuron cultures, the degeneration results from the MeHg-induced downregulation of

Rac1, which normally promotes the outgrowth of neurites (Fujimura *et al.* 2009, Fujimura *et al.* 2011). Nrf2-dependent stress response pathways have been shown to inhibit MeHg- and PD-associated toxicant pathologies (Jakel *et al.* 2007, Toyama *et al.* 2007). Considering SKN-1 inhibits MeHg-induced animal death and is expressed in DA neurons, we asked whether the transcription factor may also mitigate toxicant-associated DA neuron vulnerability. First, the effectiveness of feeding RNAi for gene knockdown in the DA neurons was determined. RJ928 nematodes were grown on RNAi bacteria expressing dsRNA that targets GFP. In second-generation L4 stage animals, less than 20% of animals had normal GFP expression, indicating that the RNAi is effective (data not shown). Then L1 stage RJ928 nematodes were grown on plates containing 0.5 to 2 μ M MeHg and seeded with *skn-1* RNAi bacteria for 4 days. DA neuron viability was assessed *in vivo* as previously described (Settivari *et al.* 2009). We found that chronic exposure to sub-lethal MeHg concentrations caused a significant loss of DA neurons (up to 30% of the animals exposed to 1 μ M MeHg) in animals with a reduction of *skn-1* mRNA within 96 hours at all concentrations tested (**Fig. 22**). The DA neuron degeneration appears similar to our prior PD-associated toxicant studies in which we characterized the cellular pathology by loss of DA neuron GFP expression, decreased DA levels and loss of DA neuron integrity by electron microscopy (Nass *et al.* 2002, Settivari *et al.* 2009). The DA neurotoxicity appears to occur without large-scale cellular death as animals exposed at these concentrations for up to 5 days did not display any decrease in viability. Only 10% of *skn-1* RNAi animals had died after 6 days of exposure on the highest concentration (**Fig. 23**), consistent with the decrease in longevity of *skn-1* mutants (Oliveira *et al.* 2009). These results indicate that the *C. elegans* DA neurons are vulnerable to MeHg, and the expression of SKN-1 inhibits the toxicant-induced DA neuron degeneration.

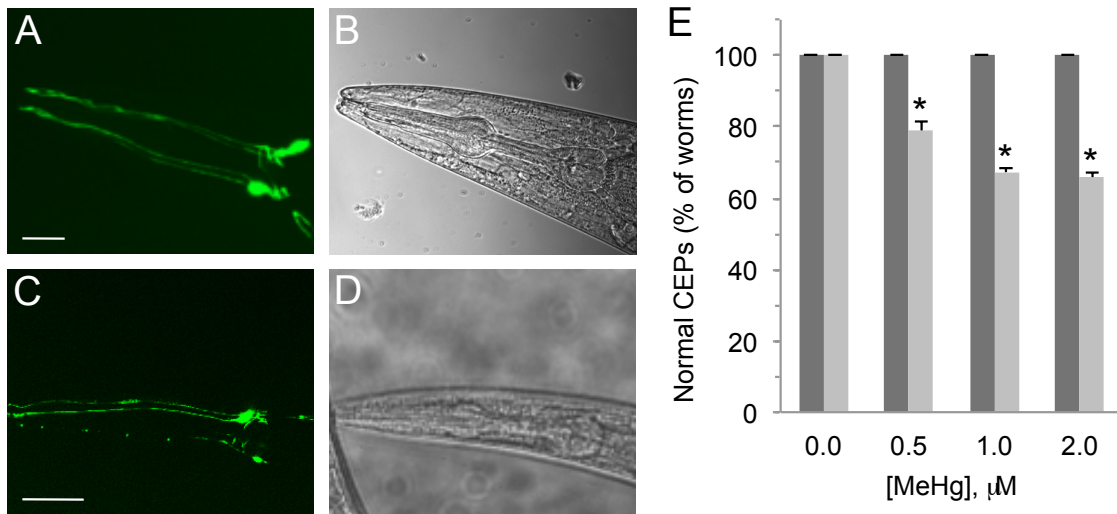


Figure 22. SKN-1 inhibits MeHg-induced DA neuron degeneration. Synchronized L1 stage RJ928 nematodes were grown on the indicated concentrations of MeHg for 4 days and the animals were scored for DA neuron degeneration. (A) GFP-expressing DA neurons within the head of a WT nematode exposed to MeHg and (B) DIC image of the corresponding animal. (C) GFP-expressing DA neurons in the head of a *skn-1* RNAi animal exposed to MeHg; image chose emphasizes significant loss of CEP cell bodies and dendrites. (D) DIC animals of the corresponding animal. (E) Quantification of DA neuron integrity in WT and *skn-1* RNAi animals, shown are mean values \pm SE of three replicates. Data was analyzed using two-way ANOVA followed by Bonferroni post test. * indicates a significant difference between *skn-1* RNAi and WT at each concentration, $p < 0.01$. Within the *skn-1* RNAi group, all the MeHg groups were significantly different ($p < 0.03$) from the 0 μ M MeHg group.

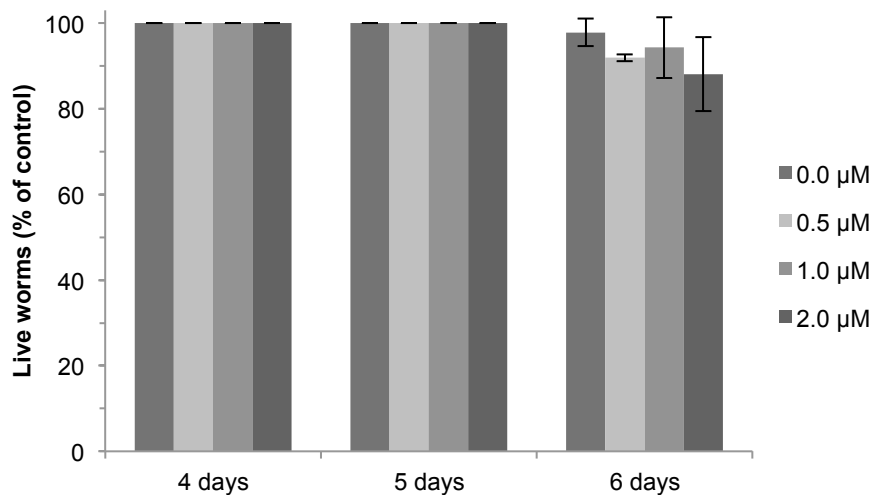


Figure 23. Viability of *skn-1* RNAi nematodes exposed to low concentrations of MeHg is not decreased for up to 5 days. L1 stage RJ928 animals were grown on *skn-1* RNAi plates containing MeHg for the indicated amount of time, and the number of live animals was determined each day.

In addition to its role in oxidative stress, SKN-1 may also control the expression of genes involved in DA regulation and signaling. Interestingly, the DA-associated genes *cat-4* (human GTPCH, GTP cyclohydrolase I), *ptps-1* (human PTPS, 6-pyruvoyl tetrahydrobiopterin synthase) and *bas-1* (human AAADC, aromatic amino acid decarboxylase) were identified to contain multiple SKN-1 binding sites and are upregulated in a SKN-1-dependent manner after arsenite stress (Oliveira *et al.* 2009). GTPCH and PTPS are involved in the synthesis of tetrahydrobiopterin (BH₄), a cofactor of TH, which catalyzes the rate-limiting step in DA synthesis. AAADC catalyzes the conversion of L-DOPA to dopamine, so altered expression of any of these genes could have an effect on DA levels. GTPCH and PTPS are decreased prior to the observation of DA neuron loss in a *Drosophila* PD model and low BH₄ levels have been observed in the cerebrospinal fluid of PD patients (Lovenberg *et al.* 1979, Scherzer *et al.* 2003). Therefore, we asked if *cat-4* plays a role in MeHg-induced DA neuron degeneration. We found that RNAi knock down of *cat-4* increases DA neuron degeneration in the presence of MeHg and double knock down of *cat-4* and *skn-1* has an additive effect (Fig. 24). Dysregulation of the metabolic pathways involving *cat-4* and *ptps-1* would disrupt DA regulation in general, but could also lead to accumulation of toxic metabolites that contribute to cell death (Blau *et al.* 2001). In *C. elegans*, *cat-4* mutants exhibit increased

permeability of their cuticle due to reduced tyrosine cross-linking, so this could also contribute to overall sensitivity, possibly by increased MeHg uptake (Loer & DePaul 2002).

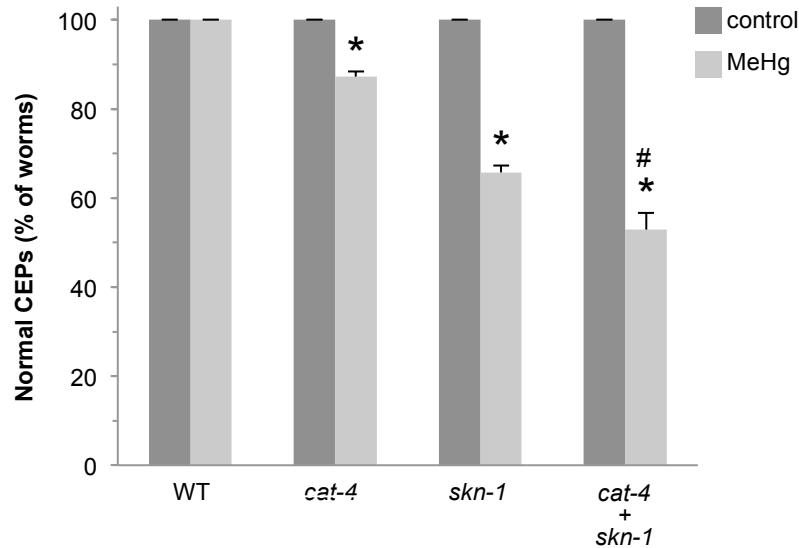


Figure 24. *cat-4* RNAi increases sensitivity to MeHg-induced DA neuron degeneration. Synchronized L1 stage RJ928 nematodes were grown on 1 μ M MeHg for 4 days and the animals were scored for DA neuron degeneration. Quantification of DA neuron integrity is shown as mean values \pm SE of three replicates. Data was analyzed using two-way ANOVA followed by Bonferroni post test. * indicates a significant difference between RNAi and WT, $p < 0.001$. # indicates a significant difference between double RNAi of *cat-4+skn-1* compared to either single RNAi, $p < 0.05$.

F. SKN-1 inhibits Aluminum-induced DA neuron degeneration

Exposure to aluminum (Al^{3+}) has been associated with the development of PD and our lab has developed a model of Al^{3+} -induced DA neuron degeneration (Zayed *et al.* 1990, VanDuyn *et al.* 2013). Al^{3+} exposure in *C. elegans* results in a decrease in mitochondrial membrane potential and ATP levels (VanDuyn *et al.* 2013). SKN-1 inhibits Al^{3+} -induced DA neuron degeneration as RNAi knockdown of *skn-1* increases the number of nematodes that exhibit DA neuron pathology (VanDuyn *et al.* 2013). Al^{3+} toxicity is facilitated by SMF-3, a protein homologous to the rice Al^{3+} transporter Nrat1 and an intracellular metal transporter in yeast, Smfp2. A strain expressing mutant *smf-3* has increased resistance to the DA neuron degeneration induced by Al^{3+} (VanDuyn *et al.* 2013). As loss of the transporter results in decreased toxicity, we hypothesized that the Al levels would be altered in the mutant strain relative to WT. Consistent with my hypothesis, I found that *smf-3* mutant animals contain higher total Al levels following

acute exposure (**Fig. 25A**). These results are consistent with a model in which SMF-3 is expressed in an intracellular compartment and transports Al^{3+} out of the compartment (**Fig. 25B**). A genetic knockout of SMF-3 would increase Al^{3+} in the intracellular compartment, sequestering the metal from the cytoplasm and other intracellular compartments, potentially inhibiting the metal-associated toxicity.

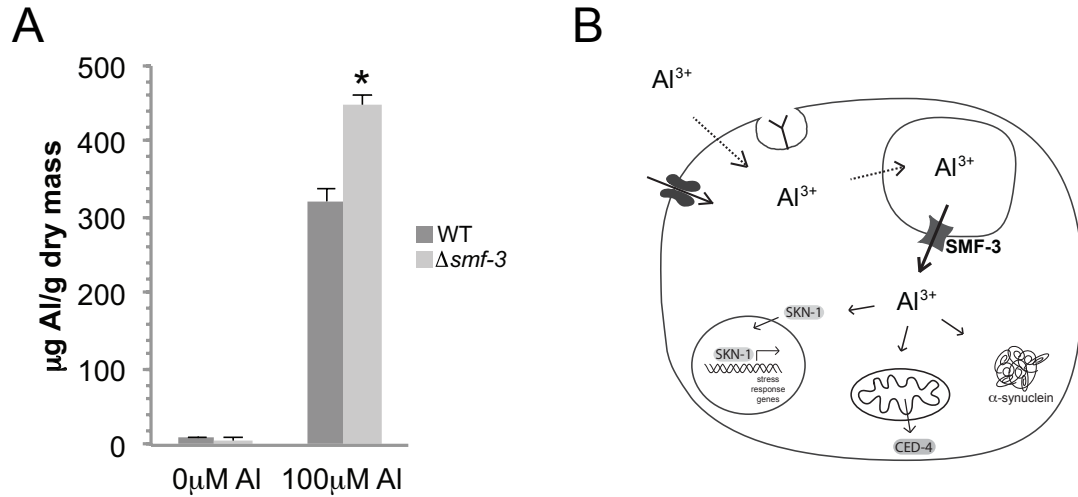


Figure 25. SMF-3 contributes to Al^{3+} -induced DA neuron degeneration. (A) Whole animal Al levels are greater in *smf-3* mutant nematodes than WT. ICP-MS was used to quantify Al following a 30 minute exposure to 100 μM Al^{3+} . (B) A model of SMF-3-associated trafficking and toxicity in DA neurons. SMF-3 promotes cytotoxicity by transporting Al^{3+} into the cytoplasm, where it can interact with SKN-1 and α -synuclein, and promote apoptosis through a pathway involving CED-4.

V. RNAi screen for mediators of MeHg toxicity

Genetic screening is a powerful tool for the identification of genes involved in a particular biological process. In a reverse genetic (RNAi) screen, the expression of individual genes is decreased and the effect of decreased gene expression is analyzed (Kamath & Ahringer 2003). I utilized this genetic tool to identify genes involved in MeHg-associated toxicity.

A. Development and implementation of a MeHg-sensitive RNAi screen

The genetic pathways and mediators of the MeHg-induced defects are largely ill-defined. In order to identify novel molecular modulators of MeHg-associated toxicity, I developed and implemented a genome wide reverse genetic screen. I have described how *C. elegans* can be used for hypothesis driven study of the mechanisms involved in MeHg toxicity for predicted targets including stress response and neuronal pathways. However, another utility of this model system lies in the ability to identify, in an unbiased fashion, molecular targets that have never before been associated with MeHg toxicity.

Over 18,500 bacteria strains, each expressing dsRNA for a specific *C. elegans* gene, were fed individually to the nematode in liquid media in 96-well plates and consumption of the bacteria results in a reduction of protein expression coded by the dsRNA-associated gene (**Fig. 26A**) (Kamath *et al.* 2001). Nematodes were grown in the RNAi bacteria for 2 days and then MeHg was added at a concentration that was not lethal to WT animals (5 μ M). After 2 more days, the OD₆₀₀ of each well was measured in a plate reader. The OD₆₀₀ indicates the amount of bacteria remaining in the wells. In wells with a high OD₆₀₀, the bacteria were not consumed and the animals may have become too sick to eat or had died. This suggests that either the dsRNA-associated gene codes for a protein necessary for growth and development under non-stressed conditions or for a protein required for maintaining viability under MeHg-associated stress. Approximately 900 genes were identified in the first round of the screen.

In order to determine if the protein targeted by the RNAi clone is necessary for viability in normal conditions or may be involved in inhibiting MeHg-associated toxicity, a second round of screening was performed in liquid media including a control well to compare to MeHg treatment (**Fig. 26B**). If both the control and MeHg containing well had low bacteria density, the initial identification of the dsRNA conferring MeHg resistance was likely a false positive due to a technical error and this gene was excluded

from further analysis. If both wells contained a high concentration of bacteria, the knockdown of gene expression likely reduced viability independent of the MeHg exposure, and these genes were also excluded. If the control well had a significantly reduced bacteria level and the MeHg-containing well had a high density of bacteria, the protein coded by the targeted gene likely inhibits MeHg toxicity, and the gene was tested in a third and final round of screening (**Fig. 26C**). The first two rounds of the screen were done with relatively low stringency to ensure that I did not miss a gene that plays a role in inhibiting MeHg-associated animal death. Numerical cut-off values for the OD₆₀₀ measurements were established and followed as described in the Methods section, but if a clone that did not meet the cut-off seemed to inhibit growth by visual inspection under a dissecting microscope, or the results were questionable, it was placed on the list to evaluate in the next round.

The first two rounds of the screen provided an indirect measurement of animal viability, quantifying the amount of bacteria consumed. For the third round, nematodes were grown on RNAi plates, exposed to MeHg and the viability of each animal was directly assessed as described for the previous live-dead assays. RNAi clones that significantly reduced viability relative to HT115 (WT control) were considered “screen hits”.

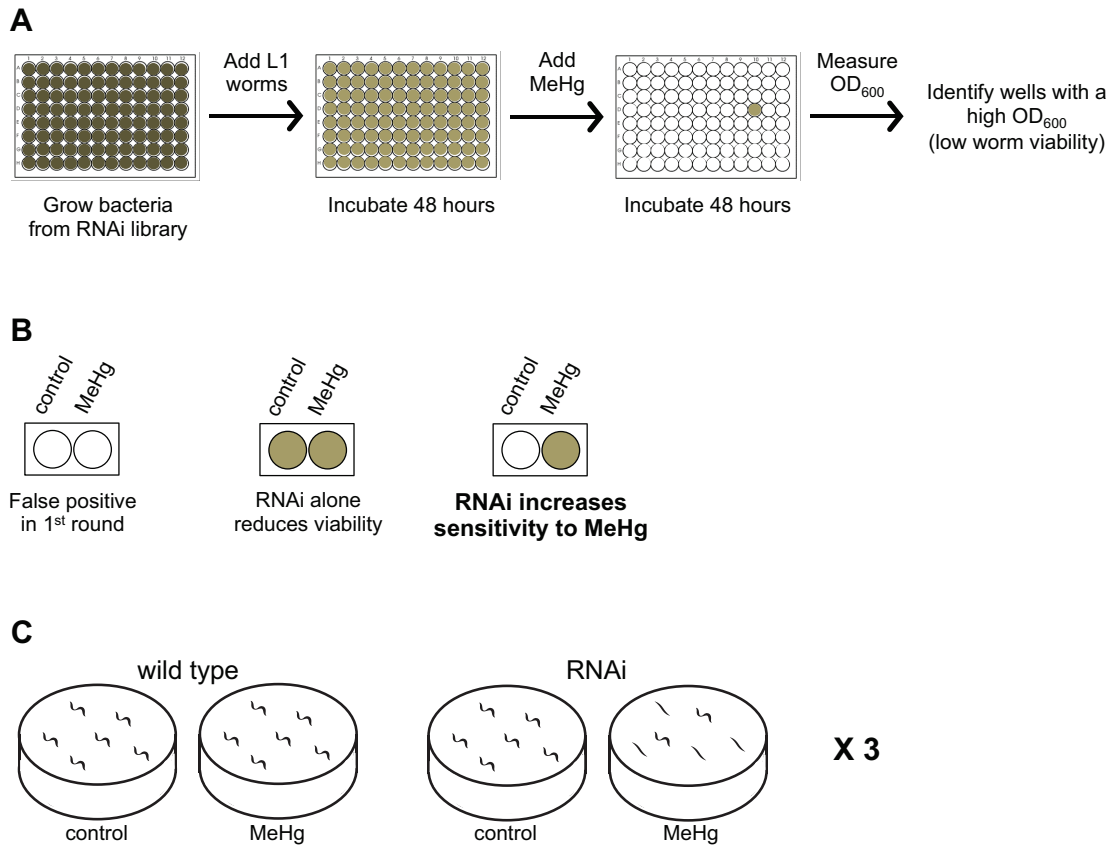


Figure 26. Work-flow diagram for the genome wide RNAi screen. In the first round screen (A), all clones were exposed to MeHg and assayed for viability. The MeHg concentration (5 μ M) allows WT nematodes to grow and consume all bacteria from the well (low OD₆₀₀) so any wells that retain bacteria (high OD₆₀₀) contain an RNAi clone that causes a change from WT. This includes genes that increase sensitivity to MeHg but also genes that are necessary for growth or development in the absence of toxicant. The second round screen (B) included a control and a MeHg treated well for each clone and allowed for differentiation between these possibilities and also identified false positives from the first round. Clones for which the control and MeHg wells were different in the second round were tested on agar plates for a direct measure of animal viability (C). At least 20 animals per plate were assayed, and the experiment was repeated three times for each clone.

Note

The screen was inadvertently performed using a media lacking some recommended additives. Standard protocols for *C. elegans* RNAi by feeding in liquid culture call for the use of S medium to resuspend the bacterial pellet. S medium contains 1 liter S basal, 10 ml 1 M potassium citrate, 10 ml trace metals solution, 3 ml 1 M CaCl₂, 3 ml 1 M MgSO₄ (Stiernagle 1999). However, I used S basal without adding the additional

ingredients. The key difference is the absence of Ca^{2+} and Mg^{2+} in S basal, resulting in a significant reduction in these elements in the final growth media. The compositions of standard nematode growth media (NGM) plates, S basal and S medium are listed in **Table 4**.

Component	Agar plates	S medium	S Basal
BactoAgar	17 g/L		
BactoPeptone	2.5 g/L		
NaCl	51.3 mM	100.1 mM	100.1 mM
K_2HPO_4	2.5 mM	5.7 mM	5.7 mM
KH_2PO_4	10 mM	44.1 mM	44.1 mM
cholesterol	5 $\mu\text{g/ml}$	5 $\mu\text{g/ml}$	5 $\mu\text{g/ml}$
CaCl_2	1.1 – 2.2 mM	2.9 mM	10-15 μM^*
MgSO_4	1.0 – 1.7 mM	2.9 mM	20 μM^*
Ampicillin	100 $\mu\text{g/ml}$	100 $\mu\text{g/ml}$	100 $\mu\text{g/ml}$
IPTG	1 mM	1 mM	1 mM
potassium citrate, pH 6.0		9.75 mM	
<u>trace metals solution</u>			
disodium EDTA		48.7 μM	
FeSO_4		24.2 μM	6 μM^*
MnCl_2		9.8 μM	
ZnSO_4		9.8 μM	
CuSO_4		0.975 μM	

Table 4. Composition of *C. elegans* growth media. * indicates the concentration is estimated based on the amount present in the *E. coli* culture.

To determine if the different growth medias may affect nematode viability as determined by bacteria consumption under my screening conditions, 96 well plates were prepared containing HT115 bacteria suspended in S medium, S basal, S medium minus Ca^{2+} or S medium minus Mg^{2+} . The OD_{600} was measured each day for 4 days, and the results were expressed as the bacteria remaining (% of day 0) (**Fig. 27**). There was no significant difference between S medium and S basal, or when the Ca^{2+} or Mg^{2+} were excluded from the S medium. Although the bacteria remaining in the no Ca^{2+} /MeHg

group appears increased at day 3 and 4 (**Fig. 27C**), the variability is such that the difference is not significant. Viability assays were also performed with various concentrations of Ca^{2+} and Mg^{2+} added to S basal solution and no differences were observed (data not shown).

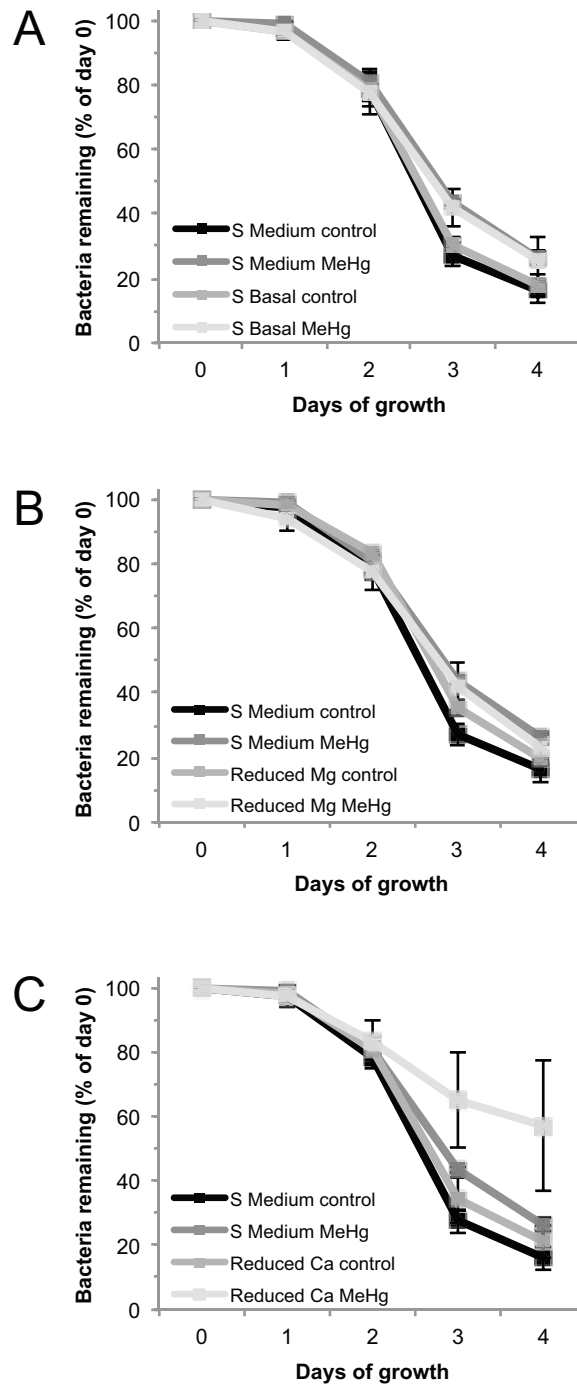


Figure 27. The reduction of Ca^{2+} or Mg^{2+} levels does not significantly affect nematode growth. NL2099 strain nematodes were grown in 96 well plates following the conditions of the RNAi screen using the indicated solutions to resuspend the HT115 (WT) bacteria. MeHg was added on day 2 to 5 μM . The OD_{600} was measured each day and presented as the % of day 0. Comparisons were made between S medium and S basal (A), S medium and S medium with reduced Mg (B) and S medium and S medium with reduced Ca^{2+} (C).

Ca²⁺ and Mg²⁺ are required for animal viability, however under the conditions of my screen, there appeared to be little effect from the reduction of these elements. During the screen knockdown of 242 genes in the Open Biosystems library decreased the growth or viability of the nematodes in the absence of MeHg. 216 of these genes (89%) have been previously reported to produce developmental or lethal phenotypes in literature. I also observed phenotypes (dumpy, clear, protruding vulva, sterile) that have been reported in other RNAi screens, indicating that the overall effectiveness of RNAi was not significantly impaired by the modified media. Also, several genes were identified as screen hits that have been previously implicated in MeHg toxicity: *skn-1* (Nrf2 in mammals); *eft-3*, *eft-4*, *cyc-1* (zebrafish muscle microarray data); *ubc-1* (MEF microarray data); proteasome-associated genes (yeast and MEF data). The third round of screening was carried out on RNAi agar plates, which contained normal levels of the elements found in the standard media. Overall, the reduction of Ca²⁺ and Mg²⁺ levels appear to have had minimal impact on the results of the screen. However, it is possible that some genes may not have been identified in the modified media that would have been in normal media.

B. Results

Of the approximately 18,500 genes that were screened, 92 genes were identified to code for proteins whose expression increases resistance to MeHg-associated animal death. These genes are strongly biased towards mechanisms that affect the mitochondria, transcription, translation, and calcium signaling, and will be reported in a future publication (**Table 5, Fig. 28**). SKN-1 was identified in the screen, providing further validation of the method to identify genes whose expression inhibits MeHg-associated animal death.

Cellular process	Number of genes
signaling	19
translation	16
transcription	12
protein degradation	8
transport	8
energetics	7
mRNA processing	7
structure	7
replication	3
endocytosis	3
apoptosis	2

Table 5. Groups of genes whose reduced expression increases MeHg-associated animal death. The screen hits are grouped into classes based on the cellular process that they are likely involved in. If the function of the *C. elegans* gene has not been reported or predicted, the function of the human homologue was used for classification.

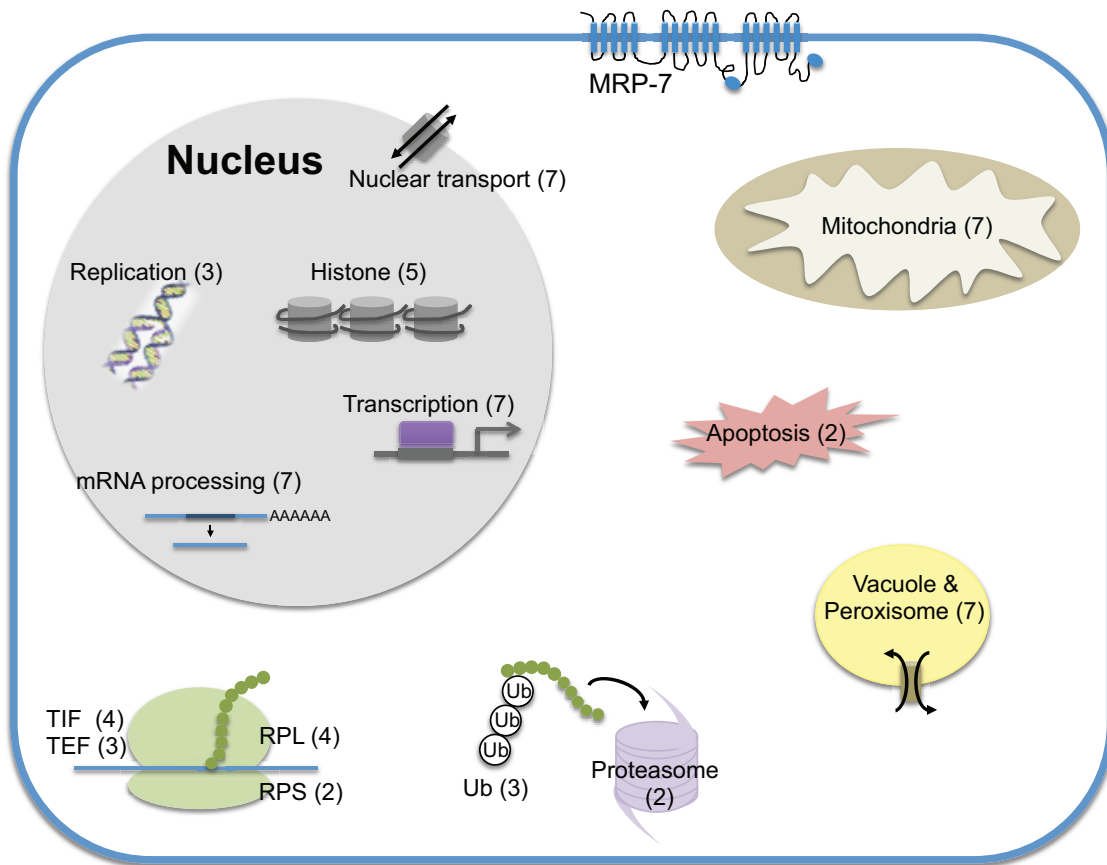


Figure 28. A summary of the screen results. The number in parentheses represents the number of genes associated with that organelle or cellular process.

One of the more robust hits observed in the screen was produced by the clone in well III-6J08 of the Source BioScience library (Kamath & Ahringer 2003). Library annotation labeled this clone as C51G7.a and this primer set produces an amplicon that overlaps the *wah-1* gene (genomic location III:11,995,030..11,997,474). The sub-library containing only the Source BioScience clones not present in the Open Biosystems library was created based on the provided library annotation. It has been reported that mistakes exist in the Source BioScience library and its annotation (Qu *et al.* 2011). Also, the names given to the original GenePairs primers may now correspond to another sequence name as the *C. elegans* genome has been updated, so the different names may result in some genes being targeted by clones in both libraries. The different nomenclature led to the inclusion of C51G7.a in the sub-library despite the presence of *wah-1* in the Open Biosystems library. Interestingly, *wah-1* was not a positive hit when

screened in the Open Biosystems library. The strong phenotype of this clone labeled C51G7.a and the discrepancy between the libraries led me to investigate further and sequence both clones. The Open Biosystems *wah-1* sequencing result matched *wah-1* in the *C. elegans* genome. The results for the clone labeled C51G7.a mapped to the gene *mrp-7*, a predicted ABC transporter (www.WormBase.org).

VI. The transporter MRP-7 inhibits MeHg toxicity

MRP-7 was the most robust hit from the RNAi screen and this gene was previously uncharacterized in *C. elegans*. Given the role of ABC transporters in MeHg toxicity, I further investigated the role of MRP-7 in the *C. elegans* response to MeHg.

A. MRP-7 is homologous to human MRP1

A BLAST search of the *C. elegans* MRP-7 sequence revealed that 14 human proteins match with an E value of 0.0, with identity scores ranging from 31-43%. MRP1 (ABCC1) shares 43% identity and 61% similarity with MRP-7, the highest of any of the MRPs, so a sequence alignment was prepared between these proteins. Human MRP1 (accession NP_004987.2) was obtained from the NCBI Protein database and *C. elegans* MRP-7 sequence was obtained from Wormbase.org. ClustalW was used to align the sequences (**Fig. 29**). Fully conserved residues are highlighted in dark gray and residues that are similar between the two sequences are highlighted in light gray (this includes both strongly and weakly similar residues as defined by ClustalW). The transmembrane helices of MRP1 are indicated by a thick black line (Bakos *et al.* 1996). The Walker A, Walker B and the ABC signature sequences of MRP1 are indicated in boxes (Frelet & Klein 2006). There is high conservation of these consensus sequences between the human and *C. elegans* proteins. Walker A and B are nucleotide binding domains that have a conserved sequence between a wide array of proteins that bind ATP (Walker *et al.* 1982). The ABC signature sequence, also called Walker C, is required for ATPase activity (Ren *et al.* 2004). The similarity between the protein sequences suggests that MRP-7 may have similar substrates to MRP1, one of which is MeHg (Rush *et al.* 2012).

```

MRP1  MALRGFCSADGSDPLWDWNVTWNTSNPDFTKCFONTVLVWVPCFYLWACFFFY--FLYLSRHRDGYIQMTPLNKTKTALG 78
MRP-7  -MLESFPCGDG-----HPFSTGLPNVSIQAQHTVLVWVPAAFFLLTLPFLSAQCHLTAQRFAFLPFSAHFIIKLLLV 70

MRP1  FLLWIVCWADLFYSFWERSRGIFLAPVFLVSPTELLGITMLLATFLIQLER-RKGVOSSGIMLTFWLVALVICALAILRSKI 157
MRP-7  AFLAANSLATWCYVLFSSKNS---YAAAYVYVPLGW-VLVWTGTFLVHLIRLRCLVSSGQHVTSLIFLLCGAPEFYQWI 146

MRP1  MTALKEDAQVDL-----FRDITFYVYFSLLLIQLVLSCFSDRSPLFSETIHDPN---PCPESSASFLSRITFWWITGL 227
MRP-7  RMENSNSFPNDLTTTDSAQFLSIAYLSWYSALLIYTFSLCFADPRGAKTDEKASSKSAASPELQSSFLNRLTLWWFNSI 226

MRP1  IVRGYRQPLEGSDLWLNKEDTSEQVVPVLVKNWKKKCAKTRKQPVKVYVSSKDPAPKESKVDANEVEEVALIVKSPQK 307
MRP-7  PWTGARRDLEIDDFELNERSGTEFLSELWESFWEPKRLKYIHD--TSIWAKKDPSE-----QEKDPVVI----- 289

MRP1  EWNPSLFKVLKTFGPYFLMSFFFKAIHDLMMFSGPOILKLLIKFVNDTKAPDWQGYFYTVLLEFVTACLQTLVLHQQFYH 387
MRP-7  ---PSVVSSLFMMFRWELLASTLKFVSDTMQFASPFLLHELLNFI SAKNAPFWKGMALSILMFSVSELRSLLNGFYVI 366

MRP1  CFVSGMRIKTAVIGAVYRKALVITNSARKSSTVGEIVNLSVDAQRFMDLATYINMIWSAPLQVILALYLLWNLGQPSVL 467
MRP-7  MFRMGTKIQTSLTAAVYKKTLLISNSARDRVGEIVNLMADIVERFQMITPQIQQFWSQYQITFALVYLFITLGYSA 446

MRP1  AGVAVMVLMPVNAVMAAMKTKTYQVAHMKSKDNRIKLMNEILNGIKVLKLYAWELAFKDKVLAIRQEEELKVLKKSAYLSA 547
MRP-7  PGVIMVIFVPMNIISSMIVRKWQEQMKLKBERTKMNVEVLNGIKVVKLYAWEVPEAYIDEIRTKELALIKKSAMVRN 526

MRP1  VGTFTWVCTPFLVALCTFAVYVTIDENNILDAQTAQFVSLALFNILRFPLNILPMVISSIVQASVSLKRLRIFLSHEEELP 627
MRP-7  ILDSFNATASPFLVALFSEGTFLSNPSHLLTPQIAFVSLALFNQLRSPMTMIALLINQAVQAVVSNKRLKEFLVAEELDE 606
Walker A
MRP1  DSIERRPVKDGCGTNSITVRNATFTWARS DPP--TLNGITFSIPEGALVAVVGOVCGKSSLLSALLAEMDKVEGHVAI 704
MRP-7  KCVDR-SVNIERSHNAVRVENLTASWDPEEAAGEKTLQDQVDTAPRNSLIAVVGVKVGSGKSSLLQALLGEMGKLRGRIGV 685
ABC signature
MRP1  KGSVAYVPQQAWIQNDSLRENILFCQLEEPYRSVIQACALLPDLIELPSGDRTEIGEKGVNLSGGQKQVSLARAVYS 784
MRP-7  NGRVAYVPQQPWIQNMTLRDNITFGRPFDRKRYDQVLYACALKADIKILPAGDQTEIGEKGINLSGGQKARVSLARAVYQ 765
Walker B
MRP1  NADIVLFDPLSAVDAHVKHIFENVIGPKGMLKNKTRILVTHSMSVLPQVDVIVMSGGKISEMGSYOELLARDGAFAB 864
MRP-7  NLDVYLLDDPLSAVDAHVGRHIFEKVIQGNLLREKTRILVTHGLTYTKMADELVMLEKIEESGTFEHLIKRRLGDFD 845

MRP1  FLRTYAS----TEQEQDAEENGVTGVSQPGKEAKQMEGLVTDTSAGKQLQRQLSSSSSYSGDISRHHNSTAELQKAEAK 940
MRP-7  FMEEYKSGSDNSSEAGSODDDFEAIGGEIQDYMNPEDVVLTVTNDLDETIPTPELTTQISTMSSPEKPTGTSPAATE 925

MRP1  KEETWKLMEADKAQTGOVKLSVYWDYMKAIGLFISFLSFLFMCNHSALASNYWLSLWTDPIVNGTQEHKTKVR---LS 1017
MRP-7  SQN--KLIKKEGIAQGVKVEIATYQLYVKAAGYLLSIAFICFFIVYMTLQTLRSFWLSAWSDEYDPSAHPMAKGWRLG 1003

MRP1  VYGALGISQGIAVEGYSMAVSIIGGILASRCLHVDLLHSILRSPMSFFERTPSGNLVNRFKELDVTDSMIPEVIMKFMGS 1097
MRP-7  VYGALGFSETACFFVALLALVFGORASKNLHGPLIHNLMRSPMSFYDTPLGRILNRCADIDETIDMMLPMNFRYLVMC 1083

MRP1  LFNVIACIVILLATPIAIIIPPLGLIYFFVQRFYVASSRQLKRLSVSRSPVYSHFNETLLGVSVIRAFEEQERFIHQ 1177
MRP-7  VLOVAFTLIVIIISTPLFAVVILPLALYILFLRYVPTSRQLKRLSVHRSPYIYSHFGETIQGAASIRAFQKVDDEFROD 1163

MRP1  SDLKVDENQKAYPISIVANRWLAVRLECVGNCIVLFAALFAVISRHSS--LSAGLVGLSVSYSLQVTTYLNWLVMSSEM 1254
MRP-7  SGRILDTFIRCRYSSLVSNRWLAVRLEFVGNCFIIFAAALFAVLSKEFGWITSPGVIGVSVSYALNITEVLNFAVRQVSEI 1243
Walker A
MRP1  ETNIVAVERLKEYSETEKEAPWQIQETAPPSSWPQVGRVEFRNYCLRYREDLDFVLRHINVTINGGEKVGIVGRTGAGKS 1334
MRP-7  EANIVSVERVNEYTNPNEAPWRIEGREPAPGWPSRGVVKFDGYSTRYREGLDLVLDHISADVAAGEKIGIVGRTGAGKS 1323

MRP1  SLTLGLFRINESAEGEIIDIIGINIAKIGLHDLRFKTIITIPQDPVLFSGSLRMNLDPFSSQYSDEEVWTSLELAHLKDFVSA 1414
MRP-7  SFALALFRMIEAAGGRIVDDVEVSQIGLHDLRSNITITIPQDPVLFSGTLRFNLDPFPTYSDDQIWRALELAHLKHAAG 1403
ABC signature Walker B
MRP1  LPDKLDHECAEGGENLSVQORQLVCLARALLRKTILVLDDEATAAVDLETDDLQSTIRTOFEDCTVLTIAHRLNTIMDY 1494
MRP-7  LPDGLLYKISEAGENLSVQORQLVALARALLRHTRVLVLDDEATAAVDVATDALIQETIREEFKECTVFTIAHRLNTIMDY 1483

MRP1  TRVIVLDKGETQEYGAPSDLLQOR-GLFYMAKDAGLV---- 1531
MRP-7  DRIMVLDKGSILEFDTDPALMADKNSAFKMOVADAAEQDKHE 1525

```

Figure 29. Sequence alignment of human MRP1 with *C. elegans* MRP-7. ClustalW was used to align human MRP1 (accession NP_004987.2) with *C. elegans* MRP-7 (accession NP_507812.3). Identical residues are highlighted in dark gray and similar residues are highlighted in light gray. Thick black lines indicate the transmembrane domains of MRP1 and the conserved Walker A, Walker B and ABC signature sequences are boxed.

B. MRP-7 inhibits MeHg-induced animal death

RNAi mediated knock down of *mrp-7* was found to reduce animal viability in the screen, resulting in 0% live animals on 10 μM MeHg. Nematodes were then grown on *mrp-7* RNAi bacteria and the reduction in *mrp-7* RNAi levels was confirmed by RT-PCR (data not shown). Animals were transferred to plates containing MeHg from 0 to 10 μM MeHg and the number of live animals was counted 48 hours later. The reduction in *mrp-7* expression results in a dramatic decrease in animal viability, resulting in an LC50 of 5 μM (Fig. 30). These results indicate that MRP-7 inhibits MeHg-induced animal death in a concentration dependent manner. Vertebrate MRPs have been shown to confer increased resistance to toxic substrates in a dose-dependent manner, largely by pumping substances out of the cell (Leslie *et al.* 2004). MRP-7 may also be inhibiting toxicity through limiting MeHg accumulation within the cell.

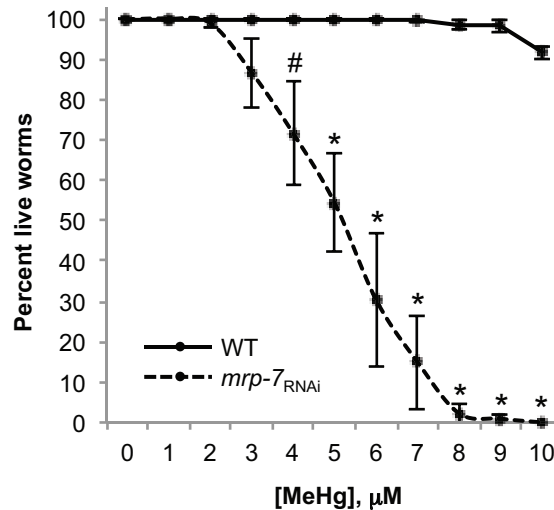


Figure 30. MRP-7 inhibits MeHg-induced whole animal death. RNAi sensitive NL2099 nematodes were grown on RNAi bacteria to knock down *mrp-7* expression or empty vector for WT control and 2nd generation L3 animals were exposed to the indicated concentrations of MeHg for 48 hours. The number of live animals was counted and indicated as the percent of the total number of animals (> 50 per condition). The data is presented as mean \pm SEM of 4 independent replicates. Data was analyzed by two-way ANOVA with Bonferroni post-tests. *mrp-7* RNAi is significantly different from WT with $p < 0.05$ (#) or $p < 0.001$ (*).

There are 8 MRP genes in *C. elegans*, but *mrp-7* was the only ABC transporter identified in the screen. As there is high homology among the MRPs, I wanted to verify that the other transporters were not playing a role in MeHg-associated animal viability. I

utilized RNAi to knock down gene expression of *mrp-1* – *8* and exposed the nematodes to 10 μ M MeHg as described above. All knockdown groups showed similar viability as WT except for *mrp-7* (**Fig. 31**). Although these studies do not exclude a role for other MRP transporters in MeHg toxicity, under these conditions their expression does not appear to affect MeHg-induced lethality.

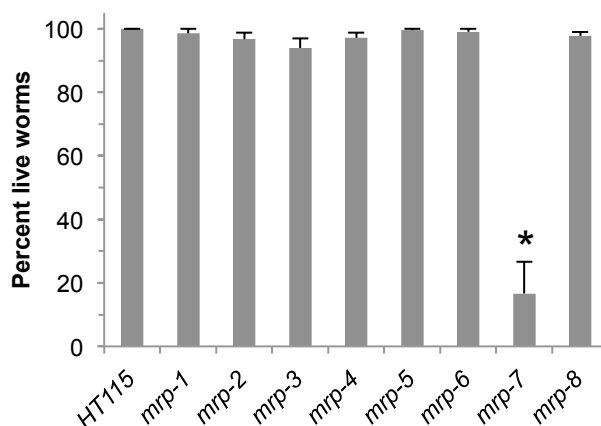


Figure 31. Other MRPs do not affect MeHg-induced lethality. RNAi sensitive NL2099 nematodes were grown on RNAi bacteria to knock down gene expression or empty vector for WT control and second-generation animals were exposed to 10 μ M MeHg for 48 hours. The number of live animals was counted and indicated as the percent of the total number of animals (> 50 per condition). The data is presented as mean \pm SEM of 3 independent replicates. Data was analyzed by one-way ANOVA with a Bonferroni post-test, * indicates $p < 0.001$.

C. MRP-7 inhibits accumulation of Hg

Expression of MRP1 confers resistance to a variety of toxicants, including metals and GSH conjugates, by increasing their excretion (Dallas *et al.* 2006). Considering the high homology between MRP1 and MRP-7, I asked whether MRP-7 may be involved in regulating cellular Hg levels. To determine if MRP-7 expression can modulate whole animal Hg levels, WT and *mrp-7* RNAi adult animals were grown on 1 μ M MeHg for up to 48 hours and whole animal Hg levels were determined by ICP-MS. Chronic MeHg exposure resulted in approximately 2-fold higher levels of Hg in *mrp-7* RNAi versus WT animals at the later time points (**Fig. 32**). Other experiments using different stage nematodes have shown a significant difference as early as 24 hours (data not shown). These results indicate that MRP-7 may be inhibiting MeHg toxicity by increasing cellular export of the compound.

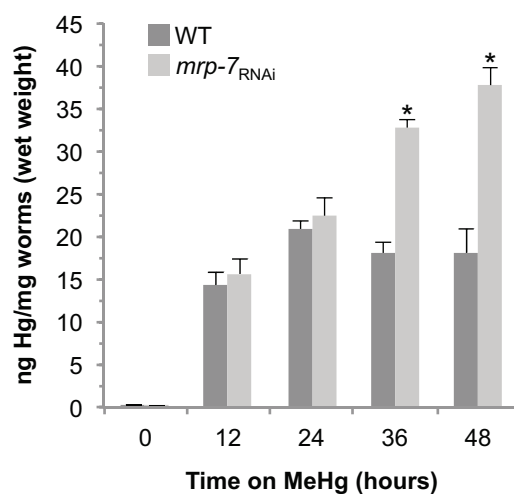


Figure 32. MRP-7 inhibits the accumulation of MeHg. RNAi sensitive NL2099 nematodes were grown on RNAi bacteria knocking down *mrp-7* expression or empty vector for WT control and second-generation adult animals were exposed to 1 μ M MeHg for the indicated amount of time. Following exposure, animals were collected and the Hg content was measured by ICP-MS. Hg content was normalized to the wet weight of the nematode samples and the data is presented as mean \pm SEM of 4 independent replicates. Data was analyzed by two-way ANOVA with Bonferroni post-tests. *mrp-7* RNAi is significantly different from WT with $p < 0.001$ (*).

The amount of Hg that accumulates in WT nematodes (~ 20 ppm) is in the range of that found in the brains of humans and other mammals following MeHg exposure. The brain of an infant that died in Iraq following *in utero* MeHg exposure contained 13.7 ppm total Hg (Choi *et al.* 1978). After 8 weeks of MeHg consumption, adult mice had brain Hg concentrations as high as 23 ppm (Fujimura *et al.* 2009). Most studies suggest that brain Hg levels above 1 ppm could begin to lead to neurological changes in humans, so while these cases may be at the higher end of the spectrum, the amounts of MeHg used in my *C. elegans* studies are within the range and highly relevant to human and vertebrate studies. Furthermore, the amount of MeHg necessary to elicit DA neuron degeneration in *C. elegans* ($\sim 0.5 - 1$ μ M) is as low or lower than the concentrations used in cell culture experiments. For example, cell death is observed in about 50% of cortical neurons exposed to 100 nM MeHg for 3 days (Fujimura *et al.* 2011). PC12 cells exhibit significant cell death after 2 hour exposure to 5 μ M MeHg (Tiernan *et al.* 2013). In SH-SY5Y cells, 1 μ M for 6 hours was a sub-lethal dose that induced significant changes in gene expression (Toyama *et al.* 2011b).

D. MRP-7 expression reduces the MeHg-associated stress response

I have shown that MeHg exposure increases ROS and induces a stress response indicated by the increased expression of GSTs in WT animals (**Fig. 13 and 14**). The greater sensitivity and higher Hg levels in *mrp-7* RNAi animals led me to further investigate the gene expression changes in these animals. RT-PCR was performed following acute (4 hours on 25 μ M MeHg) or chronic (4 days on 400 nM MeHg) exposure. Acute MeHg exposure results in an induction of *gst-38* and *hsp-16.1*, and there is no significant difference between the WT response and that of *mrp-7* RNAi animals (**Fig. 33A and B**). There is also no difference in cellular Hg content between WT and *mrp-7* RNAi at early time points of exposure (**Fig. 32**), suggesting that the stress levels may be similar. Chronic MeHg exposure in *mrp-7* RNAi animals may result in greater intracellular stress compared to WT as *gst-1*, *hsp-4* and *hsp-6* mRNA levels are significantly increased following chronic exposure but not in WT animals (**Fig. 33C and D**). The gene expression changes are consistent with the ICP-MS data in that higher Hg levels are observed in *mrp-7* RNAi animals compared to WT at later time points (**Fig. 32**). Acute exposure (2, 4 or 8 hours) to MeHg in WT animals did not increase *gst-1* levels (**Fig. 14 and Fig. 33A**), however a significant increase was observed under the chronic exposure conditions that result in higher total Hg levels (4 days).

The HSP genes selected for analysis are indicative of stress in specific cellular compartments. HSP-4 is homologous to the human BiP/GRP78 and is upregulated in response to ER stress and the UPR (Kaufman 1999, Shen *et al.* 2001). HSP-6 is specifically activated by the mitochondrial UPR (Yoneda *et al.* 2004). HSP-16.1 is in the family of small HSPs that function in stress resistance in *C. elegans* and was found to be localized to the Golgi apparatus (Kourtis *et al.* 2012). Therefore, the increased expression of these genes not only indicates cellular stress induced by MeHg, but also may suggest that the ER, mitochondria and Golgi apparatus are cellular targets of MeHg.

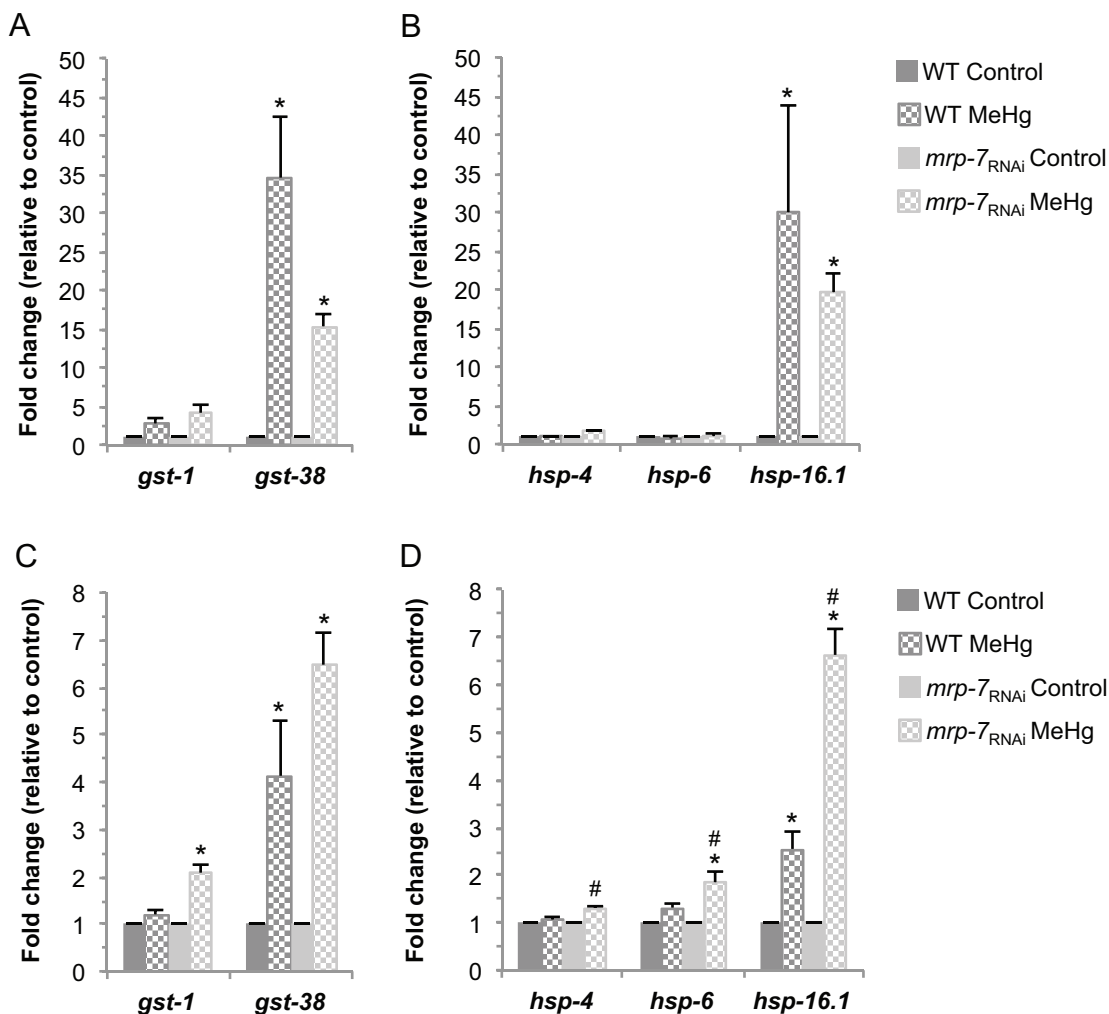


Figure 33. GST and HSP mRNA expression are increased following MeHg exposure. Animals were exposed to 25 μ M MeHg for 4 hours (A and B) or 400 nM MeHg for 4 days (C and D) and mRNA expression was measured by RT-PCR and analyzed using the ddCt method with normalization to GAPDH. dCt values for each gene were analyzed by one-way ANOVA followed by a Bonferroni post-test, * indicates a significant difference from the control treated group at $p < 0.001$ (A), $p < 0.01$ (B and D) or $p < 0.05$ (C), # indicates a significant difference between the WT and *mrp-7* RNAi MeHg treated groups at $p < 0.05$.

E. *mrp-7* mRNA levels are increased following MeHg exposure

The microarray and RT-PCR studies presented in this thesis demonstrate that the expression of numerous genes that may contribute to inhibiting the toxicity of MeHg are upregulated following exposure to the toxicant. Therefore, I hypothesized that *mrp-7* expression may also be upregulated following MeHg exposure. Short-term exposure to MeHg resulted in no change in *mrp-7* mRNA levels (data not shown), however a 4 day

exposure to 400 nM MeHg caused a significant increase in *mrp-7* expression (**Fig. 34**). This is consistent with studies in vertebrate cell culture. Exposure of a fish cell line to HgCl_2 induced expression of 4 *abcc* (MRP) mRNAs (Della Torre *et al.* 2012). Inorganic Hg also increases expression of MRP1 and MRP2 at both the gene and protein level in Madin-Darby canine kidney (MDCK) cells (Aleo *et al.* 2005). MeHg could be causing an increase in expression of the transporter in an attempt to lower cellular Hg levels and decrease toxicity.

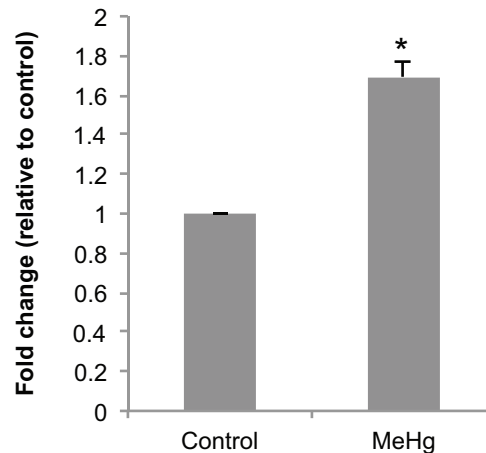


Figure 34. *mrp-7* mRNA levels are increased following chronic MeHg exposure. NL2099 L1 stage nematodes were grown on 400 nM MeHg for 4 days and *mrp-7* mRNA expression was measured by RT-PCR and analyzed using the ddCt method with normalization to GAPDH. dCt values for control and MeHg groups were compared using a student's t-test. * indicates a significant difference, $p < 0.05$.

F. MRP-7 inhibits DA neuron degeneration

As MRP-7 contributes to whole animal death, I asked if the transporter may function in DA neurons to reduce cytotoxicity. L1 animals were grown on plates containing various concentrations of MeHg and seeded with RNAi bacteria targeting *mrp-7* or containing an empty vector. Initially, 1 μM MeHg was used as in the *skn-1* experiments, but this concentration resulted in delayed development of *mrp-7* RNAi nematodes, so concentrations were reduced to 100 – 500 nM. Following a 96 hour exposure to MeHg, the DA neurons were evaluated under a fluorescent dissecting microscope. Chronic exposure of *mrp-7* RNAi animals to MeHg results in a significant loss of DA neurons at concentrations as low as 300 nM. Exposure to 400 nM MeHg results in approximately 60% of the *mrp-7* RNAi animals displaying significant DA neurodegeneration, while none of the WT animals' DA neurons degenerate (**Fig. 35C and E**). The neurodegeneration

often presented as the loss of one or more complete CEP process. Importantly, there are no gross morphological differences, or differences in growth and development between WT and *mrp-7* RNAi animals for this exposure condition, suggesting that the toxicant is not causing wide-spread cell death (**Fig. 35A and C**).

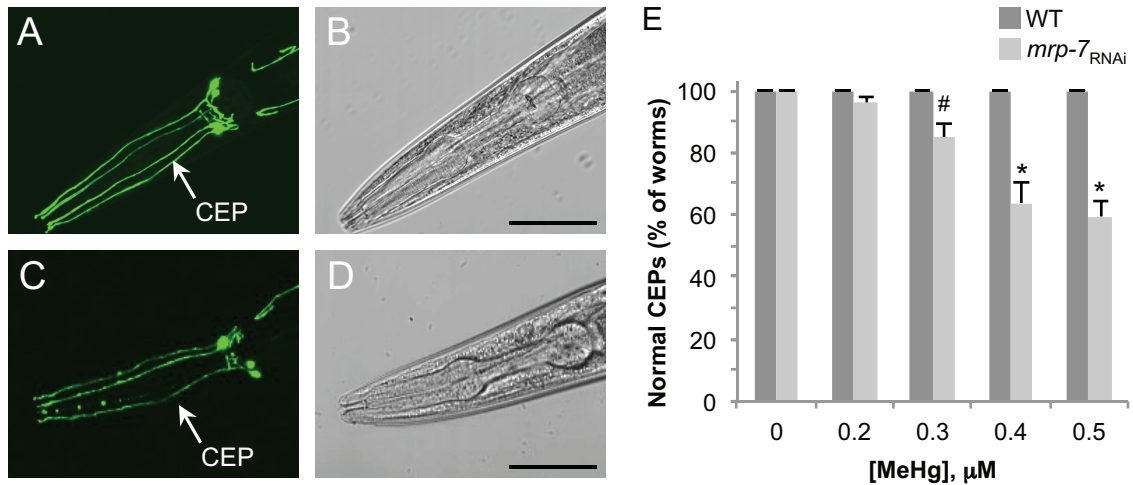


Figure 35. MRP-7 inhibits MeHg-associated DA neuron degeneration. RNAi sensitive RJ928 L1 stage nematodes were grown on plates containing MeHg and seeded with RNAi bacteria targeting *mrp-7* or empty vector. After 4 days, the DA neurons were visualized using a fluorescent microscope and scored for degeneration. Nematodes are considered normal if all 4 CEP processes are intact from the cell body to the tip of the nose. MeHg (0.5 μM) does not affect the DA neurons in WT animals (A) however exposure to 0.5 μM MeHg causes degeneration of the DA neurons in the absence of *mrp-7* (C). The DIC images (B, D) illustrate that there are no gross morphological differences between WT and *mrp-7* RNAi, and the animals are of similar size (scale bar is 50 μM). Quantification of degeneration is presented as the percent of animals with normal CEPs (E). The data is presented as mean \pm SEM of 5 independent replicates. Data was analyzed by two-way ANOVA with Bonferroni post-tests. *mrp-7* RNAi is significantly different from WT with $p < 0.01$ (#) or $p < 0.001$ (*).

G. MRP-7 is expressed in DA neurons

MRPs reduce cellular toxicity by transporting substrates out of the cell, and MRP-7 inhibits accumulation of Hg in *C. elegans*, supportive of a role of MRP-7 in MeHg transport (Sharom 2008). As a decrease in *mrp-7* results in MeHg-induced DA neurodegeneration, I asked if MRP-7 may be expressed in the DA neurons and generated a transgenic reporter strain to determine the expression pattern of MRP-7.

Transgenic animals expressing transcriptional fusions with fluorescent proteins are often used to determine the expression pattern of a gene (Boulin *et al.* 2006). The

BC *C. elegans* Gene Expression Consortium has generated promoter::GFP fusions for numerous *C. elegans* genes (Hunt-Newbury *et al.* 2007). As mentioned above, reporters may not always show the full endogenous expression pattern, however the work of the Consortium has shown good agreement between the expression patterns determined by GFP reporters and the patterns determined by SAGE analysis of mRNA expression (Hunt-Newbury *et al.* 2007). Their results suggest that transcriptional reporters can be useful tools for investigating gene expression patterns, provided the potential limitations are acknowledged. The Consortium website provides the primers used to isolate the promoter region for each construct, which are designed to amplify about 3 kb upstream of the start codon unless an upstream gene requires shortening (Hunt-Newbury *et al.* 2007). A strain expressing P_{mrp-7} ::GFP (BC10031) was generated by their group and is available from the CGC. Their studies suggest MRP-7 expression in the “intestine, body wall muscle, head neurons” (www.WormBase.org). As there are several types of neurons in the head of the nematode, I wanted to determine if MRP-7 is expressed in the DA neurons. CFP and YFP are two fluorophores that are commonly used together to determine co-localization as their excitation and emission wavelengths have minimal overlap, so genetic constructs were generated to express CFP behind the *mrp-7* promoter (as determined by the Consortium) and YFP behind the *dat-1* promoter (Miller *et al.* 1999, Nass *et al.* 2002). In the transgenic nematodes (RJ1089), *dat-1* expression is localized to the DA neurons (**Fig. 36B**) as in the original P_{dat-1} ::GFP strain, BY250 (Nass *et al.* 2002). CFP fluorescence is observed in the intestine and what appear to be two continuous lines down either the side of the animal, possibly seam cells or alae of the epidermis (**Fig. 36C**). There is also CFP expression in the head, but it is difficult to observe if there is overlap with the P_{dat-1} ::YFP expression in the whole animal *in vivo* (**Fig. 36D**).

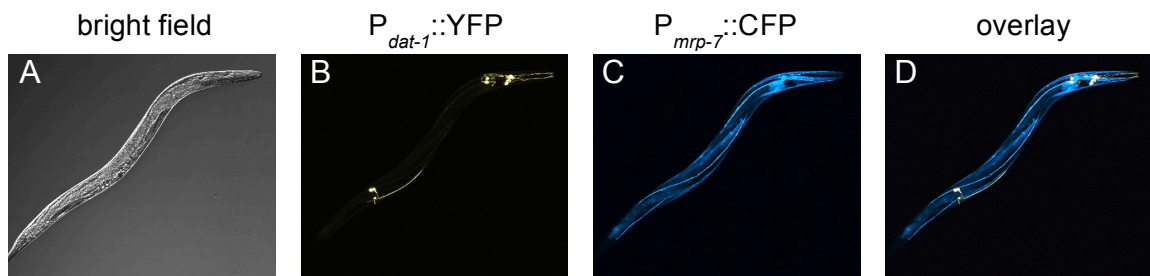


Figure 36. Expression pattern of P_{mrp-7} ::CFP in whole animals. RJ1089 strain young adult nematodes were visualized by confocal microscopy. YFP and CFP were viewed with the appropriate lasers, and no interference was detected between the signals.

As the visualization of whole nematodes did not conclusively show expression of MRP-7 in the DA neurons, primary cultures were prepared from the RJ1089 animals. As observed previously in primary cultures, the DA neurons express yellow fluorescence and form processes (**Fig. 37B**) (Settivari *et al.* 2009). CFP was expressed in several, but not all cells, including DA neurons (**Fig. 37C**), indicating that the 3466 kb promoter of MRP-7 is sufficient to drive the expression of the MRP protein. All DA neurons expressed CFP (**Fig. 37D**). Future experiments could utilize neuronal subtype specific antibodies or fluorescent reporters to further characterize the cellular localization of MRP-7. These results indicate that MRP-7 is likely expressed in DA neurons and may function to inhibit MeHg-associated DA neurodegeneration.

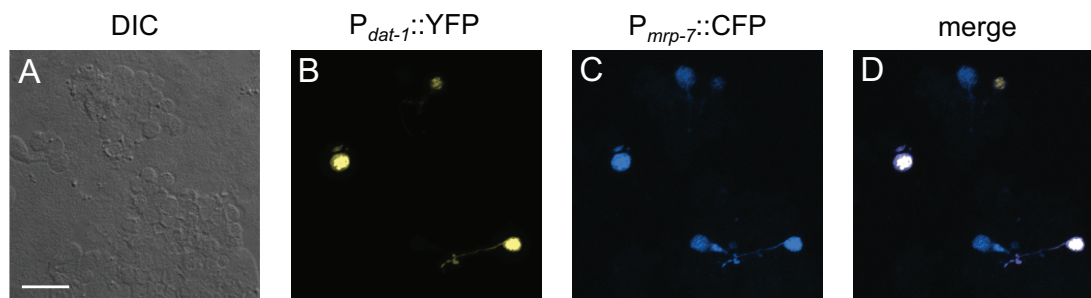


Figure 37. MRP-7 is expressed in *C. elegans* DA neurons. Transgenic animals [$P_{dat-1}::YFP$; $P_{mrp-7}::CFP$] were used to generate primary cultures. Confocal imaging was used to visualize the expression of the fluorophores. DA neurons were identified by the presence of YFP (B). MRP-7 expression (C) was detected in the DA neurons as well as other cells (D), but not all cells (A).

H. Other types of neurons do not degenerate following MeHg exposure

Individual transgenic strains with specific neuronal types labeled with GFP are available from the CGC. I crossed each strain with the *rrf-3* mutant strain NL2099 to generate strains that have GFP-expressing neurons that are sensitive to RNAi. The types of neurons expressing GFP include GABA, glutamatergic, cholinergic, serotonergic and the ASI neurons. Each strain was exposed to 0.5 or 1 μ M MeHg following knockdown of *mrp-7* or *skn-1* and no significant changes in neuronal morphology were observed under these conditions. A representative image of GABA neurons following MeHg exposure is shown (**Fig. 38**). The selective degeneration of the DA neurons is consistent with vertebrate literature suggesting these neurons are more sensitive to stress and cell death relative to other types of neurons (Petrucci & Dickson 2008). As the DA quinone

and MeHg both react with GSH, the GSH levels may be depleted faster or to a greater extent by MeHg than in other neurons, contributing to the selective sensitivity (Cuadrado *et al.* 2009).

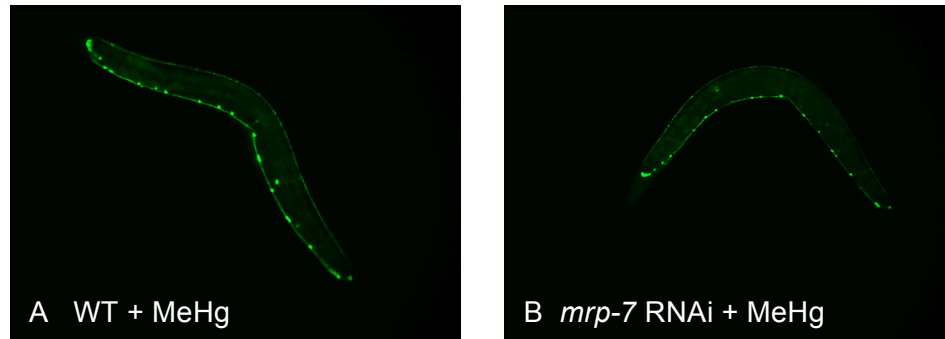


Figure 38. MeHg exposure does not cause GABA neuron degeneration. RJ1040 [$P_{unc-47}::GFP$; $rrf-3(pk1426)$] nematodes were grown on RNAi plates seeded with HT115 or *mrp-7* RNAi bacteria containing 0.5 μ M MeHg for 4 days. GFP is expressed in GABA neurons. There were no observable breaks in the dorsal or ventral nerve cord. The cell bodies may be slightly smaller in *mrp-7* RNAi nematodes, but overall the GABA neurons were essentially normal following MeHg exposure.

VII. Discussion

The studies presented in this thesis describe a novel *C. elegans* model of MeHg toxicity and DA neuron degeneration, and the identification of genes involved in modulating the toxicity. Several cellular processes have been associated with MeHg toxicity, yet the genetic and molecular bases of the toxicity remain largely undefined. Acute MeHg exposure in mice and rats can cause DA release, and DA-related behaviors are altered following chronic MeHg exposure, however it is difficult to investigate the molecular basis of the pathology in these systems due to the complexity of the mammalian brain (Faro *et al.* 1997, Bourdineaud *et al.* 2011). As MeHg exposure has been linked epidemiologically to PD, the prevalence of MeHg in the environment and the increasing incidence of PD indicate that determining the contribution of the toxicant to the disease could provide significant benefit to public health.

C. elegans has been established as a model system for elucidating the molecular mechanisms of both gene-associated and toxicant-induced DA neuron cell death (Nass *et al.* 2008). My studies show that exposure to MeHg induces DA neuron degeneration in *C. elegans*, thus establishing a whole animal model for studying the molecular basis of MeHg-associated DA neuron pathology. I have utilized gene expression and hypothesis-driven studies as well as a genome wide reverse genetic screen to identify genes involved in MeHg toxicity. The increased expression of GSTs and other stress response genes following MeHg exposure led to the discovery that the transcription factor SKN-1/Nrf2 inhibits MeHg toxicity in the whole animal as well as DA neurons. A novel RNAi screen identified genes required for viability in the presence of MeHg, including the ABC transporter MRP-7, which plays a significant role in MeHg excretion and inhibits MeHg-induced DA neuron degeneration.

A. Viability

My studies show that *C. elegans* recapitulates several of the key features of MeHg toxicity in mammals. Chronic exposure results in animal death, which is reduced by co-exposure with Se. In mammals, the brain of the developing fetus is more sensitive to the damage induced by MeHg than the adult brain (Clarkson *et al.* 2003). In *C. elegans* exposed to MeHg, I find significant effects on several parameters of reproduction and development including developmental delay, impaired reproductive capacity and embryonic defects.

Effects on *C. elegans* viability and development are commonly monitored in toxicological studies and have been employed as endpoints in high throughput toxicity screening (Boyd *et al.* 2012). However, observations of animal death or delayed development following toxicant exposure provide little information regarding the mechanisms of toxicity as multiple processes may be involved in producing the effect. Biochemical assays may be useful in *C. elegans* to suggest molecular effects of toxicant exposure. I utilized the dye DCFDA to show that MeHg increases ROS levels in the nematode, consistent with observations in mammals (Ali *et al.* 1992). Furthermore, the genetic techniques available in *C. elegans* provide an excellent opportunity to identify genes involved with cellular processes (Boulin & Hobert 2012). The genes and molecular pathways involved in biological processes such as development, neuronal function and cell death are highly conserved between *C. elegans* and humans (Shaye & Greenwald 2011). Therefore, the identification of genes and pathways that are associated with a toxicant in the nematode may provide insight into the mechanisms of toxicity in humans and other vertebrates.

The gene expression profile following toxicant exposure provides information about both the cellular processes disrupted by the toxicant and the defense mechanisms that the cell has activated. Microarray analysis of gene expression is sensitive and can detect cellular changes before visible toxicity or cell death occurs, contributing to its utility in toxicology (Nuwaysir *et al.* 1999). Microarray analysis following MeHg exposure has been completed in several organisms, but these studies are mostly tissue specific (ex. brain, liver). I used microarray analysis to identify MeHg-induced changes in gene expression in the whole nematode and approximately 500 genes were found to be upregulated over 2-fold after MeHg exposure. DAVID analysis of the list of upregulated genes indicates an enrichment of genes involved in stress response (GSTs, HSPs, CYPs) and the ubiquitin proteasome pathway. Similar results were found by microarray analysis of MEF cells following MeHg exposure; there was an enrichment of genes involved in glutathione metabolism, Nrf2-mediated stress response and protein ubiquitination pathways, among other processes (Yu *et al.* 2010). The gene response profile in my microarray is consistent with those obtained from mammalian studies, suggesting that the molecular pathways involved in MeHg toxicity are likely similar between *C. elegans* and vertebrates.

Microarrays have been the standard technique for global analysis of gene expression for several years, however new technologies have led to the development of

a method called RNA-seq that offers several advantages over traditional microarray for transcriptome profiling (Wang *et al.* 2009b). RNA-seq uses high-throughput sequencing to identify all cDNAs in the cell at a given time. Microarray analysis is limited to the genes represented on the chip, however there is no such bias with RNA-seq and a comprehensive gene expression profile can be obtained. The technology can also be more sensitive, identifying transcripts that may not be detected by microarray (Wang *et al.* 2009b). We, along with our collaborator Dr. Garry Wong and his colleagues, have utilized RNA-seq to analyze gene expression following MeHg exposure in *C. elegans*. As reported in Rudgalvyte *et al.* 2013, the RNA-seq data indicates upregulation of GSTs, HSPs, UGTs and CYPs (Rudgalvyte *et al.* 2013). Furthermore, 5 of the top 20 genes from RNA-seq were also identified by my microarray analysis (Rudgalvyte *et al.* 2013). The RNA-seq analysis was performed after chronic exposure to 10 μ M MeHg and the microarray results in this thesis indicate changes following acute exposure to MeHg. The RNA-seq study results are consistent with my microarray data, suggesting that similar classes of stress response genes are induced by MeHg exposure following different exposure conditions.

B. SKN-1

My gene expression studies show that MeHg exposure increases expression of specific GSTs, prompting me to investigate the mechanisms involved in regulating the expression of these genes. Phase II detoxification enzymes, including GSTs in mammals and *C. elegans*, can be regulated by the transcription factor Nrf2/SKN-1 and Nrf2 has been implicated in MeHg toxicity (Toyama *et al.* 2007, Oliveira *et al.* 2009, Yu *et al.* 2010). I found that SKN-1 is required for the transcription of *gst-4* and *gst-38*, and there are likely more genes upregulated by MeHg that are regulated by SKN-1 (Oliveira *et al.* 2009). RNAi knockdown of *skn-1* increases sensitivity to MeHg, suggesting that SKN-1 plays a significant role in managing MeHg-associated toxicity, likely by increasing the expression of genes with protective functions. MeHg increases cellular ROS levels and SKN-1 may upregulate antioxidant genes that can reduce ROS. SKN-1 target genes also include members of the UPS and regulators of transcription and translation. As MeHg can bind and damage proteins, the SKN-1 response could facilitate the removal of damaged proteins and the production of new proteins to promote cell survival. SKN-1 is known to upregulate GSTs and may control the expression of transporters such as MRP-7, which could promote the conjugation of MeHg to GSH and

then excretion through the transporters (Oliveira *et al.* 2009). Therefore, the protective role of SKN-1 likely involves downstream pathways and systems that contribute to survival in the presence of MeHg.

SKN-1 has been shown to be localized in the cytoplasm of intestinal cells under normal conditions, and oxidative stress results in translocation of the protein to the nucleus (An & Blackwell 2003). In the nucleus, SKN-1 can bind to ARE sequences and enhance the transcription of stress response genes. SKN-1 has also been observed in the ASI neurons, which are two chemosensory neurons in the head of the nematode, and the protein is constitutively nuclear in these cells (Bishop & Guarente 2007). The expression of SKN-1 in the ASI neurons is involved in longevity, as dietary restriction causes SKN-1 to initiate signals that result in increased lifespan (Bishop & Guarente 2007). The reported expression pattern of SKN-1 did not include DA neurons, however it was based on observations of a translational reporter strain, which may not always reveal the true expression patterns of a protein (Boulin *et al.* 2006). Studies in mammalian cells have shown that Nrf2 is expressed in and can inhibit cytotoxicity in DA neurons (Siebert *et al.* 2009). Therefore, I hypothesized that SKN-1 may be expressed in *C. elegans* DA neurons. Immunoreactivity of a SKN-1 antibody in DA neurons in primary cultures supports this hypothesis and shows that SKN-1 is expressed in *C. elegans* DA neurons (**Fig. 20**).

The discovery of SKN-1 expression in the DA neurons has contributed to other studies in our lab and we have reported that SKN-1 also inhibits DA neuron degeneration induced by Al³⁺, Mn, rotenone and 6-OHDA (Settivari *et al.* 2013, VanDuyn *et al.* 2013, data not shown). Further genetic studies of Al³⁺-induced DA neuron degeneration revealed a role for SMF-3, a *C. elegans* homologue of the mammalian divalent metal transporter. *smf-3* mutants have increased resistance to Al³⁺, and given its role as a transporter, we hypothesized that the decreased toxicity was due to decreased Al levels. I utilized ICP-MS to measure total Al levels following an acute exposure to Al and found a significant increase in *smf-3* mutants compared to WT (**Fig. 25**). These results are consistent with a model that includes SMF-3 localization in an intracellular compartment where the transporter facilitates movement of Al³⁺ into the cytosol. Our identification of SMF-3 is the first report of an Al transporter in any animal. Collectively, our studies underscore the crucial role of SKN-1 in DA neurons in response to toxicant-induced stress and suggest that oxidative stress is involved in the cellular response to a variety of PD-associated neurotoxicants.

C. RNAi Screen

Genome-wide RNAi screens provide a relatively unbiased approach to discover new genes associated with a specific cellular process or phenotype (Sugimoto 2004). In contrast, the results of hypothesis driven experiments may be limited by the initial question being asked. For example, we have utilized strains with mutations in PD-associated genes to determine if loss of function in those genes may increase sensitivity to DA neurotoxicants. In this targeted approach, our results are specific for the mutants and may limit the identification of other genes involved in the DA neuron degeneration. My screen largely assumes no a priori knowledge of genes involved in MeHg toxicity. I screened two RNAi libraries for suppressors of MeHg-induced lethality utilizing the OD₆₀₀ of the bacterial culture as the indicator of viability. A plate reader was utilized to measure the OD₆₀₀ of each well in the 96-well microtiter plate, which allowed for the whole plate to be analyzed in approximately a minute. *skn-1* RNAi was used to optimize the MeHg concentration that would allow the detection of nematodes with increased sensitivity relative to WT. I chose the highest concentration of MeHg that allowed viability of WT animals, but significantly decreased the viability of MeHg-exposed *skn-1* RNAi animals. *skn-1* RNAi also served as the positive control during the second round of the screen. For *skn-1*, the bacteria in control wells are consumed and results in an OD₆₀₀ near 0 while wells with MeHg have an OD₆₀₀ near 1 at the end of the exposure. Obtaining this result in the control suggested that both the RNAi and MeHg are likely effective. Furthermore, the observation of decreased viability for genes with previously reported growth defective phenotypes throughout the screen suggested that the RNAi was effective. It is possible that not every RNAi clone efficiently knocked its target gene, which may have resulted in false negatives (genes involved in MeHg toxicity that were not identified due to the conditions of the screen). However, the goal was to identify genes that likely play a significant role in MeHg toxicity, not to definitively identify every gene that affects MeHg-associated animal sensitivity.

At the completion of the screen, 92 RNAi clones were identified that significantly inhibit animal viability in the presence of MeHg. The genes were largely organized into groups based on their function (or predicted function) as annotated in WormBase (www.WormBase.org). If no information was available for the *C. elegans* gene, it was classified based on the function of the closest human homolog. The protein sequence for nearly all *C. elegans* genes is available at WormBase.org, so NCBI BLAST was used to search for the human homologue of each screen hit. Over 90% of the screen hits

have an identifiable human homologue. This is supportive of my hypothesis that the screen in *C. elegans* will identify genes that likely play a role in MeHg toxicity in humans.

The screen identified several genes that have been associated previously with MeHg toxicity, as well as new genes that previously have not been implicated. Seven genes associated with the mitochondria were identified, including ETC subunits. The mitochondria are known to be a cellular target of MeHg (Atchison & Hare 1994). Also, RNAi knockdown of the mitochondria-associated genes may impair mitochondrial function, increasing ROS and intracellular calcium, and sensitizing the cells to further insult by MeHg.

The effects of MeHg on protein homeostasis reported in the literature are consistent with my screen results (Syversen 1977). Eight genes involved in protein degradation, specifically the UPS, were found to increase sensitivity to MeHg. This is consistent with the studies in yeast that show overexpression of UPS genes can confer resistance to MeHg (Furuchi *et al.* 2002, Hwang *et al.* 2009). Impairment of protein synthesis also appears to increase sensitivity to MeHg, as several translation initiation and elongation factors and ribosomal subunits were identified in the screen.

Consistent with mammalian literature showing an important role for calcium in the response to MeHg, knockdown of two genes that encode regulators of Ca homeostasis was found to increase sensitivity to MeHg (Hare *et al.* 1993). Genes related to homeostasis of other ions and vacuole and peroxisome function were identified, which may be involved in cellular detoxification. The screen hits may also provide insight into the mechanisms of cell death caused by MeHg, as two apoptosis-related genes and three genes associated with endocytosis (often linked to autophagy) were found to increase sensitivity to MeHg.

MeHg targets the nervous system in mammals and causes DA neuron degeneration in *C. elegans*, however few genes involved in nervous system development or function were identified in the screen. This is likely because the endpoint of the screen was animal death and few neurons in the worm are required for viability (Bargmann 1993). A more sensitive assay using a lower MeHg concentration and a behavioral phenotype as the endpoint may identify genes involved in nervous system function. Also, the MeHg exposure began at L4 stage, so MeHg-associated genes involved in embryonic or early larval development may not have been identified. Altering the time points or other parameters of the screen may also allow for the identification of additional genes involved in MeHg-associated toxicity.

My microarray analysis identified genes for which expression is increased following MeHg exposure, and the RNAi screen identified genes that inhibit MeHg toxicity. It may be expected that genes inhibiting MeHg toxicity are preferentially upregulated following exposure. However, I found minimal overlap between the genes identified by the microarray and the genes identified in the screen; only 4 of the screen hits were upregulated by MeHg in the microarray results and one screen hit was found to be upregulated in the RNA-seq results. The genes identified in the screen are necessary for animal viability in the presence of MeHg. These genes may code for stress response proteins or detoxification enzymes that play a specific role in the cell's response to MeHg exposure (i.e. SKN-1 and MRP-7). However, the genes could also play a role in a normal cellular process, that when inhibited by gene knockdown, results in an increase in the cell's sensitivity to MeHg insult. For example, knockdown of a gene involved in mitochondrial function may result in damage to the mitochondria, sensitizing the organelle to the effects of subsequent MeHg exposure. The upregulation of one individual gene by MeHg may also not have a significant effect on cellular toxicity, and that gene could be indicated in the microarray but not identified by the screen. For example, several GSTs are upregulated by MeHg yet RNAi knockdown of an individual GST does not affect MeHg toxicity. However, knockdown of SKN-1 increases sensitivity, which likely results in decreased expression of several GSTs, among other genes.

My genetic screen identified RNAi clones that caused increased sensitivity to MeHg and therefore genes involved in inhibiting MeHg toxicity. To identify genes for which knockdown increases resistance to MeHg, a screen could be performed with a higher concentration of MeHg that would result in the lethality of WT animals. Here, RNAi clones that allow survival in the presence of MeHg would be identified. As knockdown of these genes results in enhanced survival in the presence of MeHg, the function of the gene would facilitate MeHg toxicity. For example, a gene that acts in a pathway of apoptosis could be activated in the presence of MeHg, and knockdown of this gene may inhibit apoptosis and promote survival. Negative regulators of pathways that inhibit toxicity could also be identified. For example, *wdr-23* should be identified in such a screen and could be used as a positive control, as I have shown knockdown of this gene results in increased expression of SKN-1 and increased animal survival. This screen could produce a list of genes with the potential to further elucidate the pathways involved in MeHg toxicity.

Following the observation that MRP-7 was mis-annotated, I determined if any of the other Ahringer library hits may be incorrectly labeled. The reliability of all clones in the Ahringer library has been predicted based on bioinformatic gene analysis and clone sequencing and is provided in an online database (<http://biocompute.bmi.ac.cn/CeIRNAi/>) (Qu *et al.* 2011). Thirty of the screen hits were from the Ahringer library and 12 of these, including MRP-7, were reported in the database as “marginal”, suggesting that there is a possibility the clone may target a different gene than was indicated in the original library database. Therefore it is likely important in future studies to verify the identity of the clones by sequencing.

D. MRP-7

Cellular detoxification often involves reactions in three phases (Klaassen & Lu 2008). Phase I and phase II detoxification metabolize and conjugate the chemical or toxicant, which prepares it for excretion from the cell during phase III. Phase I and II enzymes were found to be upregulated by MeHg exposure as determined by microarray analysis and loss of a key regulator of phase II enzyme expression, SKN-1, increases sensitivity to MeHg. MeHg is able to bind numerous proteins and cause widespread cellular damage, so conjugation and the SKN-1 antioxidant response may not be enough to fully mitigate the toxicity. A single phase III transporter was identified in the RNAi screen, MRP-7, and knockdown of this protein results in greater sensitivity to MeHg than loss of SKN-1. These results suggest that excretion from the cell may be a more effective method of reducing MeHg toxicity than phase I or II detoxification.

ABC transporter literature largely focuses on roles in chemoresistance or excretion, likely functioning on the plasma membrane to facilitate removal of substrates from the cell (Sharom 2008). *mrp-7* RNAi animals contain higher Hg levels following exposure to MeHg than WT, suggesting that MRP-7 functions to inhibit the intracellular accumulation of MeHg. My studies are supportive of a model in which MRP-7 is located on the plasma membrane. MeHg can enter the cell via diffusion across the plasma membrane, or through Ca²⁺ channels or amino acid transporters (Lakowicz & Anderson 1980, Kerper *et al.* 1992, Marty & Atchison 1997). Intracellular MeHg is transported out of the cell, against the concentration gradient, via the action of MRP-7 (**Fig. 39**). This model is consistent with the function of MRP2 in MeHg transport in the kidney. MeHg accumulates in the epithelial cells of the proximal tubules and is then transported by MRP2 out of the cell and into the lumen of the kidney for excretion (Zalups & Bridges

2009). Subcellular localization studies utilizing an antibody to MRP-7 or a translational fluorescent reporter could help to confirm that MRP-7 is expressed on the plasma membrane.

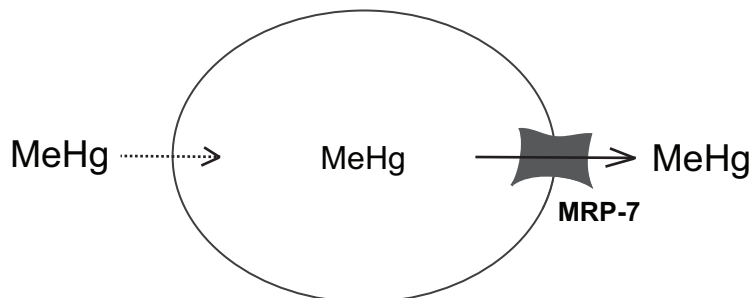


Figure 39. A model for MRP-7 mediated transport of MeHg. The dashed line represents an undefined mechanism of movement into the cell. MRP-7 is likely expressed on the plasma membrane and pumps intracellular MeHg out of the cell.

Regardless of the specificity or localization of MRP-7, it is clear that loss of the transporter increases the amount of MeHg in the cell and therefore likely increases cellular stress. The gene expression changes following MeHg exposure in *mrp-7* RNAi animals provide insight into the molecular pathways that are perturbed by the toxicant. The upregulation of *gst-38* is expected as this gene is also increased in WT animals following MeHg (**Fig. 14**). The increase in *gst-1*, *hsp-4* and *hsp-6* expression in the *mrp-7* RNAi animals after chronic, but not acute, exposure is consistent with the increased Hg levels at later time points. It appears that when the Hg levels are higher, the cells are under greater stress, and induce different or additional genes in response to this stress.

GST π plays a role in PD and the *C. elegans* homologue *gst-1* has been shown to be expressed in *C. elegans* DA neurons and is involved in DA neuron sensitivity to Mn (Settivari *et al.* 2013). Upregulation of this gene following MeHg exposure in *mrp-7* RNAi animals suggests that the DA neurons may be under stress, and the observation of DA neuron degeneration following MeHg exposure in *mrp-7* RNAi animals is consistent with this hypothesis.

hsp-4 is a homologue of the protein BiP that is upregulated during ER stress (Ient *et al.* 2012). Induction of *hsp-4* in *mrp-7* RNAi animals indicates that MeHg may be contributing to an ER stress response. The accumulation of unfolded proteins is also a cause of ER stress (Gorbatyuk & Gorbatyuk 2013). Therefore, the upregulation of *hsp-4*

could be a direct effect of MeHg exposure or a consequence of the activation of the UPR by MeHg.

There is also evidence for a UPR activated specifically in the mitochondria (Haynes & Ron 2010). *hsp-6* is a chaperone that is upregulated in response to this mitochondrial UPR (Yoneda *et al.* 2004). Insults that are known to cause ER stress and increase *hsp-4* levels, such as tunicamycin and heat stress, had no effect on *hsp-6* expression, suggesting that the upregulation of *hsp-6* occurs specifically following mitochondrial disruption (Yoneda *et al.* 2004). Oxidative stress can activate the *hsp-6* mitochondrial UPR response, so the increase in ROS by MeHg could contribute to the *hsp-6* induction following exposure. However, MeHg may also activate *hsp-6* in another manner as *hsp-6* can be upregulated in the absence of ROS (Yoneda *et al.* 2004). MeHg could potentially disrupt mitochondrial proteins through its interaction with thiol groups which could also activate the mitochondrial UPR and *hsp-6*.

hsp-16.1 is a member of the small HSP family, which are known to function as chaperones to stabilize protein folding and prevent the accumulation of mis-folded proteins (Jakob *et al.* 1993). In *C. elegans*, HSP-16.1 is localized specifically to the Golgi apparatus, an organelle which participates in the processing and packaging of proteins (Kourtis *et al.* 2012). The Golgi also stores and regulates intracellular Ca^{2+} through the function of the Ca^{2+} and Mg^{2+} ATPase, PMR-1 (Van Baelen *et al.* 2001). Stress can induce the release of Ca^{2+} from the Golgi to increase intracellular Ca^{2+} levels that ultimately contribute to cell death (Kourtis *et al.* 2012). HSP-16.1 contributes to cellular protection by functioning with PMR-1 to prevent high intracellular Ca^{2+} levels. MeHg has been shown to increase intracellular Ca^{2+} by releasing the cation from the ER and mitochondria, and the upregulation of HSP-16.1 in *C. elegans* suggests that Golgi-related Ca^{2+} release may also contribute to MeHg-induced cellular toxicity (Marty & Atchison 1997). Overall, these gene expression studies suggest that the level of cellular stress appears to be higher following MeHg exposure in *mrp-7* RNAi animals relative to WT.

MRP-7 plays a role in inhibiting toxicity in *C. elegans* following MeHg exposure, and consistent with its role in promoting survival, *mrp-7* mRNA levels are increased in the presence of MeHg (**Fig. 34**). Mammalian studies have shown that Nrf2 can contribute to the regulation of MRPs (Ji *et al.* 2013). As the expression of *C. elegans* homologues of several Nrf2-regulated genes, including ABC transporters, is regulated by SKN-1 and there are two SKN-1 binding sites in the promoter of *mrp-7*, I hypothesized

that *mrp-7* expression is dependent on SKN-1 (Oliveira *et al.* 2009). *skn-1* expression was reduced with RNAi and *mrp-7* mRNA levels were measured by RT-PCR. After RT-PCR with several independent biological replicates, the results were inconclusive due to variability. Two replicates showed a decrease in *mrp-7*, two replicates showed an increase in *mrp-7* and two replicates showed no change in expression levels. SKN-1 may play a role in the regulation of *mrp-7*, but a conclusion cannot be drawn from these results. Further investigations could use alternative methods for measuring gene or protein expression. A primary antibody to MRP-7 could be generated and used for Western blotting. The $P_{mrp-7}::CFP$ strain (RJ1089) contains the *mrp-7* promoter with both SKN-1 binding sites, so decreased CFP fluorescence following *skn-1* RNAi may indicate that SKN-1 regulates MRP-7 protein expression. The inability to perform *skn-1* RNAi for more than one generation may decrease the success of these experiments (Hamilton *et al.* 2005). If the *mrp-7* mRNA or protein is present in the embryo or first larval stage, there would be detectable *mrp-7* expression before *skn-1* is knocked down. If *mrp-7* is not highly upregulated following MeHg exposure, or has a long biological half-life and is not transcribed at high levels under normal conditions, a loss of SKN-1 may have little effect as the initial *mrp-7* could still be detected. If *skn-1* RNAi could be performed on multiple generations, *mrp-7* may not be transcribed in the second-generation progeny in the absence of SKN-1 allowing for a detectable difference.

E. Implications in PD

I have identified several cellular responses to MeHg in *C. elegans* that have also been reported in models of DA neuron degeneration or PD. Furthermore, genes identified to play a role in MeHg toxicity have also been associated with PD. Chronic exposure of the nematode to MeHg results in degeneration of the DA neurons while no effect is observed on the morphology other neuronal types. In PD, death of the DA neurons in the SN is observed while other cell types remain largely unaffected (Petrucci & Dickson 2008). A hypothesis for this selective sensitivity of DA neurons is that these cells have an intrinsically elevated level of ROS and therefore less external insult is needed to disrupt the oxidative balance and cause oxidative stress (Drechsel & Patel 2008). I have shown that MeHg increases ROS, so it is possible that the DA neurons have a lower threshold for ROS thus making these cells more sensitive than others. Furthermore, the DA neurons in *C. elegans* are not required for animal viability. Therefore, the loss of the DA neurons specifically can be observed without widespread cell death in the whole

animal. The selective death of DA neurons makes *C. elegans* an attractive model for investigating the role of MeHg in DA neuron degeneration.

GSH is an antioxidant molecule with important functions in both MeHg toxicity and PD. MeHg exposure can decrease GSH levels and the brains of PD patients also have reduced GSH content (Yee & Choi 1996, Zeevalk *et al.* 2008). Decreased GSH disrupts the oxidative balance of cells and reduces the ability to tolerate increased ROS. In MeHg toxicity and PD, GSH also plays a role in conjugation and excretion of substances from the cell, either MeHg itself or quinones formed from DA auto-oxidation (Zeevalk *et al.* 2008, Rush *et al.* 2012). My results show that the GSH system is involved in MeHg toxicity, as several GSTs are upregulated following exposure, and SKN-1 could be regulating the expression of additional genes in the GSH pathways. GSTs likely facilitate the conjugation of GSH to MeHg and polymorphisms in GSTs have been associated with elevated MeHg levels as well as an increased risk of PD (Schlätwicke Engström *et al.* 2008, Shi *et al.* 2009). MeHg-GSH conjugates can be removed from the cell by MRPs, and this may also be true for MRP-7 (Rush *et al.* 2012). It has yet to be determined if MRPs may participate in the excretion of substances from DA neurons in PD. However, I have shown that MRP-7 is expressed in *C. elegans* DA neurons, suggesting that MRPs may play a role in inhibiting DA neuron cytotoxicity in humans.

The transcription factor Nrf2 has been implicated in PD and modulation of its activity could be a promising therapy for the disease (Cuadrado *et al.* 2009). Nrf2 also inhibits MeHg toxicity (Toyama *et al.* 2007). I have shown that the Nrf2 homologue SKN-1 inhibits MeHg-induced animal death and DA neuron degeneration in *C. elegans*. Furthermore, Nrf2/SKN-1 regulates gene expression to decrease ROS and increase GSH (Kensler *et al.* 2007). Other SKN-1 regulated genes may also have implications in DA neuron physiology or pathology. The *C. elegans* gene *cat-4* is involved in the synthesis of DA and is regulated by SKN-1 (Oliveira *et al.* 2009). CAT-4, homologous to human GTP cyclohydrolase I, inhibits MeHg-induced DA neuron degeneration in our model, suggesting that altered DA regulation may contribute to the sensitivity of these cells. CAT-4/GTPCH is involved in the synthesis of BH₄, and in humans reduced BH₄ levels have been found in PD patients and mutations in GTPCH have been correlated with developing parkinsonism (Lovenberg *et al.* 1979, Nygaard *et al.* 1992, Blau *et al.* 2001). DA can activate Nrf2, but the contribution of Nrf2 in the regulation of DA

synthesis is largely unknown and our model may provide an opportunity for further investigation into the role of Nrf2 and the possible significance to PD (Shih *et al.* 2007).

The UPS likely plays a role in inhibiting cytotoxicity following MeHg exposure. MeHg exposure increases expression of UPS genes and overexpression of UPS components in yeast confers resistance to the toxicant (Hwang *et al.* 2009, Yu *et al.* 2010). The studies in my thesis are also supportive of a role for protein degradation in the cellular response to MeHg exposure. The high affinity between MeHg and thiol groups provides the potential for MeHg to bind, modify or disrupt proteins (Clarkson 1987). If damaged, these proteins could become substrates for the UPS. This thesis also provides evidence for a role of the UPS in MeHg toxicity. Microarray analysis shows an induction of F-box and SKp1 related genes, both related to ubiquitination. In the RNAi screen, 8 genes were identified that have putative roles in the UPS and protein degradation.

My studies also show an induction of *hsp-4* in *mrp-7* RNAi animals following chronic MeHg exposure (**Fig. 33D**). The ER chaperone protein BiP (*hsp-4* in *C. elegans*) binds newly synthesized proteins and ensures proper trafficking into the ER for protein folding (lent *et al.* 2012). BiP can also promote the recycling of damaged proteins through the UPS (Kaufman 1999). BiP levels have been shown to be elevated by many sources of ER stress, including exposure to MeHg in *C. elegans* (*hsp-4*) and rats (Grp78) (Helmcke & Aschner 2010, Zhang *et al.* 2013). These reports and my data suggest that ER stress may be activated by high levels of MeHg or MeHg-associated stress.

The accumulation or aggregation of damaged or misfolded proteins may be a contributor to the DA neuron cytotoxicity observed in PD (Hoozemans *et al.* 2007). Impairment of the UPS can produce PD-like effects in model systems, and the overall function of the UPS is decreased in PD models and human PD patients (Lim & Tan 2007). Also, one mutation associated with familial PD occurs in the parkin gene, which is a component of the E3 ubiquitin ligase complex (Vistbakka *et al.* 2012). Mutations in another ubiquitination-related gene, UCH-L1, are considered a risk factor for PD (Klein & Westenberger 2012). The PD-associated toxicant 6-OHDA can induce expression of BiP, suggesting the involvement of ER stress and the UPR in DA neuron toxicity (Chen *et al.* 2004). BiP overexpression can mediate the neurotoxicity of α -synuclein in DA neurons (Gorbatyuk *et al.* 2012). These studies suggest that damaged proteins and UPS dysfunction contribute to the neuronal degeneration observed in PD. Furthermore,

the therapeutic potential of BiP activators is now being demonstrated in animal models of PD (Gorbatyuk & Gorbatyuk 2013).

MeHg exposure could impair the UPS in DA neurons, sensitizing them to additional insults and contributing to the development of PD. Alternatively, it is possible that the impairment of the UPS in PD could exacerbate the effects of MeHg exposure in the DA neurons. Nematode fluorescent reporter strains are available for direct observation of protein turnover and UPS function in particular *C. elegans* cell types (Hamer *et al.* 2010). This could allow for further investigation of the role of the UPS in MeHg toxicity in DA neurons. Impairment of the UPS by MeHg in the DA neurons would provide significant support for a role of the toxicant in contributing to DA neuron death observed in PD. PD mutant strains in which the DA neurons are already vulnerable could also be tested for sensitivity to MeHg.

My studies have identified several genes and pathways involved in MeHg toxicity, and many of these are also implicated in PD. MeHg may be contributing to the degeneration of DA neurons through multiple mechanisms as suggested by literature and the studies presented in this thesis. The possible pathways and organelles involved in MeHg cytotoxicity are diagrammed in **Figure 40** and described below. Although the molecular mechanisms by which MeHg contributes to DA neuron pathology are largely undefined, the model described in this thesis provides a solid basis to begin to address this question.

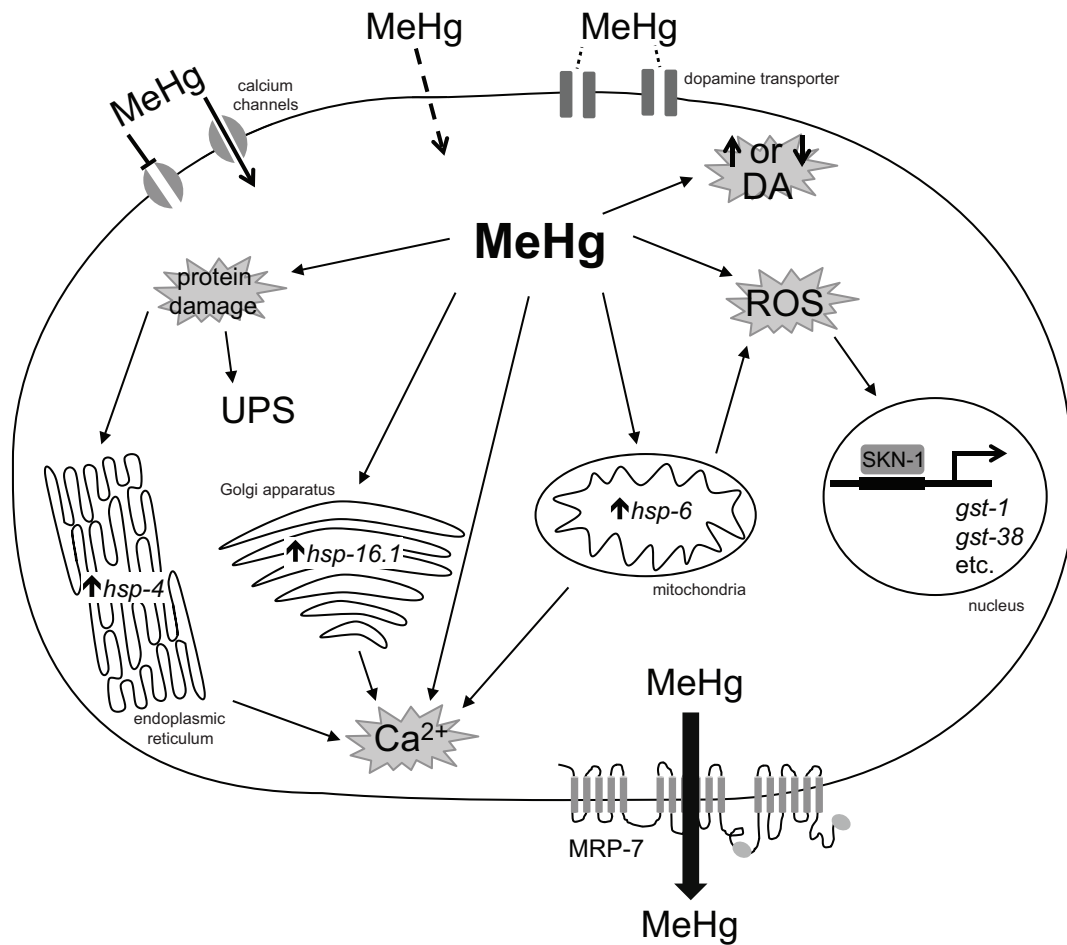


Figure 40. A model for MeHg-associated DA neuron cytotoxicity. Extracellularly, MeHg may interact with membrane proteins including Ca²⁺ channels and the dopamine transporter. Routes of MeHg entry into the cell include Ca²⁺ channels and diffusion through the plasma membrane. Intracellularly, MeHg can cause protein damage that activates the UPS as indicated by an upregulation of the ER-associated *hsp-4*. MeHg may also target the mitochondria, resulting in an increase in *hsp-6* expression. Furthermore, intracellular MeHg may result in Ca²⁺ release from the ER, Golgi apparatus and mitochondria. MeHg-associated oxidative stress may result in the nuclear localization of SKN-1 and the upregulation of SKN-1 target genes including GSTs, and alter DA homeostasis.

MeHg is known to bind to –SH groups, which can cause disruption of protein folding or damage to the proteins (Clarkson 1987). My studies are consistent with literature suggesting an initiation of the UPR following MeHg exposure and the involvement of the UPS in mediating MeHg-induced cellular damage. MeHg causes an increase in *hsp-4* mRNA, which is expressed in the ER and an indicator of the UPR (**Fig. 33**). Damaged proteins can be degraded and removed from the cell to prevent cellular

toxicity by the UPS. I have shown that components of the UPS are upregulated by MeHg exposure, and RNAi knockdown of several UPS components increases the sensitivity of *C. elegans* to MeHg (**Table 3, Table 5**). The UPS also plays a role in the cellular pathology associated with PD (Lim & Tan 2007). Therefore, accumulation of unfolded or damaged proteins in the DA neurons may contribute to the cytotoxicity caused by MeHg.

MeHg has been shown to cause an increase in intracellular ROS (Kaur *et al.* 2006, Mori *et al.* 2011). I have shown that total ROS are also increased in *C. elegans* exposed to MeHg (**Fig. 13**). Also, I have found that the transcription factor SKN-1, which is often induced by oxidative stress, plays an important role in mediating MeHg toxicity. SKN-1 target genes (ex. *gst-1, gst-38*) are upregulated following MeHg exposure (**Fig. 18, Fig. 33**). Also, knockdown of SKN-1 increases whole animal and DA neuron sensitivity to MeHg, likely due in part to a reduced ability to buffer ROS (**Fig. 16, Fig. 22**). Oxidative stress contributes to DA neuron cell death in PD; many PD-associated toxicants increase ROS and mutations in DJ-1, which protects cells against oxidative damage, are the most common cause of early-onset PD (Ariga *et al.* 2013).

Disruption of mitochondrial function or mitochondrial damage may also play a role in MeHg-induced degeneration of DA neurons. Numerous studies in mammalian systems implicate the mitochondria in MeHg toxicity (Atchison & Hare 1994). My studies show that MeHg induces *hsp-6* expression, a marker of the mitochondrial UPR, and RNAi knockdown of mitochondria-associated genes renders animals more vulnerable to MeHg (**Table 5, Fig. 33**). Furthermore, mitochondrial dysfunction can produce ROS and contribute to oxidative stress as well as releasing pro-apoptotic factors to promote cell death (Turrens 2003). The mitochondria are a common target of PD-associated toxicants that cause DA neuron cell death and PINK1 is a mitochondrial protein that when mutated causes PD (Exner *et al.* 2012).

Another effect of MeHg exposure that could contribute to MeHg-induced DA neuron toxicity is a disruption of intracellular calcium levels. MeHg has been shown to enter cells through calcium channels as well as inhibit Ca^{2+} transport (Sirois & Atchison 1996). Exposure of cells to MeHg can cause the release of Ca^{2+} from intracellular stores, including the mitochondria, ER and Golgi apparatus followed by an influx of extracellular Ca^{2+} (Marty & Atchison 1997, Limke *et al.* 2003, Kourtis *et al.* 2012). My studies have shown that MeHg affects these organelles, suggesting that Ca^{2+} levels may also be altered by MeHg exposure in *C. elegans* (**Fig. 33**). Also, two mediators of Ca^{2+}

homeostasis were identified in my RNAi screen (data not shown). Excess intracellular Ca^{2+} can have multiple effects on the cell, including promoting cell death through apoptosis (Orrenius *et al.* 2003). Ca^{2+} may play a role in the selective vulnerability of DA neurons in PD as these neurons display autonomous pacemaking involving Ca^{2+} currents (Chan *et al.* 2009). The intrinsic disruption in Ca^{2+} homeostasis in these neurons may predispose them to further insult by toxicants that also affect Ca^{2+} levels, such as MeHg.

DA may also contribute to the intrinsic vulnerability of DA neurons to damage by toxicants. DA is reactive and auto-oxidation can produce quinones and lead to oxidative stress (Shih *et al.* 2007). There are reports in literature that suggest both an increase and a decrease in DA release following MeHg exposure and disruption of DA homeostasis could cause damage to the cells (Faro *et al.* 1997, Faro *et al.* 2002a). MeHg can also interact with and disrupt the function of the DAT, possibly contributing to the changes in intracellular DA content (Dreiem *et al.* 2009).

Increases in intracellular MeHg concentrations could lead to increased toxicity and the damage may be more severe in cells intrinsically sensitive to insult, such as DA neurons. My studies show that the transporter MRP-7 is expressed in DA neurons in *C. elegans* and may be involved in Hg efflux to inhibit cellular toxicity (**Fig. 32, Fig. 37**). Although an MRP has not been previously identified in DA neurons, my studies suggest the transporter may mediate neuronal vulnerability to neurotoxicants.

VIII. Future directions

A. Cell-type specific RNAi

SKN-1 and MRP-7 inhibit MeHg-induced DA neuron degeneration. RNAi mediated knockdown of *skn-1* or *mrp-7* exclusively in the DA neurons could provide an opportunity to further characterize the role of the proteins in these neurons. Cell-type specific knockdown of *skn-1* or *mrp-7* in other cells could also be utilized to determine in which cells the proteins play a role in animal viability and how the proteins may function to inhibit toxicity in the developing embryo. A method for cell-type specific RNAi takes advantage of the gene *sid-1*. SID-1 is a dsRNA channel that is required for uptake of the dsRNA into cells and *sid-1* mutants are essentially resistant to RNAi (Calixto *et al.* 2010). Therefore, SID-1 can be expressed behind cell-type specific promoters in *sid-1* mutants and RNAi will result in gene knockdown only in cells that express the channel. Cell-type specific RNAi could also allow knockdown of a gene necessary for development or viability in a subset of cells while maintaining normal expression in the rest of the animal. For example, SKN-1 knockdown exclusively in the DA neurons may allow the RNAi to be continued through multiple generations as the expression the cells necessary for embryonic development would not be affected.

B. Epigenetics, acetylation and ubiquitination

Epigenetics is a rapidly-advancing area of study in toxicology, but few papers exist regarding epigenetics in MeHg toxicity. Mice exposed to MeHg *in utero* and for 7 days after birth had increased methylation and decreased acetylation of the histones at the BDNF promoter (Onishchenko *et al.* 2008). mRNA levels of the DNA methyltransferase (DNMT-1) were decreased and methylation of CpG sites in the promoter of p16(INK4a), a tumor suppressor gene, was reduced following MeHg exposure in rats (Desaulniers *et al.* 2009). These studies suggest that epigenetic changes may be affecting gene expression following MeHg exposure, but the larger implications of these observations are still unknown. Our *C. elegans* model provides a convenient opportunity for *in utero* exposure and analysis of offspring, that may facilitate MeHg-associated epigenetic studies. As the larvae develop quickly, and the animals have a lifespan of only 2-3 weeks, the effects of *in utero* MeHg exposure may be monitored at various time points from birth to death.

In addition to histones, other proteins can be acetylated with varying consequences on cellular function. Acetylation can be detected with antibodies or through liquid chromatography – mass spectrometry (LC-MS) (Choudhary *et al.* 2009). Analysis of the acetylation state of individual proteins is helpful for hypothesis driven studies. This would allow us to determine if acetylation is altered by MeHg exposure and which proteins may be the target of this acetylation. The identification of acetylated proteins could also provide insight into the acetyltransferases or deacetylases that are affected by MeHg (Choudhary *et al.* 2009). The combination of this sensitive technology and with our model for MeHg toxicity may provide insight into the role of MeHg in protein acetylation.

The strong association between the UPS and MeHg and the UPS and PD warrants further investigation into how the UPS is contributing to pathology. The *C. elegans* model of MeHg described here provides an opportunity for these studies. First, nematode fluorescent reporter strains are available for direct observation of protein turnover and UPS function in particular *C. elegans* cell types (Hamer *et al.* 2010). This could allow for further investigation into the role of the UPS in MeHg toxicity in DA neurons. Impairment of the UPS by MeHg in the DA neurons would provide support for a role of the toxicant in contributing to DA neuron death observed in PD. PD-associated mutant strains in which the DA neurons are already vulnerable could also be tested for sensitivity to MeHg. Additionally, ubiquitinated proteins can be detected and identified using LC-MS, allowing the identification of which proteins in the nematode become ubiquitinated following MeHg exposure. This technique may identify the proteins or protein classes that are damaged by MeHg and targeted for degradation. It would also be interesting to determine how ubiquitination or UPS function are affected following knockdown of the ubiquitin-related genes identified in the genetic screen.

C. Further studies on RNAi screen hits

My RNAi screen identified 92 genes involved in inhibiting MeHg toxicity. This list of genes provides opportunities for follow-up studies that have the potential to identify new molecular pathways involved in MeHg toxicity. Below I have provided examples of how three genes (*eat-6*, *gob-1* and C39E9.10) that were identified in the screen may be contributing to MeHg toxicity, based on their proposed function and current literature. Further characterization would provide both information about the function of the protein in *C. elegans* biology and how the protein may contribute to MeHg toxicity. I have also

described how the screen may have revealed novel regulators of SKN-1 as knockdown of any gene upstream of SKN-1 could result in a similar phenotype as SKN-1 RNAi. Based on their predicted functions, two genes could be involved in the phosphorylation or stabilization of SKN-1. Genes involved in nuclear transport were identified in the screen and, as the mechanism of SKN-1 nuclear translocation is undefined, may provide insight into this important step in the activation of SKN-1.

eat-6 encodes the a subunit of a Na⁺/K⁺ ATPase and mutation leads to a reduction in the ion gradients necessary for action potentials and a slowed pharyngeal pumping rate (Davis *et al.* 1995). In *Drosophila*, mutations in the α -subunit of the Na⁺/K⁺ ATPase result in hyperexcitability and neuronal degeneration (Palladino *et al.* 2003). Mutations in the human gene (ATP1A4) can lead to rapid-onset dystonia-parkinsonism, which causes some symptoms similar to PD but is not responsive to L-dopa therapy and does not cause loss of DAT or significant neuronal loss (de Carvalho Aguiar *et al.* 2004). MeHg can bind to the ATPase and inhibit its function. The depolarization of the membrane caused by loss of Na⁺/K⁺ ATPase function could increase Ca²⁺ entry into the cell and increase ROS to contribute to cytotoxicity (Huang *et al.* 2008). Loss of *eat-6* by RNAi could also lead to elevated intracellular Ca²⁺ and ROS, sensitizing the cells to further insult by MeHg. Future studies could determine if *eat-6* is expressed in DA neurons and contributes to neurotoxicity in *C. elegans*.

C39E9.10 is homologous to the human SPNS1 (protein spinster homolog isoform 1), originally labeled HSpin1 (Yanagisawa *et al.* 2003). In *Drosophila*, the spin gene is required for programmed cell death and loss of this protein results in degeneration of neurons and the accumulation of lipofuscin in the lysosomes (Nakano *et al.* 2001). The human HSpin1 interacts with Bcl-2/Bcl-xL to induce autophagy and a decrease in this protein could impair normal cell death pathways and contribute to neurodegeneration (Yanagisawa *et al.* 2003). Lipofuscin can be measured in *C. elegans* and determining the role of C39E9.10 may provide insight into the role of autophagy in MeHg toxicity and DA neuron degeneration.

The *gob-1* gene encodes the trehalose-6-phosphatase enzyme that converts trehalose-6-phosphate (T-6-P) to trehalose (Kormish & McGhee 2005). Trehalose is a sugar that protects cells against the stress from multiple types of insults in plants and other organisms including *C. elegans*. Trehalose also prevents the accumulation of unfolded proteins (Singer & Lindquist 1998). RNAi knockdown of *gob-1* decreases the levels of trehalose while increasing levels of the potentially toxic T-6-P. Treatment with

exogenous trehalose extends life span in *C. elegans*, so it is possible that a reduction of this compound in the nematode may increase basal stress levels and sensitize the animal to further insult by MeHg (Honda *et al.* 2010).

nekl-2 is a kinase that is predicted to phosphorylate SKN-1 to facilitate its entry into the nucleus. This kinase was identified in a screen and it was shown that RNAi knockdown results in decreased SKN-1 nuclear localization, decreased stress resistance and decreased life span (Kell *et al.* 2007). The human homologue of *nekl-2* is NEK8 which plays a role in the cytoskeleton and cell cycle progression. Mutations in the human and mice NEK8 genes result in cystic kidney disease (Liu *et al.* 2002, Zalli *et al.* 2012). Although the neurotoxic effects are the primary concern for MeHg toxicity, effects on the kidneys have been reported in numerous animal studies.

K03H1.10 is homologous to *C. elegans cbp-1* and the mammalian p300/CBP transcriptional coactivator (Shi & Mello 1998). Based on the predicted sequence, K03H1.10 contains the domains necessary for interaction with the transcription factor CREB and another binding domain, however it lacks the HAT domain. *cbp-1* promotes the stabilization and activation of SKN-1 in *C. elegans* development and p300/CBP interacts with and acetylates Nrf2 in mammalian systems (Shi & Mello 1998, Sun *et al.* 2009). Without the HAT domain, K03H1.10 is unlikely to acetylate SKN-1, however it may still participate in the binding and stabilization of SKN-1 in gene promoters.

Currently the mechanism of SKN-1 entry into the nucleus is undefined. In mammals, Nrf2 nuclear translocation is facilitated by importin α and importin β (Theodore *et al.* 2008). As SKN-1 nuclear localization is necessary for survival in the presence of MeHg, loss of any upstream regulators may also decrease viability after MeHg exposure. The screen identified *ima-3* and *imb-3* (homologues of importin α and importin β), *nxt-1* (NXT2), *ran-4* (NTF2) and three members of the nuclear pore complex (NUP 98, 160, 205). NTF2 (nuclear transport factor 2) is necessary to bind RanGDP and facilitate its entry into the nucleus through the NPC (nuclear pore complex) (Ribbeck *et al.* 1998). Ran is being constantly depleted from the nucleus as it is necessary for transport of many substrates out of the nucleus (as RanGTP). NXT1 is a nuclear export factor that also participates in Ran-mediated transport. Disruption of nuclear transport in general can lead to many types of dysfunction in the cell and has been linked to neurodegenerative disease including PD (Patel & Chu 2011).

IX. References

- 40612, T. S. A. N. (2008) Determination of Hg in urine using the Thermo Scientific XSERIES 2 ICP-MS. In: *Application Note 40612*, (T. F. Scientific ed.). Thermo Fisher Scientific.
- Abe, T., Haga, T. and Kurokawa, M. (1975) Blockage of axoplasmic transport and depolymerisation of reassembled microtubules by methyl mercury. *Brain Res*, **86**, 504-508.
- Affymetrix GeneChip C. elegans Genome Array. Vol. 2013.
- Ahringer, J. (2006) Reverse Genetics. *WormBook*.
- Al-Abbasi, A. H., Kostyniak, P. J. and Clarkson, T. W. (1978) An extracorporeal complexing hemodialysis system for the treatment of methylmercury poisoning. III. Clinical applications. *J Pharmacol Exp Ther*, **207**, 249-254.
- Aleo, M. F., Morandini, F., Bettoni, F., Giuliani, R., Rovetta, F., Steimberg, N., Apostoli, P., Parrinello, G. and Mazzoleni, G. (2005) Endogenous thiols and MRP transporters contribute to Hg²⁺ efflux in HgCl₂-treated tubular MDCK cells. *Toxicology*, **206**, 137-151.
- Ali, S. F., LeBel, C. P. and Bondy, S. C. (1992) Reactive oxygen species formation as a biomarker of methylmercury and trimethyltin neurotoxicity. *Neurotoxicology*, **13**, 637-648.
- Altschul, S. F., Gish, W., Miller, W., Myers, E. W. and Lipman, D. J. (1990) Basic local alignment search tool. *Journal of Molecular Biology*, **215**, 403-410.
- An, J. H. and Blackwell, T. K. (2003) SKN-1 links C. elegans mesendodermal specification to a conserved oxidative stress response. *Genes & Development*, **17**, 1882-1893.
- An, J. H., Vranas, K., Lucke, M., Inoue, H., Hisamoto, N., Matsumoto, K. and Blackwell, T. K. (2005) Regulation of the Caenorhabditis elegans oxidative stress defense protein SKN-1 by glycogen synthase kinase-3. *Proceedings of the National Academy of Sciences of the United States of America*, **102**, 16275-16280.
- Andersen, H. R. and Andersen, O. (1993) Effects of dietary alpha-tocopherol and beta-carotene on lipid peroxidation induced by methyl mercuric chloride in mice. *Pharmacol Toxicol*, **73**, 192-201.
- Antoshechkin, I. and Sternberg, P. W. (2007) The versatile worm: genetic and genomic resources for Caenorhabditis elegans research. *Nat Rev Genet*, **8**, 518-532.
- Ariga, H., Takahashi-Niki, K., Kato, I., Maita, H., Niki, T. and Iguchi-Ariga, S. M. (2013) Neuroprotective function of DJ-1 in Parkinson's disease. *Oxid Med Cell Longev*, **2013**, 683920.

- Armstrong, R. N. (1997) Structure, catalytic mechanism, and evolution of the glutathione transferases. *Chem Res Toxicol*, **10**, 2-18.
- Ashrafi, K., Chang, F. Y., Watts, J. L., Fraser, A. G., Kamath, R. S., Ahringer, J. and Ruvkun, G. (2003) Genome-wide RNAi analysis of *Caenorhabditis elegans* fat regulatory genes. *Nature*, **421**, 268-272.
- Asikainen, S., Vartiainen, S., Lakso, M., Nass, R. and Wong, G. (2005) Selective sensitivity of *Caenorhabditis elegans* neurons to RNA interference. *NeuroReport*, **16**, 1995-1999.
- Atchison, W. D. (2005) Is chemical neurotransmission altered specifically during methylmercury-induced cerebellar dysfunction? *Trends in Pharmacological Sciences*, **26**, 549-557.
- Atchison, W. D. and Hare, M. F. (1994) Mechanisms of methylmercury-induced neurotoxicity. *FASEB J.*, **8**, 622-629.
- Atchison, W. D. and Narahashi, T. (1982) Methylmercury-induced depression of neuromuscular transmission in the rat. *Neurotoxicology*, **3**, 37-50.
- Audhya, A., Hyndman, F., McLeod, I. X., Maddox, A. S., Yates, J. R., 3rd, Desai, A. and Oegema, K. (2005) A complex containing the Sm protein CAR-1 and the RNA helicase CGH-1 is required for embryonic cytokinesis in *Caenorhabditis elegans*. *J Cell Biol*, **171**, 267-279.
- Avery, L. and You, Y. J. (2012) *C. elegans* feeding. *WormBook*, doi/10.1895/wormbook.1.150.1.
- Ayyadevara, S., Dandapat, A., Singh, S. P., Siegel, E. R., Shmookler Reis, R. J., Zimniak, L. and Zimniak, P. (2007) Life span and stress resistance of *Caenorhabditis elegans* are differentially affected by glutathione transferases metabolizing 4-hydroxynon-2-enal. *Mechanisms of ageing and development*, **128**, 196-205.
- Ayyadevara, S., Engle, M. R., Singh, S. P., Dandapat, A., Lichti, C. F., Benes, H., Shmookler Reis, R. J., Liebau, E. and Zimniak, P. (2005) Lifespan and stress resistance of *Caenorhabditis elegans* are increased by expression of glutathione transferases capable of metabolizing the lipid peroxidation product 4-hydroxynonenal. *Aging Cell*, **4**, 257-271.
- Bailey, J. M., Hutsell, B. A. and Newland, M. C. (2013) Dietary nimodipine delays the onset of methylmercury neurotoxicity in mice. *Neurotoxicology*, **37**, 108-117.
- Bakir, F., Damluji, S. F., Amin-Zaki, L. et al. (1973) Methylmercury poisoning in Iraq. *Science*, **181**, 230-241.
- Bakos, E., Hegedüs, T., Holló, Z., Welker, E., Tusnády, G. E., Zaman, G. J., Flens, M. J., Váradi, A. and Sarkadi, B. (1996) Membrane topology and glycosylation of the human multidrug resistance-associated protein. *J Biol Chem*, **271**, 12322-12326.

- Ballatori, N., Lieberman, M. W. and Wang, W. (1998) N-acetylcysteine as an antidote in methylmercury poisoning. *Environ Health Perspect*, **106**, 267-271.
- Ballatori, N. and Villalobos, A. R. (2002) Defining the molecular and cellular basis of toxicity using comparative models. *Toxicol Appl Pharmacol*, **183**, 207-220.
- Bargmann, C. I. (1993) Genetic and Cellular Analysis of Behavior in *C. elegans*. *Annual Review of Neuroscience*, **16**, 47-71.
- Bargmann, C. I. (1998) Neurobiology of the *Caenorhabditis elegans* Genome. *Science*, **282**, 2028-2033.
- Barone, M. C., Sykiotis, G. P. and Bohmann, D. (2011) Genetic activation of Nrf2 signaling is sufficient to ameliorate neurodegenerative phenotypes in a *Drosophila* model of Parkinson's disease. *Dis Model Mech*, **4**, 701-707.
- Bartels, A. L., Kortekaas, R., Bart, J., Willemsen, A. T., de Klerk, O. L., de Vries, J. J., van Oostrom, J. C. and Leenders, K. L. (2009) Blood-brain barrier P-glycoprotein function decreases in specific brain regions with aging: a possible role in progressive neurodegeneration. *Neurobiol Aging*, **30**, 1818-1824.
- Bassett, T., Bach, P. and Chan, H. M. (2012) Effects of methylmercury on the secretion of pro-inflammatory cytokines from primary microglial cells and astrocytes. *Neurotoxicology*, **33**, 229-234.
- Belletti, S., Orlandini, G., Vettori, M. V., Mutti, A., Uggeri, J., Scandroglio, R., Alinovi, R. and Gatti, R. (2002) Time course assessment of methylmercury effects on C6 glioma cells: submicromolar concentrations induce oxidative DNA damage and apoptosis. *J Neurosci Res*, **70**, 703-711.
- Berg, K., Puntervoll, P., Valdersnes, S. and Goksøyr, A. (2010) Responses in the brain proteome of Atlantic cod (*Gadus morhua*) exposed to methylmercury. *Aquat Toxicol*, **100**, 51-65.
- Bianchi, L. and Driscoll, M. (2006) Culture of embryonic *C. elegans* cells for electrophysiological and pharmacological analyses. *WormBook*, 1-15.
- Bianchi, L., Driscoll, M. (2006) Culture of embryonic *C. elegans* cells for electrophysiological and pharmacological analyses. In: *WormBook*, (W. The *C. elegans* Research Community ed.), Vol. doi/10.1895/wormbook.1.122.1.
- Bishop, N. A. and Guarente, L. (2007) Two neurons mediate diet-restriction-induced longevity in *C. elegans*. *Nature*, **447**, 545-549.
- Blau, N., Bonafe, L. and Thony, B. (2001) Tetrahydrobiopterin deficiencies without hyperphenylalaninemia: diagnosis and genetics of dopa-responsive dystonia and sepiapterin reductase deficiency. *Molecular genetics and metabolism*, **74**, 172-185.

- Bloom, D. A. and Jaiswal, A. K. (2003) Phosphorylation of Nrf2 at Ser40 by protein kinase C in response to antioxidants leads to the release of Nrf2 from INrf2, but is not required for Nrf2 stabilization/accumulation in the nucleus and transcriptional activation of antioxidant response element-mediated NAD(P)H:quinone oxidoreductase-1 gene expression. *J Biol Chem*, **278**, 44675-44682.
- Bonnet, J. J., Benmansour, S., Amejdki-Chab, N. and Costentin, J. (1994) Effect of CH₃HgCl and several transition metals on the dopamine neuronal carrier; peculiar behaviour of Zn²⁺. *Eur J Pharmacol*, **266**, 87-97.
- Borst, P., Evers, R., Kool, M. and Wijnholds, J. (2000) A family of drug transporters: the multidrug resistance-associated proteins. *J Natl Cancer Inst*, **92**, 1295-1302.
- Boulin, T., Etchberger, J. and Hobert, O. (2006) Reporter gene fusions. *WormBook*.
- Boulin, T. and Hobert, O. (2012) From genes to function: the *C. elegans* genetic toolbox. *Wiley Interdiscip Rev Dev Biol*, **1**, 114-137.
- Bourdineaud, J. P., Fujimura, M., Laclau, M., Sawada, M. and Yasutake, A. (2011) Deleterious effects in mice of fish-associated methylmercury contained in a diet mimicking the Western populations' average fish consumption. *Environ Int*, **37**, 303-313.
- Bourdineaud, J. P., Marumoto, M., Yasutake, A. and Fujimura, M. (2012) Dietary mercury exposure resulted in behavioral differences in mice contaminated with fish-associated methylmercury compared to methylmercury chloride added to diet. *J Biomed Biotechnol*, **2012**, 681016.
- Bowerman, B., Eaton, B. A. and Priess, J. R. (1992) *skn-1*, a maternally expressed gene required to specify the fate of ventral blastomeres in the early *C. elegans* embryo. *Cell*, **68**, 1061-1075.
- Boyd, W. A., McBride, S. J., Rice, J. R., Snyder, D. W. and Freedman, J. H. (2010) A high-throughput method for assessing chemical toxicity using a *Caenorhabditis elegans* reproduction assay. *Toxicol Appl Pharmacol*, **245**, 153-159.
- Boyd, W. A., Smith, M. V., Kissling, G. E. and Freedman, J. H. (2012) Medium- and high-throughput screening of neurotoxicants using *C. elegans*. *Neurotoxicology and Teratology*, **In Press, Corrected Proof**.
- Braak, H., Del Tredici, K., Rüb, U., de Vos, R. A., Jansen Steur, E. N. and Braak, E. (2003) Staging of brain pathology related to sporadic Parkinson's disease. *Neurobiol Aging*, **24**, 197-211.
- Braungart, E., Gerlach, M., Riederer, P., Baumeister, R. and Hoener, M. C. (2004) *Caenorhabditis elegans* MPP⁺ model of Parkinson's disease for high-throughput drug screenings. *Neurodegener Dis*, **1**, 175-183.
- Brenner, S. (1974) The genetics of *Caenorhabditis elegans*. *Genetics*, **77**, 71-94.

- Bridges, C. C., Joshee, L. and Zalups, R. K. (2009) Effect of DMPS and DMSA on the placental and fetal disposition of methylmercury. *Placenta*, **30**, 800-805.
- Bridges, C. C., Joshee, L. and Zalups, R. K. (2011) MRP2 and the handling of mercuric ions in rats exposed acutely to inorganic and organic species of mercury. *Toxicol Appl Pharmacol*, **251**, 50-58.
- Bridges, C. C., Joshee, L. and Zalups, R. K. (2012) Placental and fetal disposition of mercuric ions in rats exposed to methylmercury: role of Mrp2. *Reprod Toxicol*, **34**, 628-634.
- Broeks, A., Gerrard, B., Allikmets, R., Dean, M. and Plasterk, R. H. (1996) Homologues of the human multidrug resistance genes MRP and MDR contribute to heavy metal resistance in the soil nematode *Caenorhabditis elegans*. *EMBO J*, **15**, 6132-6143.
- Burton, N. C., Kensler, T. W. and Guilarte, T. R. (2006) In vivo modulation of the Parkinsonian phenotype by Nrf2. *Neurotoxicology*, **27**, 1094-1100.
- Calixto, A., Chelur, D., Topalidou, I., Chen, X. and Chalfie, M. (2010) Enhanced neuronal RNAi in *C. elegans* using SID-1. *Nature methods*, **7**, 554-559.
- Cambier, S., Bénard, G., Mesmer-Dudons, N., Gonzalez, P., Rossignol, R., Brèthes, D. and Bourdineaud, J. P. (2009) At environmental doses, dietary methylmercury inhibits mitochondrial energy metabolism in skeletal muscles of the zebra fish (*Danio rerio*). *The International Journal of Biochemistry & Cell Biology*, **41**, 791-799.
- Cambier, S., Gonzalez, P., Durrieu, G., Maury-Brachet, R., Boudou, A. and Bourdineaud, J. P. (2010) Serial analysis of gene expression in the skeletal muscles of zebrafish fed with a methylmercury-contaminated diet. *Environ Sci Technol*, **44**, 469-475.
- Cambier, S., Gonzalez, P., Mesmer-Dudons, N., Brèthes, D., Fujimura, M. and Bourdineaud, J. P. (2012) Effects of dietary methylmercury on the zebrafish brain: histological, mitochondrial, and gene transcription analyses. *Biometals*, **25**, 165-180.
- Candido, E. P., Jones, D., Dixon, D. K., Graham, R. W., Russnak, R. H. and Kay, R. J. (1989) Structure, organization, and expression of the 16-kDa heat shock gene family of *Caenorhabditis elegans*. *Genome*, **31**, 690-697.
- Cannon, J. R. and Greenamyre, J. T. (2013) Gene-environment interactions in Parkinson's disease: specific evidence in humans and mammalian models. *Neurobiol Dis*, **57**, 38-46.
- Carew, M. W. and Leslie, E. M. (2010) Selenium-dependent and -independent transport of arsenic by the human multidrug resistance protein 2 (MRP2/ABCC2): implications for the mutual detoxification of arsenic and selenium. *Carcinogenesis*, **31**, 1450-1455.

- Carvalho, M. C., Nazari, E. M., Farina, M. and Muller, Y. M. R. (2008) Behavioral, Morphological, and Biochemical Changes after In Ovo Exposure to Methylmercury in Chicks. *Toxicol. Sci.*, **106**, 180-185.
- Carvelli, L., McDonald, P. W., Blakely, R. D. and Defelice, L. J. (2004) Dopamine transporters depolarize neurons by a channel mechanism. *Proc Natl Acad Sci U S A*, **101**, 16046-16051.
- Castoldi, A. F., Barni, S., Turin, I., Gandini, C. and Manzo, L. (2000) Early acute necrosis, delayed apoptosis and cytoskeletal breakdown in cultured cerebellar granule neurons exposed to methylmercury. *J Neurosci Res*, **59**, 775-787.
- Caudle, W. M., Guillot, T. S., Lazo, C. R. and Miller, G. W. (2012) Industrial toxicants and Parkinson's disease. *Neurotoxicology*, **33**, 178-188.
- Ceccatelli, S., Daré, E. and Moors, M. (2010) Methylmercury-induced neurotoxicity and apoptosis. *Chem Biol Interact*, **188**, 301-308.
- Chan, C. S., Gertler, T. S. and Surmeier, D. J. (2009) Calcium homeostasis, selective vulnerability and Parkinson's disease. *Trends Neurosci*, **32**, 249-256.
- Chang, J. Y. and Tsai, P.-F. (2008) Prevention of methylmercury -induced mitochondrial depolarization, glutathione depletion and cell death by 15-deoxy-delta-12,14-prostaglandin J2. *Neurotoxicology*, **29**, 1054-1061.
- Chen, G., Bower, K. A., Ma, C., Fang, S., Thiele, C. J. and Luo, J. (2004) Glycogen synthase kinase 3beta (GSK3beta) mediates 6-hydroxydopamine-induced neuronal death. *FASEB J*, **18**, 1162-1164.
- Chen, P. C., Vargas, M. R., Pani, A. K., Smeyne, R. J., Johnson, D. A., Kan, Y. W. and Johnson, J. A. (2009) Nrf2-mediated neuroprotection in the MPTP mouse model of Parkinson's disease: Critical role for the astrocyte. *Proc Natl Acad Sci U S A*, **106**, 2933-2938.
- Choe, K. P., Przybysz, A. J. and Strange, K. (2009) The WD40 repeat protein WDR-23 functions with the CUL4/DDB1 ubiquitin ligase to regulate nuclear abundance and activity of SKN-1 in *Caenorhabditis elegans*. *Mol Cell Biol*, **29**, 2704-2715.
- Choi, B. H., Lapham, L. W., Amin-Zaki, L. and Saleem, T. (1978) Abnormal neuronal migration, deranged cerebral cortical organization, and diffuse white matter astrocytosis of human fetal brain: A major effect of methylmercury poisoning in utero. *J. Neuropath. Exp. Neurol.*, **37**, 719-733.
- Choudhary, C., Kumar, C., Gnad, F., Nielsen, M. L., Rehman, M., Walther, T. C., Olsen, J. V. and Mann, M. (2009) Lysine acetylation targets protein complexes and co-regulates major cellular functions. *Science*, **325**, 834-840.
- Christensen, M., Estevez, A., Yin, X., Fox, R., Morrison, R., McDonnell, M., Gleason, C., Miller, D. M. and Strange, K. (2002) A primary culture system for functional analysis of *C. elegans* neurons and muscle cells. *Neuron*, **33**, 503-514.

- Clarkson, T. W. (1987) Metal toxicity in the central nervous system. *Environ Health Perspect*, **75**, 59-64.
- Clarkson, T. W. and Magos, L. (2006) The toxicology of mercury and its chemical compounds. *Crit Rev Toxicol*, **36**, 609-662.
- Clarkson, T. W., Magos, L., Cox, C., Greenwood, M. R., Amin-Zaki, L., Majeed, M. A. and Al-Damluji, S. F. (1981) Tests of efficacy of antidotes for removal of methylmercury in human poisoning during the Iraq outbreak. *J Pharmacol Exp Ther*, **218**, 74-83.
- Clarkson, T. W., Magos, L. and Myers, G. J. (2003) The toxicology of mercury--current exposures and clinical manifestations. *N Engl J Med*, **349**, 1731-1737.
- Cole, R. D., Anderson, G. L. and Williams, P. L. (2004) The nematode *Caenorhabditis elegans* as a model of organophosphate-induced mammalian neurotoxicity. *Toxicol Appl Pharmacol*, **194**, 248-256.
- Conseil, G., Deeley, R. G. and Cole, S. P. (2005) Polymorphisms of MRP1 (ABCC1) and related ATP-dependent drug transporters. *Pharmacogenet Genomics*, **15**, 523-533.
- Corti, O., Lesage, S. and Brice, A. (2011) What genetics tells us about the causes and mechanisms of Parkinson's disease. *Physiol Rev*, **91**, 1161-1218.
- Cuadrado, A., Moreno-Murciano, P. and Pedraza-Chaverri, J. (2009) The transcription factor Nrf2 as a new therapeutic target in Parkinson's disease. *Expert Opin Ther Targets*, **13**, 319-329.
- Cuello, S., Goya, L., Madrid, Y., Campuzano, S., Pedrero, M., Bravo, L., Cámara, C. and Ramos, S. (2010) Molecular mechanisms of methylmercury-induced cell death in human HepG2 cells. *Food and chemical toxicology : an international journal published for the British Industrial Biological Research Association*, **48**, 1405-1411.
- Cui, Y., McBride, S., Boyd, W., Alper, S. and Freedman, J. (2007) Toxicogenomic analysis of *Caenorhabditis elegans* reveals novel genes and pathways involved in the resistance to cadmium toxicity. *Genome Biology*, **8**, R122.
- Cuomo, V., Ambrosi, L., Annau, Z., Cagiano, R., Brunello, N. and Racagni, G. (1984) Behavioural and neurochemical changes in offspring of rats exposed to methyl mercury during gestation. *Neurobehav Toxicol Teratol*, **6**, 249-254.
- Curle, D. C., Ray, M. and Persaud, T. V. (1987) In vivo evaluation of teratogenesis and cytogenetic changes following methylmercuric chloride treatment. *Anat Rec*, **219**, 286-295.
- Dallas, S., Miller, D. S. and Bendayan, R. (2006) Multidrug resistance-associated proteins: expression and function in the central nervous system. *Pharmacol Rev*, **58**, 140-161.

- Dalman, M. R., Deeter, A., Nimishakavi, G. and Duan, Z. H. (2012) Fold change and p-value cutoffs significantly alter microarray interpretations. *BMC Bioinformatics*, **13 Suppl 2**, S11.
- Damier, P., Hirsch, E. C., Agid, Y. and Graybiel, A. M. (1999) The substantia nigra of the human brain. II. Patterns of loss of dopamine-containing neurons in Parkinson's disease. *Brain*, **122 (Pt 8)**, 1437-1448.
- Daré, E., Fetissov, S., Hökfelt, T., Hall, H., Ogren, S. O. and Ceccatelli, S. (2003) Effects of prenatal exposure to methylmercury on dopamine-mediated locomotor activity and dopamine D2 receptor binding. *Naunyn Schmiedebergs Arch Pharmacol*, **367**, 500-508.
- David, H. E., Dawe, A. S., de Pomerai, D. I., Jones, D., Candido, E. P. and Daniells, C. (2003) Construction and evaluation of a transgenic hsp16-GFP-lacZ *Caenorhabditis elegans* strain for environmental monitoring. *Environ Toxicol Chem*, **22**, 111-118.
- Davidson, P. W., Cory-Slechta, D. A., Thurston, S. W. et al. (2011) Fish consumption and prenatal methylmercury exposure: cognitive and behavioral outcomes in the main cohort at 17 years from the Seychelles child development study. *Neurotoxicology*, **32**, 711-717.
- Davis, J. R., Li, Y. and Rankin, C. H. (2008) Effects of Developmental Exposure to Ethanol on *Caenorhabditis elegans*. *Alcoholism: Clinical and Experimental Research*, **32**, 853-867.
- Davis, M. W., Somerville, D., Lee, R. Y., Lockery, S., Avery, L. and Fambrough, D. M. (1995) Mutations in the *Caenorhabditis elegans* Na,K-ATPase alpha-subunit gene, eat-6, disrupt excitable cell function. *J Neurosci*, **15**, 8408-8418.
- Dawson, T. M. and Dawson, V. L. (2003) Molecular pathways of neurodegeneration in Parkinson's disease. *Science*, **302**, 819-822.
- de Carvalho Aguiar, P., Sweadner, K. J., Penniston, J. T. et al. (2004) Mutations in the Na⁺/K⁺ -ATPase alpha3 gene ATP1A3 are associated with rapid-onset dystonia parkinsonism. *Neuron*, **43**, 169-175.
- Dean, M., Rzhetsky, A. and Allikmets, R. (2001) The human ATP-binding cassette (ABC) transporter superfamily. *Genome Res*, **11**, 1156-1166.
- Della Torre, C., Zaja, R., Loncar, J., Smital, T., Focardi, S. and Corsi, I. (2012) Interaction of ABC transport proteins with toxic metals at the level of gene and transport activity in the PLHC-1 fish cell line. *Chem Biol Interact*, **198**, 9-17.
- Dengg, M. and van Meel, J. C. (2004) *Caenorhabditis elegans* as model system for rapid toxicity assessment of pharmaceutical compounds. *J Pharmacol Toxicol Methods*, **50**, 209-214.

- Dennis, J. L., Mutwakil, M. H. A. Z., Lowe, K. C. and de Pomerai, D. I. (1997) Effects of metal ions in combination with a non-ionic surfactant on stress responses in a transgenic nematode. *Aquatic Toxicology*, **40**, 37-50.
- Desaulniers, D., Xiao, G. H., Lian, H., Feng, Y. L., Zhu, J., Nakai, J. and Bowers, W. J. (2009) Effects of mixtures of polychlorinated biphenyls, methylmercury, and organochlorine pesticides on hepatic DNA methylation in prepubertal female Sprague-Dawley rats. *Int J Toxicol*, **28**, 294-307.
- Dhawan, R., Dusenbery, D. B. and Williams, P. L. (1999) Comparison of lethality, reproduction, and behavior as toxicological endpoints in the nematode *Caenorhabditis elegans*. *J Toxicol Environ Health A*, **58**, 451-462.
- Dhawan, R., Dusenbery, D. B. and Williams, P. L. (2000) A comparison of metal-induced lethality and behavioral responses in the nematode *Caenorhabditis elegans*. *Environmental Toxicology and Chemistry*, **19**, 3061-3067.
- Dinkova-Kostova, A. T., Holtzclaw, W. D., Cole, R. N., Itoh, K., Wakabayashi, N., Katoh, Y., Yamamoto, M. and Talalay, P. (2002) Direct evidence that sulfhydryl groups of Keap1 are the sensors regulating induction of phase 2 enzymes that protect against carcinogens and oxidants. *Proc Natl Acad Sci U S A*, **99**, 11908-11913.
- Drechsel, D. A. and Patel, M. (2008) Role of reactive oxygen species in the neurotoxicity of environmental agents implicated in Parkinson's disease. *Free Radic Biol Med*, **44**, 1873-1886.
- Dreiem, A., Shan, M., Okoniewski, R. J., Sanchez-Morrissey, S. and Seegal, R. F. (2009) Methylmercury inhibits dopaminergic function in rat pup synaptosomes in an age-dependent manner. *Neurotoxicol Teratol*, **31**, 312-317.
- Dreuw, A., Hermanns, H. M., Heise, R. et al. (2005) Interleukin-6-type cytokines upregulate expression of multidrug resistance-associated proteins in NHEK and dermal fibroblasts. *J Invest Dermatol*, **124**, 28-37.
- Driscoll, C. T., Mason, R. P., Chan, H. M., Jacob, D. J. and Pirrone, N. (2013) Mercury as a global pollutant: sources, pathways, and effects. *Environ Sci Technol*, **47**, 4967-4983.
- Drożdżik, M., Białecka, M., Myśliwiec, K., Honczarenko, K., Stankiewicz, J. and Sych, Z. (2003) Polymorphism in the P-glycoprotein drug transporter MDR1 gene: a possible link between environmental and genetic factors in Parkinson's disease. *Pharmacogenetics*, **13**, 259-263.
- Du, M. and Wang, D. (2009) The neurotoxic effects of heavy metal exposure on GABAergic nervous system in nematode *Caenorhabditis elegans*. *Environ Toxicol Pharmacol*, **27**, 314-320.
- Duerr, J. S., Frisby, D. L., Gaskin, J., Duke, A., Asermely, K., Huddleston, D., Eiden, L. E. and Rand, J. B. (1999) *The cat-1 gene of Caenorhabditis elegans encodes a vesicular monoamine transporter required for specific monoamine-dependent behaviors.*

- Dutheil, F., Beaune, P., Tzourio, C., Lorient, M. A. and Elbaz, A. (2010) Interaction between ABCB1 and professional exposure to organochlorine insecticides in Parkinson disease. *Arch Neurol*, **67**, 739-745.
- Eaton, D. and Bammler, T. (1999) Concise Review of the glutathione s-transferases and their significance to toxicology. *Toxicological Sciences*, **49**, 156-164.
- Ekino, S., Susa, M., Ninomiya, T., Imamura, K. and Kitamura, T. (2007) Minamata disease revisited: An update on the acute and chronic manifestations of methyl mercury poisoning. *Journal of the Neurological Sciences*, **262**, 131-144.
- Eto, K., Marumoto, M. and Takeya, M. (2010) The pathology of methylmercury poisoning (Minamata disease). *Neuropathology*.
- Evans, T. C. (2006) Transformation and microinjection. *WormBook*, doi/10.1895/wormbook.1.108.1.
- Exner, N., Lutz, A. K., Haass, C. and Winklhofer, K. F. (2012) Mitochondrial dysfunction in Parkinson's disease: molecular mechanisms and pathophysiological consequences. *EMBO J*, **31**, 3038-3062.
- Fahn, S. (2008) *Parkinson's Disease: Molecular and Therapeutic Insights from Model Systems*. Elsevier Academic Press, New York, NY.
- Falcão, A. S., Bellarosa, C., Fernandes, A., Brito, M. A., Silva, R. F., Tiribelli, C. and Brites, D. (2007) Role of multidrug resistance-associated protein 1 expression in the in vitro susceptibility of rat nerve cell to unconjugated bilirubin. *Neuroscience*, **144**, 878-888.
- Farina, M., Campos, F., Vendrell, I., Berenguer, J., Barzi, M., Pons, S. and Suñol, C. (2009) Probucol increases glutathione peroxidase-1 activity and displays long-lasting protection against methylmercury toxicity in cerebellar granule cells. *Toxicol Sci*, **112**, 416-426.
- Faro, L. R., do Nascimento, J. L., Alfonso, M. and Durán, R. (2002a) Mechanism of action of methylmercury on in vivo striatal dopamine release. Possible involvement of dopamine transporter. *Neurochem Int*, **40**, 455-465.
- Faro, L. R., do Nascimento, J. L., Alfonso, M. and Durán, R. (2002b) Protection of methylmercury effects on the in vivo dopamine release by NMDA receptor antagonists and nitric oxide synthase inhibitors. *Neuropharmacology*, **42**, 612-618.
- Faro, L. R., do Nascimento, J. L., Campos, F., Vidal, L., Alfonso, M. and Durán, R. (2005) Protective effects of glutathione and cysteine on the methylmercury-induced striatal dopamine release in vivo. *Life Sci*, **77**, 444-451.
- Faro, L. R., Durán, R., do Nascimento, J. L., Alfonso, M. and Picanço-Diniz, C. W. (1997) Effects of methyl mercury on the in vivo release of dopamine and its acidic metabolites DOPAC and HVA from striatum of rats. *Ecotoxicol Environ Saf*, **38**, 95-98.

- Finkelstein, Y., Vardi, J., Kesten, M. M. and Hod, I. (1996) The enigma of parkinsonism in chronic borderline mercury intoxication, resolved by challenge with penicillamine. *Neurotoxicology*, **17**, 291-295.
- Fire, A., Xu, S., Montgomery, M. K., Kostas, S. A., Driver, S. E. and Mello, C. C. (1998) Potent and specific genetic interference by double-stranded RNA in *Caenorhabditis elegans*. *Nature*, **391**, 806-811.
- Forman, H. J., Zhang, H. and Rinna, A. (2009) Glutathione: overview of its protective roles, measurement, and biosynthesis. *Mol Aspects Med*, **30**, 1-12.
- Fox, J. H., Patel-Mandlik, K. and Cohen, M. M. (1975) Comparative effects of organic and inorganic mercury on brain slice respiration and metabolism. *J Neurochem*, **24**, 757-762.
- Franco, J. L., Posser, T., Dunkley, P. R. et al. (2009) Methylmercury neurotoxicity is associated with inhibition of the antioxidant enzyme glutathione peroxidase. *Free Radic Biol Med*, **47**, 449-457.
- Freire, C. and Koifman, S. (2012) Pesticide exposure and Parkinson's disease: epidemiological evidence of association. *Neurotoxicology*, **33**, 947-971.
- Frelet, A. and Klein, M. (2006) Insight in eukaryotic ABC transporter function by mutation analysis. *FEBS Lett*, **580**, 1064-1084.
- Frokjaer-Jensen, C. (2003) Cameleon imaging of calcium transients in cultured mechanosensory neurons in *Caenorhabditis elegans*. In: *Niels Bohr Institute*. University of Copenhagen.
- Fujimura, M., Usuki, F., Kawamura, M. and Izumo, S. (2011) Inhibition of the Rho/ROCK pathway prevents neuronal degeneration in vitro and in vivo following methylmercury exposure. *Toxicol Appl Pharmacol*, **250**, 1-9.
- Fujimura, M., Usuki, F., Sawada, M., Rostene, W., Godefroy, D. and Takashima, A. (2009) Methylmercury exposure downregulates the expression of Rac1 and leads to neuritic degeneration and ultimately apoptosis in cerebrocortical neurons. *Neurotoxicology*, **30**, 16-22.
- Fujiyama, J., Hirayama, K. and Yasutake, A. (1994) Mechanism of methylmercury efflux from cultured astrocytes. *Biochem Pharmacol*, **47**, 1525-1530.
- Furuchi, T., Hwang, G. W. and Naganuma, A. (2002) Overexpression of the ubiquitin-conjugating enzyme Cdc34 confers resistance to methylmercury in *Saccharomyces cerevisiae*. *Mol Pharmacol*, **61**, 738-741.
- Gailer, J., George, G. N., Harris, H. H., Pickering, I. J., Prince, R. C., Somogyi, A., Buttigieg, G. A., Glass, R. S. and Denton, M. B. (2002) Synthesis, purification, and structural characterization of the dimethyldiselenoarsinate anion. *Inorg Chem*, **41**, 5426-5432.

- Giménez-Llort, L., Ahlbom, E., Daré, E., Vahter, M., Ögren, S. and Ceccatelli, S. (2001) Prenatal exposure to methylmercury changes dopamine-modulated motor activity during early ontogeny: age and gender-dependent effects. *Environ Toxicol Pharmacol*, **9**, 61-70.
- Glover, C. N., Zheng, D., Jayashankar, S., Sales, G. D., Hogstrand, C. and Lundebye, A. K. (2009) Methylmercury speciation influences brain gene expression and behavior in gestationally-exposed mice pups. *Toxicol Sci*, **110**, 389-400.
- Gorbatyuk, M. S. and Gorbatyuk, O. S. (2013) The Molecular Chaperone GRP78/BiP as a Therapeutic Target for Neurodegenerative Disorders: A Mini Review. *J Genet Syndr Gene Ther*, **4**.
- Gorbatyuk, M. S., Shabashvili, A., Chen, W. et al. (2012) Glucose regulated protein 78 diminishes α -synuclein neurotoxicity in a rat model of Parkinson disease. *Mol Ther*, **20**, 1327-1337.
- Götz, M. E., Koutsilieri, E., Riederer, P., Ceccatelli, S. and Daré, E. (2002) Methylmercury induces neurite degeneration in primary culture of mouse dopaminergic mesencephalic cells. *J Neural Transm*, **109**, 597-605.
- Grandjean, P., Weihe, P., White, R. F. et al. (1997) Cognitive deficit in 7-year-old children with prenatal exposure to methylmercury. *Neurotoxicol Teratol*, **19**, 417-428.
- Gromer, S., Eubel, J. K., Lee, B. L. and Jacob, J. (2005) Human selenoproteins at a glance. *Cell Mol Life Sci*, **62**, 2414-2437.
- Guyen, K. and de Pomerai, D. (1995) Differential expression of HSP70 proteins in response to heat and cadmium in *Caenorhabditis elegans*. *J Thermal Biol*, **20**, 355-363.
- Guyen, K., Duce, J. A. and de Pomerai, D. I. (1995) Calcium moderation of cadmium stress explored using a stress-inducible transgenic strain of *Caenorhabditis elegans*. *Comp Biochem Physiol C Pharmacol Toxicol Endocrinol*, **110**, 61-70.
- Hamer, G., Matilainen, O. and Holmberg, C. I. (2010) A photoconvertible reporter of the ubiquitin-proteasome system in vivo. *Nature methods*, **7**, 473-478.
- Hamilton, B., Dong, Y., Shindo, M., Liu, W., Odell, I., Ruvkun, G. and Lee, S. S. (2005) A systematic RNAi screen for longevity genes in *C. elegans*. *Genes Dev*, **19**, 1544-1555.
- Harada, M. (1995) Minamata disease: methylmercury poisoning in Japan caused by environmental pollution. *Crit Rev Toxicol*, **25**, 1-24.
- Hare, M. F., McGinnis, K. M. and Atchison, W. D. (1993) Methylmercury increases intracellular concentrations of Ca^{++} and heavy metals in NG108-15 cells. *J Pharmacol Exp Ther*, **266**, 1626-1635.

- Hartz, A. M. and Bauer, B. (2010) Regulation of ABC transporters at the blood-brain barrier: new targets for CNS therapy. *Mol Interv*, **10**, 293-304.
- Hartz, A. M. and Bauer, B. (2011) ABC transporters in the CNS - an inventory. *Curr Pharm Biotechnol*, **12**, 656-673.
- Hasegawa, K. and Miwa, J. (2010) Genetic and cellular characterization of *Caenorhabditis elegans* mutants abnormal in the regulation of many phase II enzymes. *PLoS One*, **5**, e11194.
- Hasegawa, K., Miwa, S., Isomura, K., Tsutsumiuchi, K., Taniguchi, H. and Miwa, J. (2008) Acrylamide-responsive genes in the nematode *Caenorhabditis elegans*. *Toxicol Sci*, **101**, 215-225.
- Hayashi, A., Suzuki, H., Itoh, K., Yamamoto, M. and Sugiyama, Y. (2003) Transcription factor Nrf2 is required for the constitutive and inducible expression of multidrug resistance-associated protein 1 in mouse embryo fibroblasts. *Biochem Biophys Res Commun*, **310**, 824-829.
- Hayes, J. D., Flanagan, J. U. and Jowsey, I. R. (2005) Glutathione transferases. *Annu Rev Pharmacol Toxicol*, **45**, 51-88.
- Haynes, C. M. and Ron, D. (2010) The mitochondrial UPR - protecting organelle protein homeostasis. *J Cell Sci*, **123**, 3849-3855.
- Heath, J. C., Banna, K. M., Reed, M. N., Pesek, E. F., Cole, N., Li, J. and Newland, M. C. (2010) Dietary selenium protects against selected signs of aging and methylmercury exposure. *Neurotoxicology*, **31**, 169-179.
- Helmcke, K. J. and Aschner, M. (2010) Hormetic effect of methylmercury on *Caenorhabditis elegans*. *Toxicol Appl Pharmacol*, **248**, 156-164.
- Henderson, S. T. and Johnson, T. E. (2001) daf-16 integrates developmental and environmental inputs to mediate aging in the nematode *Caenorhabditis elegans*. *Current Biology*, **11**, 1975-1980.
- Hershko, A. and Ciechanover, A. (1998) The ubiquitin system. *Annu Rev Biochem*, **67**, 425-479.
- Heschl, M. F. and Baillie, D. L. (1990) The HSP70 multigene family of *Caenorhabditis elegans*. *Comp Biochem Physiol B*, **96**, 633-637.
- Hirrlinger, J. and Dringen, R. (2005) Multidrug resistance protein 1-mediated export of glutathione and glutathione disulfide from brain astrocytes. *Methods Enzymol*, **400**, 395-409.
- Hirrlinger, J., Schulz, J. B. and Dringen, R. (2002) Effects of dopamine on the glutathione metabolism of cultured astroglial cells: implications for Parkinson's disease. *J Neurochem*, **82**, 458-467.

- Honda, Y., Tanaka, M. and Honda, S. (2010) Trehalose extends longevity in the nematode *Caenorhabditis elegans*. *Aging Cell*, **9**, 558-569.
- Hoozemans, J. J., van Haastert, E. S., Eikelenboom, P., de Vos, R. A., Rozemuller, J. M. and Scheper, W. (2007) Activation of the unfolded protein response in Parkinson's disease. *Biochem Biophys Res Commun*, **354**, 707-711.
- Hope, I. A. (1999) *C. elegans: A practical approach*. Oxford University Press, New York, NY.
- Huang, C. F., Hsu, C. J., Liu, S. H. and Lin-Shiau, S. Y. (2008) Neurotoxicological mechanism of methylmercury induced by low-dose and long-term exposure in mice: oxidative stress and down-regulated Na⁺/K⁺-ATPase involved. *Toxicol Lett*, **176**, 188-197.
- Huang, d. W., Sherman, B. T. and Lempicki, R. A. (2009) Systematic and integrative analysis of large gene lists using DAVID bioinformatics resources. *Nat Protoc*, **4**, 44-57.
- Hunt-Newbury, R., Viveiros, R., Johnsen, R. et al. (2007) High-Throughput In Vivo Analysis of Gene Expression in *Caenorhabditis elegans*. *PLoS Biology*, **5**, e237.
- Hwang, G. W., Furuchi, T. and Naganuma, A. (2002) A ubiquitin-proteasome system is responsible for the protection of yeast and human cells against methylmercury. *FASEB J*, **16**, 709-711.
- Hwang, G. W., Furuoya, Y., Hiroshima, A., Furuchi, T. and Naganuma, A. (2005) Overexpression of Bop3 confers resistance to methylmercury in *Saccharomyces cerevisiae* through interaction with other proteins such as Fkh1, Rts1, and Msn2. *Biochem Biophys Res Commun*, **330**, 378-385.
- Hwang, G. W., Hayashi, T., Kita, K., Takahashi, T., Kuge, S. and Naganuma, A. (2007) siRNA-mediated inhibition of phosphatidylinositol glycan Class B (PIGB) confers resistance to methylmercury in HEK293 cells. *J Toxicol Sci*, **32**, 581-583.
- Hwang, G. W., Tobita, M., Takahashi, T., Kuge, S., Kita, K. and Naganuma, A. (2010) siRNA-mediated AMPKalpha1 subunit gene PRKAA1 silencing enhances methylmercury toxicity in HEK293 cells. *J Toxicol Sci*, **35**, 601-604.
- Hwang, G. W., Wada, N., Kuge, S. and Naganuma, A. (2009) Overexpression of the novel F-box protein Ymr258c confers resistance to methylmercury in *Saccharomyces cerevisiae*. *J Toxicol Sci*, **34**, 413-416.
- lent, B., Edwards, R., Mould, R., Hannah, M., Holden-Dye, L. and O'Connor, V. (2012) HSP-4 endoplasmic reticulum (ER) stress pathway is not activated in a *C. elegans* model of ethanol intoxication and withdrawal. *Invert Neurosci*, **12**, 93-102.
- Innamorato, N. G., Jazwa, A., Rojo, A. I. et al. (2010) Different susceptibility to the Parkinson's toxin MPTP in mice lacking the redox master regulator Nrf2 or its target gene heme oxygenase-1. *PLoS One*, **5**, e11838.

- Inoue, H., Hisamoto, N., An, J. H., Oliveira, R. P., Nishida, E., Blackwell, T. K. and Matsumoto, K. (2005) The *C. elegans* p38 MAPK pathway regulates nuclear localization of the transcription factor SKN-1 in oxidative stress response. *Genes & Development*, **19**, 2278-2283.
- InSug, O., Datar, S., Koch, C. J., Shapiro, I. M. and Shenker, B. J. (1997) Mercuric compounds inhibit human monocyte function by inducing apoptosis: evidence for formation of reactive oxygen species, development of mitochondrial membrane permeability transition and loss of reductive reserve. *Toxicology*, **124**, 211-224.
- Itoh, K., Chiba, T., Takahashi, S. et al. (1997) An Nrf2/small Maf heterodimer mediates the induction of phase II detoxifying enzyme genes through antioxidant response elements. *Biochem Biophys Res Commun*, **236**, 313-322.
- Itoh, K., Wakabayashi, N., Katoh, Y., Ishii, T., Igarashi, K., Engel, J. D. and Yamamoto, M. (1999) Keap1 represses nuclear activation of antioxidant responsive elements by Nrf2 through binding to the amino-terminal Neh2 domain. *Genes Dev*, **13**, 76-86.
- Jain, A. K. and Jaiswal, A. K. (2007) GSK-3beta acts upstream of Fyn kinase in regulation of nuclear export and degradation of NF-E2 related factor 2. *J Biol Chem*, **282**, 16502-16510.
- Jaiswal, A. K. (2004) Nrf2 signaling in coordinated activation of antioxidant gene expression. *Free Radical Biology and Medicine*, **36**, 1199-1207.
- Jakel, R. J., Townsend, J. A., Kraft, A. D. and Johnson, J. A. (2007) Nrf2-mediated protection against 6-hydroxydopamine. *Brain Research*, **1144**, 192-201.
- Jakob, U., Gaestel, M., Engel, K. and Buchner, J. (1993) Small heat shock proteins are molecular chaperones. *J Biol Chem*, **268**, 1517-1520.
- Jankovic, J. (2008) Parkinson's disease: clinical features and diagnosis. *J Neurol Neurosurg Psychiatry*, **79**, 368-376.
- Jayanthi, L. D., Apparsundaram, S., Malone, M. D., Ward, E., Miller, D. M., Eppler, M. and Blakely, R. D. (1998) The *Caenorhabditis elegans* gene T23G5.5 encodes an antidepressant- and cocaine-sensitive dopamine transporter. *Mol Pharmacol*, **54**, 601-609.
- Jazwa, A., Rojo, A. I., Innamorato, N. G., Hesse, M., Fernández-Ruiz, J. and Cuadrado, A. (2011) Pharmacological targeting of the transcription factor Nrf2 at the basal ganglia provides disease modifying therapy for experimental parkinsonism. *Antioxid Redox Signal*, **14**, 2347-2360.
- Ji, L., Li, H., Gao, P., Shang, G., Zhang, D. D., Zhang, N. and Jiang, T. (2013) Nrf2 pathway regulates multidrug-resistance-associated protein 1 in small cell lung cancer. *PLoS One*, **8**, e63404.

- Johnson, J. A., Johnson, D. A., Lee, J.-M., Li, J., Kraft, A. D., Calkins, M. J. and Jakel, R. J. (2007) The Nrf2-ARE pathway: A potential therapeutic target for neurodegenerative diseases. *International Congress Series*, **1302**, 143-153.
- Jones, P. M. and George, A. M. (2002) Mechanism of ABC transporters: a molecular dynamics simulation of a well characterized nucleotide-binding subunit. *Proc Natl Acad Sci U S A*, **99**, 12639-12644.
- Jope, R. S. and Johnson, G. V. (2004) The glamour and gloom of glycogen synthase kinase-3. *Trends Biochem Sci*, **29**, 95-102.
- Juárez, B. I., Martínez, M. L., Montante, M., Dufour, L., García, E. and Jiménez-Capdeville, M. E. (2002) Methylmercury increases glutamate extracellular levels in frontal cortex of awake rats. *Neurotoxicol Teratol*, **24**, 767-771.
- Kahn, N. W., Rea, S. L., Moyle, S., Kell, A. and Johnson, T. E. (2008) Proteasomal dysfunction activates the transcription factor SKN-1 and produces a selective oxidative-stress response in *Caenorhabditis elegans*. *Biochem J*, **409**, 205-213.
- Kalisch, B. E. and Racz, W. J. (1996) The effects of methylmercury on endogenous dopamine efflux from mouse striatal slices. *Toxicol Lett*, **89**, 43-49.
- Kamath, R. S. and Ahringer, J. (2003) Genome-wide RNAi screening in *Caenorhabditis elegans*. *Methods*, **30**, 313-321.
- Kamath, R. S., Fraser, A. G., Dong, Y. et al. (2003) Systematic functional analysis of the *Caenorhabditis elegans* genome using RNAi. *Nature*, **421**, 231-237.
- Kamath, R. S., Martinez-Campos, M., Zipperlen, P., Fraser, A. G. and Ahringer, J. (2001) Effectiveness of specific RNA-mediated interference through ingested double-stranded RNA in *Caenorhabditis elegans*. *Genome Biol*, **2**, RESEARCH0002.
- Kampkötter, A., Nkwonkam, C. G., Zurawski, R. F., Timpel, C., Chovolou, Y., Wätjen, W. and Kahl, R. (2007) Investigations of protective effects of the flavonoids quercetin and rutin on stress resistance in the model organism *Caenorhabditis elegans*. *Toxicology*, **234**, 113-123.
- Kanaoka, Y., Ago, H., Inagaki, E. et al. (1997) Cloning and crystal structure of hematopoietic prostaglandin D synthase. *Cell*, **90**, 1085-1095.
- Kanaoka, Y. and Urade, Y. (2003) Hematopoietic prostaglandin D synthase. *Prostaglandins, Leukotrienes and Essential Fatty Acids*, **69**, 163-167.
- Karlsson, M., Kurz, T., Brunk, U. T., Nilsson, S. E. and Frennesson, C. I. (2010) What does the commonly used DCF test for oxidative stress really show? *Biochem J*, **428**, 183-190.
- Kasama, H., Itoh, K., Omata, S. and Sugano, H. (1989) Differential effects of methylmercury on the synthesis of protein species in dorsal root ganglia of the rat. *Arch Toxicol*, **63**, 226-230.

- Kauffmann, H. M., Pfannschmidt, S., Zöller, H., Benz, A., Vorderstemann, B., Webster, J. I. and Schrenk, D. (2002) Influence of redox-active compounds and PXR-activators on human MRP1 and MRP2 gene expression. *Toxicology*, **171**, 137-146.
- Kaufman, R. J. (1999) Stress signaling from the lumen of the endoplasmic reticulum: coordination of gene transcriptional and translational controls. *Genes Dev*, **13**, 1211-1233.
- Kaur, P., Aschner, M. and Syversen, T. (2006) Glutathione modulation influences methyl mercury induced neurotoxicity in primary cell cultures of neurons and astrocytes. *Neurotoxicology*, **27**, 492-500.
- Kawai, Y., Garduño, L., Theodore, M., Yang, J. and Arinze, I. J. (2011) Acetylation-deacetylation of the transcription factor Nrf2 (nuclear factor erythroid 2-related factor 2) regulates its transcriptional activity and nucleocytoplasmic localization. *J Biol Chem*, **286**, 7629-7640.
- Kell, A., Ventura, N., Kahn, N. and Johnson, T. E. (2007) Activation of SKN-1 by novel kinases in *Caenorhabditis elegans*. *Free Radical Biology and Medicine*, **43**, 1560-1566.
- Kennedy, S., Wang, D. and Ruvkun, G. (2004) A conserved siRNA-degrading RNase negatively regulates RNA interference in *C. elegans*. *Nature*, **427**, 645-649.
- Kensler, T. W., Wakabayashi, N. and Biswal, S. (2007) Cell survival responses to environmental stresses via the Keap1-Nrf2-ARE pathway. *Annu Rev Pharmacol Toxicol*, **47**, 89-116.
- Kerper, L. E., Ballatori, N. and Clarkson, T. W. (1992) Methylmercury transport across the blood-brain barrier by an amino acid carrier. *Am J Physiol*, **262**, R761-765.
- Khan, M. A. and Wang, F. (2009) Mercury-selenium compounds and their toxicological significance: toward a molecular understanding of the mercury-selenium antagonism. *Environ Toxicol Chem*, **28**, 1567-1577.
- Kim, N. S. and Lee, B. K. (2010) Blood total mercury and fish consumption in the Korean general population in KNHANES III, 2005. *Sci Total Environ*, **408**, 4841-4847.
- Kim, Y. and Sun, H. (2007) Functional genomic approach to identify novel genes involved in the regulation of oxidative stress resistance and animal lifespan. *Aging Cell*, **6**, 489-503.
- Klaassen, C. D. and Lu, H. (2008) Xenobiotic transporters: ascribing function from gene knockout and mutation studies. *Toxicol Sci*, **101**, 186-196.
- Klein, C. and Westenberger, A. (2012) Genetics of Parkinson's disease. *Cold Spring Harb Perspect Med*, **2**, a008888.
- Kormish, J. D. and McGhee, J. D. (2005) The *C. elegans* lethal gut-obstructed *gob-1* gene is trehalose-6-phosphate phosphatase. *Dev Biol*, **287**, 35-47.

- Kourtis, N., Nikolettou, V. and Tavernarakis, N. (2012) Small heat-shock proteins protect from heat-stroke-associated neurodegeneration. *Nature*, **490**, 213-218.
- Kunimoto, M. and Suzuki, T. (1997) Migration of granule neurons in cerebellar organotypic cultures is impaired by methylmercury. *Neurosci Lett*, **226**, 183-186.
- Lagido, C., Pettitt, J., Flett, A. and Glover, L. A. (2008) Bridging the phenotypic gap: real-time assessment of mitochondrial function and metabolism of the nematode *Caenorhabditis elegans*. *BMC Physiol*, **8**, 7.
- Lakowicz, J. R. and Anderson, C. J. (1980) Permeability of lipid bilayers to methylmercuric chloride: quantification by fluorescence quenching of a carbazole-labeled phospholipid. *Chem Biol Interact*, **30**, 309-323.
- Lakso, M., Vartiainen, S., Moilanen, A. M., Sirviö, J., Thomas, J. H., Nass, R., Blakely, R. D. and Wong, G. (2003) Dopaminergic neuronal loss and motor deficits in *Caenorhabditis elegans* overexpressing human alpha-synuclein. *J Neurochem*, **86**, 165-172.
- Lamitina, T., Huang, C. G. and Strange, K. (2006) Genome-wide RNAi screening identifies protein damage as a regulator of osmoprotective gene expression. *Proc Natl Acad Sci U S A*, **103**, 12173-12178.
- Łania-Pietrzak, B., Michalak, K., Hendrich, A. B., Mosiadz, D., Gryniewicz, G., Motohashi, N. and Shirataki, Y. (2005) Modulation of MRP1 protein transport by plant, and synthetically modified flavonoids. *Life Sci*, **77**, 1879-1891.
- Lant, B. and Storey, K. B. (2010) An overview of stress response and hypometabolic strategies in *Caenorhabditis elegans*: conserved and contrasting signals with the mammalian system. *Int J Biol Sci*, **6**, 9-50.
- Larkin, M. A., Blackshields, G., Brown, N. P. et al. (2007) Clustal W and Clustal X version 2.0. *Bioinformatics*, **23**, 2947-2948.
- LeBel, C. P., Ali, S. F., McKee, M. and Bondy, S. C. (1990) Organometal-induced increases in oxygen reactive species: the potential of 2',7'-dichlorofluorescein diacetate as an index of neurotoxic damage. *Toxicol Appl Pharmacol*, **104**, 17-24.
- Lee, C. G., Tang, K., Cheung, Y. B. et al. (2004) MDR1, the blood-brain barrier transporter, is associated with Parkinson's disease in ethnic Chinese. *J Med Genet*, **41**, e60.
- Lee, J. Y., Hwang, G. W. and Naganuma, A. (2009) Rip1 enhances methylmercury toxicity through production of reactive oxygen species (ROS) in budding yeast. *J Toxicol Sci*, **34**, 715-717.
- Leiers, B., Kampkotter, A., Grevelding, C. G., Link, C. D., Johnson, T. E. and Henkle-Duhrsen, K. (2003) A stress-response glutathione S-transferase confers resistance to oxidative stress in *Caenorhabditis elegans*.

- Leslie, E. M., Haimeur, A. and Waalkes, M. P. (2004) Arsenic transport by the human multidrug resistance protein 1 (MRP1/ABCC1). Evidence that a tri-glutathione conjugate is required. *J Biol Chem*, **279**, 32700-32708.
- Leung, M. C., Williams, P. L., Benedetto, A., Au, C., Helmcke, K. J., Aschner, M. and Meyer, J. N. (2008) *Caenorhabditis elegans*: an emerging model in biomedical and environmental toxicology. *Toxicol Sci*, **106**, 5-28.
- Leviel, V. (2011) Dopamine release mediated by the dopamine transporter, facts and consequences. *J Neurochem*, **118**, 475-489.
- Li, J., Cai, T., Wu, P. et al. (2009) Proteomic analysis of mitochondria from *Caenorhabditis elegans*. *Proteomics*, **9**, 4539-4553.
- Li, Q., Zhang, S. H., Yu, Y. H., Wang, L. P., Guan, S. W. and Li, P. F. (2012) Toxicity of sodium fluoride to *Caenorhabditis elegans*. *Biomed Environ Sci*, **25**, 216-223.
- Liao, V. H. and Freedman, J. H. (1998) Cadmium-regulated genes from the nematode *Caenorhabditis elegans*. Identification and cloning of new cadmium-responsive genes by differential display. *J Biol Chem*, **273**, 31962-31970.
- Lim, K. L. and Tan, J. M. (2007) Role of the ubiquitin proteasome system in Parkinson's disease. *BMC Biochem*, **8 Suppl 1**, S13.
- Limke, T. L. and Atchison, W. D. (2002) Acute exposure to methylmercury opens the mitochondrial permeability transition pore in rat cerebellar granule cells. *Toxicol Appl Pharmacol*, **178**, 52-61.
- Limke, T. L., Heidemann, S. R. and Atchison, W. D. (2004) Disruption of intraneuronal divalent cation regulation by methylmercury: are specific targets involved in altered neuronal development and cytotoxicity in methylmercury poisoning? *Neurotoxicology*, **25**, 741-760.
- Limke, T. L., Otero-Montanez, J. K. and Atchison, W. D. (2003) Evidence for interactions between intracellular calcium stores during methylmercury-induced intracellular calcium dysregulation in rat cerebellar granule neurons. *J Pharmacol Exp Ther*, **304**, 949-958.
- Lindblom, T. H. and Dodd, A. K. (2006) Xenobiotic detoxification in the nematode *Caenorhabditis elegans*. *Journal of Experimental Zoology Part A: Comparative Experimental Biology*, **305A**, 720-730.
- Link, C. D., Cypser, J. R., Johnson, C. J. and Johnson, T. E. (1999) Direct observation of stress response in *Caenorhabditis elegans* using a reporter transgene. *Cell Stress Chaperones*, **4**, 235-242.
- Lints, R. and Emmons, S. W. (1999) Patterning of dopaminergic neurotransmitter identity among *Caenorhabditis elegans* ray sensory neurons by a TGFbeta family signaling pathway and a Hox gene. *Development*, **126**, 5819-5831.

- Liu, S., Lu, W., Obara, T., Kuida, S., Lehoczky, J., Dewar, K., Drummond, I. A. and Beier, D. R. (2002) A defect in a novel Nek-family kinase causes cystic kidney disease in the mouse and in zebrafish. *Development*, **129**, 5839-5846.
- Loer, C. M. and DePaul, S. (2002) The cat-4/GTP cyclohydrolase I/F32G8.6 gene of *C. elegans*. In: *West Coast Worm Meeting*.
- LoPachin, R. M. and Barber, D. S. (2006) Synaptic cysteine sulfhydryl groups as targets of electrophilic neurotoxicants. *Toxicol Sci*, **94**, 240-255.
- Lovenberg, W., Levine, R. A., Robinson, D. S., Ebert, M., Williams, A. C. and Calne, D. B. (1979) Hydroxylase cofactor activity in cerebrospinal fluid of normal subjects and patients with Parkinson's disease. *Science*, **204**, 624-626.
- Lund, M. E., Banner, W., Clarkson, T. W. and Berlin, M. (1984) Treatment of acute methylmercury ingestion by hemodialysis with N-acetylcysteine (Mucomyst) infusion and 2,3-dimercaptopropane sulfonate. *J Toxicol Clin Toxicol*, **22**, 31-49.
- Madejczyk, M. S., Aremu, D. A., Simmons-Willis, T. A., Clarkson, T. W. and Ballatori, N. (2007) Accelerated urinary excretion of methylmercury following administration of its antidote N-acetylcysteine requires Mrp2/Abcc2, the apical multidrug resistance-associated protein. *J Pharmacol Exp Ther*, **322**, 378-384.
- Maduro, M. F., Meneghini, M. D., Bowerman, B., Broitman-Maduro, G. and Rothman, J. H. (2001) Restriction of mesendoderm to a single blastomere by the combined action of SKN-1 and a GSK-3beta homolog is mediated by MED-1 and -2 in *C. elegans*. *Mol Cell*, **7**, 475-485.
- Malhotra, D., Portales-Casamar, E., Singh, A. et al. (2010) Global mapping of binding sites for Nrf2 identifies novel targets in cell survival response through ChIP-Seq profiling and network analysis. *Nucleic Acids Res*, **38**, 5718-5734.
- Mancini, J. D., Autio, D. M. and Atchison, W. D. (2009) Continuous exposure to low concentrations of methylmercury impairs cerebellar granule cell migration in organotypic slice culture. *Neurotoxicology*, **30**, 203-208.
- Mandel, S. A., Fishman-Jacob, T. and Youdim, M. B. (2009) Modeling sporadic Parkinson's disease by silencing the ubiquitin E3 ligase component, SKP1A. *Parkinsonism Relat Disord*, **15 Suppl 3**, S148-151.
- Marr, J., Nilsen, T. W. and Komuniecki, R. W. (2003) *Molecular Medical Parasitology*. Academic Press, London, UK.
- Marty, M. S. and Atchison, W. D. (1997) Pathways mediating Ca²⁺ entry in rat cerebellar granule cells following in vitro exposure to methyl mercury. *Toxicol Appl Pharmacol*, **147**, 319-330.
- Marty, M. S. and Atchison, W. D. (1998) Elevations of intracellular Ca²⁺ as a probable contributor to decreased viability in cerebellar granule cells following acute exposure to methylmercury. *Toxicol Appl Pharmacol*, **150**, 98-105.

- Miao, Z. H. and Ding, J. (2003) Transcription factor c-Jun activation represses mdr-1 gene expression. *Cancer Res*, **63**, 4527-4532.
- Miller, D. M., Desai, N. S., Hardin, D. C., Piston, D. W., Patterson, G. H., Fleenor, J., Xu, S. and Fire, A. (1999) Two-color GFP expression system for *C. elegans*. *Biotechniques*, **26**, 914-918, 920-911.
- Mineva, I., Stamenova, M., Gartner, W. and Wagner, L. (2008) Expression of the small heat shock protein alphaB-crystallin in term human placenta. *Am J Reprod Immunol*, **60**, 440-448.
- Minich, T., Riemer, J., Schulz, J. B., Wielinga, P., Wijnholds, J. and Dringen, R. (2006) The multidrug resistance protein 1 (Mrp1), but not Mrp5, mediates export of glutathione and glutathione disulfide from brain astrocytes. *J Neurochem*, **97**, 373-384.
- Minnema, D. J., Cooper, G. P. and Greenland, R. D. (1989) Effects of methylmercury on neurotransmitter release from rat brain synaptosomes. *Toxicol Appl Pharmacol*, **99**, 510-521.
- Miura, K. and Clarkson, T. W. (1993) Reduced methylmercury accumulation in a methylmercury-resistant rat pheochromocytoma PC12 cell line. *Toxicol Appl Pharmacol*, **118**, 39-45.
- Miura, N., Kaneko, S., Hosoya, S., Furuchi, T., Miura, K., Kuge, S. and Naganuma, A. (1999) Overexpression of L-glutamine:D-fructose-6-phosphate amidotransferase provides resistance to methylmercury in *Saccharomyces cerevisiae*. *FEBS Lett*, **458**, 215-218.
- Mori, N., Yasutake, A. and Hirayama, K. (2007) Comparative study of activities in reactive oxygen species production/defense system in mitochondria of rat brain and liver, and their susceptibility to methylmercury toxicity. *Arch Toxicol*, **81**, 769-776.
- Mori, N., Yasutake, A., Marumoto, M. and Hirayama, K. (2011) Methylmercury inhibits electron transport chain activity and induces cytochrome c release in cerebellum mitochondria. *J Toxicol Sci*, **36**, 253-259.
- Myers, G. J., Thurston, S. W., Pearson, A. T., Davidson, P. W., Cox, C., Shamlaye, C. F., Cernichiari, E. and Clarkson, T. W. (2009) Postnatal exposure to methyl mercury from fish consumption: a review and new data from the Seychelles Child Development Study. *Neurotoxicology*, **30**, 338-349.
- Naganuma, A., Miura, K., Tanaka-Kagawa, T., Kitahara, J., Seko, Y., Toyoda, H. and Imura, N. (1998) Overexpression of manganese-superoxide dismutase prevents methylmercury toxicity in HeLa cells. *Life Sci*, **62**, PL157-161.
- Nakano, Y., Fujitani, K., Kurihara, J. et al. (2001) Mutations in the novel membrane protein spinster interfere with programmed cell death and cause neural degeneration in *Drosophila melanogaster*. *Mol Cell Biol*, **21**, 3775-3788.

- Nakaso, K., Nakamura, C., Sato, H., Imamura, K., Takeshima, T. and Nakashima, K. (2006) Novel cytoprotective mechanism of anti-parkinsonian drug deprenyl: PI3K and Nrf2-derived induction of antioxidative proteins. *Biochem Biophys Res Commun*, **339**, 915-922.
- Nass, R. and Blakely, R. D. (2003) The *Caenorhabditis elegans* dopaminergic system: opportunities for insights into dopamine transport and neurodegeneration. *Annu Rev Pharmacol Toxicol*, **43**, 521-544.
- Nass, R., Hall, D. H., Miller, D. M., 3rd and Blakely, R. D. (2002) Neurotoxin-induced degeneration of dopamine neurons in *Caenorhabditis elegans*. *Proc Natl Acad Sci U S A*, **99**, 3264-3269.
- Nass, R. and Hamza, I. (2007) The nematode *C. elegans* as an animal model to explore toxicology in vivo: solid and axenic growth culture conditions and compound exposure parameters. *Current Protocols in Toxicology*, 1.9.1-1.9.18.
- Nass, R., Merchant, K. and Ryan, T. (2008) *C. elegans* in Parkinson's disease drug discover: addressing an unmet medical need. *Molecular Interventions*, **8**.
- Nass, R., Miller, D. M. and Blakely, R. D. (2001) *C. elegans*: a novel pharmacogenetic model to study Parkinson's disease. *Parkinsonism Relat Disord*, **7**, 185-191.
- Nass, R. and Settivari, R. (2008) *C. elegans* models of Parkinson's Disease: A Robust Genetic System to Identify and Characterize Endogenous and Environmental Components Involved in Dopamine Neuron Degeneration. In: *Parkinson's Disease: Molecular and Therapeutic Insights from Model Systems*, (R. Nass and S. Przedborski eds.), pp. 347-360. Elsevier Academic Press, New York, NY.
- Ngim, C. H. and Devathanan, G. (1989) Epidemiologic study on the association between body burden mercury level and idiopathic Parkinson's disease. *Neuroepidemiology*, **8**, 128-141.
- Nguyen, T., Nioi, P. and Pickett, C. B. (2009) The Nrf2-antioxidant response element signaling pathway and its activation by oxidative stress. *J Biol Chem*, **284**, 13291-13295.
- Ni, M., Li, X., Yin, Z., Jiang, H., Sidoryk-Węgrzynowicz, M., Milatovic, D., Cai, J. and Aschner, M. (2010) Methylmercury induces acute oxidative stress, altering Nrf2 protein level in primary microglial cells. *Toxicol Sci*, **116**, 590-603.
- Ni, M., Li, X., Yin, Z., Sidoryk-Węgrzynowicz, M., Jiang, H., Farina, M., Rocha, J. B., Syversen, T. and Aschner, M. (2011) Comparative study on the response of rat primary astrocytes and microglia to methylmercury toxicity. *Glia*, **59**, 810-820.
- Niu, W., Lu, Z. J., Zhong, M. et al. (2011) Diverse transcription factor binding features revealed by genome-wide ChIP-seq in *C. elegans*. *Genome Res*, **21**, 245-254.
- Novillo, A., Won, S. J., Li, C. and Callard, I. P. (2005) Changes in Nuclear Receptor and Vitellogenin Gene Expression in Response to Steroids and Heavy Metal in *Caenorhabditis elegans*. *Integr Comp Biol*, **45**, 61-71.

- Nuwaysir, E. F., Bittner, M., Trent, J., Barrett, J. C. and Afshari, C. A. (1999) Microarrays and toxicology: the advent of toxicogenomics. *Mol Carcinog*, **24**, 153-159.
- Nuytemans, K., Theuns, J., Cruts, M. and Van Broeckhoven, C. (2010) Genetic etiology of Parkinson disease associated with mutations in the SNCA, PARK2, PINK1, PARK7, and LRRK2 genes: a mutation update. *Hum Mutat*, **31**, 763-780.
- Nygaard, T. G., Takahashi, H., Heiman, G. A., Snow, B. J., Fahn, S. and Calne, D. B. (1992) Long-term treatment response and fluorodopa positron emission tomographic scanning of parkinsonism in a family with dopa-responsive dystonia. *Ann Neurol*, **32**, 603-608.
- Ogura, H., Takeuchi, T. and Morimoto, K. (1996) A comparison of the 8-hydroxydeoxyguanosine, chromosome aberrations and micronucleus techniques for the assessment of the genotoxicity of mercury compounds in human blood lymphocytes. *Mutat Res*, **340**, 175-182.
- Ohlson, C. G. and Hogstedt, C. (1981) Parkinson's disease and occupational exposure to organic solvents, agricultural chemicals and mercury--a case-referent study. *Scand J Work Environ Health*, **7**, 252-256.
- Oliveira, R. P., Abate, J. P., Dilks, K., Landis, J., Ashraf, J., Murphy, C. T. and Blackwell, T. K. (2009) Condition-adapted stress and longevity gene regulation by *Caenorhabditis elegans* SKN-1/Nrf. *Aging Cell*, **8**, 524-541.
- Onishchenko, N., Karpova, N., Sabri, F., Castrén, E. and Ceccatelli, S. (2008) Long-lasting depression-like behavior and epigenetic changes of BDNF gene expression induced by perinatal exposure to methylmercury. *J Neurochem*, **106**, 1378-1387.
- Orrenius, S., Zhivotovsky, B. and Nicotera, P. (2003) Regulation of cell death: the calcium-apoptosis link. *Nat Rev Mol Cell Biol*, **4**, 552-565.
- Owuor, E. D. and Kong, A. N. (2002) Antioxidants and oxidants regulated signal transduction pathways. *Biochem Pharmacol*, **64**, 765-770.
- Pacyna, J. M., Sundseth, K., Pacyna, E. G., Jozewicz, W., Munthe, J., Belhaj, M. and Aström, S. (2010) An assessment of costs and benefits associated with mercury emission reductions from major anthropogenic sources. *J Air Waste Manag Assoc*, **60**, 302-315.
- Page, A. P. and Johnstone, I. L. (2007) The cuticle. *WormBook*, doi/10.1895/wormbook.1.138.1.
- Palladino, M. J., Bower, J. E., Kreber, R. and Ganetzky, B. (2003) Neural dysfunction and neurodegeneration in *Drosophila* Na⁺/K⁺ ATPase alpha subunit mutants. *J Neurosci*, **23**, 1276-1286.
- Parcellier, A., Schmitt, E., Brunet, M., Hammann, A., Solary, E. and Garrido, C. (2005) Small heat shock proteins HSP27 and alphaB-crystallin: cytoprotective and oncogenic functions. *Antioxid Redox Signal*, **7**, 404-413.

- Parížek, J. and Ostádalová, I. (1967) The protective effect of small amounts of selenite in sublimate intoxication. *Experientia*, **23**, 142-143.
- Park, S.-K., Tedesco, P. M. and Johnson, T. E. (2009) Oxidative stress and longevity in *Caenorhabditis elegans* as mediated by SKN-1. *Aging Cell*, **8**, 258-269.
- Parks, J. M., Johs, A., Podar, M. et al. (2013) The genetic basis for bacterial mercury methylation. *Science*, **339**, 1332-1335.
- Patel, V. P. and Chu, C. T. (2011) Nuclear transport, oxidative stress, and neurodegeneration. *Int J Clin Exp Pathol*, **4**, 215-229.
- Petersen, M. S., Halling, J., Bech, S., Wermuth, L., Weihe, P., Nielsen, F., Jørgensen, P. J., Budtz-Jørgensen, E. and Grandjean, P. (2008) Impact of dietary exposure to food contaminants on the risk of Parkinson's disease. *Neurotoxicology*, **29**, 584-590.
- Peterson, R. T., Nass, R., Boyd, W. A., Freedman, J. H., Dong, K. and Narahashi, T. (2008) Use of non-mammalian alternative models for neurotoxicological study. *Neurotoxicology*, **29**, 546-555.
- Petrucci, L. and Dickson, D. W. (2008) *Parkinson's Disease: Molecular and Therapeutic Insights from Model Systems*. Elsevier Academic Press, New York, NY.
- Ponka, P. (1999) Cell biology of heme. *Am J Med Sci*, **318**, 241-256.
- Poulain, A. J. and Barkay, T. (2013) Environmental science. Cracking the mercury methylation code. *Science*, **339**, 1280-1281.
- Prahlad, V. and Morimoto, R. I. (2009) Integrating the stress response: lessons for neurodegenerative diseases from *C. elegans*. *Trends in Cell Biology*, **19**, 52-61.
- Pratt, S., Shepard, R. L., Kandasamy, R. A., Johnston, P. A., Perry, W. and Dantzig, A. H. (2005) The multidrug resistance protein 5 (ABCC5) confers resistance to 5-fluorouracil and transports its monophosphorylated metabolites. *Mol Cancer Ther*, **4**, 855-863.
- Pretera, T., Zhang, Y., Spencer, S. R., Wilczak, C. A. and Talalay, P. (1993) The electrophile counterattack response: protection against neoplasia and toxicity. *Adv Enzyme Regul*, **33**, 281-296.
- Qu, W., Ren, C., Li, Y. et al. (2011) Reliability analysis of the Ahringer *Caenorhabditis elegans* RNAi feeding library: a guide for genome-wide screens. *BMC Genomics*, **12**, 170.
- Ralston, N. V., Blackwell, J. L. and Raymond, L. J. (2007) Importance of molar ratios in selenium-dependent protection against methylmercury toxicity. *Biol Trace Elem Res*, **119**, 255-268.
- Ralston, N. V. and Raymond, L. J. (2010) Dietary selenium's protective effects against methylmercury toxicity. *Toxicology*, **278**, 112-123.

- Rand, M. D., Bland, C. E. and Bond, J. (2008) Methylmercury Activates Enhancer-of-Split and Bearded Complex Genes Independent of the Notch Receptor. *Toxicol. Sci.*, **104**, 163-176.
- Rand, M. D., Dao, J. C. and Clason, T. A. (2009) Methylmercury disruption of embryonic neural development in *Drosophila*. *Neurotoxicology*, **30**, 794-802.
- Rasband, W. S. (1997-2012) ImageJ. U.S. National Institutes of Health, Bethesda, MD, USA, <http://imagej.nih.gov/ij/>.
- Reed, M. N. and Newland, M. C. (2009) Gestational methylmercury exposure selectively increases the sensitivity of operant behavior to cocaine. *Behavioral Neuroscience*, **123**, 408-417.
- Reid, G., Wielinga, P., Zelcer, N., De Haas, M., Van Deemter, L., Wijnholds, J., Balzarini, J. and Borst, P. (2003) Characterization of the transport of nucleoside analog drugs by the human multidrug resistance proteins MRP4 and MRP5. *Mol Pharmacol*, **63**, 1094-1103.
- Ren, X. Q., Furukawa, T., Haraguchi, M., Sumizawa, T., Aoki, S., Kobayashi, M. and Akiyama, S. (2004) Function of the ABC signature sequences in the human multidrug resistance protein 1. *Mol Pharmacol*, **65**, 1536-1542.
- Reyes, L. H., Mizanur Rahman, G. M., Fahrenholz, T. and Skip Kingston, H. M. (2008) Comparison of methods with respect to efficiencies, recoveries, and quantitation of mercury species interconversions in food demonstrated using tuna fish. *Anal Bioanal Chem*, **390**, 2123-2132.
- Rheinberger, C. M. and Hammitt, J. K. (2012) Risk trade-offs in fish consumption: a public health perspective. *Environ Sci Technol*, **46**, 12337-12346.
- Ribbeck, K., Lipowsky, G., Kent, H. M., Stewart, M. and Görlich, D. (1998) NTF2 mediates nuclear import of Ran. *EMBO J*, **17**, 6587-6598.
- Rice, D. C., Schoeny, R. and Mahaffey, K. (2003) Methods and rationale for derivation of a reference dose for methylmercury by the U.S. EPA. *Risk Anal*, **23**, 107-115.
- Riddle, D. L. (1988) *The Nematode Caenorhabditis elegans*. Cold Spring Harbor Laboratory Press, Cold Spring Harbor.
- Roberts, R. A., Laskin, D. L., Smith, C. V., Robertson, F. M., Allen, E. M., Doorn, J. A. and Slikker, W. (2009) Nitrate and oxidative stress in toxicology and disease. *Toxicol Sci*, **112**, 4-16.
- Robinson, J. F., Guerrette, Z., Yu, X., Hong, S. and Faustman, E. M. (2010) A systems-based approach to investigate dose- and time-dependent methylmercury-induced gene expression response in C57BL/6 mouse embryos undergoing neurulation. *Birth Defects Res B Dev Reprod Toxicol*, **89**, 188-200.

- Roh, J.-Y., Jung, I.-H., Lee, J.-Y. and Choi, J. (2007) Toxic effects of di(2-ethylhexyl)phthalate on mortality, growth, reproduction and stress-related gene expression in the soil nematode *Caenorhabditis elegans*. *Toxicology*, **237**, 126-133.
- Rojo, A. I., Rada, P., Egea, J., Rosa, A. O., López, M. G. and Cuadrado, A. (2008a) Functional interference between glycogen synthase kinase-3 beta and the transcription factor Nrf2 in protection against kainate-induced hippocampal cell death. *Mol Cell Neurosci*, **39**, 125-132.
- Rojo, A. I., Sagarra, M. R. and Cuadrado, A. (2008b) GSK-3beta down-regulates the transcription factor Nrf2 after oxidant damage: relevance to exposure of neuronal cells to oxidative stress. *J Neurochem*, **105**, 192-202.
- Ronaldson, P. T., Persidsky, Y. and Bendayan, R. (2008) Regulation of ABC membrane transporters in glial cells: relevance to the pharmacotherapy of brain HIV-1 infection. *Glia*, **56**, 1711-1735.
- Rossi, A. D., Ahlbom, E., Ogren, S. O., Nicotera, P. and Ceccatelli, S. (1997) Prenatal exposure to methylmercury alters locomotor activity of male but not female rats. *Exp Brain Res*, **117**, 428-436.
- Rual, J. F., Ceron, J., Koreth, J. et al. (2004) Toward improving *Caenorhabditis elegans* phenome mapping with an ORFeome-based RNAi library. *Genome Res*, **14**, 2162-2168.
- Rudgalvyte, M., VanDuyn, N., Aarnio, V., Heikkinen, L., Peltonen, J., Lakso, M., Nass, R. and Wong, G. (2013) Methylmercury exposure increases lipocalin related (*lpr*) and decreases activated in blocked unfolded protein response (*abu*) genes and specific miRNAs in *Caenorhabditis elegans*. *Toxicology Letters*, **Accepted for publication**.
- Rush, T., Liu, X., Nowakowski, A. B., Petering, D. H. and Lobner, D. (2012) Glutathione-mediated neuroprotection against methylmercury neurotoxicity in cortical culture is dependent on MRP1. *Neurotoxicology*, **33**, 476-481.
- Rusyniak, D. E., Arroyo, A., Acciani, J., Froberg, B., Kao, L. and Furbee, B. (2010) Heavy metal poisoning: management of intoxication and antidotes. *EXS*, **100**, 365-396.
- Sachs, C. and Jonsson, G. (1975) Mechanisms of action of 6-hydroxydopamine. *Biochem Pharmacol*, **24**, 1-8.
- Sager, P. R. and Syversen, T. L. (1984) Differential responses to methylmercury exposure and recovery in neuroblastoma and glioma cells and fibroblasts. *Exp Neurol*, **85**, 371-382.
- Saha, S., Guillily, M. D., Ferree, A. et al. (2009) LRRK2 modulates vulnerability to mitochondrial dysfunction in *Caenorhabditis elegans*. *J Neurosci*, **29**, 9210-9218.

- Sakamoto, M., Ikegami, N. and Nakano, A. (1996) Protective effects of Ca²⁺ channel blockers against methyl mercury toxicity. *Pharmacol Toxicol*, **78**, 193-199.
- Salonen, J. T., Seppänen, K., Lakka, T. A., Salonen, R. and Kaplan, G. A. (2000) Mercury accumulation and accelerated progression of carotid atherosclerosis: a population-based prospective 4-year follow-up study in men in eastern Finland. *Atherosclerosis*, **148**, 265-273.
- Salonen, J. T., Seppänen, K., Nyysönen, K. et al. (1995) Intake of mercury from fish, lipid peroxidation, and the risk of myocardial infarction and coronary, cardiovascular, and any death in eastern Finnish men. *Circulation*, **91**, 645-655.
- Samali, A. and Orrenius, S. (1998a) Heat shock proteins: regulators of stress response and apoptosis. *Cell Stress Chaperones*, **3**, 228-236.
- Samali, A. and Orrenius, S. (1998b) Heat shock proteins: regulators of stress response and apoptosis. *Cell Stress Chaperones*, **3**, 228-236.
- Sanders, B. (1993) Stress proteins in aquatic organisms: an environmental perspective. *Critical Reviews in Toxicology*, **23**, 49-75.
- Sarafian, T. and Verity, M. A. (1991) Oxidative mechanisms underlying methyl mercury neurotoxicity. *Int J Dev Neurosci*, **9**, 147-153.
- Sarafian, T. A., Bredesen, D. E. and Verity, M. A. (1996) Cellular resistance to methylmercury. *Neurotoxicology*, **17**, 27-36.
- Sass, J. B., Haselow, D. T. and Silbergeld, E. K. (2001) Methylmercury-induced decrement in neuronal migration may involve cytokine-dependent mechanisms: a novel method to assess neuronal movement in vitro. *Toxicol Sci*, **63**, 74-81.
- Sawin, E. R., Ranganathan, R. and Horvitz, H. R. (2000) *C. elegans* locomotory rate is modulated by the environment through a dopaminergic pathway and by experience through a serotonergic pathway. *Neuron*, **26**, 619-631.
- Scherzer, C. R., Jensen, R. V., Gullans, S. R. and Feany, M. B. (2003) Gene expression changes presage neurodegeneration in a *Drosophila* model of Parkinson's disease. *Hum Mol Genet*, **12**, 2457-2466.
- Schläwicke Engström, K., Strömberg, U., Lundh, T., Johansson, I., Vessby, B., Hallmans, G., Skerfving, S. and Broberg, K. (2008) Genetic variation in glutathione-related genes and body burden of methylmercury. *Environ Health Perspect*, **116**, 734-739.
- Schober, S. E., Sinks, T. H., Jones, R. L. et al. (2003) Blood Mercury Levels in US Children and Women of Childbearing Age, 1999-2000. *JAMA*, **289**, 1667-1674.
- Schulz, T. J., Zarse, K., Voigt, A., Urban, N., Birringer, M. and Ristow, M. (2007) Glucose Restriction Extends *Caenorhabditis elegans* Life Span by Inducing Mitochondrial Respiration and Increasing Oxidative Stress. *Cell Metabolism*, **6**, 280-293.

- Seidler, A., Hellenbrand, W., Robra, B. P., Vieregge, P., Nischan, P., Joerg, J., Oertel, W. H., Ulm, G. and Schneider, E. (1996) Possible environmental, occupational, and other etiologic factors for Parkinson's disease: a case-control study in Germany. *Neurology*, **46**, 1275-1284.
- Settivari, R., Levora, J. and Nass, R. (2009) The divalent metal transporter homologues SMF-1/2 mediate dopamine neuron sensitivity in caenorhabditis elegans models of manganism and parkinson disease. *J Biol Chem*, **284**, 35758-35768.
- Settivari, R., Vanduyn, N., Levora, J. and Nass, R. (2013) The Nrf2/SKN-1-dependent glutathione S-transferase π homologue GST-1 inhibits dopamine neuron degeneration in a Caenorhabditis elegans model of manganism. *Neurotoxicology*.
- Shafer, T. J., Meacham, C. A. and Barone, S. (2002) Effects of prolonged exposure to nanomolar concentrations of methylmercury on voltage-sensitive sodium and calcium currents in PC12 cells. *Brain Res Dev Brain Res*, **136**, 151-164.
- Shanker, G., Mutkus, L. A., Walker, S. J. and Aschner, M. (2002) Methylmercury enhances arachidonic acid release and cytosolic phospholipase A2 expression in primary cultures of neonatal astrocytes. *Brain Res Mol Brain Res*, **106**, 1-11.
- Sharma, R. P., Aldous, C. N. and Farr, C. H. (1982) Methylmercury induced alterations in brain amine syntheses in rats. *Toxicol Lett*, **13**, 195-201.
- Sharom, F. J. (2008) ABC multidrug transporters: structure, function and role in chemoresistance. *Pharmacogenomics*, **9**, 105-127.
- Shaye, D. D. and Greenwald, I. (2011) OrthoList: a compendium of C. elegans genes with human orthologs. *PLoS One*, **6**, e20085.
- Shen, X., Ellis, R. E., Lee, K. et al. (2001) Complementary Signaling Pathways Regulate the Unfolded Protein Response and Are Required for C. elegans Development. *Cell*, **107**, 893-903.
- Shenker, B. J., Guo, T. L., O, I. and Shapiro, I. M. (1999) Induction of apoptosis in human T-cells by methyl mercury: temporal relationship between mitochondrial dysfunction and loss of reductive reserve. *Toxicol Appl Pharmacol*, **157**, 23-35.
- Sheps, J. A., Ralph, S., Zhao, Z., Baillie, D. L. and Ling, V. (2004) The ABC transporter gene family of Caenorhabditis elegans has implications for the evolutionary dynamics of multidrug resistance in eukaryotes. *Genome Biol*, **5**, R15.
- Shi, M., Bradner, J., Bammler, T. K., Eaton, D. L., Zhang, J., Ye, Z., Wilson, A. M., Montine, T. J. and Pan, C. (2009) Identification of glutathione S-transferase π as a protein involved in Parkinson disease progression. *Am J Pathol*, **175**, 54-65.
- Shi, Y. and Mello, C. (1998) A CBP/p300 homolog specifies multiple differentiation pathways in Caenorhabditis elegans. *Genes Dev*, **12**, 943-955.

- Shih, A. Y., Erb, H. and Murphy, T. H. (2007) Dopamine activates Nrf2-regulated neuroprotective pathways in astrocytes and meningeal cells. *Journal of Neurochemistry*, **101**, 109-119.
- Shinkai, Y., Sumi, D., Fukami, I., Ishii, T. and Kumagai, Y. (2006) Sulforaphane, an activator of Nrf2, suppresses cellular accumulation of arsenic and its cytotoxicity in primary mouse hepatocytes. *FEBS Lett*, **580**, 1771-1774.
- Siebert, A., Desai, V., Chandrasekaran, K., Fiskum, G. and Jafri, M. S. (2009) Nrf2 activators provide neuroprotection against 6-hydroxydopamine toxicity in rat organotypic nigrostriatal cocultures. *Journal of Neuroscience Research*, **87**, 1659-1669.
- Simmer, F., Moorman, C., van der Linden, A. M., Kuijk, E., van den Berghe, P. V. E., Kamath, R. S., Fraser, A. G., Ahringer, J. and Plasterk, R. H. A. (2003) Genome-Wide RNAi of *C. elegans* Using the Hypersensitive rrf-3 Strain Reveals Novel Gene Functions. *PLoS Biol*, **1**, e12.
- Simmer, F., Tijsterman, M., Parrish, S., Koushika, S. P., Nonet, M. L., Fire, A., Ahringer, J. and Plasterk, R. H. (2002) Loss of the putative RNA-directed RNA polymerase RRF-3 makes *C. elegans* hypersensitive to RNAi. *Curr Biol*, **12**, 1317-1319.
- Singer, M. A. and Lindquist, S. (1998) Multiple effects of trehalose on protein folding in vitro and in vivo. *Mol Cell*, **1**, 639-648.
- Sirois, J. E. and Atchison, W. D. (1996) Effects of mercurials on ligand- and voltage-gated ion channels: a review. *Neurotoxicology*, **17**, 63-84.
- Sokolowski, K., Falluel-Morel, A., Zhou, X. and DiCicco-Bloom, E. (2011) Methylmercury (MeHg) elicits mitochondrial-dependent apoptosis in developing hippocampus and acts at low exposures. *Neurotoxicology*, **32**, 535-544.
- Stacchiotti, A., Lavazza, A., Rezzani, R., Borsani, E., Rodella, L. and Bianchi, R. (2004) Mercuric chloride-induced alterations in stress protein distribution in rat kidney. *Histol Histopathol*, **19**, 1209-1218.
- Steenland, K., Hein, M. J., Cassinelli, R. T., Prince, M. M., Nilsen, N. B., Whelan, E. A., Waters, M. A., Ruder, A. M. and Schnorr, T. M. (2006) Polychlorinated biphenyls and neurodegenerative disease mortality in an occupational cohort. *Epidemiology*, **17**, 8-13.
- Stefani, M. and Dobson, C. M. (2003) Protein aggregation and aggregate toxicity: new insights into protein folding, misfolding diseases and biological evolution. *J Mol Med (Berl)*, **81**, 678-699.
- Stiernagle, T. (1999) *C. elegans: A practical approach*. Oxford University Press, New York.
- Strange, K. (2006) *C. Elegans: Methods and Applications: Methods in Molecular Biology*. Humana Press, Totowa, NJ.

- Strange, K., Christensen, M. and Morrison, R. (2007) Primary culture of *Caenorhabditis elegans* developing embryo cells for electrophysiological, cell biological and molecular studies. *Nat Protoc*, **2**, 1003-1012.
- Sugimoto, A. (2004) High-throughput RNAi in *Caenorhabditis elegans*: genome-wide screens and functional genomics. *Differentiation*, **72**, 81-91.
- Suh, J. H., Shenvi, S. V., Dixon, B. M., Liu, H., Jaiswal, A. K., Liu, R. M. and Hagen, T. M. (2004) Decline in transcriptional activity of Nrf2 causes age-related loss of glutathione synthesis, which is reversible with lipoic acid. *Proc Natl Acad Sci U S A*, **101**, 3381-3386.
- Sulston, J., Dew, M. and Brenner, S. (1975) Dopaminergic neurons in the nematode *Caenorhabditis elegans*. *J Comp Neurol*, **163**, 215-226.
- Sun, Z., Chin, E. and Zhang, D. (2009) Acetylation of Nrf2 by p300/CBP Augments promoter-specific DNA binding of Nrf2 during antioxidant response. *MCB*.
- Sundseth, K., Pacyna, J. M., Pacyna, E. G., Munthe, J., Belhaj, M. and Aström, S. (2010) Economic benefits from decreased mercury emissions: Projections for 2020. *Journal of Cleaner Production*, **18**, 386-394.
- Surmeier, D. J., Guzman, J. N. and Sanchez-Padilla, J. (2010) Calcium, cellular aging, and selective neuronal vulnerability in Parkinson's disease. *Cell Calcium*, **47**, 175-182.
- Swain, S., Wren, J. F., Stürzenbaum, S. R. et al. (2010) Linking toxicant physiological mode of action with induced gene expression changes in *Caenorhabditis elegans*. *BMC Syst Biol*, **4**, 32.
- Sykiotis, G. P. and Bohmann, D. (2010) Stress-activated cap'n'collar transcription factors in aging and human disease. *Sci Signal*, **3**, re3.
- Syversen, T. (1977) Effects of methylmercury on in vivo protein synthesis in isolated cerebral and cerebellar neurons. *Neuropathology and Applied Neurobiology*, **3**, 225-236.
- Takeuchi, T. (1982) Pathology of Minamata disease. With special reference to its pathogenesis. *Acta Pathol Jpn*, **32 Suppl 1**, 73-99.
- Tamm, C., Duckworth, J., Hermanson, O. and Ceccatelli, S. (2006) High susceptibility of neural stem cells to methylmercury toxicity: effects on cell survival and neuronal differentiation. *J Neurochem*, **97**, 69-78.
- Tanner, C. M., Kamel, F., Ross, G. W. et al. (2011) Rotenone, paraquat, and Parkinson's disease. *Environ Health Perspect*, **119**, 866-872.
- Tatara, C. P., Newman, M. C., McCloskey, J. T. and Williams, P. L. (1997) Predicting relative metal toxicity with ion characteristics: *Caenorhabditis elegans* LC50. *Aquat Toxicol*, **39**, 279-290.

- Theodore, M., Kawai, Y., Yang, J., Kleshchenko, Y., Reddy, S. P., Villalta, F. and Arinze, I. J. (2008) Multiple nuclear localization signals function in the nuclear import of the transcription factor Nrf2. *J Biol Chem*, **283**, 8984-8994.
- Thimmulappa, R. K., Mai, K. H., Srisuma, S., Kensler, T. W., Yamamoto, M. and Biswal, S. (2002) Identification of Nrf2-regulated genes induced by the chemopreventive agent sulforaphane by oligonucleotide microarray. *Cancer Res*, **62**, 5196-5203.
- Thomas, B. and Beal, M. F. (2011) Molecular insights into Parkinson's disease. *F1000 Med Rep*, **3**, 7.
- Tiernan, C. T., Edwin, E. A., Goudreau, J. L., Atchison, W. D. and Lookingland, K. J. (2013) The role of de novo catecholamine synthesis in mediating methylmercury-induced vesicular dopamine release from rat pheochromocytoma (PC12) cells. *Toxicol Sci*, **133**, 125-132.
- Timmons, L., Court, D. L. and Fire, A. (2001) Ingestion of bacterially expressed dsRNAs can produce specific and potent genetic interference in *Caenorhabditis elegans*. *Gene*, **263**, 103-112.
- Tofighi, R., Johansson, C., Goldoni, M., Ibrahim, W. N., Gogvadze, V., Mutti, A. and Ceccatelli, S. (2011) Hippocampal neurons exposed to the environmental contaminants methylmercury and polychlorinated biphenyls undergo cell death via parallel activation of calpains and lysosomal proteases. *Neurotox Res*, **19**, 183-194.
- Toyama, T., Shinkai, Y., Sumi, D. and Kumagai, Y. (2010) Carbon monoxide derived from heme oxygenase-2 mediates reduction of methylmercury toxicity in SH-SY5Y cells. *Toxicol Appl Pharmacol*, **249**, 86-90.
- Toyama, T., Shinkai, Y., Yasutake, A., Uchida, K., Yamamoto, M. and Kumagai, Y. (2011a) Isothiocyanates reduce mercury accumulation via an Nrf2-dependent mechanism during exposure of mice to methylmercury. *Environ Health Perspect*, **119**, 1117-1122.
- Toyama, T., Sumi, D., Shinkai, Y., Yasutake, A., Taguchi, K., Tong, K. I., Yamamoto, M. and Kumagai, Y. (2007) Cytoprotective role of Nrf2/Keap1 system in methylmercury toxicity. *Biochemical and Biophysical Research Communications*, **363**, 645-650.
- Toyama, T., Yoshida, E., Shinkai, Y. and Kumagai, Y. (2011b) DNA microarray analysis of human neuroblastoma SH-SY5Y cells exposed to methylmercury. *J Toxicol Sci*, **36**, 843-845.
- Trasande, L., Landrigan, P. J. and Schechter, C. (2005) Public health and economic consequences of methylmercury toxicity to the developing brain. *Environmental Health Perspectives*, **113**.

- Traunspurger, W., Haitzer, M., Hoss, S., Beier, S., Ahlf, W. and C., S. (1997) Ecotoxicological assessment of aquatic sediments with *Caenorhabditis elegans* (nematoda) - a method for testing liquid medium and whole-sediment samples. *Environmental Toxicology and Chemistry*, **16**, 245-250.
- Tullet, J. M., Hertweck, M., An, J. H., Baker, J., Hwang, J. Y., Liu, S., Oliveira, R. P., Baumeister, R. and Blackwell, T. K. (2008) Direct inhibition of the longevity-promoting factor SKN-1 by insulin-like signaling in *C. elegans*. *Cell*, **132**, 1025-1038.
- Tuomisto, J. and Komulainen, H. (1983) Release and inhibition of uptake of 5-hydroxytryptamine in blood platelets in vitro by copper and methyl mercury. *Acta Pharmacol Toxicol (Copenh)*, **52**, 292-297.
- Turrens, J. F. (2003) Mitochondrial formation of reactive oxygen species. *J Physiol*, **552**, 335-344.
- USEPA (2001) Water Quality Criterion for the Protection of Human Health: Methylmercury. Vol. EPA-823-R-01-001. U.S. Environmental Protection Agency, Office of Water, Washington, DC.
- USEPA (2009) The National Study of Chemical Residues in Lake Fish Tissue. Vol. EPA-823-R-09-006. U.S. Environmental Protection Agency, Office of Water, Washington, DC.
- USEPA (2010) Guidance for implementing the January 2001 methylmercury water quality criterion. Vol. EPA 823-R-10-001. U.S. Environmental Protection Agency, Office of Water, Washington, DC.
- USFDA (2001) An important message for pregnant women and women of childbearing age who may become pregnant about the risks of mercury in fish. Vol. Advisory 3872. U.S. Food and Drug Administration, Center for Food Safety and Applied Nutrition, Washington, DC.
- Usuki, F., Fujita, E. and Sasagawa, N. (2008) Methylmercury activates ASK1/JNK signaling pathways, leading to apoptosis due to both mitochondria- and endoplasmic reticulum (ER)-generated processes in myogenic cell lines. *Neurotoxicology*, **29**, 22-30.
- Uversky, V. N., Li, J. and Fink, A. L. (2001) Metal-triggered structural transformations, aggregation, and fibrillation of human alpha-synuclein. A possible molecular link between Parkinson's disease and heavy metal exposure. *J Biol Chem*, **276**, 44284-44296.
- Van Baelen, K., Vanoevelen, J., Missiaen, L., Raeymaekers, L. and Wuytack, F. (2001) The Golgi PMR1 P-type ATPase of *Caenorhabditis elegans*. Identification of the gene and demonstration of calcium and manganese transport. *J Biol Chem*, **276**, 10683-10691.

- van de Water, F. M., Masereeuw, R. and Russel, F. G. (2005) Function and regulation of multidrug resistance proteins (MRPs) in the renal elimination of organic anions. *Drug Metab Rev*, **37**, 443-471.
- van Rossum, A. J., Brophy, P. M., Tait, A., Barrett, J. and Jefferies, J. R. (2001) Proteomic identification of glutathione S-transferases from the model nematode *Caenorhabditis elegans*. *Proteomics*, **1**, 1463-1468.
- van Wijngaarden, E., Beck, C., Shamlaye, C. F., Cernichiari, E., Davidson, P. W., Myers, G. J. and Clarkson, T. W. (2006) Benchmark concentrations for methyl mercury obtained from the 9-year follow-up of the Seychelles Child Development Study. *Neurotoxicology*, **27**, 702-709.
- VanDuyn, N., Settivari, R., LeVora, J., Zhou, S., Unrine, J. and Nass, R. (2013) The metal transporter SMF-3/DMT-1 mediates aluminum-induced dopamine neuron degeneration. *J Neurochem*, **124**, 147-157.
- VanDuyn, N., Settivari, R., Wong, G. and Nass, R. (2010) SKN-1/Nrf2 inhibits dopamine neuron degeneration in a *Caenorhabditis elegans* model of methylmercury toxicity. *Toxicol Sci*.
- Vatamaniuk, O. K., Bucher, E. A., Sundaram, M. V. and Rea, P. A. (2005) CeHMT-1, a putative phytochelatin transporter, is required for cadmium tolerance in *Caenorhabditis elegans*. *J Biol Chem*, **280**, 23684-23690.
- Verity, M. A., Brown, W. J. and Cheung, M. (1975) Organic mercurial encephalopathy: in vivo and in vitro effects of methyl mercury on synaptosomal respiration. *J Neurochem*, **25**, 759-766.
- Verschuuren, H. G., Kroes, R., Den Tonkelaar, E. M., Berkvens, J. M., Helleman, P. W., Rauws, A. G., Schuller, P. L. and Van Esch, G. J. (1976) Toxicity of methylmercury chloride in rats I. Short-term study. *Toxicology*, **6**, 85-96.
- Virtanen, J. K., Rissanen, T. H., Voutilainen, S. and Tuomainen, T. P. (2007) Mercury as a risk factor for cardiovascular diseases. *J Nutr Biochem*, **18**, 75-85.
- Vistbakka, J., VanDuyn, N., Wong, G. and Nass, R. (2012) *C. elegans* as a genetic model system to identify Parkinson's disease-associated therapeutic targets. *CNS Neurol Disord Drug Targets*, **11**, 957-964.
- Vollrath, V., Wielandt, A. M., Iruetagoiena, M. and Chianale, J. (2006) Role of Nrf2 in the regulation of the Mrp2 (ABCC2) gene. *Biochem J*, **395**, 599-609.
- von Otter, M., Landgren, S., Nilsson, S. et al. (2010) Association of Nrf2-encoding NFE2L2 haplotypes with Parkinson's disease. *BMC Med Genet*, **11**, 36.
- Wagner, G. C., Reuhl, K. R., Ming, X. and Halladay, A. K. (2007) Behavioral and neurochemical sensitization to amphetamine following early postnatal administration of methylmercury (MeHg). *Neurotoxicology*, **28**, 59-66.

- Walker, A. K., See, R., Batchelder, C., Kophengnavong, T., Gronniger, J. T., Shi, Y. and Blackwell, T. K. (2000) A Conserved Transcription Motif Suggesting Functional Parallels between *Caenorhabditis elegans* SKN-1 and Cap'n'Collar-related Basic Leucine Zipper Proteins. *J. Biol. Chem.*, **275**, 22166-22171.
- Walker, J. E., Saraste, M., Runswick, M. J. and Gay, N. J. (1982) Distantly related sequences in the alpha- and beta-subunits of ATP synthase, myosin, kinases and other ATP-requiring enzymes and a common nucleotide binding fold. *EMBO J*, **1**, 945-951.
- Wang, J., Robida-Stubbs, S., Tullet, J. M., Rual, J. F., Vidal, M. and Blackwell, T. K. (2010) RNAi screening implicates a SKN-1-dependent transcriptional response in stress resistance and longevity deriving from translation inhibition. *PLoS Genet*, **6**.
- Wang, L., Jiang, H., Yin, Z., Aschner, M. and Cai, J. (2009a) Methylmercury Toxicity and Nrf2-dependent Detoxification in Astrocytes. *Toxicol. Sci.*, **107**, 135-143.
- Wang, S., Zhao, Y., Wu, L., Tang, M., Su, C., Hei, T. K. and Yu, Z. (2007) Induction of germline cell cycle arrest and apoptosis by sodium arsenite in *Caenorhabditis elegans*. *Chem Res Toxicol*, **20**, 181-186.
- Wang, Z., Gerstein, M. and Snyder, M. (2009b) RNA-Seq: a revolutionary tool for transcriptomics. *Nat Rev Genet*, **10**, 57-63.
- Weihe, P. and Joensen, H. D. (2012) Dietary recommendations regarding pilot whale meat and blubber in the Faroe Islands. *Int J Circumpolar Health*, **71**, 18594.
- Weimer, R. M., Richmond, J. E., Davis, W. S., Hadwiger, G., Nonet, M. L. and Jorgensen, E. M. (2003) Defects in synaptic vesicle docking in unc-18 mutants. *Nat Neurosci*, **6**, 1023-1030.
- Weis, J. S. (2009) Reproductive, developmental, and neurobehavioral effects of methylmercury in fishes. *J Environ Sci Health C Environ Carcinog Ecotoxicol Rev*, **27**, 212-225.
- Weiss, B. (2010) Lead, manganese, and methylmercury as risk factors for neurobehavioral impairment in advanced age. *Int J Alzheimers Dis*, **2011**, 607543.
- Weiss, B., Clarkson, T. W. and Simon, W. (2002) Silent latency periods in methylmercury poisoning and in neurodegenerative disease. *Environ Health Perspect*, **110 Suppl 5**, 851-854.
- White, J. G., Southgate, E., Thomson, J. N. and Brenner, S. (1986) The structure of the nervous system of the nematode *Caenorhabditis elegans*. *Philos Trans R Soc Lond B Biol Sci*, **314**, 1-340.
- Wilbur, S. M. and Soffey, E. (2003) Tips for the Analysis of Mercury by ICP-MS. *Agilent ICP-MS Journal*.

- Wilce, M. C. J. and Parker, M. W. (1994) Structure and function of glutathione S-transferases. *Biochimica et Biophysica Acta (BBA) - Protein Structure and Molecular Enzymology*, **1205**, 1-18.
- Wilson, D. T., Polunas, M. A., Zhou, R., Halladay, A. K., Lowndes, H. E. and Reuhl, K. R. (2005) Methylmercury alters Eph and ephrin expression during neuronal differentiation of P19 embryonal carcinoma cells. *Neurotoxicology*, **26**, 661-674.
- Wood, J. M. (1974) Biological cycles for toxic elements in the environment. *Science*, **183**, 1049-1052.
- Woods, J. S. (1996) Altered porphyrin metabolism as a biomarker of mercury exposure and toxicity. *Can J Physiol Pharmacol*, **74**, 210-215.
- Yabe, T., Suzuki, N., Furukawa, T., Ishihara, T. and Katsura, I. (2005) Multidrug resistance-associated protein MRP-1 regulates dauer diapause by its export activity in *Caenorhabditis elegans*. *Development*, **132**, 3197-3207.
- Yadatie, F., Karlsen, O. A., Lanzén, A., Berg, K., Olsvik, P., Hogstrand, C. and Goksøyr, A. (2013) Global transcriptome analysis of Atlantic cod (*Gadus morhua*) liver after in vivo methylmercury exposure suggests effects on energy metabolism pathways. *Aquat Toxicol*, **126**, 314-325.
- Yamazaki, M., Li, B., Louie, S. W. et al. (2005) Effects of fibrates on human organic anion-transporting polypeptide 1B1-, multidrug resistance protein 2- and P-glycoprotein-mediated transport. *Xenobiotica*, **35**, 737-753.
- Yan, R., Urdaneta-Marquez, L., Keller, K., James, C. E., Davey, M. W. and Prichard, R. K. (2012) The role of several ABC transporter genes in ivermectin resistance in *Caenorhabditis elegans*. *Vet Parasitol*, **190**, 519-529.
- Yanagisawa, H., Miyashita, T., Nakano, Y. and Yamamoto, D. (2003) HSpin1, a transmembrane protein interacting with Bcl-2/Bcl-xL, induces a caspase-independent autophagic cell death. *Cell Death Differ*, **10**, 798-807.
- Yang, L., Ho, N. Y., Müller, F. and Strähle, U. (2010) Methyl mercury suppresses the formation of the tail primordium in developing zebrafish embryos. *Toxicol Sci*, **115**, 379-390.
- Yao, C., El Khoury, R., Wang, W. et al. (2010) LRRK2-mediated neurodegeneration and dysfunction of dopaminergic neurons in a *Caenorhabditis elegans* model of Parkinson's disease. *Neurobiol Dis*, **40**, 73-81.
- Yee, S. and Choi, B. H. (1994) Methylmercury poisoning induces oxidative stress in the mouse brain. *Exp Mol Pathol*, **60**, 188-196.
- Yee, S. and Choi, B. H. (1996) Oxidative stress in neurotoxic effects of methylmercury poisoning. *Neurotoxicology*, **17**, 17-26.

- Yin, Z., Milatovic, D., Aschner, J. L., Syversen, T., Rocha, J. B., Souza, D. O., Sidoryk, M., Albrecht, J. and Aschner, M. (2007) Methylmercury induces oxidative injury, alterations in permeability and glutamine transport in cultured astrocytes. *Brain Res*, **1131**, 1-10.
- Yoneda, T., Benedetti, C., Urano, F., Clark, S. G., Harding, H. P. and Ron, D. (2004) Compartment-specific perturbation of protein handling activates genes encoding mitochondrial chaperones. *J Cell Sci*, **117**, 4055-4066.
- Yorifuji, T., Tsuda, T., Inoue, S., Takao, S. and Harada, M. (2011) Long-term exposure to methylmercury and psychiatric symptoms in residents of Minamata, Japan. *Environ Int*, **37**, 907-913.
- Yorifuji, T., Tsuda, T., Takao, S. and Harada, M. (2008) Long-term exposure to methylmercury and neurologic signs in Minamata and neighboring communities. *Epidemiology*, **19**, 3-9.
- Yoshida, E., Toyama, T., Shinkai, Y., Sawa, T., Akaike, T. and Kumagai, Y. (2011) Detoxification of methylmercury by hydrogen sulfide-producing enzyme in Mammalian cells. *Chem Res Toxicol*, **24**, 1633-1635.
- Yu, R., Chen, C., Mo, Y. Y., Hebbar, V., Owuor, E. D., Tan, T. H. and Kong, A. N. (2000) Activation of mitogen-activated protein kinase pathways induces antioxidant response element-mediated gene expression via a Nrf2-dependent mechanism. *J Biol Chem*, **275**, 39907-39913.
- Yu, X., Robinson, J. F., Sidhu, J. S., Hong, S. and Faustman, E. M. (2010) A system-based comparison of gene expression reveals alterations in oxidative stress, disruption of ubiquitin-proteasome system and altered cell cycle regulation after exposure to cadmium and methylmercury in mouse embryonic fibroblast. *Toxicol Sci*, **114**, 356-377.
- Yu, Z., Yang, X. and Wang, K. (2006) Metal ions induced heat shock protein response by elevating superoxide anion level in HeLa cells transformed by HSE-SEAP reporter gene. *Toxicology*, **223**, 1-8.
- Zalli, D., Bayliss, R. and Fry, A. M. (2012) The Nek8 protein kinase, mutated in the human cystic kidney disease nephronophthisis, is both activated and degraded during ciliogenesis. *Hum Mol Genet*, **21**, 1155-1171.
- Zalups, R. K. and Bridges, C. C. (2009) MRP2 involvement in renal proximal tubular elimination of methylmercury mediated by DMPS or DMSA. *Toxicol Appl Pharmacol*, **235**, 10-17.
- Zayed, J., Campanella, G., Panisset, J. C., Ducic, S., Andre, P., Masson, H. and Roy, M. (1990) [Parkinson disease and environmental factors]. *Rev Epidemiol Sante Publique*, **38**, 159-160.
- Zeevalk, G. D., Razmpour, R. and Bernard, L. P. (2008) Glutathione and Parkinson's disease: is this the elephant in the room? *Biomed Pharmacother*, **62**, 236-249.

- Zhang, D. D., Lo, S. C., Cross, J. V., Templeton, D. J. and Hannink, M. (2004a) Keap1 is a redox-regulated substrate adaptor protein for a Cul3-dependent ubiquitin ligase complex. *Mol Cell Biol*, **24**, 10941-10953.
- Zhang, H., Feng, X., Zhu, J., Sapkota, A., Meng, B., Yao, H., Qin, H. and Larssen, T. (2012) Selenium in soil inhibits mercury uptake and translocation in rice (*Oryza sativa* L.). *Environ Sci Technol*, **46**, 10040-10046.
- Zhang, Y., Lu, R., Liu, W. et al. (2013) Hormetic effects of acute methylmercury exposure on grp78 expression in rat brain cortex. *Dose Response*, **11**, 109-120.
- Zhang, Y., Schuetz, J. D., Elmquist, W. F. and Miller, D. W. (2004b) Plasma membrane localization of multidrug resistance-associated protein homologs in brain capillary endothelial cells. *J Pharmacol Exp Ther*, **311**, 449-455.
- Zhou, J., Liu, M., Aneja, R., Chandra, R., Lage, H. and Joshi, H. C. (2006) Reversal of P-glycoprotein-mediated multidrug resistance in cancer cells by the c-Jun NH2-terminal kinase. *Cancer Res*, **66**, 445-452.
- Zimmer, B., Schildknecht, S., Kuegler, P. B., Tanavde, V., Kadereit, S. and Leist, M. (2011) Sensitivity of dopaminergic neuron differentiation from stem cells to chronic low-dose methylmercury exposure. *Toxicol Sci*, **121**, 357-367.
- Zipper, L. M. and Mulcahy, R. T. (2000) Inhibition of ERK and p38 MAP kinases inhibits binding of Nrf2 and induction of GCS genes. *Biochem Biophys Res Commun*, **278**, 484-492.
- Zong, W. X. and Thompson, C. B. (2006) Necrotic death as a cell fate. *Genes Dev*, **20**, 1-15.
- Zuckerman, D., Gallo, A. and Levin, M. (2007) Can eating fish be dangerous? The facts about methylmercury. *National Research Center for Women & Families*, <http://www.center4research.org>.

CURRICULUM VITAE

Natalia M. VanDuyn

Education

Ph.D. in Toxicology
Department of Pharmacology and Toxicology
Indiana University, Indianapolis, IN
August 2007 – March 2014

B.S. with High Distinction
Major: Biology
Minors: Chemistry, Psychology
Indiana University, Bloomington, IN
August 2003 – May 2007

Research

Dissertation Research, March 2008 – December 2014
Identification and characterization of molecular modulators of methylmercury-induced toxicity and dopamine neuron degeneration in *Caenorhabditis elegans*
Mentor: Dr. Richard Nass
Department of Pharmacology and Toxicology, Indiana University School of Medicine, Indianapolis, IN

Student Research Training in Alternative Methods sponsored by Colgate-Palmolive, June 2011
Evaluating the role of intracellular calcium and mitochondrial membrane potential in a novel *C. elegans* model of methylmercury toxicity
Mentor: Dr. Bill Atchison
Department of Pharmacology & Toxicology, Michigan State University, East Lansing, MI

Laboratory Assistant, September 2005 – May 2006
Mentor: Dr. Jeffrey Palmer
Department of Biology, Indiana University, Bloomington, IN

Publications

Sanford JR, Wang X, Mort M, **VanDuyn N**, Cooper DN, Mooney SD, Edenberg HJ, Liu Y. (2009) Splicing factor SFRS1 recognizes a functionally diverse landscape of RNA transcripts. *Genome Res.* 19(3):381-94.

VanDuyn N, Settivari R, Wong G, Nass R. (2010) SKN-1/Nrf2 inhibits dopamine neuron degeneration in a *Caenorhabditis elegans* model of methylmercury toxicity. *Tox Sci.* 118(2):613-624.

Vistbakka J*, **VanDuyn N***, Wong G, Nass R. (2012) *C. elegans* as a genetic model system to identify Parkinson's disease-associated therapeutic targets. *CNS Neurol Disord Drug Targets*. 11(8):957-64. [*co-first authors]

VanDuyn N, Settivari R, LeVora J, Zhou S, Unrine J, Nass R. (2013) The metal transporter SMF-3/DMT-1 mediates aluminum-induced dopamine neuron degeneration. *J Neurochem*. 124(1):147-57.

Settivari R, **VanDuyn N**, LeVora J, Nass R. (2013) The Nrf2/SKN-1-dependent glutathione S-transferase π homologue GST-1 inhibits dopamine neuron degeneration in a *Caenorhabditis elegans* model of manganism. *Neurotoxicology*. 38:51-60.

Rudgalvyte M, **VanDuyn N**, Aarnio V, Heikkinen L, Peltonen J, Lakso M, Nass R, Wong, G. (2013) Methylmercury exposure increases lipocalin related (lpr) and decreases activated in blocked unfolded protein response (abu) genes and specific miRNAs in *Caenorhabditis elegans*. *Toxicol Lett*. 222(2):189-96.

N VanDuyn and R Nass. (2013) The putative multidrug resistance protein MRP-7 inhibits methylmercury-associated animal toxicity and dopamine neurodegeneration in *Caenorhabditis elegans*. *J Neurochem*. Accepted Article doi: 10.1111/jnc.12515.

Abstracts

R Nass and **N VanDuyn**. A reverse genetic screen identifies the putative multidrug resistance protein MRP-7 as an inhibitor of methylmercury-associated animal toxicity and dopamine neuron degeneration. Gordon Research Conference: Cellular & Molecular Mechanisms of Toxicity. Andover, NH, 2013.

VanDuyn N, Nass R. Identification and characterization of plasma membrane and intracellular transporters involved in MeHg-induced whole animal and DA neuron pathology. Society of Toxicology, San Antonio, TX, 2013.

***Awarded the Occupational & Public Health Specialty Section Best Abstract by a Student Award**

Jamadar S, **VanDuyn N**, Nass R. Generation and characterization of a humanized *C. elegans* transgenic animal that results in early onset, age-dependent complete loss of DA neurons. Society of Toxicology, San Antonio, TX, 2013.

Nass R, Ghosh S, Shah K, Trinidad J, **VanDuyn N**. Identification of novel genes and epigenetic mechanisms in *C. elegans* models of idiopathic Parkinson's disease and manganism. Society of Toxicology, San Antonio, TX, 2013.

VanDuyn N, Settivari R, Nass R. Identification and characterization of molecular modulators of methylmercury-induced toxicity and dopamine neuron degeneration in *C. elegans*. Society of Toxicology, San Francisco, CA, 2012.

Nass R, Settivari R, LeVora J, Zhou S, Unrine J, **VanDuyn N**. Identification and characterization of a dopamine neuron-associated aluminum transporter that confers aluminum-induced neurodegeneration. Society of Toxicology, San Francisco, CA, 2012.

VanDuyn N. Identification and characterization of molecular modulators involved in methylmercury –induced cellular stress. EPA STAR Graduate Fellowship Conference. Washington, DC, 2011.

***Poster selected for presentation at a Capitol Hill Reception**

VanDuyn N, Settivari R, Sinclair G, Nass R. Identification and characterization of molecular modulators of methylmercury-induced whole animal and dopamine neuron pathology in *C. elegans*. International *C. elegans* Meeting. Los Angeles, CA, 2011.

Settivari R, Zhou S, **VanDuyn N,** LeVora J, Sinclair G, Nass R. Role of Nrf2/SKN-1 dependent and ER stress proteins in *C. elegans* models of Parkinson's disease and manganism. International *C. elegans* Meeting. Los Angeles, CA, 2011.

Nass R, Settivari R, **VanDuyn N,** Zhou S. Identification of molecular modulators of methylmercury-induced dopamine neuron degeneration in *C. elegans*. 13th International Neurotoxicology Association Meeting, Xi'an, China, 2011.

Nass R, Settivari R, **VanDuyn N,** Zhou S. Role of Nrf2/SKN-1 dependent proteins in *C. elegans* models of Parkinson's disease and manganism. 13th International Neurotoxicology Association Meeting, Xi'an, China, 2011.

VanDuyn N, Settivari R, Sinclair G, Nass R. Identification and characterization of molecular modulators of methylmercury-induced dopamine neuron pathology in *C. elegans*. Society of Toxicology, Washington, DC, 2011.

Settivari R, LeVora J, **VanDuyn N,** Zhou S, Sinclair G, Nass R. GST-PI inhibits dopamine neuron degeneration in *C. elegans* models of Parkinson's disease and manganism. Society of Toxicology, Washington, DC, 2011.

Nass R, LeVora J, **VanDuyn N,** Settivari R. NRF2/SKN-1-dependent GST-PI inhibits dopamine neurodegeneration in *Caenorhabditis elegans* models of Parkinson's disease and manganism. Society for Neuroscience, San Diego, CA, 2010.

VanDuyn N, Settivari R, Zhou S, Nass R. Identification of molecular modulators of methylmercury-induced animal vulnerability and dopamine neuron degeneration in *C. elegans*. Aging, Metabolism, Pathogenesis, Stress and Small RNAs in *C. elegans* Topics Meeting, Madison, WI, 2010.

Settivari R, Sinclair G, LeVora J, **VanDuyn N,** Zhou S, Nass R. SKN-1 dependent GST-Pi inhibits dopamine neuron degeneration in *C. elegans* models of Parkinson's disease and manganism. Aging, Metabolism, Pathogenesis, Stress and Small RNAs in *C. elegans* Topics Meeting, Madison, WI, 2010.

VanDuyn N, Settivari R, Nass R. SKN-1/Nrf2 inhibits cellular stress in a novel *C. elegans* model of methylmercury neurotoxicity. Society of Toxicology, Salt Lake City, UT, 2010.

***Awarded the Metals Specialty Section Third Place Graduate Student Award**

VanDuyn N, Settivari R, Asikainen S, Rudgalvyte M, Wong G, Nass R. Molecular and genetic analysis in a novel model of methylmercury neurotoxicity. International *C. elegans* Meeting, Los Angeles, CA, 2009.

VanDuyn N, Settivari R, Chen L, Braun AK, Nass R. Molecular and genetic analysis in a novel model of methylmercury neurotoxicity. Society of Toxicology, Baltimore, MD, 2009.

VanDuyn N, Settivari R, Asikainen S, Rudgalvytes M, Hradsky J, Chen L, Braun AK, Wong G, Nass R. Molecular and genetic analysis in a novel model of methylmercury neurotoxicity. Society for Neuroscience, Washington DC, 2008.

Honors and Awards

U.S. EPA Science to Achieve Results (STAR) Graduate Fellowship

Title: Mechanisms of methylmercury-induced cellular stress in *Caenorhabditis elegans*
September 2010 – September 2013
Total Award: \$37,500 per year for 3 years

PhRMA Foundation Pre Doctoral Fellowship in Pharmacology/Toxicology

Title: Mechanisms of methylmercury-induced cellular stress in *Caenorhabditis elegans*
January – August 2010
Total Award: \$20,000 per year for 2 years

Colgate-Palmolive Award for Student Research Training in Alternative Methods

Title: Evaluating the role of intracellular calcium and mitochondrial membrane potential in a novel *C. elegans* model of methylmercury toxicity
Society of Toxicology, January 2010
Total Award: \$3,500

K. K. Chen Distinguished Graduate Student Fellowship

IUSM Department of Pharmacology and Toxicology, 2012
Total Award: \$1,500

Occupational & Public Health Specialty Section Best Abstract by a Student Award

Society of Toxicology, March 2013
Total Award: \$500

Metals Specialty Section Third Place Graduate Student Award

Society of Toxicology, March 2010
Total Award: \$100

Travel Stipend Award

7th International Conference on Frontotemporal Dementias, Indianapolis, IN, October 2010
Total Award: \$560

Educational Enhancement Grant

IUPUI Graduate Student Organization, April 2009
Total Award: \$500

University Fellowship for Graduate Study

Indiana University School of Medicine, 2007
Total Award: one year of tuition, stipend, insurance and \$800 for travel

Professional Organizations

Society of Toxicology (SOT), 2009 – Present
SOT Metals Specialty Section, 2009 – Present
SOT Neurotoxicology Specialty Section, 2009 – Present
Genetics Society of America (GSA), 2009 – 2012
Society for Neuroscience (SfN), 2008 – 2009

Activities

Indiana University School of Medicine Graduate Student Mentor, 2008 – 2011
Indiana University School of Medicine New Student Recruiter, 2008 – 2012
Pharmacology and Toxicology Graduate Student Organization, 2008 – 2013